Thermoelectric heating and air conditioning with double flux ventilation in passive houses

DOCTORAL THESIS

Sergio Díaz de Garayo Balsategui

Supervisors

David Astrain Ulibarrena

Álvaro Martínez Echeverria

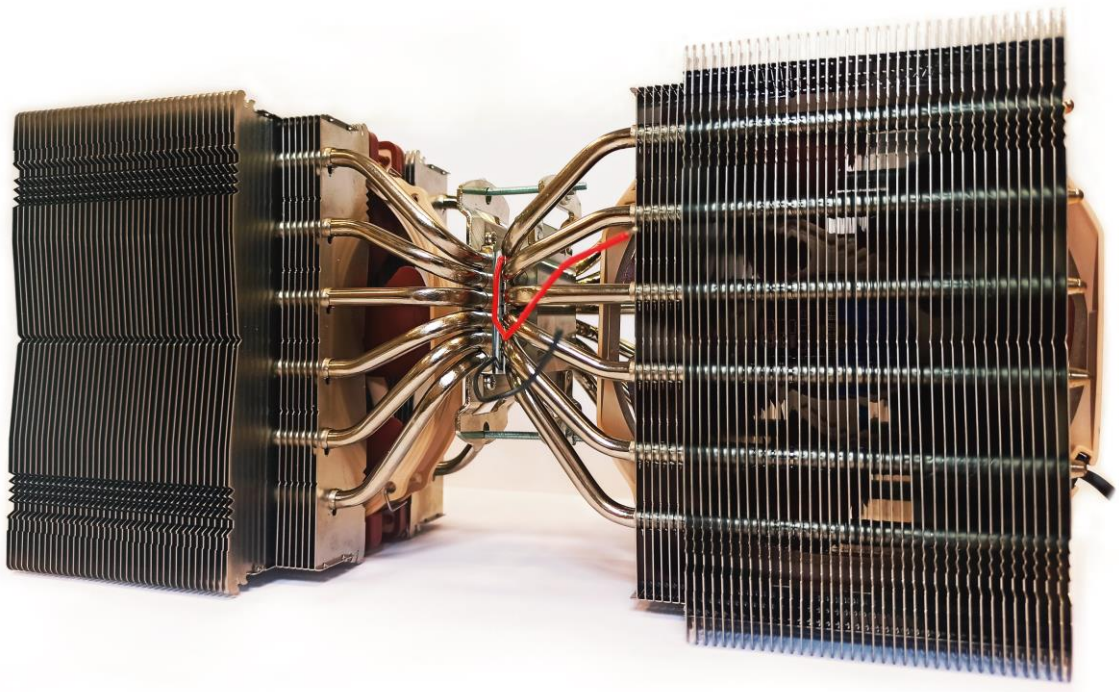

Pamplona, 2nd February 2022

Engineering Department

Public University of Navarre

https://doi.org/10.48035/Tesis/2454/42629

Compendium of Publications

The present Ph. D. dissertation is a compendium of the following publications:

- P. Aranguren, S. Díaz de Garayo, A. Martínez, D. Astrain. **Heat pipes thermal performance for a reversible thermoelectric cooler-heat pump for a nZEB**. Enery & Buildings 187 (2019) 163-172. DOI: 10.1016/j.enbuild.2019.01.039

- S. Díaz de Garayo, A. Martínez, P. Aranguren, D. Astrain. **Prototype of an air to air thermoelectric heat pump integrated with a double flux mechanical ventilation system for passive houses**. Applied Thermal Engineering 190 (2021) 116801. DOI: 10.1016/j.applthermaleng.2021.116801

- S. Díaz de Garayo, A. Martínez, P. Aranguren, D. Astrain. **Optimal combination of an air-to-air thermoelectric heat pump with a heat recovery system to HVAC a passive house dwelling.** Applied Energy 309 (2022) 118443. DOI: 10.1016/j.apenergy.2021.118443

- S. Díaz de Garayo, A. Martínez, P. Aranguren, D. Astrain. **Annual energy performance of a thermoelectric heat pump combined with a heat recover unit to HVAC one passive house dwelling.** Applied Thermal Engineering 204 (2022) 117832. DOI: 10.1016/j.applthermaleng.2021.117832

All the articles have been published in high-quality JCR journals, whose quality indicators are summarized as follows:

- Energy & Buildings
  Impact factor (2019): 9.9
  Category: Mechanical Engineering
  Rank: 22/585
  Quartile: Q1

- Applied Thermal Engineering
  Impact factor (2020): 10.1
  Category: Energy Engineering and Power Technology
  Rank: 18/216
  Quartile: Q1

- Applied Energy
  Impact factor (2020): 9.746
  Category: Engineering, Chemical.
  Rank: 6/143
  Quartile: Q1

Furthermore, since the articles have been performed in co-authorship, the contributions of each author are detailed below:

- P. Aranguren, S. Díaz de Garayo, A. Martínez, M. Araiz, D. Astrain. **Heat pipes thermal performance for a reversible thermoelectric cooler-heat pump for a nZEB**. Enery & Buildings 187 (2019) 163-172. DOI: 10.1016/j.enbuild.2019.01.039

  Patricia Aranguren: Methodology, Lab. Tests, Writing - original draft, Writing – Review & Edition, Visualization.

  Sergio Díaz de Garayo: Methodology, Prototype Design & Construction, Computational Model, Analysis of results, Writing – original draft.

  Álvaro Martínez: Conceptualization, Review & Edition.

  Miguel Araiz: Review & Edition, Visualization.

  David Astrain: Conceptualization, Writing – Review & Edition, Supervision.

- S. Díaz de Garayo, A. Martínez, P. Aranguren, D. Astrain. **Prototype of an air to air thermoelectric heat pump integrated with a double flux mechanical ventilation system for passive houses**. Applied Thermal Engineering 190 (2021) 116801. DOI: 10.1016/j.applthermaleng.2021.116801

  Sergio Díaz de Garayo: Funding acquisition, Prototype Design & Construction, Investigation, Lab. Tests, Writing - original draft, Writing – Review & Edition Project Administration.

  Álvaro Martínez: Conceptualization, Methodology, Review & Edition.

  Patricia Aranguren: Methodology Lab. Tests, Methodology, Writing – Review.

  David Astrain: Conceptualization, Writing – Review & Edition, Supervision.

- S. Díaz de Garayo, A. Martínez, D. Astrain. **Optimal combination of an air-to-air thermoelectric heat pump with a heat recovery system to HVAC a passive house dwelling**. Applied Energy 309 (2022) 118443. DOI: 10.1016/j.apenergy.2021.118443

  Sergio Díaz de Garayo: Conceptualization, Methodology, Formal analysis, Software, Validation, Investigation, Data curation, Visualization, Writing - original draft.

  Álvaro Martínez: Conceptualization, Methodology, Formal analysis, Validation, Writing - review & editing.

  David Astrain: Conceptualization, Validation, Visualization, Supervision.

- S. Díaz de Garayo, A. Martínez, D. Astrain. **Annual energy performance of a thermoelectric heat pump combined with a heat recover unit to HVAC one passive house dwelling.** Applied Thermal Engineering 204 (2022) 117832. DOI: 10.1016/j.applthermaleng.2021.117832

  Sergio Díaz de Garayo: Conceptualization, Computational Model, Investigation, Analysis of results, Writing - original draft, Writing – Review & Edition, Visualization.
  Álvaro Martínez: Methodology, Analysis of results, Formal analysis, Writing - review & editing.
  David Astrain: Conceptualization, Validation, Visualization, Supervision.

Abstract

The fight against climate change has determined the need to decarbonize our economies. In this context, buildings, which are responsible for 30 % of world energy consumption (40 % in Europe) and 28 % of CO_2 emissions (36 % in Europe), will change a lot in the coming years. The new building codes and the massive rehabilitation of envelopes will reduce the specific heating demand (kWh/m^2), while cooling demand will be increased, due to global warming and the more stringent comfort demand. This fact, together with the need to phase out fossil fuel boilers, will massively promote the use of heat pumps for air conditioning in buildings.

Although the vapor-compression cycle is the dominant technology in this sector, the IEA foresees in the "2030 sustainable development scenario" that 1.5 of the 14.5 TW of thermal power of the heat pumps deployed in the coming years will come from alternative technologies to the vapor-compression cycle, contributing to the phase out of HFC refrigerants. This thesis proposes the use of heat pumps based on thermoelectricity, whose main advantages are related with the absence of moving parts and refrigerants. Specifically, this thesis focuses on the design and construction of an air-to-air heat pump device integrated with double flux ventilation in homes, with a surface area limited to 100 m^2, and a highly energy efficient, as "Passive House", where the reduced heating load (<10 W/m^2) enables the possibility to provide enough heating by solely rising the temperature of the ventilation air flow, taking advantage of the residual heat from the renovated air.

Given the importance of heat exchangers in the overall efficiency of the system, two alternatives have been tested: finned heat sinks and finned heat-pipes. Heat-pipes have demonstrated to perform best in the temperature and flow ranges of this application; even in the case of the cold air duct, where heat-pipes work contrary to their original design. The prototype with the heat-pipes is lighter and narrower (which facilitates its installation in false ceilings), thanks to the thermal characterization of the heat exchangers, which determined that their behavior in the horizontal position was equivalent to the vertical one.

Following the heat exchangers investigation, one prototype of an air-to-air thermoelectric heat pump was manufactured with a heating power of 1,250 W and 375 W for cooling with a variable COP 1.5-4 and 0.5-2.5, respectively. The prototype has been tested with the help of a climatic chamber in different winter and summer scenarios, working with different temperature gaps, air flows and voltages. Based on the empirical results, a fast and reliable

computational model has been developed, capable of representing both, the thermoelectric effects in the thermocouples, as well as the variable thermal resistance of the exchangers as a function of the ventilation flow rate and the heat flow, under different operating conditions. Simulation results have been adjusted and validated with the empirical results.

In a subsequent computational study, the number of modules of the heat pump was optimized for different heating and cooling needs, obtaining the maximum possible COP and enabling the comparison of two potential integration layouts of the heat pump with the double flux ventilation system. The stand-alone option as active heat recovery unit has been discarded, in favor of its integration with a passive heat recovery unit, commonly installed in "Passive House" buildings. This combination is more efficient in all the cases analyzed, requiring 5 times less modules. Additionally, the optimization of the seasonal coefficient of performance SCOP in three European climates, following the Directive 2010/30 / EU methodology for heat pumps, concludes that the optimal number of modules in the three cases is 15, which is a promising principle for the standardization of a thermoelectric heat pump model that could reach the market, oriented to "Passive House" dwellings.

Finally, a pilot case has been investigated in a 74.3 m^2 dwelling in a "Passive House" apartment block in Pamplona (Spain). The previously validated model was integrated with a simulation of the building, based on its "Passive House" certificate. The proposed HVAC system maintains stable comfort conditions both in winter and summer, thanks to the precise regulation system allowed by the thermoelectric modules. The system consumes 1,143 kWh/year (15.3 kWh/m^2year) of electricity, which can be produced on-site using 4 photovoltaic panels of 250 Wp. This system is then compared with a vapor-compression cycle heat pump. This technology saves 20.9 % of energy with respect to thermoelectricity, but this only means saving one 250 Wp panel per home.

The results derived from this doctoral thesis show that thermoelectricity can be a real alternative to the construction of heat pumps for the air conditioning of "Passive House" dwellings, given the big advantages (silent, robust system, lightweight design and easily installed on ceilings false, easy regulation, integrability with photovoltaic installations and potential savings in manufacturing costs) compared with its lower efficiency, that can be easily compensated with the increase of photovoltaic production integrated in the building.

Resumen

La lucha contra el cambio climático ha determinado la necesidad de descarbonizar nuestras economías. En este contexto, los edificios, responsables del 30 % del consumo de energía mundial (40 % en Europa) y el 28 % de las emisiones de CO_2 (36 % en Europa), van a cambiar mucho en los próximos años. Los nuevos códigos de la edificación y la rehabilitación masiva de envolventes van a reducir la demanda de calefacción específica (kWh/m^2), si bien es esperable que la demanda de refrigeración aumente, debido al calentamiento global y la mayor demanda de confort. Este hecho, junto con la necesidad de abandonar las calderas de combustibles fósiles, van a promocionar masivamente el uso de las bombas de calor para la climatización de los edificios, tanto para calefacción como para refrigeración.

Si bien el ciclo de compresión de vapor es la tecnología dominante en el sector, la AIE prevé en su "escenario de desarrollo sostenible 2030", que 1.5 de los 14.5 TW de potencia térmica de las bombas de calor instaladas en los próximos años provendrá de tecnologías alternativas al ciclo de compresión, contribuyendo al abandono de los refrigerantes HFC. Esta tesis propone el uso de bombas de calor basadas en termoelectricidad, cuyas ventajas competitivas se basan fundamentalmente en la ausencia de partes móviles y de refrigerantes. Concretamente, esta tesis se centra en el diseño y construcción de un dispositivo de bomba de calor air-aire integrado con la ventilación de doble flujo en viviendas con una superficie inferior a 100 m^2 y una envolvente de alta eficiencia energética tipo "Passive House", donde la reducida carga de calefacción (<10 W/m^2) permite climatizar el espacio con el caudal de aire de ventilación, aprovechando el calor residual del aire renovado.

Dada la importancia de los intercambiadores de calor en la eficiencia total del sistema, se ha experimentado con dos alternativas: perfiles de aluminio extrusionado y heat-pipes con aletas. Se ha demostrado que los heat-pipes funcionan mejor en los rangos de temperatura y caudal de la aplicación, incluso en el conducto de aire frío, donde los heat-pipes funcionan de forma contraria a su diseño original. El prototipo con los heat-pipes es más ligero y estrecho (lo que facilita su instalación en techos falsos), gracias a la caracterización térmica de los intercambiadores, que determinó que su comportamiento en posición horizontal era equivalente al vertical.

A partir de los resultados obtenidos se fabricó un prototipo de bomba de calor termoeléctrica aire-aire con una potencia de calefacción de 1,250 W y 375 W de refrigeración con un COP

variable 1.5-4 y 0.5-2.5, respectivamente. El prototipo ha sido ensayado con la ayuda de una cámara climática en diferentes escenarios de invierno y verano, trabajando con diferentes saltos térmicos, caudales de aire y voltajes. A partir de los resultados obtenidos se ha desarrollado un modelo computacional rápido y fiable, capaz de representar tanto los efectos termoeléctricos que tienen lugar en los módulos, como la resistencia térmica variable de los intercambiadores en función del caudal de ventilación y el flujo de calor, en diferentes condiciones de funcionamiento, pudiendo validar los resultados con los datos experimentales del prototipo.

En un estudio computacional posterior se optimizó el número de módulos de la bomba de calor para diferentes necesidades de calefacción y refrigeración, obteniendo el máximo COP posible, pudiendo comparar dos posibles disposiciones de la bomba de calor en el sistema de ventilación de doble flujo. La posibilidad de su instalación "stand-alone" como recuperador activo se descartó, en favor de su integración con un recuperador de calor pasivo, habitual en los edificios "Passive House". Esta combinación es más eficiente en todos los casos analizados, precisando un número de módulos al menos 5 veces inferior. Adicionalmente, la optimización del rendimiento estacional SCOP en tres climas europeos, según la metodología de la Directiva 2010/30/EU para bombas de calor, permite concluir que el número óptimo de módulos en los tres casos es de 15, lo que supone un principio prometedor para la estandarización de un modelo de bomba de calor termoeléctrica que pudiera llegar el mercado, orientada a viviendas "Passive House".

Finalmente, se ha investigado un caso piloto en un apartamento de 74.3 m^2 en un bloque de apartamentos "Passive House" en Pamplona (España). El modelo anteriormente validado se integró con una simulación del edificio, basada en su certificado "Passive House". El sistema HVAC propuesto mantiene unas condiciones estables de confort tanto en invierno, como en verano, gracias al preciso sistema de regulación que permiten los módulos termoeléctricos. El sistema consume 1,143 kWh/año (15.3 kWh/m^2año) de electricidad, que puede ser producida in-situ mediante 4 paneles fotovoltaicos de 250 Wp. Este sistema es después comparado con una bomba de calor de ciclo de compresión de vapor. La mejor eficiencia de esta tecnología permite ahorrar un 20.9% de la energía, si bien esto tan solo implicaría ahorrar un panel de 250 Wp por vivienda.

De esta manera, los resultados derivados de esta tesis doctoral demuestran que la termolectricidad puede resultar una alternativa real a la construcción de bombas de calor para la climatización de viviendas "Passive House", dada la gran cantidad de ventajas (sistema silencioso, robusto, diseño ligero y fácilmente instalable en techos falsos, fácil regulación, integrabilidad con instalaciones fotovoltaicas y potencial de ahorro en los costes de fabricación), comparado con su menor eficiencia, fácilmente compensable con el incremento de la producción fotovoltaica integrada en el edificio.

Agradecimientos

“Life is like riding a bicycle, to keep your balance you must keep moving”. Esto dicen que dijo Albert Einstein, y este era nuestro lema, el de María y mío, cuando campábamos a nuestras anchas por la columna vertebral americana. Desde que llegamos a Navarra, han sido diez las vueltas que hemos dado al sol y en nuestras alforjas caben tres intrépidas criaturas y muchas aventuras, familiares y profesionales, como el trabajo que aquí presento.

Abre la sección de dedicatorias María, mi amor y mi compañera, el pedal que hace girar la rueda cuando el mío afloja. Le siguen Ione, Ibon y Gael, los tres maravillosos satélites que nos orbitan.

A toda mi familia, a mi aita, que murió en el 2016, y a mi ama, que ha superado el confinamiento con la resignación y la fortaleza de quien ha sabido siempre imponerse a un valle de lágrimas. A los “Garaiteguis” y a la “Pedrada”.

A Xabi, amigo y socio, tanto por su contribución al presente trabajo como por habernos arrastrado en la aventura de inBiot.

A mis directores de tesis, David y Álvaro, por su cercanía y profesionalidad. Al grupo de ITF por su energía renovable y buen rollo.

A los compañeros de Energética Edificatoria y del resto de los departamentos del Centro Nacional de Energías Renovables.

A tod@s: GRACIAS.

Contents

Index of Figures

List of Acronyms

ACH	*Air Changes*
COP	*Coefficient of Peformance*
HRU	*Heat Recovery Unit*
HE	*Heat Exchanger*
HP	*Heat Pump*
HPp	*Heat Pipe*
PH	*Passive House*
PV	*Photovoltaic*
TeHP	*Thermoelectric Heat Pump*
VC	*Vapor compression*
VCHP	*Vapor compression Heat Pump*

Chapter 1. State of the Art and Objectives

1.1. Introduction

After a long list of scientific works to reveal the nature and the threat of climate change, and the never-ending negotiations of the governments to reach consensus over the measures to be undertaken by all the nations to mitigate its effects, one legally binding global climate change agreement was finally signed in December 2015 at the Paris climate conference (COP21: Conference of the Parties within the United Nations Framework Convention on Climate Change). The Paris agreement set out a global framework to contain the effects of the climate change by "limiting global warming to well below 2 °C and pursuing efforts to limit it to 1.5 °C". This goal must be achieved by reducing the emissions of greenhouse gases to the atmosphere, in order to "achieve a balance between anthropogenic emissions by sources and removals by sinks of greenhouse gases".

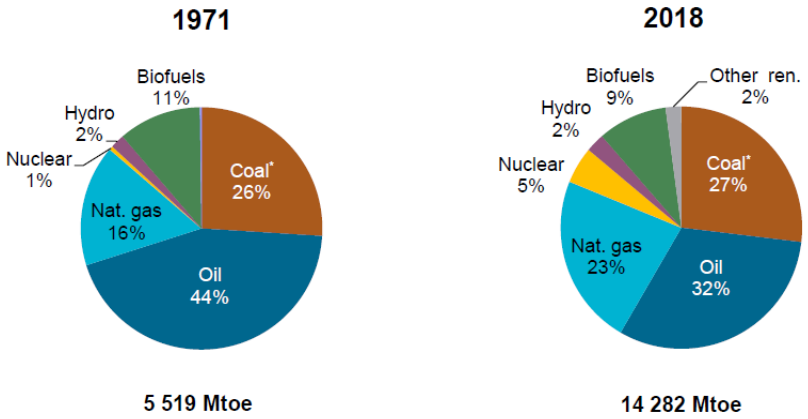

Figure 1. World energy supply by fuel. Source: IEA World Energy Balances [1]

Despite the great success of this Agreement signed by 191 nations, the world continues to highly depend on fossil fuels. According to the International Energy Agency, 81.2 % of the world's total energy supply came from fossil fuels in 2018 [1]. This share has not significantly

changed since 1971, when the fossil fuels accounted for 86.3 %. However, in these 47 years the total energy supply has been multiplied by 2.6, growing from 5,519 Mtoe to 14,282 Mtoe. This energy supply growth has not been homogeneous in all the world regions. While in 1971 the OECD countries consumed 61 % of the energy, in 2018 they only represented 38% of the world energy consumption. This is due to many factors. On the one hand, while the world population grew by 102 % (from 3,775 million people to 7,633 million people), this growth is only 43% in the OECD countries (from 905 million people to 1,302 million people). On the other hand, other factors like the emerging economies and the globalization, together with the delocalization of the production centers may explain the different evolution of the energy consumption in the world regions.

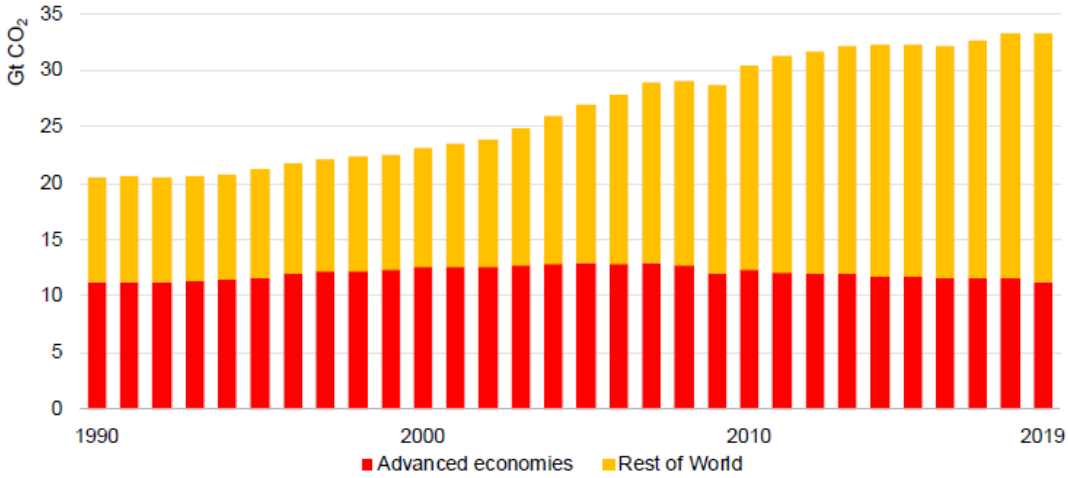

Figure 2. Energy-related CO2 emissions, 1990-2019. Source: IEA World Energy Balances [1]

The last decade has been characterized by an annual average energy demand growth rate of 1.1 %, and the energy-related CO_2 emissions have reached 33.2 Gt CO_2, 10 % higher than in 2010 and 62% with respect to 1990, the commonly used base historical year according to the Kyoto protocol. This scenario of growing energy demand has been seriously affected by the still on-going global COVID-19 pandemic. This severe illness has been widely spread, with more than 212 million cases and 4.44 million deaths confirmed. Some of the recommended prevention measures to fight the pandemic are the social distancing and the temporary lock down in many countries during 2020. As a consequence of this economic slowdown and the travel bans, the global GDP dropped by 3.5%, and the energy demand fell by 4 %, the largest decline since World War II and the largest ever absolute decline. However, energy demand is expected to rebound by 4.6% in 2021, 0.5 % above pre-Covid-19 levels.

The United Nations General Assembly identified in 2015 the Climate Action as the 13th of the Sustainable Development Goals for 2030. However, the climate continues warming: 2019 was the second warmest year on record and the end of the warmest decade (2010- 2019) ever recorded. In the meantime, if there is not a significant change in the energy policies, the CO_2 emissions are expected to keep growing, despite the temporary drop in 2020 due to the pandemic.

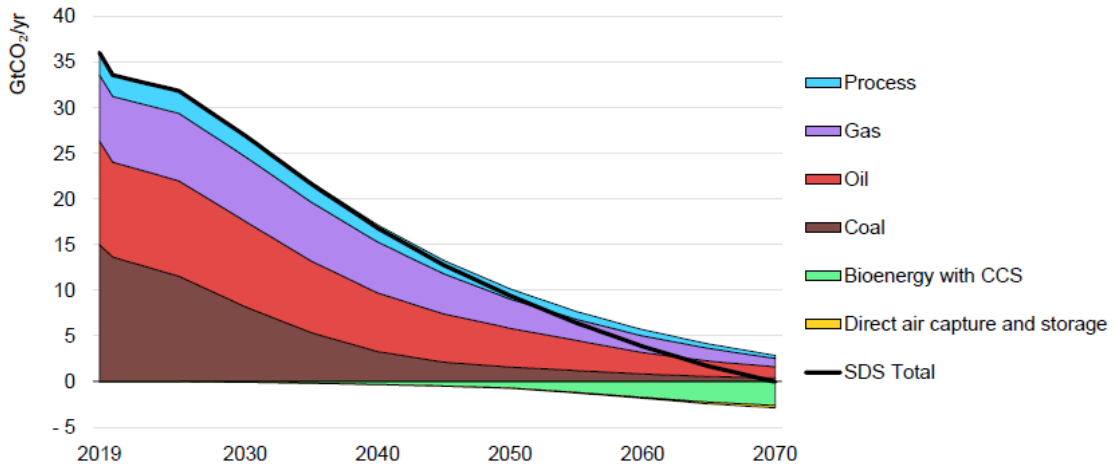

Figure 3. Global energy sector CO2 emissions by fuel and technology in the Sustainable Development Scenario, 2019-70. Notes: CCS = carbon capture and storage. SDS= Sustainable Development Scenario. Source: IEA Energy Technology Perspectives, 2020 [2]

The fight against climate change requires a wide range of measures and a complex technological transition strategy in different fields and energy end-uses. The current Ph. D. dissertation is focused and the new technological opportunities for space heating and cooling of the increased energy efficiency of buildings, integrated with on-site renewable energy production.

1.1.1. Buildings: heating and cooling

The final energy use in buildings grew from 2,818 Mtoe in 2010 to 3,057 Mtoe in 2019. This is the 30 % of the final energy consumed around the world, and it accounts for the 55 % of the overall electric consumption and the 28% of the global CO_2 emissions, what makes the decarbonization of this sector a key priority to reach climate neutrality goals.

Heating is the main end-use in building operation, being responsible for around 45 % of building emissions (4.3 Gt of CO_2 in 2019) and still relying on fossil fuels, that account for the 55 % of the final energy consumption. The heated floor area has grown 20 % in the past decade, but, fortunately, the more stringent building energy codes have reduced the thermal energy demand per square meter (i.e., 20 % in USA or 30 % in Europe, relative to 2000). In parallel to the better insulated and air sailed building envelopes, the fossil fuel-based assets need to be replaced by heat pumps, renewables and zero emissions district-heating. The sales of air-to-air heat pumps has been growing nearly 10% a year globally since 2010 with a current stock of 220 mill. units [3].

Air-conditioning is responsible for over 8 % of global electricity consumption, according to IIR estimations [3], and generates around 1 Gt CO_2, 10.5% of building emissions [4]. This is low compared with the heating end-use, but it is a fast-growing sector and it is expected to remain so over the coming decades. The stock of residential air-conditioning units is about 1.1 billion and 0.5 billion in commercial spaces. Household ownership of air-conditioners varies

enormously across countries, from 90 % in the United States, to 60 % in China and 10% in Europe. The number of air-conditioning units not only depends on the climate, but also on the income rate. India is a clear example of this, where ownership levels in high-income urban households range from 75 %-85 %, while low-income rural households does not reach the 5 %.

The world's emerging economies will continue increasing the stock of air-conditioners, as 2.8 billion people living in the hottest parts of the world only possess 8% of the current air-conditioners [3]. Furthermore, the increase of ambient temperatures and the demand of more comfortable indoor spaces will continue growing.

According to IEA, considering the likely effect of current policies and targets, global energy needs for space cooling will triple by 2030 [5]. As Figure 4 shows, from the 14.52 TW of thermal output (0.43 TW for only heating, 9.22 TW for heating-cooling and 4.87 TW for only-cooling) of heat pumps that will be deployed in the coming years, 1.5 TW will correspond to non-vapor-compression technologies.

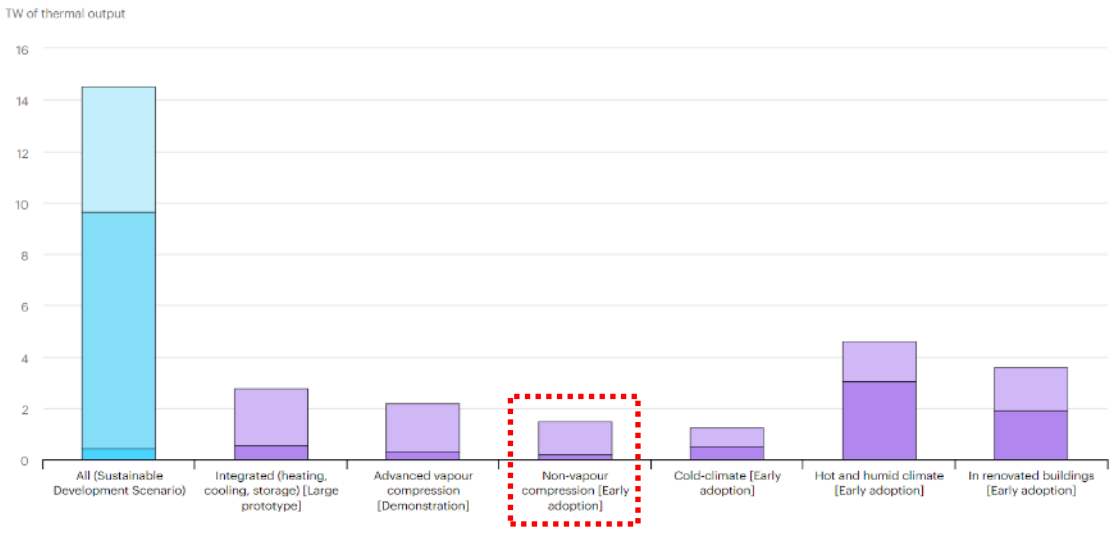

Figure 4. Heat pumping technology deployment by market segment in the Sustainable Development Scenario in 2030 and portion not deployed if innovation is delayed. Source: IEA, [5]

An estimated 33 % of households worldwide have both space heating and cooling needs. This rate is significantly higher in North America (56 %), Europe (78 %) and China (80 %). In these regions it is particularly important the promotion of reversible heat pumps to comply with the decarbonization objectives. Moreover, the provision of new services as cooling in increasingly warmer climates, could stimulate the market in favor of heat pumps in new buildings and renovations. Exploiting the synergies across heating and cooling may help to accelerate the deployment of reversible heat pumps in order to meet the buildings decarbonization objectives by phasing out fossil fuel equipment.

Nowadays the electric vapor-compression (VC) cycle is deployed in most heat pumps available in the market. This technology provides the majority of space cooling, and a substantial amount of space heating, due to its maturity, reliability, and the high efficiency. Its operation is based on a closed loop of a working fluid (refrigerant) that is compressed, condensed,

expanded, and evaporated, pumping heat from a cold reservoir (evaporator) to a hotter one (condenser). Historically, the first refrigerants deployed with this technology where chlorofluorocarbons (CFC) that were later abandoned, due to their contribution to the atmospheric ozone depletion. The CFCs were substituted by the hydrochlorofluorocarbons (HCFCs) first, and by the hydrofluorocarbons (HFCs) nowadays, aiming at reducing their impact in the climate change. Refrigerants can be toxic; they can be flammable (even explosive) or they can act as greenhouse gases with a certain global warming potential (GWP) if they are released to the atmosphere (due to leakages or by the end of the lifecycle of the unit). According to the GIZ [6][7], over 71 % of GHG emissions from refrigeration systems are due to indirect emissions from electricity generation for the unit operation, while 29 % is due to the refrigerants. This share is reduced to 10 % in the case of small refrigeration units as domestic air-conditioners.

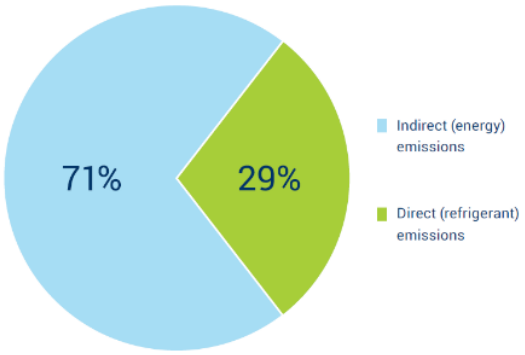

Figure 5. Global split of GHG emissions from refrigeration systems. UNEP: [8]

The use of HFCs in Europe is regulated under (EU 517/2014). The implemented phase-down will reduce the availability of F-gases continuously until 2030, what makes the search for alternatives a key challenge to the heat pump industry. Available solutions are new mixes with a lower GWP, but these substances are usually at least mildly flammable (used in small residential units). Other options are natural refrigerants like propane and butane (highly flammable), ammonia (toxic) or carbon dioxide (high operating pressure) used in industrial facilities. In any case, the progress on better sealed units as well as the skills of installers to dismantle and to recover refrigerants are important to reduce the impact of this technology and its potential risks.

The development of non-vapor compression technologies may help to comply with the decarbonization objectives, as stated by the Sustainable Development Scenario in 2030 (see Figure 4), by acting in two directions: on the one hand, increasing the heating/cooling capacity of heat pumps released to the market in applications where new alternatives may contribute with an added value; and, on the other hand, by accelerating the phase out of high global warming potential of refrigerants. The current Ph. D. dissertation aims at contributing to these objectives with the development of thermoelectric heat pumps, as an alternative to VC, in low energy demand buildings.

1.1.2. European context and buildings energy policies

The European Commission aims to become the world's first climate-neutral continent by 2050 [9]. Besides the reduction of the greenhouse gas emissions (80-95 % compared to 1990 levels), the European Commission is also taking action to adapt to the impacts of the climate change, aiming to become a climate-resilient society. One of the main challenges to meet this ambition is the decarbonization of the heating and cooling sector, as previously stated at global level, which accounts for approximately 52 % of the final energy demand (6,352 TWh) in the case of Europe. Moreover, this sector is reliant on fossil fuels. Fossil gas is the dominant energy carrier (42 %), followed by oil, biomass and electricity (all 12 %). 53 % of this primary energy is used for space heating and only 1 % for space cooling. To move to a sustainable heating and cooling sector it is essential to both invest in energy efficiency to lower overall demand and replace fossil fuels with more sustainable energy sources.

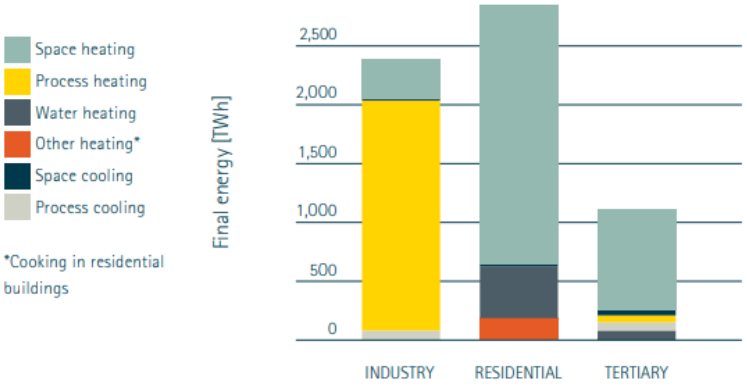

Figure 6. EU28 Final Energy demand for heating and cooling split depending on energy use and Application Area. Source:White paper - EPHA [10]

Aware that buildings are responsible for approximately 40 % of EU energy consumption and 36 % of the CO2 emission [11], this sector is one of the focus areas of the European Green Deal [9], an action plan with a set of new policies seeking to boost the efficient use of resources. The Renovation Wave [12] is one of the key initiatives of this plan, aiming at doubling the current rate of the refurbishment of buildings. Currently, roughly 75 % of the building stock is energy efficient, yet almost 85–95 % of today's buildings will still be in use in 2050. On the other hand, new buildings are assumed to comply with the nearly zero energy standard (nZEB) since 2020 (as promoted by the Energy Performance of Buildings Directive 2010/31/EU (EPBD [11]), further refunded [13]). This standard responds to different specific requirements depending on the member state and its building code, according to the different climates; but all these regulations limit the energy demand by establishing very strict minimum insulation levels of the building envelope. Both the limitation of the energy demand of new constructions and the renovation of existing buildings allow us to infer that the specific heating demand of buildings will be significantly reduced in the future.

Figure 7. Buildings new role in the 2050 climate-neutral Europe. Source: BPIE

In addition to this reduction of heating power demand given by the new regulation, the European Environmental Agency (EEA) reports significant changes in the heating and cooling loads in buildings due to climate change. Heating degree days (HDD) decreased by 6 % between the periods 1950–1980 and 1981–2017, whereas cooling degree days (CDD) increased by 33 %. According to EEA, the trend of reduction of HDD and the increase of CDDs will continue [14].

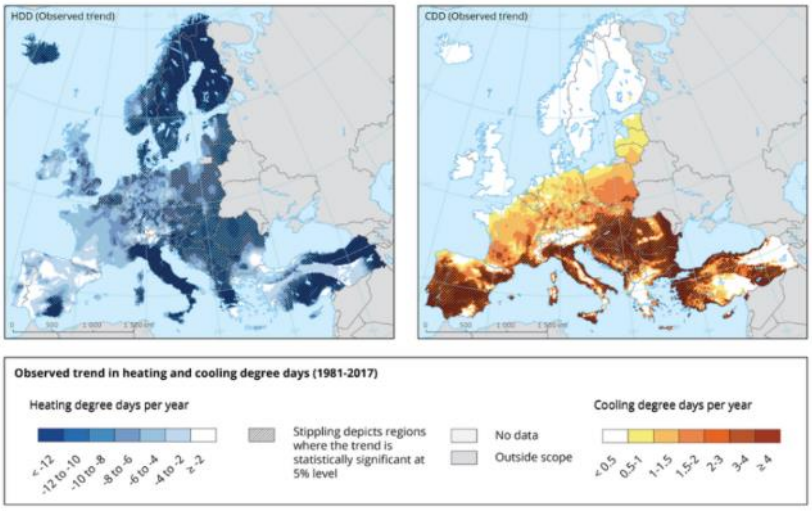

Figure 8. Degrees-days trend for heating and cooling in Europe between 1981 and 2017. Source: European Environmental Agency [14]

New better insulated buildings will, hence, require less heating but more cooling. Moreover, the need to decarbonize the heat production leads to the electrification of heat, which is expected to strongly promote the use of heat pumps in the building sector [10], in combination with other RES (biomass, solar, geothermal…)[10] and waste heat recovery systems [15].

1.1.3. Nearly Zero Energy Buildings (nZEB) and Passive Houses

The renovation of thermal envelopes and the application of nZEB standard to new buildings will then significantly change the way these buildings need to be air-conditioned. In order to identify the characteristics of these new HVAC systems, it is necessary to have a look at the basis of this new energy standard. The nZEB has been officially defined as: a "building that has a very high energy performance… the nearly zero or very low amount of energy required should be covered to a very significant extent by energy from renewable sources, including energy from renewable sources produced on-site or nearby" [11]. This definition prioritizes the energy efficiency, taking into consideration local conditions, indoor climate, the renewable energy production and, also, the cost-effectiveness. This is an important factor that is in the core of the nZEB definition. Actually, the Article 2 of the EPBD says that "(nZEB) requirements for the energy performance of buildings and building elements… should be set with a view to achieving the cost-optimal balance between the investments involved and the energy costs saved throughout the lifecycle of the building" . High performance buildings result in higher investment costs, that have been a great barrier for the adoption and deployment of this standard. In order to overcome this barrier, it has been established an optimal-cost methodology to assess the minimum performance requirements for nZEBs. This methodology is based on the establishment of an objective comparison of different packages of measures available in the market (building envelope and installed appliances) to improve the energy efficiency of buildings through their global cost (acquisition costs, maintenance, operation…) throughout the useful life of the building (30 years for the residential sector and public buildings, 20 years for the private tertiary sector) and its primary energy consumption. As shown in Figure 9, some of these packages present an optimum profitability where the investment cost is rewarded with energy savings during the useful life of the building. The area defined as nZEB, is located on the left of the graph, with primary energy consumption lower than optimal profitability and defined by solutions that can be found in the market. The nZEB is expected to trigger these solutions in the market reducing the costs and bringing them to the profitability area in a near future.

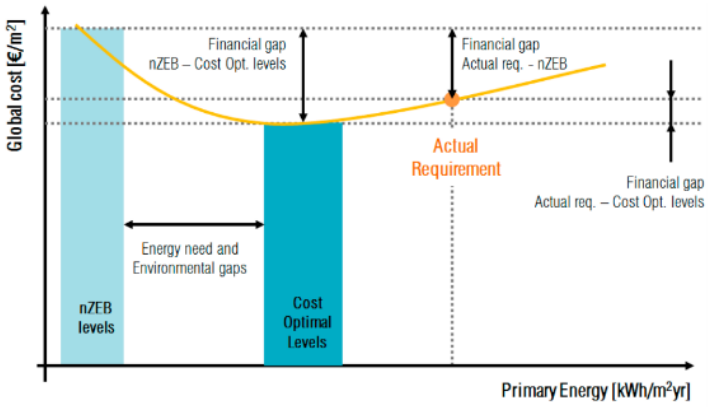

Figure 9. Energy, envirnomental and financial gaps in cost-optimal calculation to define nZEBs. Source:Ferrara M. et al. [16]

The “Passive House (PH)“ is a widely tested and clearly defined energy standard born in the nainties that perfectly fits with the definition of the nZEB and it has been a guide for the nZEB definition and implementation in many ways. On the one hand, it is a highly energy-efficient standard, what entails a nearly-zero energy demand. On the other hand, the energy efficiency level is cost-optimal from a life cycle perspective. And, finally, the on-site production of renewable energies can make a significant contribution to improve the overall performance of the building and its certificate (going from *classic*, to *premium* or *plus* categories).

Figure 10. First passive house in Darmstadt, the result of Dr. Feist's research project. Source: own

This energy standard is the result of a research project carried out in 1991, and a further success story of technological innovation [17], with more than 5,042 buildings certified all around the world [18]. One PH certified building follows the next five principles:

1) Super-insulated envelope in order to minimize the heat loss, resulting in a significantly increase of the thermal performance. Insulating has the added advantages of greater soundproofing and improved durability.

2) Airtight construction. Heat can also be lost through the envelope with the air leakage, what can also lead to discomfort due to indoor uncontrolled air movements, and localized moisture and condensation problems. A building ‘s air barrier (material layer, membrane or tape) must seal the envelope and the result must be experimentally tested with a *blower door test*.

3) High-performance glazing. Glazing systems cannot be insulated to the same level as a wall, resulting in the windows being the weakest components of the envelope in terms of heat losses. For this reason, it is crucial to improve the performance of these glazing systems by using a combination of different techniques: insulated framing, triple-glazed units when possible, argon or krypton gas fill, specific coatings…

4) Thermal-bridge-free detailing. The thermal bridges are parts of the building where different architectural features meet and they require special analysis during planning phase to avoid the heat loss in those specific areas and pay special attention during the construction.

5) Heat recovery ventilation. Due to the airtightness of these constructions, it is important to guaranty a minimum ventilation to bring in fresh air and exhaust out built-up pollutants, odours, CO_2, and moisture. This implies a heat loss that can be effectively mitigated with the installation of a double flux ventilation system integrating a heat recovery unit that may pre-heat the incoming air by cooling the expelled air flow.

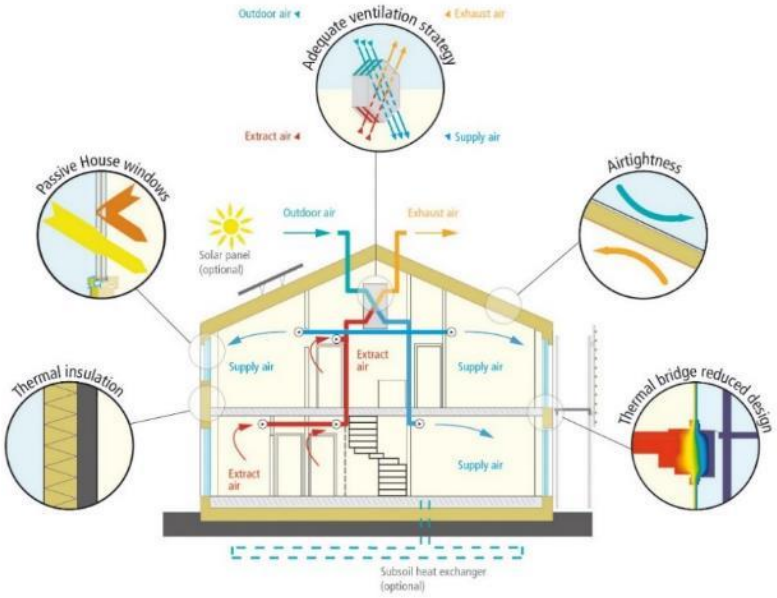

Figure 11. Five basic principles for the construction of Passive Houses. Source: PHI [19]

Following these design criteria, the building is expected to considerably reduce the heating and cooling demands, being mandatory to fulfill the following certification requirements:

- The Space Heating Energy Demand is not to exceed 15 kWh per square meter of net living space (treated floor area) per year or 10 W per square meter peak demand. In climates where active cooling is needed, the Space Cooling Energy Demand requirement roughly matches the heat demand requirements above, with an additional allowance for dehumidification.
- The Renewable Primary Energy Demand, the total energy to be used for all domestic applications (heating, hot water and domestic electricity) must not exceed 60 kWh per square meter of treated floor area per year for PH Classic. .
- In terms of Airtightness, a maximum of 0.6 air changes per hour at 50 Pascals pressure (ACH50), as verified with an onsite pressure test (in both pressurized and depressurized states).
- Thermal comfort must be met for all living areas during winter as well as in summer, with not more than 10 % of the hours in a given year over 25 °C.

1.1.4. HVAC in Passive Houses

These conditions are not arbitrary. They respond to an integrated concept behind, that constitutes the true definition of the PH:

"A Passive House is a building, for which thermal comfort (ISO 7730) can be achieved solely by post-heating or post-cooling of the fresh air mass, which is required to achieve sufficient indoor air quality conditions – without the need for additional recirculation of air"

This is, then, a functional definition with no numerical values and is essentially valid for all climates. When comfort is easily achieved by post-heating or post-cooling the air ventilation flow, then the conventional HVAC systems are rendered unnecessary, and this leads to one of the main features of this idea: the cost-efficiency. While the investment on the building is increased when the thermal envelope and the energy facilities are improved, there is a point where the peak energy demand is so low that there is no need for a conventional heat or cool distribution system (fancoils, water radiators…). The ventilation air stream can provide the air conditioning demand, and this extraordinarily simplifies the HVAC system, reducing the investment cost. This point is reached when the specific heating and cooling demands are below 10 W/m^2, as underlined by the PH standard.

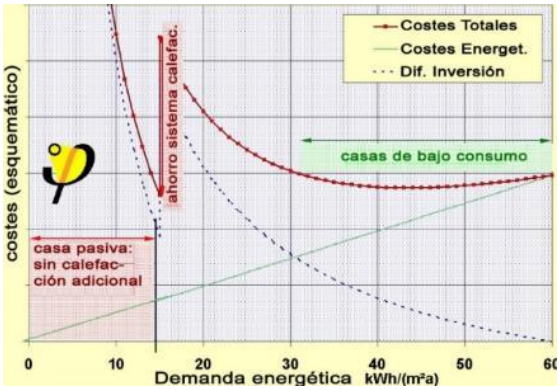

Figure 12. Cost-optimal calculation of Passive Houses. Source: PHI [19]

The double flux ventilation systems provide a continue fresh air supply that may improve the indoor wealth; specially in airtight buildings, as PH, and in long stays, as in the case for some elderly people or the lockdown experimented by many countries due to the COVID-19 pandemic [20]. Beyond the thermal comfort, a heathy indoor air quality requires a sufficient air renovation rate in order to remove indoor air pollutants and keep the concentration of CO_2 bellow 1000 ppm [21]. The ventilation is needed to maintain minimum conditions of healthiness, but it increases the energy demand, as indoor conditioned air is replaced by clean outdoor unconditioned air. A typical ventilation air flow for residential use ranges from 0.35 to 0.5 ACH [22]. Lower air ventilation rates may be insufficient to keep a healthy IAQ and reach the heating/cooling capacity, while higher ventilation rates increase the energy demand and dries the indoor air, especially in cold climates [23].

Under these conditions, the building exhaust air may be used as either a heat source or heat sink depending on the climate conditions and building needs. This is actually the working

principle of some commercial VC heat pumps integrated in the ventilation system of houses with low energy demand. Two different strategies are available in the market:

- **Active thermodynamic recovery:**

  One first option is the direct integration of the evaporator and condenser in the incoming and outgoing air ducts, with a reversible heat pump that can switch from heating to cooling mode. The ELFO Fresh^2 of CLIVET [24] is an example of this strategy (see Figure 13).

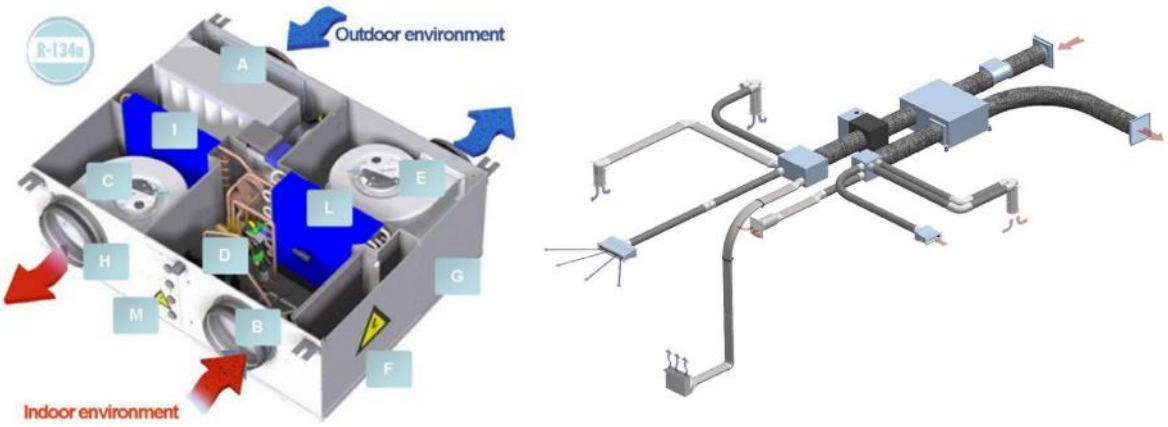

Figure 13. ELFO Fresh ^{2} model of CLIVET with thermodynamic heat recovery system of exhaust air. Source: CLIVET [24]

- **Combined unit of a heat recovery unit and a heat pump**

  Mechanical double flux ventilation systems normally include a Heat Recovery System (HRU) to passively harvest the thermal level of the outgoing air stream [25]. A typical HRU consists of a core unit, channels for fresh air and exhaust air, and blower fans. The heat is transferred from one air stream to another, with no moisture transfer and no air mixture between the air streams [26].

  This integration alternative proposes the combination of the HRU with the heat pump in the same compact unit. The incoming and outgoing air streams cross first the HRU, and then the exhaust air is used as heat reservoir to raise or lower the temperature of the fresh air, as shown in the scheme of Figure 14, in the commercial model PKOM^4 of Pichler-ORKLI [27].

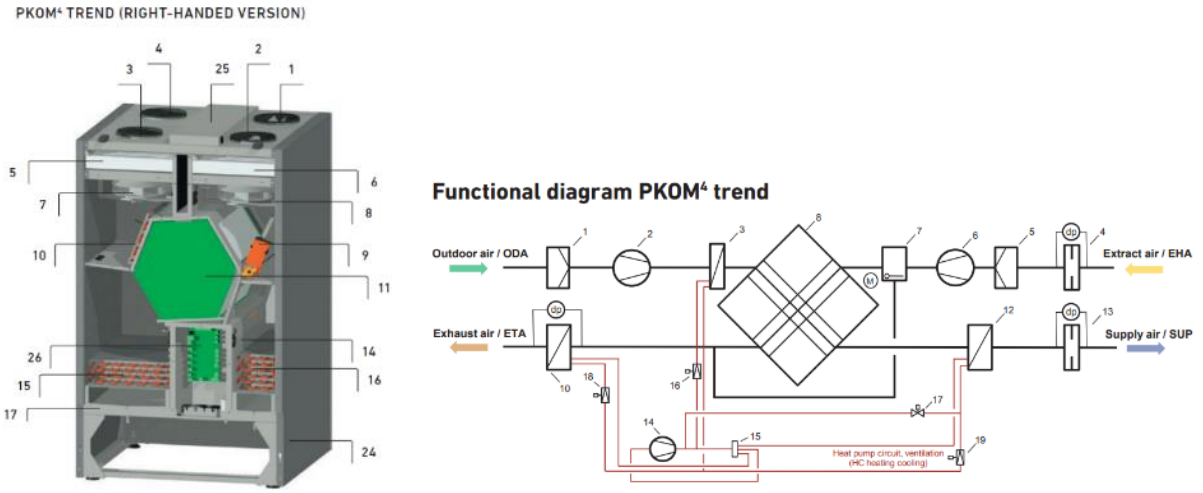

Figure 14. Compact unit PKOM [4] of Pichler combining a HRU with a heat pump. Source: Pichler-ORKLI [27]

The extreme low heating/cooling demand of PH opens the door to various potential innovations: on the one hand, there is room for alternatives to the VC cycle, preferable with small size devices that may allow a more compact design integrated with the ventilation system; on the other hand, the importance of the coefficient of performance of the heat pump is reduced, especially if costs are reduced and additional renewable energy can be produced on-site.

The current Ph. D. dissertation will investigate the potential development of thermoelectric heat pumps, as an alternative to VC, exploring the above explained two alternatives of integration with the double flux ventilation system in a PH.

1.2. State of the Art

The use of thermoelectric modules to build a thermoelectric heat pump may present many advantages, compared with the vapor-compression cycle: there are no moving parts, noise free, gas free, no chemical reaction, reliability, scalability and minimum maintenance [28]. Thus, thermoelectric modules present zero GWP (Global Warming Potential), zero ODP (Ozone Depletion Potential) and easy transition from heating to cooling mode [29]. Additionally, the thermoelectric modules require DC power supply and permit an accurate temperature control by regulating the voltage. Finally, DC supply assures an easy integration with PV panels.

This section explains the working principles of thermoelectricity and presents a state of the art of the use of thermoelectric devices as coolers and/or heaters in buildings, reviewing previous scientific literature.

1.2.1. Working principles

Thermoelectricity is the branch of thermodynamics that deals with the study of phenomena in which heat and electricity take part at the same time, and it is based in a series of interactions that were discovered in the 19th century: Joule, Seebeck, Peltier, Thomson, Hall, Nernst, Ettingshausen and Righi-Leduc. However, only the first four cause a significant macroscopic effect [30].

The Joule effect expresses the relationship between the heat generated in a conductive material and the electric current flow. Matter offers some resistance to the movement of electrons, which release kinetic energy in the collisions. This energy is dissipated as heat and it is proportional to the internal resistance of the material R_0 and the square of the intensity of the current I, as indicated in Equation 1.1.

$$\dot{Q}_{Joule} = R_0 \, I^2 \tag{1.1}$$

Seebeck effect denotes that, given a circuit formed by two different materials, “A” and “B”, connected by their ends, if these unions are maintained at a different temperature, an electromotive force (E_t) appears. This electromotive force depends on the Seebeck coefficient (α) of each of the materials as well as on the temperature difference between the unions, as depicted in Equation 1.2.

$$\frac{dE_t}{dT} = \alpha_A - \alpha_B \tag{1.2}$$

In contrast to the Seebeck effect, Peltier effect consists in the cooling or heating of the union between two materials when an electric current is flowing. This cooling or heating depends on the Seebeck coefficient of each material, the current intensity, and the temperature of the union, according to Equation 1.3.

$$\dot{Q}_{Peltier} = \pm I \, T \, (\alpha_A - \alpha_B) \tag{1.3}$$

Lastly, Thomson effect deals with the absorption or generation of heat in a material presenting a temperature gradient and in which there is an electric current flowing. Its value is indicated in Equation 1.4, where σ it the Thomson coefficient.

$$\dot{Q}_{Thomson} = -\sigma \vec{I}\,(\Delta \vec{T}) \tag{1.4}$$

This Thomson coefficient is related with Seebeck effect by means of the Kelvin relation shown in Equation 1.5.

$$\sigma = T\,\frac{\partial \alpha}{\partial T} \tag{1.5}$$

Based on the previous interactions, thermoelectric devices are capable of directly transforming heat into electricity, which is known as *thermoelectric generation*. Additionally, these devices are also capable of creating a temperature difference between both sides of the device by pumping heat from one side to the other, when an electric potential is applied. This functionality, called *thermoelectric cooling*, is the focus of the application that is investigated in the present Ph. D. dissertation.

The transformation itself occurs in the thermoelectric modules. A conventional thermoelectric module is composed of a number of N-type and P-type semiconductor junctions connected electrically in series by metallic interconnects (conducting strips made normally in copper) and thermally in parallel, forming a single-stage cooler, as shown in Figure 15. Two rigid substrates of ceramic material provide mechanical firmness to the whole system and isolate the internal circuit.

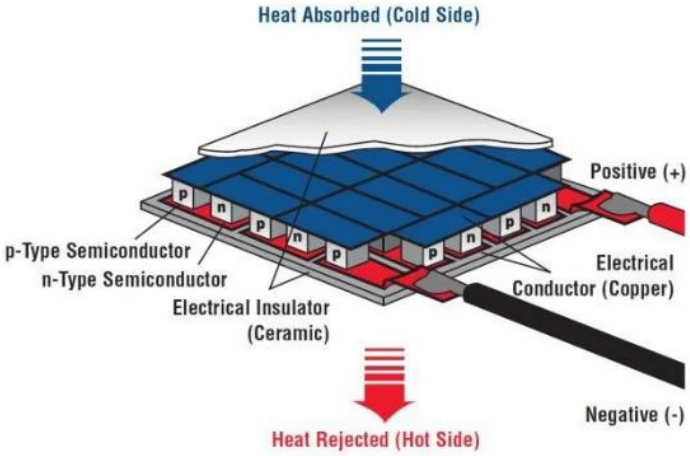

Figure 15. Thermoelectric module and thermocouple. Source: Internatinal Thermoelectric Society (ITS)

The electrical current flows from the N-type elements to the P-type elements in the cold junctions (at the top of the device). The temperature of these cold junctions decreases, and the heat is transferred from the environment to the top ceramic plate, at a lower temperature. This process happens when the electrons go from a low-energy level inside the P-type element to a high-energy level inside the N-type element trough the cold junctions. Simultaneously, the

electrons carry the absorbed heat (Q_c) to the hot junctions (at the bottom), increasing their temperature. This heat (Q_h) is dissipated by the heat sink through the bottom ceramic plate, what makes the electrons return at a lower energy level in the P-type semiconductor. Neglecting the effect of the union between semiconductors, the cooling coefficient of performance of a thermocouple, defined as the ratio between the absorbed heat flux ($\dot{Q}_c$) and the electric power consumed ($\dot{W}_{el}$), can be approximated by the following relation for an optimal electric current applied to the thermocouple ($\partial COP/\partial I = 0$):

$$COP_{Max} = \frac{\dot{Q}_c}{\dot{W}_{el}} = \frac{T_c}{T_h - T_c} \frac{\sqrt{1 + ZT_m} - \frac{T_h}{T_c}}{\sqrt{1 + ZT_m} + 1} \tag{1.6}$$

where T_m is the average temperature of the hot (T_h) and the cold (T_c) sides and Z is the figure of merit defined by next equation:

$$Z = \frac{\alpha^2}{\rho\, \lambda} \tag{1.7}$$

This figure of merit (1/K) depends on three material properties: electrical resistivity (ρ in Ωm), thermal conductivity (λ in W/mK) and the Seebeck coefficient (α in V/K). The maximum coefficient of performance is the product of the Carnot efficiency and a factor that depends on a dimensionless parameter (ZT_m) that represents the efficiency of the N-type and P-type materials that compose the thermocouple. A thermoelectric material having a higher figure of merit ZT_m is more convenient as it can carry out higher cooling power generating a higher temperature drop. This means that the coefficient of performance of the thermocouple and, by extension, of the thermoelectric module, is directly related to the capability of the material as energy converter. The ideal thermoelectric material should present a high Seebeck coefficient, thus generating a higher temperature gap for a given voltage; low electrical resistivity, in order to minimize Joule effect; and low thermal conductivity, minimizing the thermal losses through the thermoelectric module. However, this is not an easy task as the three parameters that define the figure of merit are closely related one to another, being strongly coupled through the carrier concentration [31].

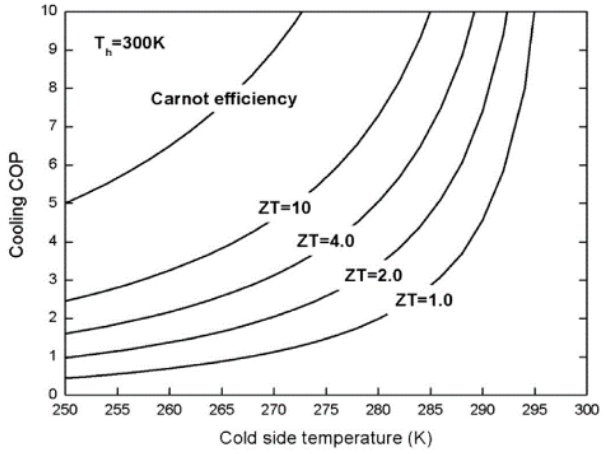

Figure 16. Cooling COP of a thermoelectric module under optimum electric current with fixed hot side temperature of 300 K. Source:Zhao D. et al. [28]

Although new research is increasingly improving the efficiency of thermoelectric modules reaching ZT_m values above 2, currently available thermoelectric materials present a ZT_m of around 1 [32], therefore, as Figure 16 shows, for cooling applications where the temperature gap between the hot and the cold sides of the thermoelectric modules goes from 30 to 50 °C, the coefficient of performance is between 0.5 and 1. This COP is low compared with VC technology, what has limited the use of these modules in commercial devices, but, as shown in next section, the cited advantages make this technology a reliable competitor of VC cycle in some specific applications.

1.2.2. Thermoelectric cooling applications in the market

The use of thermoelectricity as a heat pump has been limited so far to scientific investigations and niche applications [28], where the efficiency is not so important as the reliability and the quiet operation. However, as technology is progressing, an increased number of market opportunities have been found. This section presents six applications where the thermoelectricity has reached the market:

- **Electronic cooling applications:** electronic devices generate a huge amount of heat during operation, especially micro-processors in PCs and other systems. The past few decades have seen a dramatic increase in computing performance of microprocessors, what have entailed an increase in the power and the on-chip power density. This is commonly solved by using heat spreaders and aluminum finned heat sinks or heat pipes to dissipate the heat to the surrounding air. When the heat-flow density is high, thermoelectric coolers can enhance the cooling capacity and control, by attaching the cold plate of the TEM to the processor. This reduces the operating temperature of the processor and extends its life cycle. However, the electric consumption of the TEM is added to the electric consumption of the electronic device and there is more heat to be dissipated. This option is restricted to customized products and it is not generally offered already assembled in the market. However, there are other specific applications where the precise control of the TEMs, its compactness and the high heat-flux capacity are crucial, as in the case of the refrigeration of laser diodes and other laboratory instruments.

- **Small refrigerators:** the construction of small refrigerators cooled with TEMs present various advantages compared with their vapor-compression counterparts that outweigh the worse energy performance. One clear example of this is the minibar in hotel-rooms. In this case its silent operation may be a priority if the cooling capacity required is low. Another clear example is the portable refrigerator, where the compactness and the lightweight of the TEMs make these devices easily manageable, especially in cars, where these devices can keep drink and food cold or warm fed with the 12V DC supply of the car-battery. Additionally, these devices can incorporate their own battery for their outdoor use or be powered by solar PV panels.

- **Wine cooling:** one extrapolation of the domestic small refrigerators is the fabrication of wine cabinets. As a general rule, wine must be kept 10-15 °C for long-term storage. This, compared with the 3-5 °C in a regular fridge, is a lower temperature gap between indoor and outdoor, what significantly improves the efficiency of the TEMs, keeping a silent environment and precise temperature control.

- **Automobile cooling:** most of automobile air-conditioning systems use nowadays compression cycle equipments with R-134a as refrigerant. The leakage problem of the refrigerant in automobiles is more substantial than that in the stationary air-conditioners. Despite scientific literature presents some examples of thermoelectric air-conditioners applied to car and truck cabinets, the commercial application of the thermoelectricity was found by a car-seat temperature control made with TEMs. Gentherm (former Amarigon) company developed a Climate Control Seat (CCS) system providing active heating and cooling at seat level and individually controlled. This system was first adopted by the Ford Motor Company and introduced as an option on the model year 2000 Lincoln Navigator in 1999. Today it is available on more than 50 vehicles sold by Ford, General Motors, Toyota (Lexus), Kia, Hyundai, Nissan (Infinity), Range Rover and Jaguar Land Rover. The accommodation of the seat temperature provides more comfort to the occupant and it is expected to reduce the need for air-conditioning.

- **Medical equipment:** in addition to the previously presented advantages, the precise control of TEMs and therefore, the precise control of the temperature in a small environment, is a feature of great interest for some medical applications. In the case of medical storage chambers, the vertical stacking in benches may complicate the flow of the cold air to the top of the storage. The thermoelectric cooling systems can better distribute the cold air in the fridge and their shape accommodate the tight geometric space constrains. In the case of portable solutions, as an insulin pocket box (see Table 1), thermoelectricity is also a good solution, besides other specific applications as CO_2 incubators (where temperature stability is vital), vaccine conservation or to perform therapeutic treatments where the thermoelectric heating or cooling can be directly applied to the skin with a wristband (see https://embrlabs.com/).

- **Clothes:** in same direction as the Climate Control Seat for cars and the therapeutic treatments that control the skin temperature, there many brands that nowadays offer thermoelectric cooling vests for workers in hot environments. Even NIKE patented a technology for a new category of workout clothing for athletes based on a TEM, able to cool or warm the body to keep a core temperature. The Thin Ice 2.0 (see Table 1) developed by FUNDRAZ is an extreme example of this. It is a weight loss clothing line based on cooling the body.

Table 1. Thermoelectric cooling commercial devices.

Electronic devices cooling	Small fridge	Wine cabinets
		
Brand: TE Technology **Model:** Cold plate cooler: CP-065 (thermal stabilization of electronic components and laser diodes) **Web:** https://tetech.com/product/cp-065/	**Brand:** Brass Monkey **Model:** PORTABLE 30L COOLER / WARMER **Web:** https://brassmonkey.cool/gh1369_brass_monkey_portable_30l_cooler_warmer	**Brand:** Bartscher **Model:** Win cooler 4FL-100 **Web:** www.bartscher.com/en/New-products/Wine-cooler-4FL-100/p/700134
Car cooling	**Medical equipment**	**Cooling clothes**
		
Brand: Gentherm (AMERIGON) **Model:** CLIMATE CONTROL SEAT ® **Web:** https://gentherm.com/en/electronics/solutions/automotive	**Brand:** LABFREEZ Instruments **Model:** Pockey insulin cooler – MPR17 **Web:** https://www.labfreez.com/pocket-insulin-cooler?search=insulin	**Brand:** Fundrazr **Model:** Thin Ice 2.0 **Web:** https://fundrazr.com/thinice2.0?ref=ab_8UYHVOUvWWo8UYHVOUvWWo

1.2.3. Research lines to improve the efficiency of thermoelectric coolers

A thermoelectric heat pump (TeHP) may be described as a device that absorb heat from a cold reservoir ($\dot{Q}_c$) and emit heat to a hot one ($\dot{Q}_h$) by inserting and feeding a group of TEMs between the heat reservoirs. The heat absorbed and emitted need to be transferred through adapted heat exchangers in both sides of the TEMs, as represented in the basic layout shown in Figure 17:

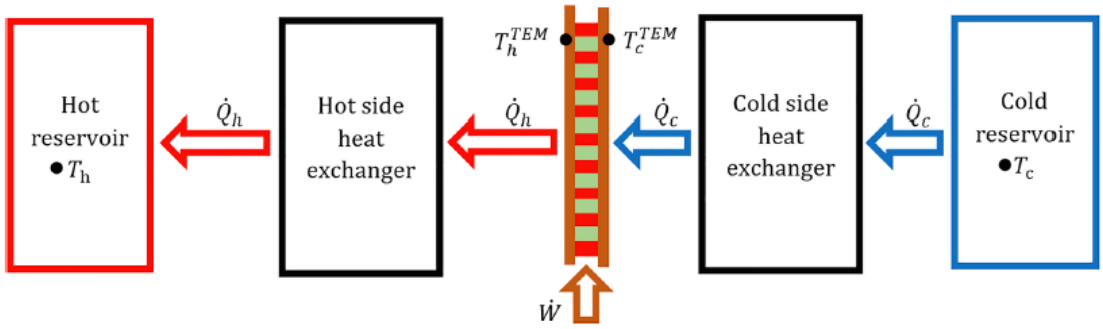

Figure 17. Basic Assembly of a TeHP. Source:Martinez A. et al. [33].

Many investigations have focused on the search for new applications where the competitive advantages of thermoelectricity represent a value in the market (as in the case of the six applications explained in previous section), seeking, as far as possible, to improve the energy efficiency of the TeHPs mainly through three research lines:

- The first research line is focused on the composition and design of the TEMs, as the essential element of a thermoelectric heat pump. The inorganic materials, such as telluride-based materials (i.e. Bi_2Te_3 and PbTe), silicon-germanium alloys (SiGe), half-Heusler alloys, skutteridites, and clathrates are the commonly most used materials in thermoelectric research, as shown in Figure 18. The highest ZT value reported was close to [34] and corresponds to bi-doped PbSeTe/PbTe (QDSL).

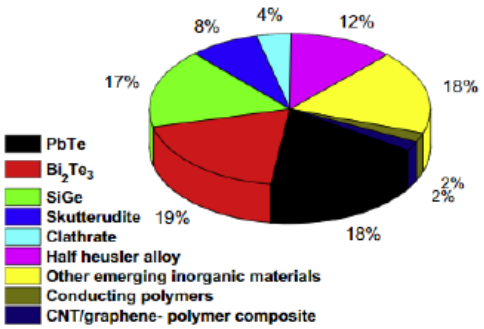

Figure 18. Contribution of various materials used in thermoelectric reserch. Source: Gayner C. et al. [35].

In the last years there has been an increase in the development of organic materials, due mainly to their cost-effectiveness, easy processing, low thermal conductivity and high flexibility [36]. However, these materials still need a lot of improvement to reach the market. Besides the thermoelectric material, a lot of research works optimize the design of the module: the number of thermocouples, their length, aspect ratio, distribution, and junctions.

- The second approach relates to the thermal design of the TeHP and its optimization. One of the factors determining the efficiency of TEMs, as either refrigerator or heater, is the temperature difference between the hot and cold sides of the thermoelectric

modules (TEMs). This line is mainly associated with the selection of the heat and cold reservoirs and the type and design of heat exchangers (HE) between the hot and cold sides of the TEMs and the heat reservoirs.

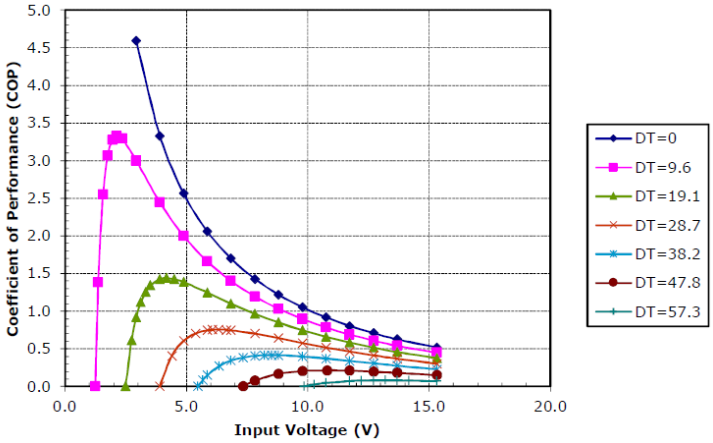

Figure 19. COP of a TEM Module (HP-127-1.4-1.15-71) depending on the suuplied voltage and temperature gap between the hot and cold sides of the TEM (DT (°C)). The hot-side temperature is fixed to 30 °C. Source: TE Technology [37]

The technical specifications of TEMs (see Figure 19 for HP-127-1.4-1.15-71) show how the COP varies depending on the temperature gap between the hot and cold faces, and the input voltage. This temperature gap is determined by the thermal equilibrium between the heat reservoirs and the TEM, which is highly affected by the thermal resistance of the HE between the TEM faces and the heat reservoirs (Astrain et al. 2016). For an air-to-air application Figure 20 shows the cold and hot sides temperature of a TEM, depending on the amperage of the DC current, and the thermal resistance of the HE. Increasing this thermal resistance from 0.2 K/W to 0.4 K/W may easily double this temperature gap, what reduces 2-3 times the maximum achievable COP.

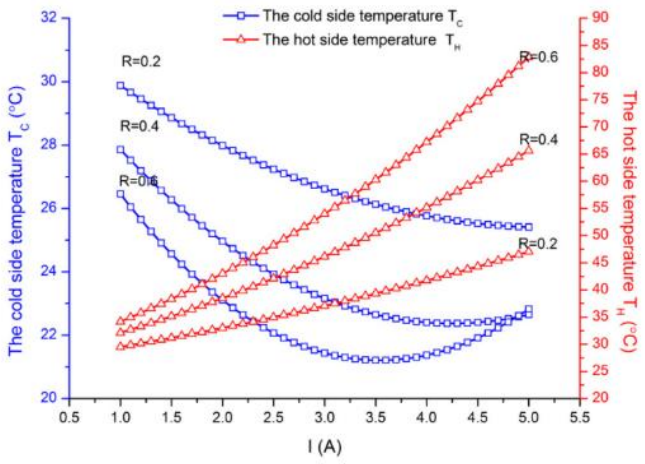

Figure 20. The cold and hot side temperature of the TEM as a function of different oper- ating currents and heat exchanger thermal resistances. Source: Han T et al. [38].

The most common HE used in the scientific literature are aluminum heat sinks and finned heat pipes (HPp). Aluminum heat sinks present a thermal resistance that depends on the convective coefficient between the heat reservoir and the fins. However, in the case of the HPp, the thermal resistance depends not only on the air flow, but also on the heat flux that crosses the heat pipe. Internally, one HPp contains a fluid in a continuing cycle of evaporation and condensation, presenting a more effective heat transfer than in a metallic conductor. A higher heat flux increments the phase change rate, what reduces the thermal resistance. The optimization of the thermal behavior of a thermoelectric device is complex and depends on the concrete application under study. As a reference, [39] experimentally measured the thermal resistance of different HE between TEMs and air, looking not only to the air flow mass, but also to the occupancy ratio (δ), this is, the ratio of the area the TEMs and the area of the HE base, as in:

$$\delta = \frac{A_{TEM}}{A_{Heat\ exchanger\ base}} \tag{1.8}$$

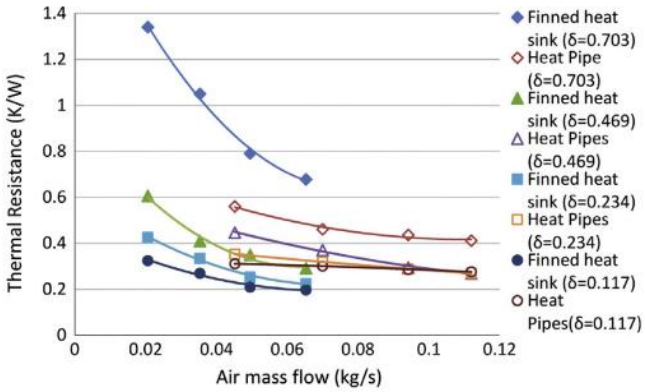

Figure 21. Thermal resistance per TEM of the finned heat sink and that of the heat pipe, as a function of the air mass flow for different values of δ – occupancy ratio. Source: Astrain D. et al. [39].

Figure 21 shows that HPp are less dependent on the air flow rate than the heat sinks. HPp commonly outperform heat sinks, but this is only true when the occupancy ratio is higher than 0.3. If not, finned-heat sinks under forced convection may be the best option.

- Finally, the third approach is the optimization of the TeHP working conditions, mainly related to the number of TEMs and regulation of the electric current input to optimize the COP of the TEMs, depending on the coolant flow rates.

Taking into account the objectives of this Ph. D. dissertation and the temperature working range of the proposed application, together with the limitation of the commercial availability of thermoelectric modules, the experimental prototypes to be developed in this Ph. D. dissertation will use Bi_2Te_3 thermoelectric modules and the research work will be focused on the second and third approaches explained above.

1.2.4. Thermoelectricity for heating and cooling in buildings

As already exposed in previous sections, there is clear need in the market to contribute with more decarbonized cooling/heating capacity to phase out fossil fuel appliances. Non-refrigerant dependent technologies can help to reduce the use of HFCs, and more specifically, thermoelectricity presents some additional advantages that can contribute to their deployment. The use of thermoelectricity to heat and/or cool buildings has not reached the market yet, but many researchers have identified this opportunity and have designed, constructed and tested many prototypes of thermoelectric heat pumps (TeHP) integrated in buildings. Many review articles ([40], [41], [42], [43] and [44]) have examined the published research studies aiming at achieving a good COP that can compete with VC cycle. The different reported investigations propose different TeHP prototypes showing a variety of TeHP designs, mathematical validated models and parametric investigations. The potential synergy of TeHP in low energy demand buildings (named as nZEBs) is firstly identified in 2016 and no specific reference to the integration of TeHPs with PH standard has been found. The different attempts to heat and/or cool buildings can be classified paying attention to the selected heat reservoirs and how the TEMs are integrated with those heat reservoirs. Next Figure 22 shows a first classification identifying the building envelope and the ventilation as the main integration possibilities of the TeHPs. The integration with the ventilation system and the outgoing and incoming air flows is analyzed in the next section, together with the potential combination with a HRU.

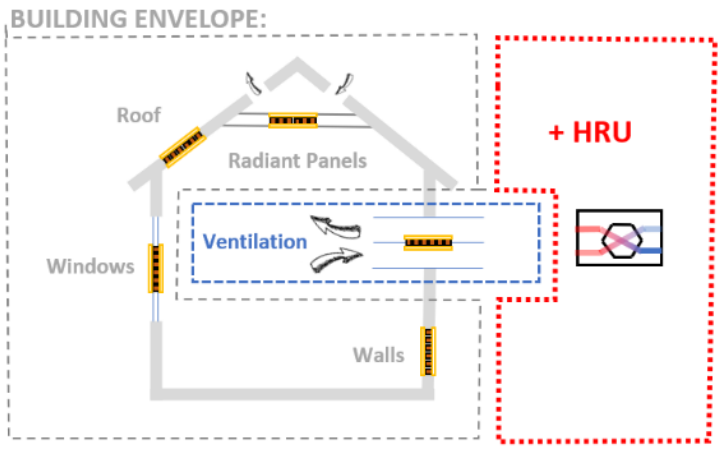

Figure 22. Figure 1. World energy supply by fuel. Source: IEA World Energy Balances Source: own.

Most of the reported research works intend to incorporate the TeHPs in the building envelope, where the TEMs are inserted in the walls, roofs, radiant panels or windows, compensating the incoming or outgoing heat flows. Next Table 2 presents the most relevant research works on this field. Six of the thirteen analyzed works are designed for only cooling, two for only heating and five of them can either cool or heat to the indoor ambient. Most of the built prototypes work between outdoor and indoor environments as hot and cold reservoirs with either natural convection or forced convection with a recirculated air flow. Seven references combine the

TeHP with PV facilities that can either provide some or all the energy consumed by the TEMs and create a ventilated façade where outdoor air can be pre-heated. The most common HE employed is finned heat sinks, only one of the prototypes analyzed in two of the reviewed references employ heat pipes for the outdoor air channel (ventilated façade), and 5 prototypes use radiant panels to provide indoor comfort, including the windowpanes. From the above references five investigations provide simulating models, two of them show empirical research with constructed prototypes and the rest six references employ empirical investigation to validate a simulating model. Table 2 shows all references listed according to the year of publication (firstly) and the main authors' surname (secondly). The information about each work includes:

- Provision of heating, cooling or both.
- Integration with a PV facility.
- Constructed prototype, simulating model or both.
- Integration strategy with the building envelope: wall, roofs & ceilings or windows.
- Scope and main remarks: where there is a brief description of the proposed work and the main achievements including the type of heat reservoirs and the heat exchangers employed.

Table 2. Research works proposing the integration of TeHPs with the building envelope.

REFERENCE	HEATING	COOLING	Integ. PV	Simul. Mod.	Prototype	Integration			SCOPE AND MAIN REMARKS
						Wall	Roof/ceil	Window	
[45]		X		X			X		• A radiative sky cooling new technology (water panels with special coating to dissipate the heat -high emissivity and low absorptivity) keeps a water tank cold. • A water circuit dissipates the heat in the hot side of the TEMs and the cold sides are used to air condition the indoor ambient with aluminum heat sinks. • Case study of one 223 m^2 house cooled with 32 m^2 radiative panels in Los Angeles.
[46]	X				X	X			• 6 TEM prototype test • Ventilated façade with water heat sinks & axial fans in the outside air chamber. Inside aluminum heat sinks are used to air condition indoor ambient. • 66-273 W heating capacity with COP ranging 2.1-1.1
[47]		X	X	X	X	X			• Integration of a 300 Wp PV facility south-faced in a room air conditioned by a 15 TEM prototype (previously investigated) • The combination of the PV production increases the COP to 1.16, compared with 0.63 in previous research. • TrnSYS simulating model.
[48]	X	X		X			X		• Dynamic state model • Validation with previous experimental study: 1.8m x 0.6 m radiant panel and 10 TEM. • Study of the system to work as radiant ceiling. Result: 48-104 W/m^2 cooling capacity – 165-343 W/m^2 heating capacity

[49]	X		X	X	X	X			• 3 TEM prototype tested heating an insulated box of 1m x 1m x 1m in a laboratory environment • Aluminum heat sinks with tangential fans in both sides of the TEMs • Simulating model to extrapolate the results to a pre-1900s mid-terrace UK dwelling
[50]	X	X	X	X	X	X			• Prototype of a ventilated façade with PV panels outside and one air ventilated air chamber • The TEMs are installed between heat pipes to exchange heat with outdoor air chamber and an aluminum panel to air condition indoor. • Scale: 1.8m x 0.6 m radiant panel and 10 TEM.
[51]		X		X	X	X			• 15 TEM prototype installed in the north façade • Aluminum heat sinks in both cold and hot sides of the TEMs • Axial fan to reduce the thermal resistance • Room 2.8 m x 2.7 m x 2.5 m air conditioned in tropical climate under real conditions • TrnSYS simulating model
[52]		X	X		X	X			• 1 TEM prototype • Ventilated façade with PV panels outside, TEM installed between two aluminum heat sinks, one indoor and the other in the air chamber • PV directly wired to the TEM
[53]		X	X	X				X	• 1 TEM prototype test • The TEM is installed between two glass panes in a window • A finite element analysis studies the optimum distribution of the TEMs in the window. • The COP ranges 0.32-0.95 for cooling and 0.44-1.1 for heating
[54]	X	X		X			X		• Roof integrated thermoelectric radiant system • Virtual case study of air conditioning of a 70 m^2 office with 90 W/m^2 cooling load and 70 W/m^2 heating load. Number of TEMs: 721-888 • Conclusions show that if the figure of merit (ZT) reaches to be greater than 1, then the system could have a better performance than conventional systems.
[55]		X	X	X				X	• Window design with a PV integrated in the glass pane and TEMs in the frame between aluminum heat sinks • The window is powered only with the incident radiation • The simulation results show that the model may decrease up to 67% the heat gains through the window
[56]	X	X		X	X			X	• 1 TEM prototype test • The TEM is installed between two glass panes in a window • A finite element analysis studies the optimum distribution of the TEMs in the window. • The COP ranges 0.32-0.95 for cooling and 0.44-1.1 for heating
[57]	X	X	X	X	X			X	• Detailed study of an 8 TEM prototype for its use in a so-called ABE (Active Building Envelope) • The paper proposes its implementation in a window and the integration with PV to improve the overall efficiency

In all the above cases, the thermal bridge created by the TEMs in the building envelope is the main weakness of the TeHP. While the building envelope receives solar radiation, a PV facility may well provide the energy required to compensate the heat flux in the envelope and even increase or reduce the indoor air temperature, pumping heat out or in, respectively. However, when there is no solar radiation, the thermal bridge cannot be easily avoided. In summertime the highest cooling need coincides with the highest solar radiation, and this strategy can be

helpful. In wintertime, the thermal losses potentially caused by the TeHP prototypes clearly affect to the overall energy balance of the building. This strategy goes against the principles of PH standard exposed in Section 1.1.3 aiming at minimizing the thermal bridges in the building envelope. Therefore, the integration of the TeHP with the building envelope has been discarded.

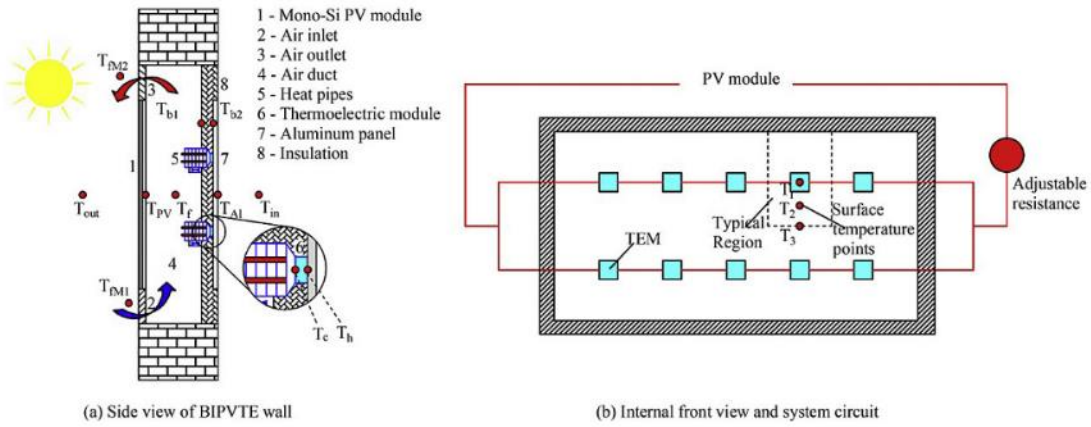

Figure 23. Prototype of buliding integrated PV thermoelectric heat pump (BIPVTE). Source: Luo Y. et al. [58]

1.2.5. Thermoelectric heat pumps integrated with air ventilation systems.

All buildings need to be adequately ventilated to ensure the health and safety of building occupants (by removing carbon dioxide, water vapor and other pollutants that are released throughout the building); and this is even more relevant when the building envelope is air-tight, as in the case of PH, in compliance with requirements of the standard (section 1.1.3). Introducing an air-to-air TeHP between fresh and exhaust air streams in a PH is the main idea defended by the present Ph. D dissertation, given the fact that PH can satisfy its heating demand rising the temperature of the ventilation air flow. This idea is not present in any of the reviewed investigations, however Table 3 collects a total of ten research works that, in one way or another, approach to this idea by proposing air-to-air TeHPs. The references are again listed according to the year of publication (firstly) and the main authors' surname (secondly), while the information about each work includes:

- Provision of heating, cooling or both.
- Integration with a PV facility.
- Constructed prototype, simulating model or both.
- Integration with an HRU.
- Scope and main remarks: where there is a brief description of the proposed work and the main achievements including the type of heat reservoirs and the heat exchangers employed.

Table 3. Research works proposing the integration of TeHPs with the ventilation system.

REFERENCE	HEATING	COOLING	Integ. PV	Integ. HRU	Simul. Mod.	Prototype	FEATURES	SCOPE AND MAIN REMARKS
[59]	X	X		X	X	X	27 TEM	• Air-to-air heat pump (aluminum heat sinks and cross flow), combined with an enthalpy wheel and a desiccant wheel to air condition one office. • Simulating results have 22% greater consumption than a reference system with vapor compression cycle system.
[60]		X			X	X	1 TEM 40 W cool	• Air-to-air heat pump. Indoor air is recirculated, while out air is used as hot reservoir. • Simulation model combines thermoelectric cooling effect and Ɛ-NTU model. • Counter flow configuration is more effective presenting a theoretical maximum of 243 W
[61]		X			X		-	• Air-to-water heat pump. Indoor air is recirculated, while heat is used for DHW. • Simulation model combines thermoelectric cooling effect and Ɛ-NTU model. • Cooling load goes 326-739 W
[62]	X		X		X	X	12 TEM 117-248 W	• Combination of an PVT for ventilation air preheating and an air-to-air heat pump. • Comparison of simulated and experimental data. • Outside conditions: 4-5.3°C and inside conditions: 15.5 °C
[63]	X	X				X	1 TEM 53.2 W heat 9.35 W cool	• Air-to-air heat pump (aluminum heat sinks and counter flow). • Air flow 5.6-11.7 m^3/h in hot side and 5.9-14.2 m^3/h in the cold side, both from same test room. • Experimental results are presented together with thermal images .
[64]	X	X	X		X		-	• Combination of thermoelectric generation (TEG attached to PV panels and between solar thermal panels and DHW) and air conditioning (air-to-air heat pump between ventilation air streams). • Overall balance is estimated to result into a positive energy building.
[65]	X	X			X	X	12 TEM	• One air-to-air prototype (heat pipes and counter flow) is presented and tested. • In winter outside temperature ranges 6-14 °C and it is regulated to reach 20 °C, while in summer 30-35 °C to reach 26 °C. • One simulation model is presented, the thermal resistance of the heat pipes is fixed to 0.4 K/W
[66]	X			X	X		-	• Simulation model of air-to-air heat pump to HVAC one nZEB with 30 W/m^2 heat load. • Three alternatives are presented: the heat pump alone, combined with an HRU and combined with an earth to air heat exchanger. In the three cases indoor air is recirculated to reach the heating load. • The number of TEMs is optimized for three climates with a range 35-60. • The thermal resistance of HE is estimated as 0.01 K/W

[67]	X	X		X		X	10 TEM 490 W heat 530 W cool	• Combination of a cross-flow aluminum HRU with a air-to-air heat pump (aluminum heat sinks and cross flow). • The incoming ventilation air (60-70 m^3/h) goes first through the heat pump and then through the HRU, so the incoming air is not supposed to over-heat nor over-cool the inside.
[68]		X			X	X	8 TEM 290 W heat 70 W cool	• One thermal diode separates inside and outside heat sinks • Winter test: 18°C inside and 1-9 °C outside. • Summer test: 21°C inside and 23-31 °C outside.

In 2006 Riffat S et al [68] presented a small air-to-air TeHP with a thermal diode that permitted to switch from cooling to heating mode by turning a thermosiphon. One extreme of the thermosiphon remained indoor while the other extreme was placed outdoor. The cooling effect occurred on the top of the thermosiphon and heating on the bottom. There is no specific integration with the ventilation air stream, but it is an ingenious way to enhance the air-TEM heat exchange.

Closer to the concept of the fresh-exhaust air heat exchange is the prototype constructed by reference Yilmazoglu M. [63] and shown in

Figure 24, with two air ducts separated by one TEM attached to two finned aluminum heat sinks. The air volumetric flow is limited to 14.2 m^3/h with a maximum cooling capacity of 9.35 W. In the laboratory tests the air blown into both ducts is taken from the indoor environment, so the results are not representative when there is temperature gap between indoor and outdoor in a building.

The first explicit reference to the integration of TeHP in nZEB is presented by Shen L et al. [64], where a combination of thermoelectric generation (TEG attached to PV panels and between solar thermal panels and DHW) and thermoelectric air conditioning is simulated.

Cai Y et al. [60] developed an air-to-air TeHP concept named ATEV (Active Thermoelectric Ventilation) between incoming and outgoing air flows in building. It was focused on air cooling, where two air ducts exchange air through the TEMs and aluminum heat sinks. The mathematical model combines the Ɛ-NTU method, and it is validated with 1 TEM prototype. The parametric study foresees a limitation of 235.8 W and 243.3 W for the cooling capacity of the ATEV when working as parallel or counter flow configurations respectively, at optimum operating conditions. A further research work [61] explores the possibility to produce domestic hot water while cooling the incoming air flow.

From the above references, only references [67], [59] and [66] investigate the combination of a HRU with the TeHP. Li T et al. [67] built in 2009 one prototype of domestic thermoelectric ventilator with heat recovery from exhaust air. The prototype combines a thermoelectric module heat exchanger and a cross flat-fin sensible heat exchanger into a device limited to 60 m^3/h. The fresh air goes through the thermoelectric modules first and then, through the aluminum cross-flow HRU, so the temperature of the incoming air is not intended to go beyond the indoor temperature. More recently, Cheon S et al. [59] built another cross-flow TeHP with aluminum heat sinks. Based on the empirical results, this research study proposes

its combination with an enthalpy wheel. In this case the fresh air stream recovers the heat from exhaust air first, and then it is conditioned by the TeHP and a desiccant wheel. The modeling results show that the energy consumption for one year is 22 % higher than a reference system composed of an HRU and a vapor compression cycle heat pump.

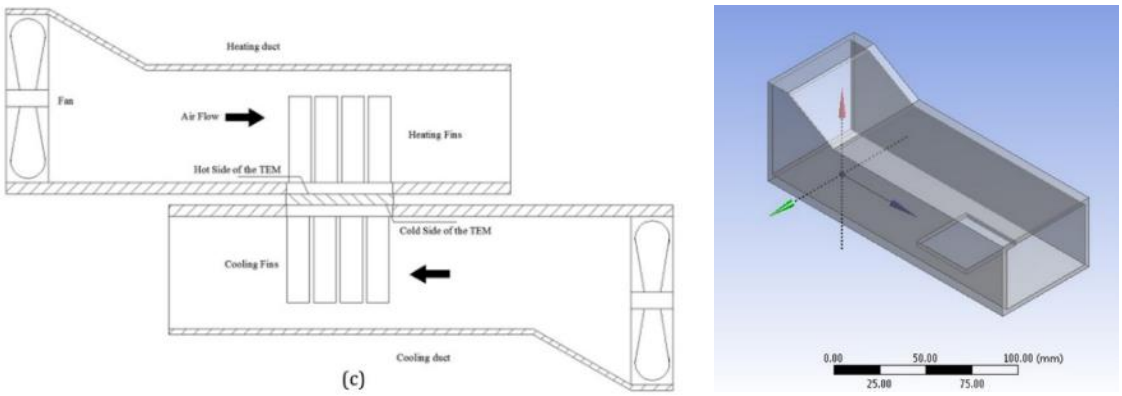

Figure 24. One TEM air-to-air TeHP with aluminum heat sinks as heat exchangers. Source: Yilmazoglu M. et al. [63]

However, in both cases, [67] and [59], the performance of the TeHP is low due to the thermal resistance of the finned heat sinks. The thermal resistance of the HE between the TEMs and the air streams is crucial in order to obtain a good energy performance of the TeHP. As previously explained in section 1.2.1, higher thermal resistance increases the temperature gap between the hot and cold sides of the TEM, what drastically reduces the COP [39]. The use of heat pipes as HE may double the energy performance of a TeHP compared with aluminum flat fin heat sinks. The relevance of the thermal resistance of these HE is remarked by Han T et al. [38], presenting a thermoelectric ventilator with heat pipes, as an evolution of a previous design made with aluminum fins [67]. The TeHP demonstrated to perform better, but the prototype is still limited to 60 m^3/h, and the tests intend to equal the indoor temperature, with no aim of extra-heating/cooling the inside. For the further analysis the thermal resistance of the HPp is set up as 0.4 K/W. This thermal resistance depends on the heat flux and the air flow, and its value in the cold side doubles the one in the hot side, since the heat pipe works contrary to the design conditions. The natural inaccuracy due to the simplifications and estimated input values for the computational models may drive to deviations higher of 30% between simulated and experimental results [69], especially if a significant aspect as the complexity related to the heat and mass transfer mechanisms in the heat pipes is not well addressed.

Finally, Kim Y et al.[66] published an interesting simulation study with the aim of heating one nZEB with a TeHP, proposing three different integration possibilities in the ventilation system. One of these three options is the combination with an HRU. The simulation results demonstrate the existence of an optimized number of modules (35-60) driven by the dissipated heat flux and the temperature difference between both sides of the flux. The TeHP has no specific physical representation and the thermal resistance of the HE between the air

streams and the TEMs is set to 0.001 K/W, based on reference [70]. Thermal resistance values for heat transfer between the TEMs and air under 0.1 K/W [39] are difficult to achieve, and the cited research [70] refers to an impinging jet system for liquid-TEM heat exchange. On the other hand, the ventilation scheme includes indoor air recirculation (3 times the ventilation air flow) to reach the estimated energy needs of the building (30 W/m^2), what makes the TeHP work against outdoor air when the HRU is integrated. As previously mentioned, the architectural conceptualization and the thermal envelope of a PH limit the heating/cooling load to 10 W/m^2 , what makes it possible the direct integration of the TeHP right after the HRU and, thus, reduce the temperature gap between air streams, and also reduce the optimized number of .

The review of previous dedicated research demonstrates the need to scale-up the air volume in the air-to-air TeHP designs investigated so far. These systems must reach a range of 50-130 m^3/h to provide sufficient renovated air for indoor spaces up to 100 m^2. On the other hand, the efficiency needs to be improved as much as possible to compete with vapor compression cycle, reducing the thermal resistance of the TEM-air heat exchangers and optimizing the design and the regulation of the TeHP. The potential integration of a TeHP with a passive house is a novel opportunity that must be analyzed, combined or not with an HRU. With this aim, it is necessary to develop a reliable computing model based on empirical evidence of a prototype, tested in real operating conditions.

1.2.6. Simulation models of thermoelectric heat pumps.

In the previous subsections many of the reviewed investigations have developed laboratory prototypes of TeHPs. However, the investigation of how these TeHPs may be integrated in buildings with different shapes, climates and bioclimatic strategies to provide comfort inside, require the use of computational models. The use of these models has become an indispensable tool for the design, analysis, and optimization of real applications, since they reduce the need of buildings prototypes and limit the number of experimental tests in order to obtain significant information, which translates into cost savings.

The computational model of a TeHP needs to not only reproduce the thermal behavior of the device but also the thermoelectric phenomena. This phenomenon happens in each of the legs of the TEMs employed. The internal heat generation/absorption is determined by the thermoelectric effects Seebeck, Peltier, Joule and Thomson, as previously exposed, and the thermoelectric material properties: the Seebeck coefficient, the Thomson coefficient, the thermal conductivity and the electric resistivity are temperature dependent.

The different simulation models emerge from the different approaches proposed to implement and solve these equations. Three are the most commonly used:

- Simple model: this model assumes one-dimensional conductive heat transfer in the legs. Also, it considers opposite Seebeck coefficient in n-doped and p-doped legs, but equal thermal conductivity and electrical resistivity, all of them introduced as constant

values. The Thomson effect is ignored, as well as the influence of the ceramic layers and shunts. All the legs are equal in base area, length, and aspect ratio. Finally, the heat generated by Joule effect distributes evenly along the legs, so that half of it goes to the hot side of the TEMs, whereas the other half goes to the cold one.

- Improved model: The improved model [71] represents the first alternative to the simple model. It goes one step further by including two different terms for the Seebeck coefficient (one for the hot side and another one for the cold side) instead of just one. This allows the consideration of the Thomson effect and the inclusion of the heat generation/absorption related to it. This heat flow is assumed to distribute evenly along the legs.

- Electrical analogy: Fraisse [71,72] and Martinez [73] provide detailed explanations of this method, by which the system is divided and transformed into an electrical circuit. At the core, a grid of connected nodes represents the p-doped and n-doped legs and the connecting shunts; thermal resistances connect the nodes, setting the conductive heat transfer between them; and heat sources over the corresponding nodes represent internal heat flows. The ceramic layers of the TEMs and the HEs can be easily included in the simulation by extending the grid.

- Others: Other solutions are also present in the literature, such as the one based on finite elements, regarded as the most reliable and accurate for TEM simulation [71]. This model allows the inclusion of all the thermoelectric effects with temperature-dependent properties even for complex TEM structures. However, it is not used in THP simulation because of its inherent high computational cost.

From the above-mentioned simulation models only, the simple model has been used in the analyzed references of TeHPs integrated with ventilations systems in buildings. Next Table 4 presents for those investigations that include a computing model information regarding the type of TEM employed, the thermoelectric properties used in the simulating model, the type of HEs in the hot and cold side and, finally, their thermal resistance.

Table 4. Simulation models of TeHPs integrated with ventilation systems in buildings.

Ref	TEM	Thermoelectric properties	Hot side HE	Cold side HE	Thermal resistance of HEs
[60]	Ferrotec 9500/127/060B	Lineykin	Heat sinks	Heat sinks	Assumed value of hot-to-cold ratio
[61]	TEC1-12708	Lineykin	Heat sinks (water duct)	Heat sinks	Assumed value of hot-to-cold ratio

[59]	HMN6040	Lineykin	Heat sinks	Heat sinks	Assumed value of hot-to-cold ratio
[62]	Ferrotec 9500/127/060B	Temperature-dependent from Ferrotec	Heat pipes	Heat pipes	Assumed value for evaporation and condensation. Empirical expressions for convection and fin efficiency.
[67]	TEC1-12706	Lineykin	Heat sinks	Heat sinks	Assumed value
[65]	Ferrotec 9500/127/120B	Constant values from Ferrotec	Heat pipes	Heat pipes	Assumed value
[66]	Ferrotec 9501/242/160B	Temperature-dependent from Melcor	[70]	[70]	Based on a water jet cooled heat sink
[68]	Melcor CP2-127-06	Temperature-dependent from Melcor	Thermal diode	Thermal diode	Empirical expressions

Computing models not only need to address the functioning of TEMs, but also the HEs and the heat transfer in the TeHP design. Additionally, the analysis of the integrability of TeHP in buildings, and more specifically in PH, need to combine the dynamic simulation of a building with the operation of the TeHP.

1.3. Motivation

The Sustainable Development Scenario in 2030 developed by the IEA foresees that 1.5 TW of the overall 14.52 TW of thermal capacity of heat pumps that are expected to be installed in the coming years, will correspond to non-vapor pumping technology, aiming at contributing to the decarbonization of the heating and cooling sector, and the phase-out of HFC refrigerants. In parallel, new and refurbished buildings are implementing stringent energy efficient measures, reducing the heating demand, while cooling demand will surely be increased due to climate warming and the more comfort requirements of occupants. This is a great market opportunity for new heat pumping technologies.

Passive House is a successful energy standard whose main principles are being followed by European directives to fight climate change and reduce the energy demand of buildings. The functional definition is based on the idea that heating / cooling demand can be reduced up to a point where thermal comfort can be provided raising or lowering the temperature of the incoming ventilation air flow. This fact permits the development of a simple and cost-effective HVAC solution, nowadays available in the market with vapor compression technology.

Thermoelectricity has demonstrated to be a robust, lightweight, reliable and scalable technology that does not require moving parts, working fluids nor auxiliary equipment. Nevertheless, their commercial use is restricted to niche applications such as small refrigerators, wine cooling, automobile cooling… while its use as heat pump in buildings is limited to the academic field.

Given the great advantages of thermoelectricity, the design of a TeHP to air condition low energy demand buildings, as PH, considering the integration with the ventilation system (combined or not with an HRU), is expected to have a great potential. The development of such application needs to be performed completely, with a proper design and optimization of the whole heat pump, as well as a proper demonstration on field, not limiting to computational or low-scale proposals. Hence, there is a necessity of a reliable computational model that considers not only the thermoelectric modules with all the thermoelectric effects, but also the heat exchangers and their integration with the building simulation, taking into account all the heat transfer mechanisms. Such a model serves as basis for the design and optimization of real prototypes that can be subsequently built and installed on field.

In this context, the present Ph.D. dissertation studies the viability of an air-to-air thermoelectric heat pump, able to air condition indoor spaces up to 100 m^2 with a ventilation need of 0.35-0.5 ACH. To this aim it is firstly necessary to propose different alternatives to optimize the heat transfer between the TEMs and air flows with an adequate design. The conclusions need be empirically tested and validated, with a built prototype operating in real conditions. The computational model reproducing the thermal behavior of the TeHP must be validated and combined with the thermal simulation of a building, to assess the performance of the HVAC system one year long. This computing model will permit to investigate the convenience of the integration of the TeHP with an HRU, the regulation alternatives, as well as the comfort conditions indoor and the comparison with a conventional heat pumps of vapor compression cycle.

In order to accomplish these purposes, the present work is contextualized with the SMART CLIMA project (PT050/2017 and PT009/2017), counting on the experience of the Ph. D. candidate in passive house building as founder of the Plataforma de Edificación Passivhaus (PEP) and current project manager at *Energy in Buildings* department of the CENER (Centro Nacional de Energías Renovables), the experience in thermoelectrics of *Thermal and Fluid Engineering research group* from the Public University of Navarre and the collaboration of ventilation equipment manufacturers.

1.4. Objectives

Considering the actual state of the art and once the motivation of the present Ph. D. dissertation has been explained, the following objective is contemplated:

Development of an air-to-air thermoelectric heat pump integrated with a double flux ventilation system to HVAC one indoor space of up to 100 m^2 with Passive House standard.

The attainment on this main objective encompasses a series of specific objectives to be developed during the thesis. The specific objectives 1 and 2 lay the empirical fundations of the thermoelectric heat pump, selecting the concrete components of final design and providing experimental data to validate the computational work, developed by objective 3. After the computational model has been validated and the TeHP optimized, next objective 4 focuses on its integration in a real case study, analyzing the feasibility and competitiviness of this new TeHP proposal.

Specific Objective 1:

As exposed in previous sections, the HE between air flows and the hot and cold faces of TEMs are key elements of the TeHPs, since they determine the temperature difference across TEMs. Therefore, the first specific objective considers the study of high-efficiency HE for their use in this application of air-to-air TeHP.

For the competitiviness of this particular application of the TeHP it is of upmost importance to to accomplish a reduced thermal resistance of the HE and obtain a reliable thermal characterization of the HE. Hence, two different types of HE will be studied both computational and experimentally: finned aluminum heat sinks and finned heat pipes. This characterization will enable analizing the influence of different factors in the operation of these devices, serving as basis for their optimization in the following specific objectives.

Specific Objective 2:

The second specific objective focuses on the design and experimental optimization of a TeHP adapted to the usual ventilation flows in an apartment with a high energy standard (nZEB), and more specifically, a PH, where the heating and cooling loads can be covered by solely rising of lowering the temperature of the ventilatin air flow. Based on the results obtained in previous specific objective, two prototypes will be designed and tested.

In this particular process, apart from the maximization of the COP of the TeHP, for which different geometries and number of TEMs will be analized, it will be of great importance to consider constructional aspects, facilitating the assembly and installation of the devices, as

well as a light-weight final design (a common individual HRU weights 20-25 Kg) able to be integrated in false ceilings (the thickness should be lower than 25 cm).

The resulting devices will be built at the laboratories of CENER, with the assitance of a ventilation company (SIBER) and the Public University of Navarre, where the peformance of the final design will be deeply analyzed with the help of a climatic chamber, making the TeHP work in real operating conditions.

Specific Objective 3:

The third specific objective deals with the development of a computational model to simulate the behaviour of the TeHP. For the refinement of the final design of the TeHP and its further integration in a simulated building, it is necessary to take into account that several aspects that have an influence: the type of HE, their geometry and materials, the nature of the heat source and sink, the number of TEMs, or the disposition and assembly of the different elements among others. Therefore, it is essential to have a versatile computational tool capable of predicting the behaviour of a TeHP, including an exhaustive discretization of the HE that considers all the heat transfer mechanism involved, and the singularities of the heat reservoirs.

The implementation of this computational model will be peformed with the numerical computing environment EES, a non-linear equations solver, that includes heat transfer subroutines and the thermodynamic properties of different substances, as psychometrics in the case of the wet air. Furthermore, the results of this model need to be validated with the empirical investigation carried out with the TeHP prototypes.

Finally, the validated computational model of the TeHP needs to be integrated with the dynamic simulation of a real building, where outside wheather conditions, the occupancy, the solar radiation and certain operating conditions, as the position of solar protection (i.e. the blinds of the windows), are constantly changing and, consecuently, need to be assessed. This integrated model will help to propose a regulation control that provides sufficient comfort conditions inside the building, minimizing the energy consumption of the TeHP.

The simulation of the building thermal behaviour will be performed with TYPE 56, inside TRNSYS numerical computing environment. TRNSYS is a transient systems simulation program with a modular structure. Many of the components that commonly make part of a thermal or electrical system can be found in the library and can be connected between them, as well as different routines to handle input of weather data or other time-dependent forcing functions and output of simulation results.

Specific Objective 4:

Based on the results of previous specific objectives, this final specific objective aims at analyzing the technical and economic feasibility of TeHP solutions in the new frame of nZEBs, as required by the EPBD and, more specifically, with the PH standard.

In this new scenario such a proposal of TeHPs is expected to compete with VCHP. VC technology is expected to have a better COP at nominal conditions, but other considerations as the more accurate regulation, and the other additional benefits of the TE (no refrigerant, no moving parts, noise free, gas free, no chemical reaction, reliability, scalability, minimum maintenance) need to be addressed in order to better understand the competitiveness of this non-VC technology in this particular application.

Moreover, the addition of more PV panels on the roof of buildings might compensate the worse energy efficiency of the TeHP with respecto to VCHP, while the construction costs may be reduced due to a more simple funcioning.

1.5. Thesis Structure

In order to accomplish the previous objectives, the present Ph. D. dissertation is structured in 6 chapters. Following to this introduction, Chapter 2 represents the first approximation to thermoelectric heat pumps. One first prototype using aluminum heat sinks as HE is built and tested. The employment of heat sinks is discarded due to the poor peformance of the protype, and, hence, the heat pipes are explored as an alternative to heat sinks. The heat pipes are thermally characterized and this characterization corresponds with the article "*Heat pipes thermal performance for a reversible thermoelectric cooler-heat pump for a nZEB"* published in Enery and buildings 187 (2019) 163-172.

Afterwards, Chapter 3 presents the contruction and the laboratory tests of a second prototype with a modular design, employing heat pipes as HE. The article *"Prototype of an air to air thermoelectric heat pump integrated with a double flux mechanical ventilation system for passive houses"* (published in Applied Thermal Engineering 190 (2021) 116801) is an in-depth investigation of the thermal performance of the prototype with different operating conditions: outside and inside temperatures, air flows and supply voltages.

Based on previous empirical results, Chapter 4 develops and validates a computational model that simulates the behaviour of the TeHP. This chapter coincides with the publication *"Optimal combination of an air-to-air thermoelectric heat pump with a heat recovery system to HVAC a passive house dwelling"*, published in Applied Energy 309 (2022) 118443. The manuscript not only makes a detailed description of the computational model including all the involved heat transfer phenomena, but also validates it thanks to the experimental tests of Chapter 2. Additionally, the publication includes a parametric investigation of the TeHP performance, comparing the stand-alone installation of the TeHP as active heat recovery with the combination with an HRU. As a result, the stand-alone installation is discarded, and an optimized number of modules is obtained based on the seasonal coefficient of performance.

Based on the previous optimization, Chapter 5 analyzes the performance of the TeHP integrated with a pilot case, simulating not only the heat pump, but also the air flows and the thermal behavior of a PH certified dwelling located in Pamplona (Spain). Hence, as developed in the article "*Annual energy performance of a thermoelectric heat pump combined with a heat recover unit to HVAC one passive house dwelling*" published in Applied Thermal Engineering 204 (2022) 117832, the viability of the TeHP is analyzed, comparing the simulated results with the performance of a VCHP and the PV production of an on-site facility.

Finally, Chapter 6 highlights the main conclusions obtained in the thesis, exposes the contributions achieved during its development, and presents the future lines arisen.

1.6. Bibliography

[1] International Energy Agency (IEA). Key World Energy Statistics 2020 2020. https://www.iea.org/reports/key-world-energy-statistics-2020 (accessed October 5, 2021).

[2] International Energy Agency (IEA). Energy Technology Perspectives 2020 2020. https://www.iea.org/reports/energy-technology-perspectives-2020 (accessed October 5, 2021).

[3] International Institute of Refrigeration (IIR). THE ROLE OF REFRIGERATION IN THE GLOBAL ECONOMY (38th Informatory Note on Refrigeration Technologies) 2019. https://iifiir.org/en/fridoc/142028 (accessed October 5, 2021).

[4] Abergel , Thibaut; Delmet C. Is cooling the future of heating? Int Energy Agency 2020. https://www.iea.org/commentaries/is-cooling-the-future-of-heating (accessed October 5, 2021).

[5] International Energy Agency (IEA). Sustainable Development Scenario 2030 2020. https://www.iea.org/reports/world-energy-model/sustainable-development-scenario (accessed October 5, 2021).

[6] Cheng TC, Cheng CH, Huang ZZ, Liao GC. Development of an energy-saving module via combination of solar cells and thermoelectric coolers for green building applications. Energy 2011;36:133–40. https://doi.org/10.1016/j.energy.2010.10.061.

[7] Dr. Johanna Gloël et al. - Deutsche Gesellschaft für Internationale Zusammenarbeit (GIZ) GmbH. Green Cooling Technologies. Program Proklima 2015;Serial num.

[8] United Nations Environment Programme (UNEP). The Importance of Energy Efficiency in the Refrigeration , and Heat Pump Sectors 2018:1–15. https://ozone.unep.org/node/3281 (accessed October 5, 2021).

[9] European Commission. The European Green Deal. Eur Comm 2019;53:24. https://doi.org/10.1017/CBO9781107415324.004.

[10] Nowak T. White paper: Heat Pumps - Integrating technologies to decarbonise heating and cooling. EPHA -European Heat Pump Assoc 2018:1–86. https://www.ehpa.org/fileadmin/user_upload/White_Paper_Heat_pumps.pdf (accessed October 5, 2021).

[11] EU. Directive 2010/31/EU of the European Parliament and of the Council of 19 May 2010 on the energy performance of buildings (recast). Off J Eur Union 2010:13–35. https://doi.org/10.3000/17252555.L_2010.153.eng.

[12] EU. A Renovation Wave for Europe - greening our buildings, creating jobs, improving lives. COM(2020) 662 Final 2020. https://ec.europa.eu/energy/sites/ener/files/eu_renovation_wave_strategy.pdf (accessed October 5, 2021).

[13] EU. Directive (EU) 2018/844 of the European Parliament and of the Council of 30 May 2018 amending Directive 2010/31/EU on the energy performance of buildings and Directive 2012/27/EU on energy efficiency. Off J Eur Union 2018;156:75–91.

[14] European Environment Agency (EEA). How is climate change affecting total and peak

energy demand for space heating and cooling across Europe? CLIM 047 2019. https://www.eea.europa.eu/data-and-maps/indicators/heating-degree-days-2/assessment (accessed October 5, 2021).

[15] Cuce P, Riffat S. A comprehensive review of heat recovery systems for building applications. Renew Sustain Energy Rev 2015;47:665–82. https://doi.org/10.1016/j.rser.2015.03.087.

[16] Ferrara M et al. Cost-Optimal Analysis for Nearly Zero Energy Buildings Design and Optimization : A Critical Review 2018. https://doi.org/10.3390/en11061478.

[17] Müller L, Berker T. Passive House at the crossroads: The past and the present of a voluntary standard that managed to bridge the energy efficiency gap. Energy Policy 2013;60:586–93. https://doi.org/10.1016/j.enpol.2013.05.057.

[18] Passive House Institute (PHI). Passive House Database n.d. https://passivehouse-database.org/index.php?lang=en#k_ (accessed October 5, 2021).

[19] Passive House Institute (PHI). Passipedia: Passive House concepts n.d. https://passipedia.org/ (accessed October 5, 2021).

[20] Tobías A, Carnerero C, Reche C, Massagué J, Via M, Minguillón MC, et al. Changes in air quality during the lockdown in Barcelona (Spain) one month into the SARS-CoV-2 epidemic. Sci Total Environ 2020;726:138540. https://doi.org/10.1016/j.scitotenv.2020.138540.

[21] Azuma K, Kagi N, Yanagi U, Osawa H. Effects of low-level inhalation exposure to carbon dioxide in indoor environments: A short review on human health and psychomotor performance. Environ Int 2018;121:51–6. https://doi.org/10.1016/j.envint.2018.08.059.

[22] Guillén-Lambea S, Rodríguez-Soria B, Marín JM. Review of European ventilation strategies to meet the cooling and heating demands of nearly zero energy buildings (nZEB)/Passivhaus. Comparison with the USA. Renew Sustain Energy Rev 2016;62:561–74. https://doi.org/10.1016/j.rser.2016.05.021.

[23] Schnieders J, Feist W, Rongen L. Passive Houses for different climate zones. Energy Build 2015;105:71–87. https://doi.org/10.1016/j.enbuild.2015.07.032.

[24] CLIVET. ELFOFresh^2. Thermodyn Heat Recover 2020. https://www.airview.nl/resources/uploads/2018/07/Technische-Manual-CPAN-U-70-650.pdf (accessed October 5, 2021).

[25] Picallo-Perez A, Sala JM, Odriozola-Maritorena M, Hidalgo JM, Gomez-Arriaran I. Ventilation of buildings with heat recovery systems: Thorough energy and exergy analysis for indoor thermal wellness. J Build Eng 2021;39:102255. https://doi.org/10.1016/j.jobe.2021.102255.

[26] Shah RK. Fundamentals of heat technology. vol. 4. 1960. https://doi.org/10.1007/bf00740254.

[27] Pishler. Heat pump combi 4 unit pkom 2015. https://www.pichlerluft.at/heat-pump-combination-unit.html (accessed October 5, 2021).

[28] Zhao D, Tan G. A review of thermoelectric cooling: Materials, modeling and applications. Appl Therm Eng 2014;66:15–24.

https://doi.org/10.1016/j.applthermaleng.2014.01.074.

[29] Sarkar J, Bhattacharyya S. Application of graphene and graphene-based materials in clean energy-related devices Minghui. Arch Thermodyn 2012;33:23–40. https://doi.org/10.1002/er.

[30] Rowe EDM, Ph D, Sc D, Group F. General principles and considerations. Thermoelectr. Handb. macro to nano. CRC Press, 2006, p. 1.1-1.14.

[31] Zhou X, Yan Y, Lu X, Zhu H, Han X, Chen G, et al. Routes for high-performance thermoelectric materials 2018;21. https://doi.org/10.1016/j.mattod.2018.03.039.

[32] Pourkiaei SM, Ahmadi MH, Sadeghzadeh M, Moosavi S, Pourfayaz F, Chen L, et al. Thermoelectric cooler and thermoelectric generator devices: A review of present and potential applications, modeling and materials. Energy 2019;186:115849. https://doi.org/10.1016/j.energy.2019.07.179.

[33] Martinez A, Díaz S, Garayo D, Aranguren P, Araiz M, Catal L. Simulation of thermoelectric heat pumps in nearly zero energy buildings : Why do all models seem to be right ? 2021;235. https://doi.org/10.1016/j.enconman.2021.113992.

[34] Harman TC, Walsh MP, Laforge BE, Turner GW. Nanostructured Thermoelectric Materials 2005;34:19–22.

[35] Gayner C, Kar KK. Progress in Materials Science Recent advances in thermoelectric materials. Prog Mater Sci 2016;83:330–82. https://doi.org/10.1016/j.pmatsci.2016.07.002.

[36] Polymers C. Recent Progress in Thermoelectric Materials Based on 2019:1–19. https://doi.org/10.3390/polym11010107.

[37] TETechnology. HP-127-1.4-1.15-71 dataheet 2018. https://tetech.com/wp-content/uploads/2013/09/HP-127-1.4-1.15-71.pdf (accessed December 17, 2018).

[38] Han T, Gong G, Liu Z, Zhang L. Optimum design and experimental study of a thermoelectric ventilator. Appl Therm Eng 2014;67:529–39. https://doi.org/10.1016/j.applthermaleng.2014.03.073.

[39] Astrain D, Aranguren P, Martínez A, Rodríguez A, Pérez MG. A comparative study of different heat exchange systems in a thermoelectric refrigerator and their influence on the efficiency. Appl Therm Eng 2016;103. https://doi.org/10.1016/j.applthermaleng.2016.04.132.

[40] Irshad K, Habib K, Saidur R, Kareem M, Saha B. Study of thermoelectric and photovoltaic facade system for energy efficient building development: A review. J Clean Prod 2019;209:1376–95. https://doi.org/10.1016/j.jclepro.2018.09.245.

[41] Liu Z, Zhang L, Gong G, Li H, Tang G. Review of solar thermoelectric cooling technologies for use in zero energy buildings. Energy Build 2015;102:207–16. https://doi.org/10.1016/j.enbuild.2015.05.029.

[42] Shen L, Pu X, Sun Y, Chen J. A study on thermoelectric technology application in net zero energy buildings. Energy 2016;113:9–24. https://doi.org/10.1016/j.energy.2016.07.038.

[43] Sarbu I, Dorca A. A comprehensive review of solar thermoelectric cooling systems. Int J Energy Res 2018;42:395–415. https://doi.org/10.1002/er.3795.

[44] Zuazua-Ros A, Martín-Gómez C, Ibáñez-Puy E, Vidaurre-Arbizu M, Gelbstein Y. Investigation of the thermoelectric potential for heating, cooling and ventilation in buildings: Characterization options and applications. Renew Energy 2019;131:229–39. https://doi.org/10.1016/j.renene.2018.07.027.

[45] Zhao D, Yin X, Xu J, Tan G, Yang R. Radiative sky cooling-assisted thermoelectric cooling system for building applications. Energy 2020;190:116322. https://doi.org/10.1016/j.energy.2019.116322.

[46] Zuazua-Ros A, Martín-Gómez C, Ibáñez-Puy E, Vidaurre-Arbizu M, Ibáñez-Puy M. Design, assembly and energy performance of a ventilated active thermoelectric envelope module for heating. Energy Build 2018;176:371–9. https://doi.org/10.1016/j.enbuild.2018.07.062.

[47] Irshad K, Habib K, Basrawi F, Saha BB. Study of a thermoelectric air duct system assisted by photovoltaic wall for space cooling in tropical climate. Energy 2017;119:504–22. https://doi.org/10.1016/j.energy.2016.10.110.

[48] Luo Y, Zhang L, Liu Z, Wu J, Zhang Y, Wu Z. Three dimensional temperature field of thermoelectric radiant panel system: Analytical modeling and experimental validation. Int J Heat Mass Transf 2017;114:169–86. https://doi.org/10.1016/j.ijheatmasstransfer.2017.06.063.

[49] Wang C, Calderón C, Wang Y. An experimental study of a thermoelectric heat exchange module for domestic space heating. Energy Build 2017;145:1–21. https://doi.org/10.1016/j.enbuild.2017.03.050.

[50] Luo Y, Zhang L, Liu Z, Wang Y, Meng F, Xie L. Modeling of the surface temperature field of a thermoelectric radiant ceiling panel system. Appl Energy 2016;162:675–86. https://doi.org/10.1016/j.apenergy.2015.10.139.

[51] Irshad K, Habib K, Thirumalaiswamy N, Saha B. Performance analysis of a thermoelectric air duct system for energy-efficient buildings. Energy 2015;91:1009–17. https://doi.org/10.1016/j.energy.2015.08.102.

[52] Piantanida P. PV & Peltier façade : preliminary experimental results. Energy Procedia 2015;78:3477–82. https://doi.org/10.1016/j.egypro.2015.11.337.

[53] Liu Z, Zhang L, Gong G. Experimental evaluation of a solar thermoelectric cooled ceiling combined with displacement ventilation system. Energy Convers Manag 2014;87:559–65. https://doi.org/10.1016/j.enconman.2014.07.051.

[54] Shen L, Xiao F, Chen H, Wang S. Investigation of a novel thermoelectric radiant air-conditioning system. Energy Build 2013;59:123–32. https://doi.org/10.1016/j.enbuild.2012.12.041.

[55] Harren-lewis T, Rangavajhala S, Messac A, Zhang J. Optimization-based feasibility study of an active thermal insulator. Build Environ 2012;53:7–15. https://doi.org/10.1016/j.buildenv.2012.01.002.

[56] Dessel S Van, Foubert B. Active thermal insulators : Finite elements modeling and parametric study of thermoelectric modules integrated into a double pane glazing

system. Energy Build 2010;42:1156–64. https://doi.org/10.1016/j.enbuild.2010.02.007.

[57] Xu X, Dessel S Van, Messac A. Study of the performance of thermoelectric modules for use in active building envelopes 2007;42:1489–502. https://doi.org/10.1016/j.buildenv.2005.12.021.

[58] Luo Y, Zhang L, Liu Z, Wu J, Zhang Y, Wu Z. Numerical evaluation on energy saving potential of a solar photovoltaic thermoelectric radiant wall system in cooling dominant climates. Energy 2018;142:384–99. https://doi.org/10.1016/j.energy.2017.10.050.

[59] Cheon S, Lim H, Jeong J. Applicability of thermoelectric heat pump in a dedicated outdoor air system. Energy 2019;173:244–62. https://doi.org/10.1016/j.energy.2019.02.012.

[60] Cai Y, Wang L, Ding W, Liu D, Zhao F. Thermal performance of an active thermoelectric ventilation system applied for built space cooling: Network model and finite time thermodynamic optimization. Energy 2019;170:915–30. https://doi.org/10.1016/j.energy.2018.12.186.

[61] Cai Y, Zhang D, Liu D, Zhao F, Wang H. Air source thermoelectric heat pump for simultaneous cold air delivery and hot water supply: Full modeling and performance evaluation. Renew Energy 2019;130:968–81. https://doi.org/10.1016/j.renene.2018.07.007.

[62] Liu Z, Zhang Y, Zhang L, Luo Y, Wu Z, Wu J, et al. Modeling and simulation of a photovoltaic thermal-compound thermoelectric ventilator system. Appl Energy 2018;228:1887–900. https://doi.org/10.1016/j.apenergy.2018.07.006.

[63] Yilmazoglu M. Experimental and numerical investigation of a prototype thermoelectric heating and cooling unit. Energy Build 2016;113:51–60. https://doi.org/10.1016/j.enbuild.2015.12.046.

[64] Shen L, Pu X, Sun Y, Chen J. A study on thermoelectric technology application in net zero energy buildings. Energy 2016;113:9–24. https://doi.org/10.1016/j.energy.2016.07.038.

[65] Han T, Gong G, Liu Z, Zhang L. Optimum design and experimental study of a thermoelectric ventilator. Appl Therm Eng 2014;67:529–39. https://doi.org/10.1016/j.applthermaleng.2014.03.073.

[66] Kim Y, Ramousse J, Fraisse G, Dalicieux P, Baranek P. Optimal sizing of a thermoelectric heat pump (THP) for heating energy-efficient buildings. Energy Build 2014;70:106–16. https://doi.org/10.1016/j.enbuild.2013.11.021.

[67] Li T, Tang G, Gong G, Zhang G, Li N, Zhang L. Investigation of prototype thermoelectric domestic-ventilator. Appl Therm Eng 2009;29:2016–21. https://doi.org/10.1016/j.applthermaleng.2008.10.007.

[68] Riffat S, Ma X, Wilson R. Performance simulation and experimental testing of a novel thermoelectric heat pump system. Appl Therm Eng 2006;26:494–501. https://doi.org/10.1016/j.applthermaleng.2005.07.016.

[69] Shen L, Tu Z, Hu Q, Tao C, Chen H. The optimization design and parametric study of thermoelectric radiant cooling and heating panel. Appl Therm Eng 2017;112:688–97. https://doi.org/10.1016/j.applthermaleng.2016.10.094.

[70] Karwa N, Stanley C, Intwala H, Rosengarten G. Development of a low thermal resistance water jet cooled heat sink for thermoelectric refrigerators. Appl Therm Eng 2017;111:1596–602. https://doi.org/10.1016/j.applthermaleng.2016.06.118.

[71] Fraisse G, Ramousse J, Sgorlon D, Goupil C. Comparison of different modeling approaches for thermoelectric elements. Energy Convers Manag 2013;65:351–6. https://doi.org/10.1016/j.enconman.2012.08.022.

[72] Fraisse G, Lazard M, Goupil C, Serrat J. Study of a thermoelement's behaviour through a modelling based on electrical analogy. Int J Heat Mass Transf 2010;53:3503–12. https://doi.org/10.1016/j.ijheatmasstransfer.2010.04.011.

[73] Martínez A, Astrain D, Rodríguez A, Aranguren P. Advanced computational model for Peltier effect based refrigerators. Appl Therm Eng 2016;95:339–47. https://doi.org/10.1016/j.applthermaleng.2015.11.021.

Chapter 2. Heat pipes as TEM-air heat exchangers

The SMART CLIMA -1 project (funded by the Government of Navarre - PT050/2016).) was the result of the collaboration of the CENER technology center, the Public University of Navarra and the company SIBER, specialized in ventilation solutions for the domestic sector. The main objective of the project was the construction of a prototype of a thermoelectric heat pump that could be integrated with SIBER's double-flow ventilation systems from a very practical perspective.

The first task was the study of all the potential integration possibilities of the heat pump with the ventilation flows in one dwelling, concluding, as detailed in the previous section, that the most suitable alternatives are the interconnection combined with the HRU and, on the other hand, the replacement of the HRU by the TeHP.

The next task was the selection of the TEMs, based on a benchmark of various manufacturers and suppliers. After analyzing the efficiency and cooling capacity of various alternatives, including flatness (which may determine the adjustment with the heat exchangers), the HP-127-1.4-1.15-71 model was selected, a high-performance TEM, fabricated by TE Technology. This 40 mm x 40 mm x 3.4mm model has a maximum cooling capacity of 80 W, presenting a complete documentation of its energy performance for different supply voltages and temperature gaps between TEM sides.

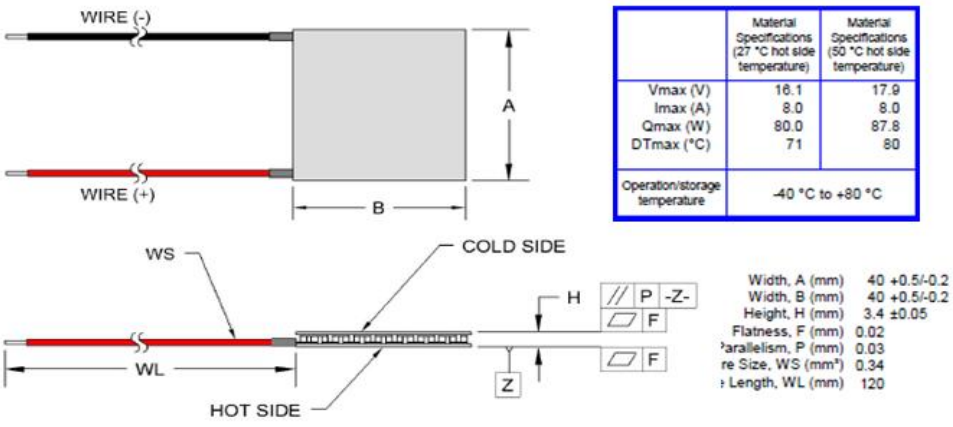

	Material Specifications (27 °C hot side temperature)	Material Specifications (50 °C hot side temperature)
Vmax (V)	16.1	17.9
Imax (A)	8.0	8.0
Qmax (W)	80.0	87.8
DTmax (°C)	71	80
Operation/storage temperature	-40 °C to +80 °C	

Width, A (mm)	40 +0.5/-0.2
Width, B (mm)	40 +0.5/-0.2
Height, H (mm)	3.4 ±0.05
Flatness, F (mm)	0.02
Parallelism, P (mm)	0.03
re Size, WS (mm²)	0.34
Length, WL (mm)	120

Figure 25. Dimensions and peformance of HP-127-1.4-1.15-71. Source: TE Technology.

All the empirical studies performed by the current Ph. D. dissertation are based on this TEM model.

On the other hand, the design of the heat pump is subject to several practical questions, which were raised by the ventilation company. The volumetric air flow must reach 130 m^3/h to satisfy the maximum ventilation requirements of an apartment of up to 100 m^2.(which is normally 100 m^3/h). The current trend of heat exchangers in the domestic sector for apartment blocks is the installation in the false ceiling, generally in the kitchen, with access to the outside through the terrace or the façade, and the interior distribution of the ventilation ducts through the false ceiling of the corridor. Additionally, power supply and access to sewage are necessary to drain the water condensation in the chilled air channel. This involves two determining factors: on the one hand, reduced weight (as a reference one HRU for such air flow volumes is ~25 Kg), which allows its handling and easy anchoring to the slab; on the other hand, the width must be limited to 25 cm, so that it can be integrated into the false ceiling. Additionally, the aim was to achieve a balance between performance and cost, which would allow it to compete with vapor compression on the market.

From this point of view, it was necessary to choose a suitable TEM-air heat exchanger, allowing for a lightweight and compact design. Given that one of the virtues of thermoelectric devices is the ease switch from cooling to heating mode, a heat-exchanger capable of working as a heat or cold sink with the same characteristics was sought. For this reason, heat sinks were chosen as the first option, selecting the K91 model from the manufacturer TECNOAL for its lightness and apparent reduced thermal resistance.

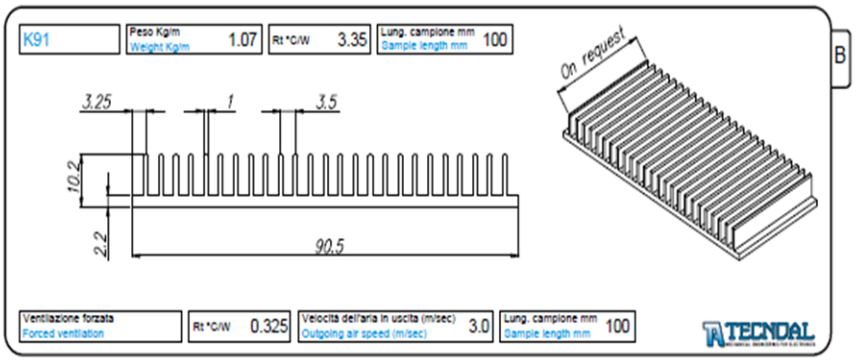

Figure 26. Dimensions and features of K91 heat sink. Source: TECNOAL.

The conceptual design carried out can be seen in Figure 27, where a cross-flow arrangement is shown. The air flow is distributed in 5 channels. In each of the fresh air channels, four K91 heatsinks exchange heat with the other two neighboring exhaust air channels through the TEMs. Each of the K91 exchangers incorporates 2 TEMs, so that a fresh air channel is heated by 8 TEMs. The rest of the surface of the K91 exchangers is insulated with an EVA foam from the neighboring exchanger. The entire TeHP is 21 x 21 x 25 cm and weights 40 Kg, employing a total of 40 TEMs.

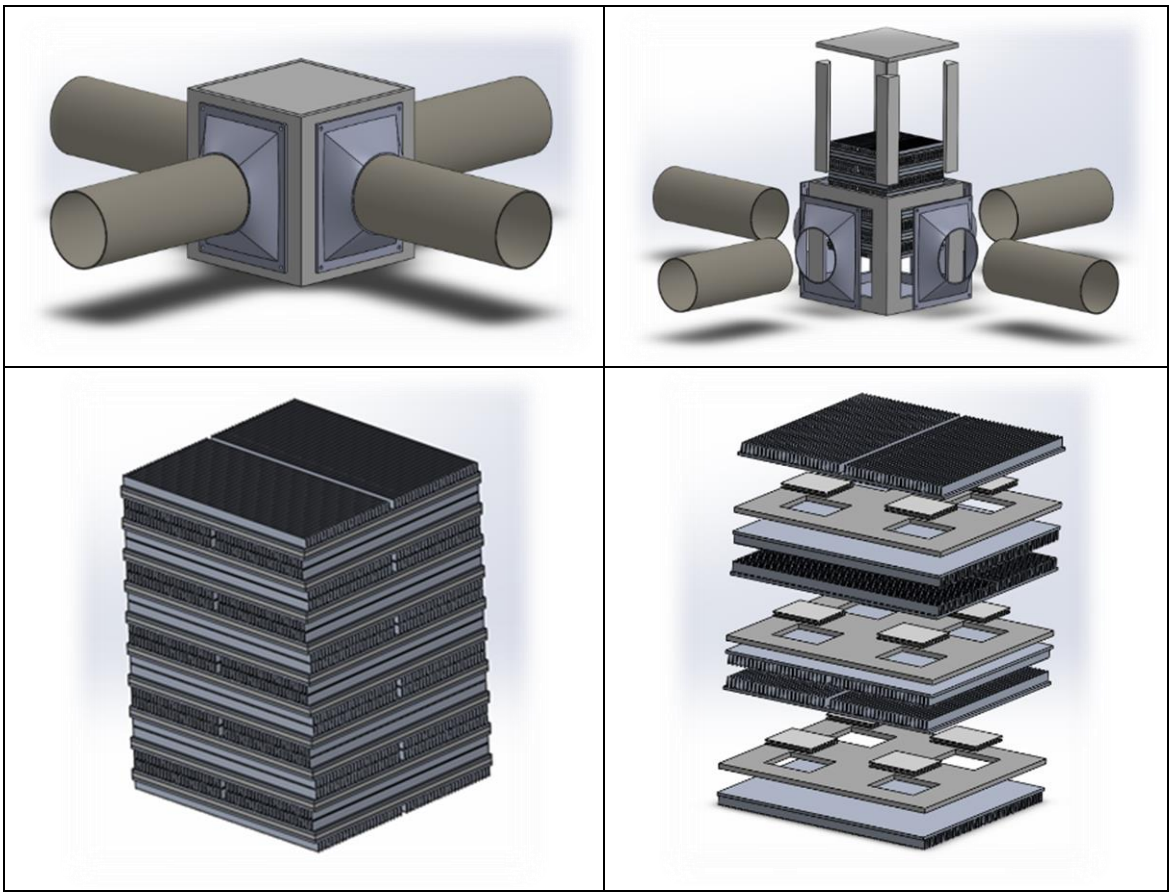

Figure 27. TeHP first prototype. Source: Project PT050/2016.

In order to empirically verify the viability of the proposed solution, a small prototype with two air channels was developed, circulating a 30 m^3/h air volumetric flow (with air directly taken from the laboratory), which is equivalent to 150 m^3/h in the original design. Inlet and outlet air temperature was measured in both air ducts, as well as the temperature on the faces of one of the TEMs and the superficial temperature of one of the heat sinks in the hot air channel (see Figure 28).

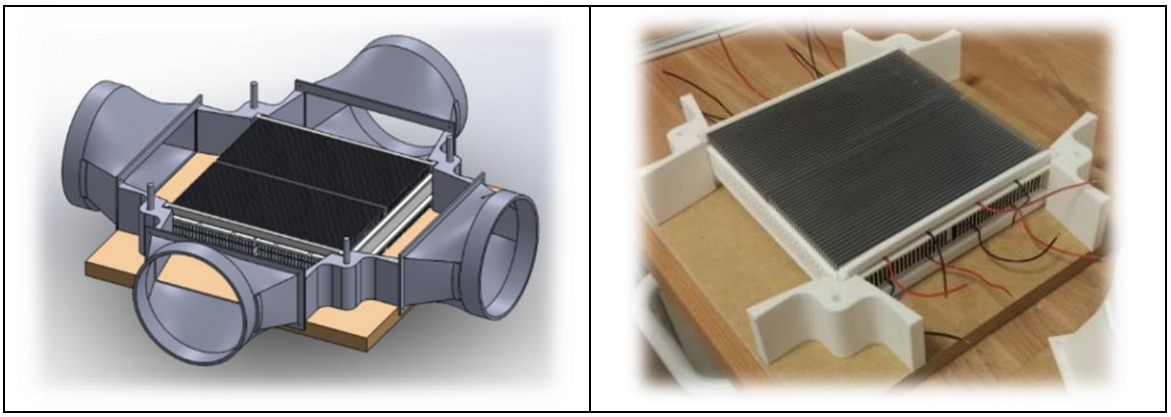

Figure 28. Built prototype for laboratory test. Source: Project PT050/2016.

The result was very poor in terms of energy performance. As shown in Figure 30, the temperature decrease in the cooled air channel is limited to 5 ° C and it drops for supply voltages higher than 7.5 V, given the deficient heat evacuation in the hot side of the TEM. The thermal resistance calculated from the measured temperatures and the heat evacuated by the hot air channel was 0.74-0.8 K/W. This thermal resistance is due, not only to the limitation of the design of the K91 heat sink, but also to the difficult assembly of the prototype. Although the tolerance of the flatness of the TEMs is guaranteed by the manufacturer, in the case of the K91, the extruded aluminum was slightly curved. At the time of disassembly, the thermal paste used for the TEM-K91 heat sink joints was non-homogeneously distributed.

The results were published in the proceedings of the 36th International Conference on Thermoelectrics, held in Pasadena (EEUU, 2017). At project level, the proposed constructive solution was discarded, given the high weight of the design and the poor energy performance, as previously shown.

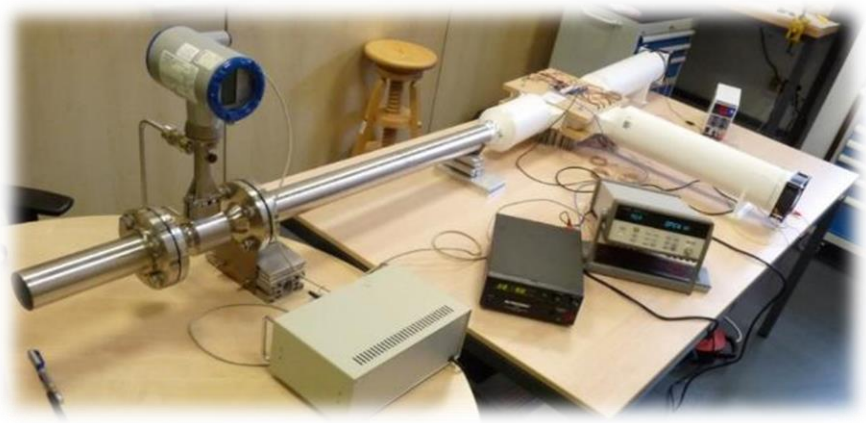

Figure 29. Lab tests of prototype-1. Source: Project PT050/2016.

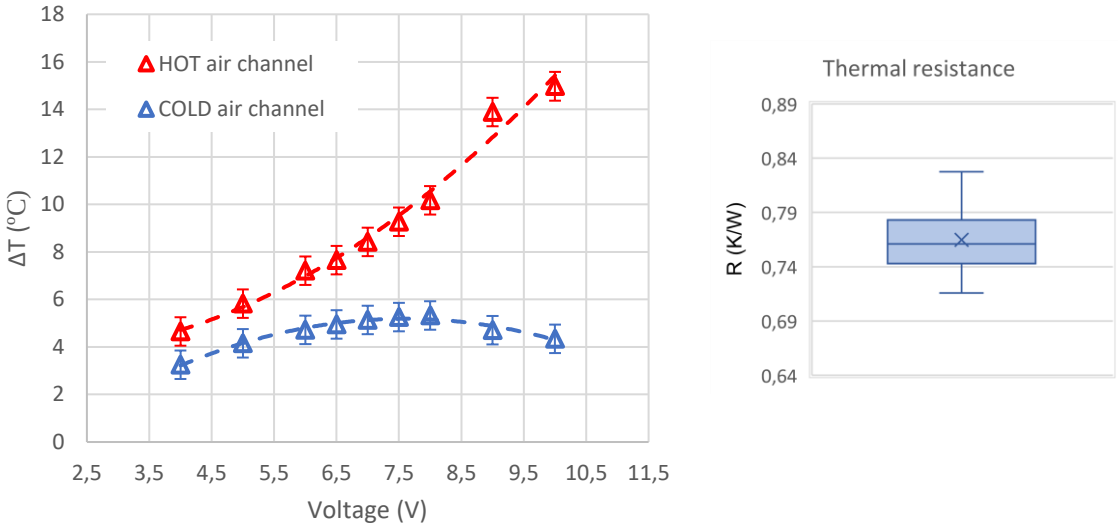

Figure 30. Left: temperature difference between inlet and outlet in both hot and cold air channels during the tests with 30 m3/h and different supply voltages. Right: estimated thermal resistance of K91 heat sink per module based on the measured superficial temperatures and the heat flux calculated with the temperature increase in the hot air channel. Source: own.

In order to improve the heat transfer between the air and the TEMs, individual heat pipes were proposed, allowing a better adjustment between TEMs and the heat pipe plates (due to the modular assembly), and the thermal behavior. The challenge, in this case, was the double dependence of the thermal resistance of the heat pipes on, not only the convection coefficient, but also the heat flow through the heat pipe, which affects to the condensation-evaporation mechanism that takes place in the fluid inside the heat-pipe. On the other hand, the design of heat-pipes, commonly marketed to evacuate heat from microprocessors, is not adapted to its use as an air channel cooler, making the system work contrary to its original conception, so that the condensation happens in the evaporator and evaporation in the condenser. For this reason, a unitary module with two heat pipes and two air ducts was built, proceeding to an in-depth study of the thermal behavior of the heat pipes. Both the methodology proposed for its empirical study, as well as the results obtained, were published in the paper: **Heat pipes thermal performance for a reversible thermoelectric cooler-heat pump for a nZEB**. (Energy & Buildings 187 (2019) 163-172. DOI: 10.1016/j.enbuild.2019.01.039) and constitute the starting point of this Ph. D. dissertation, as well as the chapter 2 of this document.

Heat pipes thermal performance for a reversible thermoelectric cooler-heat pump for a nZEB

P. Aranguren[1,2*], S. DiazDeGarayo[3], A. Martínez[1,2], D. Astrain[1,2]

[1] *Mechanical, Energy and Materials Engineering Department Public University of Navarre, 31006 Pamplona, Spain*
[2] *Smart Cities Institute, Pamplona, Spain*
[3] *National Renewable Energy Centre, 31621 Sarriguren, Spain*
[*] *e-mail:patricia.arangureng@unavarra.es*

Keywords: thermoelectric cooler; thermoelectric heat pump; nZEB; Air conditioning; computational optimization

Abstract

The nZEB standards reduce the energy demand of these buildings to a minimum, obtaining this little energy from renewable resources. Taking these aspect into consideration, a thermoelectric cooler-heat pump is proposed to achieve the comfort temperature along the whole year. The same device can provide heat in winter and it can cool down the buildings in summer just by switching the voltage supply polarity. Heat pipes are studied to work on both sides of the thermoelectric modules in order to optimize the heat transfer as these devices present really good thermal resistances and they can work in any position. However, they present pretty different thermal resistances if they work on the cold or on the hot side of the modules. A methodology to thermally characterize these heat exchangers working in both orientations is proposed and a validated computational model is developed to optimize the thermoelectric cooler-heat pump for a nZEB application. The number of thermoelectric modules, the position of the device, the ambient temperature and the air mass flow determine the operation and consequently they need to be studied in order to optimize the application.

Nomenclature

α	Seebeck coefficient	V/K
ΔT	Difference in temperature from the heat source to the heat sink	^{o}C
ρ	Density	Kg/m^3
A	Cross sectional area	m^2
$b_{R^{TEM}}$	Systematic standard uncertainty	
C_p	Specific heat	J/kgK
COP_c	Coefficient of operation of the thermoelectric cooler	
COP_{hp}	Coefficient of operation of the heat pump	
I	Current supply to the TEM	A
I_{hp}	Current supply to the heat plate	A
K	Conductance of a TEM	W/K
$\dot{m}_{air}$	Mass flow of the air	Kg/s

$\dot{Q}$	Heat flux emitted to the heat sink	W
$\dot{Q}_c$	Heat flux absorbed by the TEMs	W
$\dot{Q}_h$	Heat flux emitted by the TEMs	W
r	Electric resistivity of a TEM	Ω
R	Thermal resistance	K/W
R_h^{HP}	Thermal resistance of the hot side heat pipe	K/W
R_c^{HP}	Thermal resistance of the cold side heat pipe	K/W
$s_{\bar{R}}$	Random standard uncertainty of the mean	
T_{amb}	Ambient temperature	ºC
T_{air}	Temperature of the air	ºC
T_h	Temperature of the heat source	ºC
T_c^{TEM}	Temperature of the cold side of the TEM	ºC
T_h^{TEM}	Temperature of the hot side of the TEM	ºC
T_{air}^i	Temperature of the inlet air	ºC
T_{air}^o	Temperature of the outlet air	ºC
U_R	Expanded uncertainty	
v_{air}	Velocity of the air	m/s
V_{hp}	Voltage supply to the heat plate	V
$\dot{W}$	Power supply to the TEMs	W

1. Introduction

The International Energy Agency declared that due to rapidly growing world energy use between 1971 and 2016 the world's total final consumption was multiplied by 2.5 times [1]. The building sector consumes almost the 41 % of the world's energy consumption and constitutes roughly the 30 % of the annual greenhouse gas emissions. Residential energy use was increased in most northern and continental European countries in 2016 in response to meteorological conditions and colder climate, with reported increases between 4 and 8 % [1], meanwhile the energy demand in the building sector is expected to raise by about the 50 % in 2050, and the space cooling demand to triple between 2020 and 2050 [2]. Since buildings definitely account for a significant proportion of the total energy consumption and carbon emissions, it is necessary and urgent to decrease building energy consumption, minimizing the need for energy use through energy-efficient measures and adopting renewable energies [3]. Hence, EU regulators have published the Energy Performance of Building Directive (EPBD) which stablishes that by 2020 all new building in the EU must be "nearly-zero" energy building (nZEB), which means to reduce the building energy demand and to produce energy on building site (or nearby) [4].

The amount of the energy used in buildings for heating and cooling is approximately the 40 % of the total energy consumption, therefore and alternative energy efficient method is the main motivation of the researchers in this area [5]. Heating and cooling can be obtained by applying a voltage difference to a thermoelectric module (TEM). A thermoelectric cooler-heat pump (TECHP) is a solid-state energy converter that can create a temperature difference when an

electric potential is applied to the TEM, thanks to the Peltier effect [6]. The several advantages that these systems present, such as, high reliability, low weight, no moving parts, gas-free, no chemical reaction, environmental friendly, lengthy life spam and easiness on changing from cooling to heating mode, and vice versa [7,8], convert this technology into a promising alternative to achieve comfort into buildings, as it has been already demonstrated [9–12].

In spite of the reduced COP of thermoelectricity, due to the reduced consumption of the nZEBs, approximately 90% less energy for heating and cooling than that demanded by current building standards, the use of TECHPs for HVAC is very promising if special attention is paid to the design of the heat exchangers, which greatly influence the COP and the cooling capacity of thermoelectric systems. The COP values for heating of a thermoelectric heating and cooling unit can vary from 2.5 to 5 just by the modification of the fan speed of its ducts while the COP values for refrigeration vary from 0.4 to 1 [5]; the variation of the overall thermal conductance between 1 and 40 and the rate of thermal conductance from 0 to 2 procure an increase on the COP from 0.12 to 4.2 [11]; the use of gravity assisted heat pipes, instead of air cooled heat sinks, obtained a 64.8 % improvement in the cooling capacity [13]. Moreover, not only the heat exchanger design needs to be optimized, but also the number of TEMs and consequently their power supply in order to maximize the COP of the systems [9,14,15].

This paper presents a study of a novel TECHP including heat pipes to be located at a nZEB to obtain the comfort temperature both in winter and summer. As the thermal resistance of the heat pipes is drastically defined by their position, if they are on the hot or cold side of the TEMs, a novel thermal characterization methodology is developed. Up to now, the thermal resistances of heat pipes working as designed have been presented, but not having the evaporator at the designed condenser and vice versa, the operation of the heat pipes located on the cold side of the TEMs. This thermal characterization has been used to optimize the operation of a TECHP modifying the current supplied, the number of TEMs, the air volumetric flow and the ambient temperature thanks to the developed and validated computational model. Moreover, the obtained results are impressive for this technology.

2. Methodology for the thermal characterization of the heat pipes

A nZEB has a very high energy performance, with a nearly zero energy demand that has to be covered by energy from renewable sources produced on–site or nearby. Due to the high tightness of their envelope, mechanical ventilation is necessary in order to ensure healthiness. A waste heat recovery unit (WHR) together with a TECHP could be installed at the mechanical ventilation to obtain the comfort temperature at any time of the year. The TECHP provides heating in winter, as Figure 31 a) presents, while cooling in summer just by switching the applied voltage to the TEMs. A single TECHP system can operate both, in winter and in summer. In winter the exterior air is heated up subtracting heat from the interior air flow thanks to the applied energy to the system, as Figure 31 b) shows, while the same air flow has to be cooled down in summer, emitting heat to the interior air flow, once more thanks to the energy applied to the system.

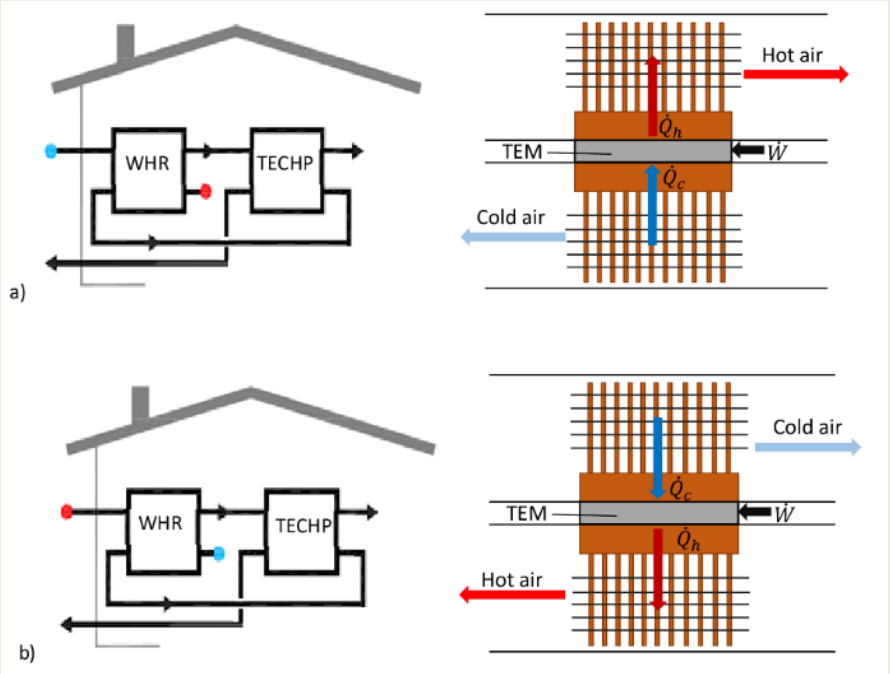

Figure 31. Thermoelectric cooler-heat pump design to be located at a nZEB, a) winter operation, b) summer operation.

A TEM is a solid-state energy converter formed by thermocouples electrically connected in series and thermally in parallel. Each thermocouple is formed by two semiconductors, one n-type and one p-type connected by metallic joints. Two ceramic plates electrically isolate the module and procure rigidity.

Bearing in mind that the heat exchangers play a very important role in the efficiency of thermoelectric systems [16,17], the use of heat pipes has been studied, as they present very good thermal resistances due to their operation principles. The TECHP proposed includes a TEM located between the two air conduits. On each side of the TEM a heat pipe in charge of emitting or absorbing the heat to or from the air flows is included, as it can be observed in Figure 32 a). The upper conduit would conduct the external air flow, once it has passed across the WHR system, to the interior of the building; meanwhile, the lower conduit would conduct the internal air flow that has passed along the WHR system to the exterior. In winter, as Figure 31 a) shows, the heat pipe that is located at the upper conduit, on the hot side of the TEM, works in conventional operation, however, the heat pipe located at the lower conduit, on the cold side of the TEM, works oppositely to its design. During summer, as Figure 31 b) shows, the upper heat pipe, located on the cold side of the TEM, works opposite to its design, while the lower one, located on the hot side of the TEM, works conventionally. Therefore, the heat pipe located on the hot side of the TEM, it does not matter if it is winter or summer, works conventionally while the one on the cold side works opposite to its design. Not only this positioning has been studied, but the same system located horizontally, both conduits laying at the same level, as Figure 32 b) presents. This configuration also presents a conventionally working heat pipe and an opposite working one, both in winter and in summer.

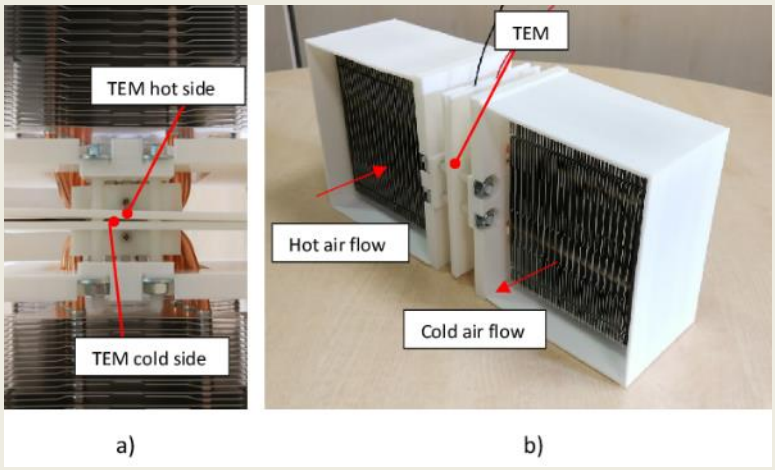

Figure 32. Thermal characterization of the heat pipes, a) detail of the location of the TEM, b) horizontal positon.

The heat pipes used have 5 copper heat pipes of diameter of 6 mm; the evaporator presents a 40 x 40 mm^2 plate to locate the TEM and condensation is helped by fins and forced convection produced by a KD1212PMS1-6A fan at each conduit. The conduits used have a diameter of 12 mm and they have been located both upstream and downstream to make sure that the air flow is ordered.

In order to thermally characterize the heat pipes working as expected and in opposite operation, a methodology has been developed. The thermal resistance of any heat exchanger can be calculated using expression (1), where ΔT stands for the difference in temperature from the heat source to the heat sink and $\dot{Q}$ is the evacuated heat to the heat sink. Thus, the temperature difference from the heat source to the heat sink needs to be known, as well as the heat flux dissipated. The heat flux emitted to the heat source could be calculated using equation (2), but unfortunately, the temperature difference between the inlet and the outlet air at these applications is normally not significant, hence the thermal resistance calculation is inaccurate.

$$R = \frac{\Delta T}{\dot{Q}} \quad (1)$$

$$\dot{Q} = \dot{m}_{air} C_p (T^i_{air} - T^o_{air}) \quad (2)$$

Therefore, the following methodology has been developed in order to accurately thermally characterize the heat pipes. Firstly, the heat pipe working as expected is characterized. To that purpose, the first assembly is done. A single heat pipe is mounted into its conduit, on its evaporator a heat plate is located. The heat plate provides a specific heat flux modifying the electrical input, and the insulation surrounding the system assures that all the heat flux created by the heat plate circulates through the heat pipe ($\dot{Q} = V_{hp} I_{hp}$). The mass flow of the air is determined measuring the velocity of the air at the duct, using an anemometer which precision and accuracy are listed on Table 5, and multiplying by the cross area and the density ($\dot{m}_{air} = v_{air} \rho A$). Figure 33 a) shows the prototype, while Figure 33 b) the diagram of the

mounting used to characterize the heat pipe. Equation (3) includes the expression used to calculate the thermal resistance of the hot side heat pipe (R_h^{HP}).

$$R_h^{HP} = \frac{T_h - T_{air}}{\dot{Q}} \tag{3}$$

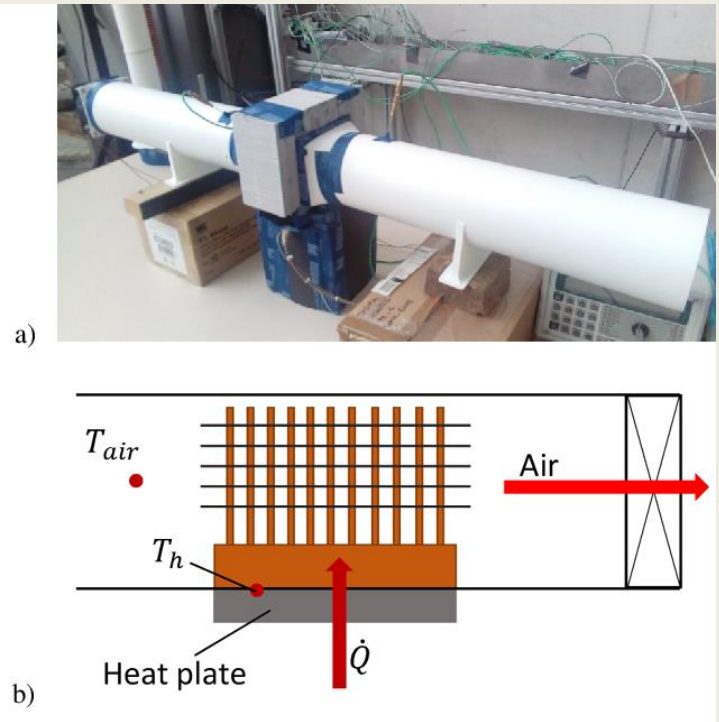

Figure 33. Assembly used to thermally characterize the hot side heat pipe, a) prototype, b) diagram of the assembly.

Table 5. Resolution and accuracy of the measurement probes used.

Sensor	Resolution	Accuracy
Temperature (ºC)	0.1	±0.5
Voltmeter (V)	0.1	±0.2
Ammeter (A)	0.01	±0.02
Anemometer (m/s)	0.01	±0.01 + 3 % measured value

The mass flow of the air ($\dot{m}_{air}$) and the heat flux to dissipate ($\dot{Q}$) determine the thermal resistance of the heat pipe, consequently different levels for both, the mass flow of the air and the heat flux to dissipate have been tested. Figure 34 presents the influence of both parameters on the thermal resistance of the hot side heat pipe for two orientations, horizontal and vertical. An increase of the heat flux to dissipate procures a reduction on the thermal resistance as the phase change heat transfer coefficients, as well as the convective coefficients, improve with an increase of the heat flux. The thermal resistance decreases from 0.194 to 0.14 K/W, a 38 % reduction, if the heat flux increases from 10 to 50 W. The air mass flow also presents a strong influence on the thermal resistance, as the convective heat transfer

coefficient determines the thermal resistance of the heat pipe, and hence improving the convective thermal resistance does have an influence on the overall thermal resistance. Looking at Figure 4 it can be concluded that the thermal resistance of the heat pipe does not change with its orientation, the maximum disagreement between thermal resistances is a 3 %, smaller than the measurement uncertainty, hence no variation of the thermal resistance is obtained if the orientation is changed.

The uncertainty study has been done through equation (4) where b_R stands for the systematic standard uncertainty, $s_{\bar{R}}$ is the random standard uncertainty and the 2 represents a confidence interval of the 95 %. The accuracies of the measurement probes can be consulted at Table 1 and the number of samples is 3 [18].

$$U_R = 2\left(b_{\bar{R}}^2 + s_{\bar{R}}^2\right)^{\frac{1}{2}} \tag{4}$$

To thermally characterize the heat pipe of the cold side of the TEM, a novel methodology is proposed. To that purpose an assembly was built, Figure 5 presents this prototype. It is formed by the two conduits, the one that introduces the external air into the building, and the one that emits the interior air of the building to the exterior. A TEM is located between the conduits and the heat pipes on both sides, one on each side respectively. The TEM is connected to a power source which can be manipulated to vary the power. Thanks to the thermal characterization of the heat pipe of the hot side, the heat flux that emits the TEM on the hot side ($\dot{Q}_h$) can be calculated if the temperatures of the hot side of the TEM and the air are known, using equation (5). The thermal resistance of the hot side heat pipe (R_h^{HP}) depends on the heat flux, hence an iterative method is used to obtain the heat flux. Knowing the heat flux emitted by the hot side of the TEM and the power supplied to the TEM ($\dot{W}$), the power absorbed by the cold side of the TEM ($\dot{Q}_c$) can be calculated using equation (6). Once this heat flux is obtained, the thermal resistance of the heat pipe located on the cold side can be calculated using equation (7).

$$\dot{Q}_h = \frac{T_h^{TEM} - T_h^{air}}{R_h^{HP}} \tag{5}$$

$$\dot{Q}_c = \dot{Q}_h - \dot{W} \tag{6}$$

$$R_c^{HP} = \frac{T_c^{air} - T_c^{TEM}}{\dot{Q}_c} \tag{7}$$

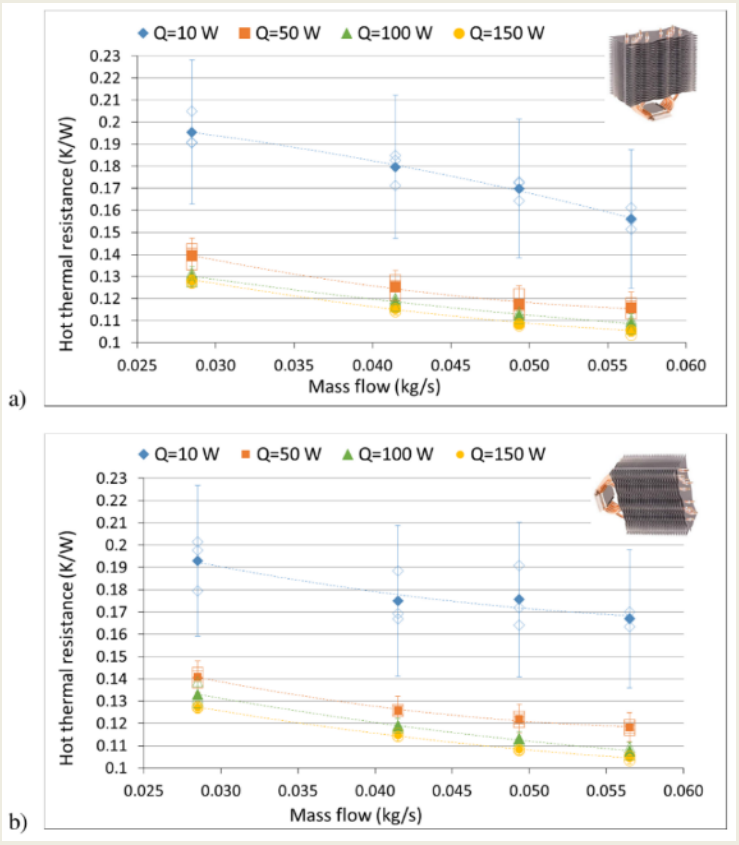

Figure 34. Thermal resistances of the hot side heat pipe, a) vertical position, b) horizontal position.

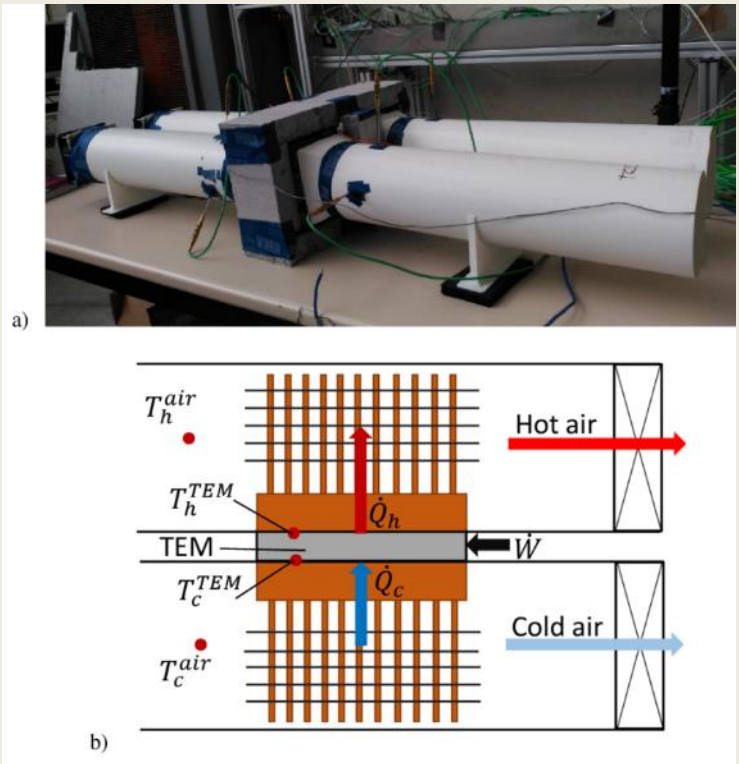

Figure 35. Assembly used to thermally characterize the cold side heat pipe, a) prototype in horizontal position, b) diagram of the assembly.

The thermal resistance of the cold side heat pipe can be observed in Figure 5, presenting two orientations, vertical position (Figure 35 a)) and horizontal position (Figure 35 b)). The heat fluxes to extract from the air flow are smaller than the ones to dissipate to the other air flow, as presented in Figure 5. The thermal resistances of the cold side heat pipe have duplicated from the ones of the hot side. When the heat pipe is located on the cold side of the TEM it has to work contrary to its design, the evaporator has to be located on the finned end of the tubes while the condenser on the plate, reducing drastically the condensation area and hence increasing its thermal resistance. Due to this operation the thermal resistance worsens drastically as it can be seen in Figure 36. Comparing Figure 36 a) and Figure 36 b), it can be concluded that the thermal resistances of the heat pipe in vertical position are better than that of the horizontal position. All the areas are similar, thus heat transfer coefficients are the responsible ones for the increase in thermal resistances. Condensation limits the overall thermal resistance, fact that is enhanced as the condensation heat transfer coefficient improves with the vertical position, as condensates leave easier the condensing area letting condensation occur. This fact is also highlighted as the thermal resistance of the cold side heat pipe is not that influenced by the air mass flow as it was the thermal resistance of the hot side heat pipe, as it is not any more the limiting one. Once more, increasing the heat flux decreases the thermal resistance, as it happened when calculating the thermal resistance of the hot side heat pipe.

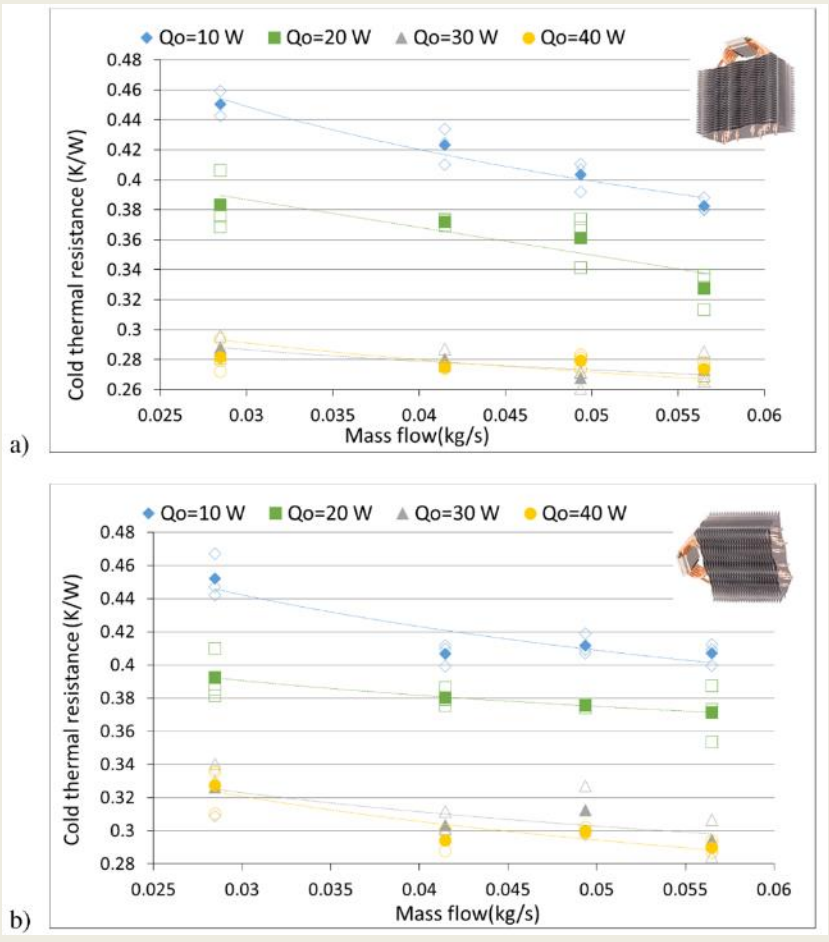

Figure 36. Thermal resistances of the cold side heat pipe, (a) vertical position, (b) horizontal position

The thermal resistance of the heat pipe gets really influenced by its operation. When two heat pipes, one on each side of the TEMs, are located, their thermal resistances are very different as their evaporators and condensers have to be swapped, harming the overall thermal resistance of the heat pipe. Hence, a study of the thermal characterization working on both sides is crucial to optimize the system.

3. Computational modelling

A model that simulates the thermoelectric behavior of the TECHP is proposed. The TECHP should be provided with heat exchangers, on both sides of the TEMs, in order to provide an optimum COP, thus the already studied heat pipes for both sides of the TEM are included into the computational model. The Engineering Equation Solver (EES) software has been used to computationally simulate the thermoelectric and the thermal phenomena. The TEMs simulated are from TE Technology, HP-127-1.4-1.15-71 which present 127 thermocouples with a cross section area of 1.4 x 1.4 mm^2 and a length of 1.15 mm [19]. As the temperatures of the heating or cooling sources are not going to drastically change, the thermoelectric properties are considered constant (at a temperature of 20 ºC), being $\alpha = 0.0541\ V/K$, $K = 0.7166\ W/K$ and $r = 1.3864\ \Omega$ for each BiTe TEM [20].

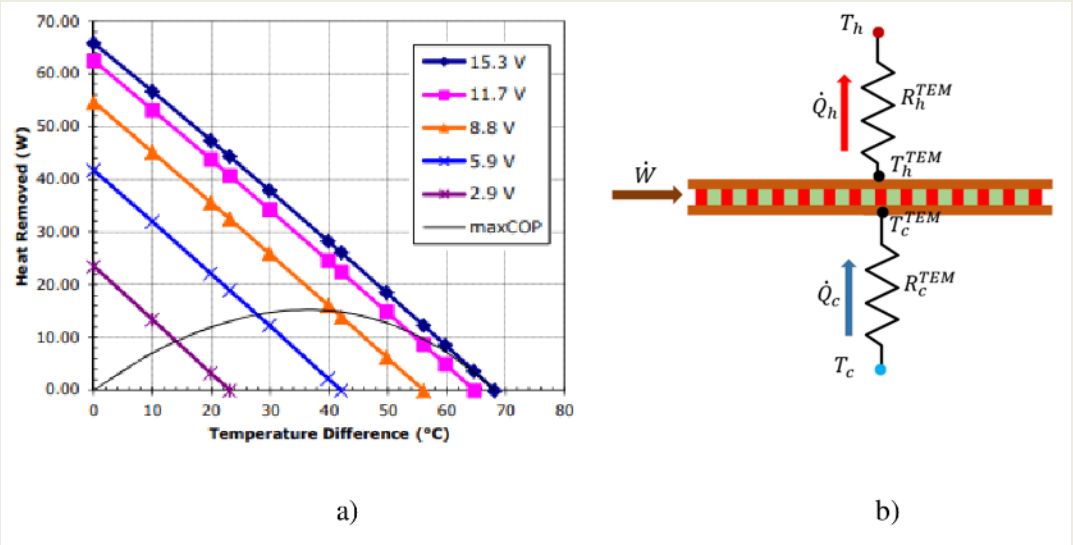

Figure 37. TECHP, a) temperature difference of the TEM in function of the applied voltage and heat removed [19], b) schematic of the TECHP.

Figure 37 a) presents the difference in temperature for the TEM as a function of the voltage applied and the heat removed. Figure 37 b) shows the schematic of the TECHP where the heat exchangers on both sides of the TEMs are present as well as the cooling and heating heat fluxes. The energy balance between the cooling or heating source and the heat exchangers can be defined by equation (8) and equation (9). The cooling and heating heat fluxes are expressed in equation (10) and equation (11), respectively, [21]. The power consumption of each TEM is calculated using equation (12), thanks to an energy balance on the TEM. The previous equations (8)-(12) have to be simultaneously met in order to solve the system, so they are all

group together by the computational program and solved, as the five equations present five unknowns (T_h^{TEM}; T_c^{TEm}; $\dot{Q}_h$; $\dot{Q}_c$; $\dot{W}$). The coefficient of performance (COP_c) of the thermoelectric cooler system evaluates the performance of the system, it is the ratio between the cooling heat flux and the consumed power, as can be seen in equation (13).

$$\dot{Q}_c = \frac{T_c - T_c^{TEM}}{R_c^{HP}} \tag{8}$$

$$\dot{Q}_h = \frac{T_h^{TEM} - T_h}{R_h^{HP}} \tag{9}$$

$$\dot{Q}_c = \alpha I T_c^{HP} - \frac{1}{2} I^2 r - K(T_h^{TEM} - T_c^{TEM}) \tag{10}$$

$$\dot{Q}_h = \alpha I T_h^{HP} + \frac{1}{2} I^2 r - K(T_h^{TEM} - T_c^{TEM}) \tag{11}$$

$$\dot{W} = \dot{Q}_h - \dot{Q}_c \tag{12}$$

$$COP_c = \frac{\dot{Q}_c}{\dot{W}} \tag{13}$$

The computational model includes the two air mass flows in counterflow arrangement, the possibility of modifying the number of TEMs used to achieve the comfort temperature within the dwelling, the thermal resistances of the heat pipes obtained in section “2. Methodology for the thermal characterization of the heat pipes”, which are a function of the heat fluxes and the air mass flow, and the possible condensation of the water vapor of the air as the temperature decreases. This model uses the values that the psychrometric chart of the wet air provides in order to account for the condensation. The enthalpy of the air flow without condensation is compared with the enthalpy at the dew point and if the first one is smaller than the second one the temperature of the air flow is recalculated including the condensation.

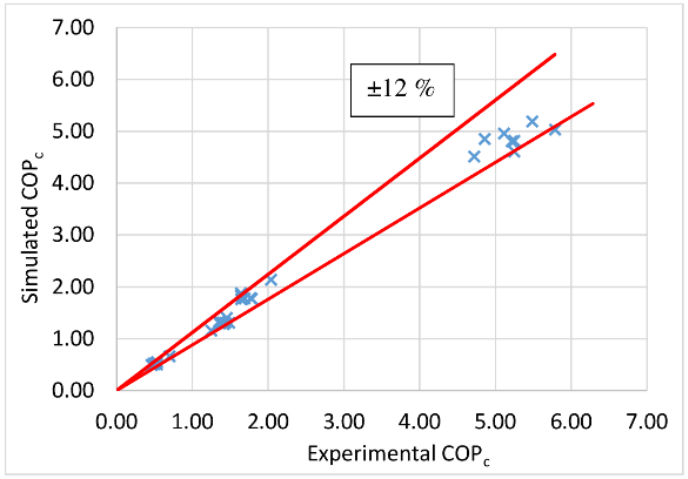

Figure 38. Simulated and experimental values of the COP.

In order to use the computational model to optimize the TECHP, firstly is validated using the obtained data from the thermal characterization of the cold side heat pipe, where the cooling heat flux was calculated to obtain the thermal resistance of the heat pipe. Four cooling heat fluxes (10, 20, 30 and 40 W) and four mass flows of the air where tested for the two configurations, horizontal and vertical position, obtaining a total of 32 experimental cases to validate the computational model. Table 2 and Table 3 include the experimental values of the cooling rate ($\dot{Q}_c$) and its experimental uncertainty, the power supplied to the TEM ($\dot{W}$) and the COP_c for the horizontal and vertical positions, meanwhile they include the computational values for the cooling rate, the consumed power and the COP_c. In order to validate the computational model a contact thermal resistance of 0.1 K/W has been added in between both heat pipes and the thermoelectric module and an electrical efficiency of the 93 %.

Table 6. Experimental and simulated results for the horizontal position used at the validation process of the computational model.

Case	Experimentation			Simulation		
$\dot{m}_{air}$ (kg/s)	$\dot{Q}_c$ (W)	$\dot{W}$ (W)	COP_c	$\dot{Q}_c$ (W)	$\dot{W}$ (W)	COP_c
0.028	10.06 ± 2.19	1.91	5.25	9.00	1.95	4.61
0.041	10.22 ± 2.40	1.73	5.79	8.97	1.78	5.03
0.049	10.31 ± 2.52	1.91	5.25	9.33	1.94	4.82
0.057	10.53 ± 2.81	1.92	5.21	9.47	1.97	4.81
0.028	19.93 ± 3.00	11.22	1.78	20.19	11.39	1.77
0.041	20.44 ± 3.00	11.31	1.77	20.86	11.67	1.79
0.049	19.71 ± 3.23	12.17	1.64	21.69	12.33	1.76
0.057	20.18 ± 3.24	11.84	1.69	21.69	12.19	1.78
0.028	29.99 ± 3.21	24.03	1.25	28.00	24.21	1.16
0.041	30.30 ± 3.67	21.24	1.41	27.48	21.46	1.28
0.049	29.83 ± 3.66	20.22	1.48	26.86	20.56	1.31
0.057	29.82 ± 3.69	20.94	1.43	27.80	21.25	1.31
0.028	39.68 ± 3.53	75.60	0.53	37.47	73.75	0.51
0.041	39.83 ± 3.87	78.62	0.51	39.59	76.09	0.52
0.049	40.31 ± 4.40	79.44	0.50	39.51	77.29	0.51
0.057	40.15 ± 4.46	57.41	0.70	37.69	56.92	0.66

The uncertainty of the cooling power has been calculated using equation (4) and the experimental tests defined in Section 2. The validated model simulates the COP with an error of the ±12 %, as Figure 8 shows.

Table 7. Experimental and simulated results for the vertical position used at the validation process of the computational model.

Case	Experimentation			Simulation		
$\dot{m}_{air}$ (kg/s)	$\dot{Q}_c$ (W)	$\dot{W}$ (W)	COP_c	$\dot{Q}_c$ (W)	$\dot{W}$ (W)	COP_c
0.028	10.23 ± 2.23	2.17	4.72	10.01	2.22	4.52
0.041	10.37 ± 2.44	2.14	4.85	9.896	2.04	4.85
0.049	10.57 ± 2.58	2.07	5.11	10.06	2.03	4.96
0.057	10.42 ± 2.78	1.90	5.49	9.88	1.90	5.19
0.028	19.50 ± 2.94	11.88	1.64	21.72	11.85	1.83
0.041	19.87 ± 2.92	12.11	1.64	22.35	12.23	1.83
0.049	19.50 ± 3.20	11.91	1.64	22.53	12.00	1.88
0.057	20.15 ± 3.24	9.89	2.04	21.13	9.89	2.14
0.028	30.60 ± 3.28	22.43	1.36	28.44	21.99	1.29
0.041	30.50 ± 3.69	21.86	1.40	28.69	21.83	1.31
0.049	30.00 ± 3.68	20.67	1.45	28.82	20.52	1.40
0.057	30.31 ± 3.75	22.42	1.35	29.65	22.22	1.33
0.028	40.29 ± 3.59	86.78	0.46	40.24	81.97	0.49
0.041	40.59 ± 3.94	76.63	0.53	40.58	73.83	0.55
0.049	39.57 ± 4.32	86.64	0.46	41.46	83.17	0.50
0.057	39.99 ± 4.45	82.08	0.49	41.45	79.09	0.52

4. Computational optimization

The validated computational model presented in the previous section simulates the behavior of a TECHP. This model is used to optimize an application where the nZEB standards are used, buildings which require very little energy for their operation, 10 W/m^2 for heating and 7 W/m^2 for cooling [22]. A room of 10 m^2 has been selected, hence in winter 100 W are necessary while in summer 70 W and the inside comfort temperature has been selected to 20 ^{o}C. To that purpose, the current of the TEMs (equation (10) and (11) is modified to meet the application criteria. A WHR system with an efficiency of the 95 % is included, as Figure 1 presents. The influence of the number of TEMs used to achieve the comfort temperature, the influence of the air volumetric flow and the position of the TECHP as well as the influence of the ambient temperature, both in summer and winter is studied using the computational model. TEMs are located one behind the other along 120 mm diameter pipes which bring the exterior air to the enclosure and conduct the interior air to the exterior, respectively.

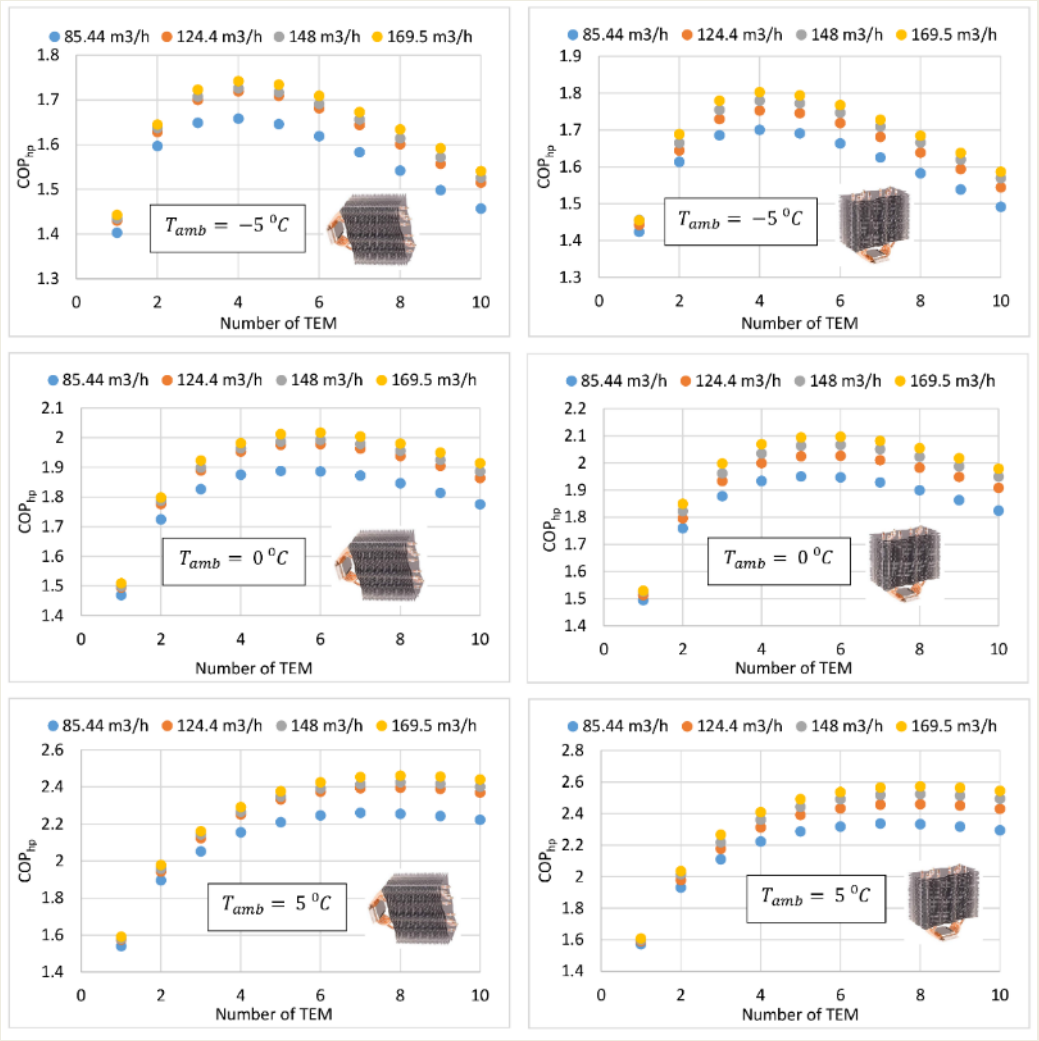

Figure 39. COP_hp for winter operation at different ambient temperatures, for different number of TEMs and air volumetric flows and for the two positions.

To test the performance of the TECHP equation (13) is used for cooling operation (in summer) while equation (14) for heating operation (in winter). As Figure 39 and Figure 40 present, the ambient temperature, the position of the TECHP, the air volumetric flows as well as the number of TEMs determine the operation of the TECHP. As the ambient temperature gets closer to the comfort temperature the COP_{hp}increases and the optimum number of TEMs varies to a greater number. Cool ambient temperatures present optimums COP_{hp} at a smaller number of TEMs, for example if the ambient temperature is $T_{amb} = -5$ ºC the optimum number of TEMs is 4 while for an ambient temperature of 5 ºC the optimum is at 8. As the number of TEMs increases, each TEM has to supply less heat to the air flow, hence each one works at a smaller current supply and thus its COP increases [23]. However, the thermal resistances of the heat exchangers located on both sides increase when the heat flux decreases, hence, an optimum for the COP can be found for each ambient temperature. When the ambient temperature is colder, the increase of the thermal resistances due to the reduction of the heat flux is more important than the reduction in the power supplied to each TEM, hence the optimum number of TEMs stays at low values. The vertical position presents

higher COPs due to the smaller thermal resistances of the heat pipes located on both sides. This configuration presents advantages for a nZEB as the TECHP is compact enough to be located on the false ceiling and it easies the parallel operation which could be really interesting for these applications.

$$COP_{hp} = \frac{\dot{Q}_h}{\dot{W}} \tag{14}$$

Figure 40 includes the operation of the TECHP in summer at different ambient temperatures, different number of TEMs, different air volumetric flows and for the two positions, horizontal and vertical. Obtaining the comfort temperature with a single TEM is not possible, thus the minimum number of TEMs is two. The same tendencies as the already mentioned for winter operation can be seen. The optimum number of TEMs shifts depending on the ambient temperature, as it is farther from the comfort temperature, the optimum number of TEMs gets smaller. The air volumetric flow has an influence on the coefficients of operation (COP_{hp}, COP_c). In both cases higher air volumetric flows procure higher COPs, as the thermal resistances of the heat pipes decrease if the air volumetric flow increases. For the horizontal position, the air volumetric flow dependency is higher than that for the vertical position, as the thermal resistances of the heat pipes vary to a greater extent if they are collocated horizontally, as Figure 4 and Figure 6 show. The vertical position procures COPs higher than the horizontal position, increases of up to 12 % are achieved in summer while 5 % in winter.

For summer and winter operation the COPs achieved are very promising, placing this technology as a strong candidate to HVAC of nZEBs. Moreover, the standards of a nZEB are to minimize the energy demand and to provide this little energy demand thanks to renewable energies. Hence, the photovoltaics and TECHPs are a very interesting synergy as both work with direct current, simplifying the electrical installation.

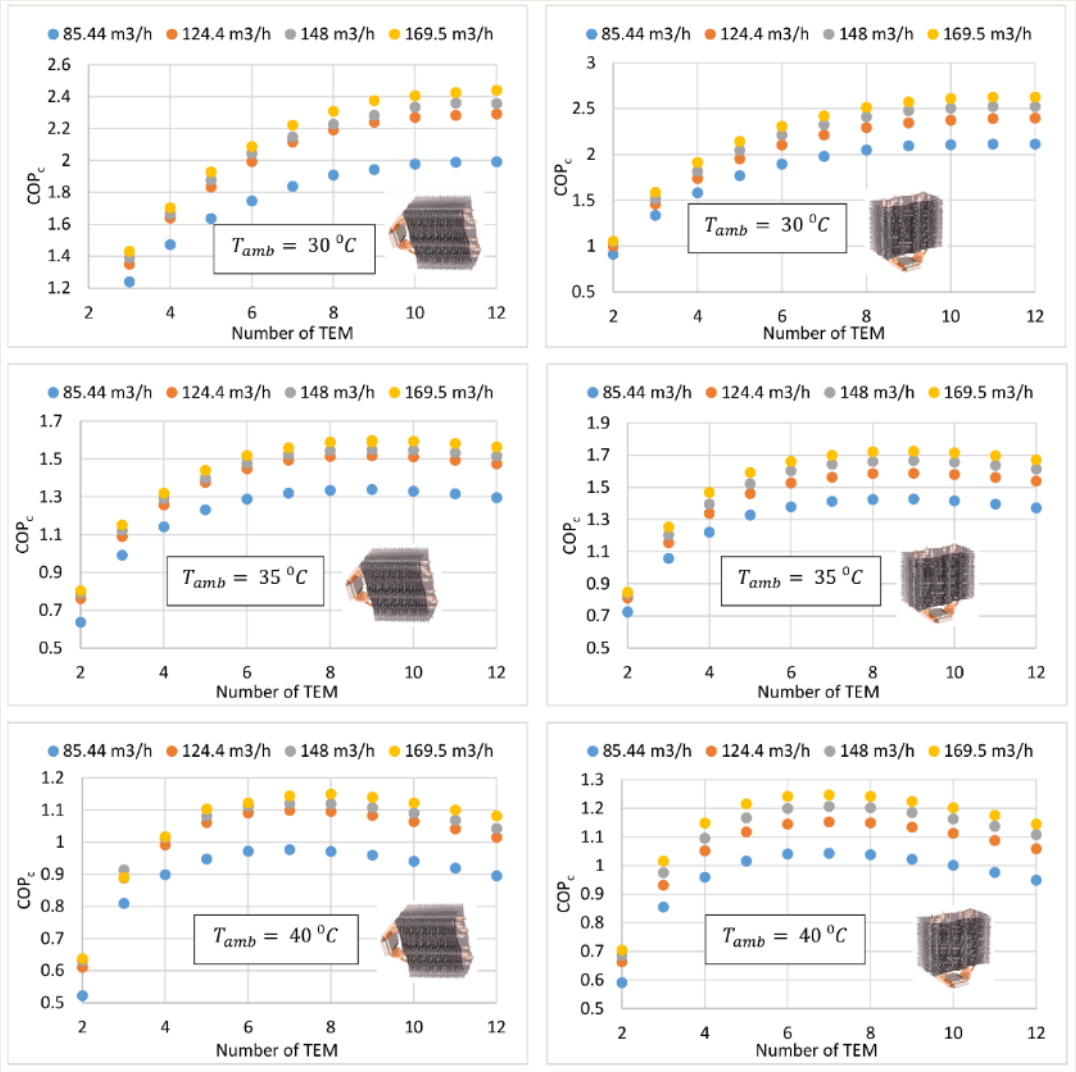

Figure 40. COP_c for summer operation at different ambient temperatures, for different number of TEMs and air volumetric flows and for the two positions.

Conclusions

The increased concern about the global warming and the rise in the pollution levels have encouraged new regulations, as the European Energy Performance of Building Directive (EPBD) which dictates public nZEB by end of 2018 and private nZEB by the end of 2020. As the energy demand of this kind of building is small, a TECHP is proposed to HVAC them, both in summer and in winter, as the same device can be used for cooling or heating just switching the power supply. To optimize the operation heat pipes have been proposed, as they present good thermal resistances and they can work both on the cold and hot sides of the TEMs. Their thermal characterization has proven that their operation gets strongly affected if located on the hot or cold side. If their evaporators need to be moved to the designed condenser, and vice versa, their thermal resistances double, hence the developed methodology as well as the thermal resistances obtained are very important to design and optimize the operation of a TECHP run with heat pipes. A validated computational model is used to optimize the TECHP provided with heat pipes on both sides of the TEMs. The number of TEMs, the ambient

temperature, the air mass flow and the position are crucial to optimize the operation. The number of TEMs presents and optimum depending on the ambient temperature, as the thermal resistances of the heat pipes increase if the heat fluxes decrease. The optimum number of TEMs decreases if the ambient temperature moves off from the comfort temperature, 20 ^{o}C.

The COPs obtained, both in winter and summer, place the thermoelectricity as a very promising technology to HVAC of nZEBs, as their energy demand is very little. The synergy between thermoelectricity and photovoltaics presents one of the solutions to cover the HVAC demand for nZEBs.

Acknowledgments

The authors are indebted to the Spanish Ministry of Economy and Competitiveness for the economic support to this work, included in the DPI2014-53158-R research project.

References

[1] I.E. Agency, World energy balances: Overview, 2018. https://webstore.iea.org/world-energy-balances-2018-overview.

[2] F. Souayfane, F. Fardoun, P.H. Biwole, Phase change materials (PCM) for cooling applications in buildings: A review, Energy Build. 129 (2016) 396–431. doi:10.1016/j.enbuild.2016.04.006.

[3] Z. Liu, L. Zhang, G. Gong, H. Li, G. Tang, Review of solar thermoelectric cooling technologies for use in zero energy buildings, Energy Build. 102 (2015) 207–216. doi:10.1016/j.enbuild.2015.05.029.

[4] O.J.E. Union, EU, Directive 2010/31/EU of the European Parliament and of the Council of 19 May 2010 on the energy performance of buildings, 2010. doi:10.3000/17252555.L_2010.153.eng.

[5] M.Z. Yilmazoglu, Experimental and numerical investigation of a prototype thermoelectric heating and cooling unit, Energy Build. 113 (2016) 51–60. doi:10.1016/j.enbuild.2015.12.046.

[6] K. Irshad, K. Habib, F. Basrawi, N. Thirumalaiswamy, R. Saidur, B.B. Saha, Thermal comfort study of a building equipped with thermoelectric air duct system for tropical climate, Appl. Therm. Eng. 91 (2015) 1141–1155. doi:10.1016/j.applthermaleng.2015.08.077.

[7] A. Rincón-Casado, A. Martinez, M. Araiz, P. Pavón-Domínguez, D. Astrain, An experimental and computational approach to thermoelectric-based conditioned mattresses, Appl. Therm. Eng. 135 (2018) 472–482. doi:10.1016/j.applthermaleng.2018.02.084.

[8] S.B. Riffat, X. Ma, Thermoelectrics: A review of present and potential applications, Appl. Therm. Eng. 23 (2003) 913–935. doi:10.1016/S1359-4311(03)00012-7.

[9] Y.W. Kim, J. Ramousse, G. Fraisse, P. Dalicieux, P. Baranek, Optimal sizing of a thermoelectric heat pump (THP) for heating energy-efficient buildings, Energy Build. 70 (2014) 106–116. doi:10.1016/j.enbuild.2013.11.021.

[10] L. Shen, X. Pu, Y. Sun, J. Chen, A study on thermoelectric technology application in net zero energy buildings, Energy. 113 (2016) 9–24. doi:10.1016/j.energy.2016.07.038.

[11] Y. Cai, S.J. Mei, D. Liu, F.Y. Zhao, H.Q. Wang, Thermoelectric heat recovery units applied in the energy harvest built ventilation: Parametric investigation and performance optimization, Energy Convers. Manag. 171 (2018) 1163–1176. doi:10.1016/j.enconman.2018.06.058.

[12] Z.B. Liu, L. Zhang, G.C. Gong, Y.Q. Luo, F.F. Meng, Experimental study and performance analysis of a solar thermoelectric air conditioner with hot water supply, Energy Build. 86 (2015) 619–625. doi:10.1016/j.enbuild.2014.10.053.

[13] X. Sun, L. Zhang, S. Liao, Performance of a thermoelectric cooling system integrated with a gravity-assisted heat pipe for cooling electronics, Appl. Therm. Eng. 116 (2017) 433–444. doi:10.1016/j.applthermaleng.2016.12.094.

[14] D. Astrain, P. Aranguren, A. Martínez, A. Rodríguez, M.G. Pérez, A comparative study of different heat exchange systems in a thermoelectric refrigerator and their influence on the efficiency, Appl. Therm. Eng. 103 (2016). doi:10.1016/j.applthermaleng.2016.04.132.

[15] A. Attar, H.S. Lee, Designing and testing the optimum design of automotive air-to-air thermoelectric air conditioner (TEAC) system, Energy Convers. Manag. 112 (2016) 328–336. doi:10.1016/j.enconman.2016.01.029.

[16] P. Aranguren, D. Astrain, A. Rodríguez, A. Martínez, Net thermoelectric power generation improvement through heat transfer optimization, Appl. Therm. Eng. 120 (2017) 496–505. doi:10.1016/j.applthermaleng.2017.04.022.

[17] M.F. Remeli, L. Tan, A. Date, B. Singh, A. Akbarzadeh, Simultaneous power generation and heat recovery using a heat pipe assisted thermoelectric generator system, Energy Convers. Manag. 91 (2015) 110–119. doi:10.1016/j.enconman.2014.12.001.

[18] H.W. Coleman, W.G. Steele, Experimentation, Validation, and Uncertainty Analysis for Engineers, 3rd ed, John Wiley & Sons, New Jersey, 2009. http://eu.wiley.com/WileyCDA/WileyTitle/productCd-0470168889.html (accessed February 16, 2016).

[19] TETechnology, HP-127-1.4-1.15-71 dataheet, (2018). https://tetech.com/wp-content/uploads/2013/09/HP-127-1.4-1.15-71.pdf (accessed December 17, 2018).

[20] A. Martínez, D. Astrain, A. Rodríguez, P. Aranguren, Advanced computational model for Peltier effect based refrigerators, Appl. Therm. Eng. 95 (2016) 339–347.

[21] D.M. Rowe, CRC Handbook of Thermoelectrics, New York. 16 (1995) 1251–1256. doi:10.1016/S0960-1481(98)00512-6.

[22] IDAE, Guia del estandar Passivhaus. Edificios de consumo energético casi nulo, 2011. https://www.fenercom.com/pdf/publicaciones/Guia-del-Estandar-Passivhaus-fenercom-2011.pdf.

[23] D. Astrain, A. Martínez, J. Gorraiz, A. Rodríguez, G. Pérez, Computational study on temperature control systems for thermoelectric refrigerators, J. Electron. Mater. 41 (2012) 1081–1090. doi:10.1007/s11664-012-2002-0.

Chapter 3. TeHP experimental results

The analysis carried out with the heat pipes, and whose main conclusions were reported in Chapter 2, was the main reason to prorogue the research project SMART CLIMA -1, with a second edition: SMART CLIMA -2 (funded by the Government of Navarre – PT009/2017), where a 2nd Prototype of air-to-air thermoelectric heat pump with heat pipes was proposed.

This protype is composed of 10 modules with 10 TEMs, aiming at reaching the heating load of a 100 m^2 dwelling. After constructed, this TeHP was tested in the same laboratory as the first prototype, blowing into both air ducts the air from the lab at same temperature. The results were significantly better in this case, increasing the temperature gap between inlet and outlet in the cold air duct, from 5 °C in the first prototype, to 8.5 °C, in this second prototype, and showing a growing tendency up to 12 V supply (see Figure 41).

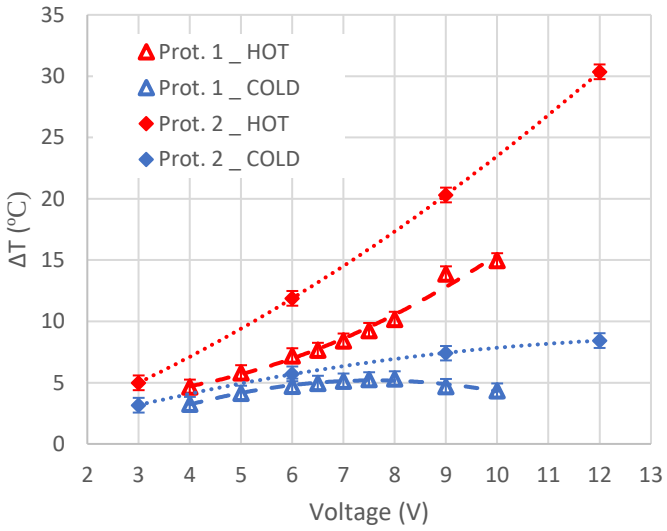

Figure 41. Temperature gap between inlet and outlet of hot and cold air ducts (150 m^3/h) in the two prototypes developed under SMART CLIMA research project (PT050/2016 & PT090/2017). Source: own.

This prototype was not only better in terms of energy performance, but it also improves the indicators related to the constructive characteristics and manageability. On the one hand, the modular design and the one-by-one TEM-heat exchanger adjustment facilitate the fabrication. On the other hand, the final TeHP weight is lower, 15 Kg compared with the estimated 40 Kg for the first prototype, and about 20-25 Kg of a regular HRU. Moreover, the thickness of the TeHP is 16.5 cm without insulation, compared with 25 cm of the first prototype, what greatly helps with its integration in false ceilings. Finally, the better energy performance is reached with 4 times less TEMs than in the first prototype.

Table 8. Features of the TeHP prototypes developed in the frame of SMART CLIMA project (PT050/2016 & PT090/2017).

	1st Prot.: HEAT SINKS	**2nd Prot.: HEAT PIPES**
Number of TEMs	10	40
Weight (Kg)	40	15
Thickness (cm)	25	16.5
Max. temp gap in the cooling air duct (°C) (150 m^3/h)	5	8.5

Once the heat pipes proved to be a better heat exchanger option for this particular application, the next step was the empirical analysis of the performance of the TeHP, with different temperature gaps between indoor and outdoor air circumstances, as in a real case, but in a controlled environment where stationary conditions can be reached, and proper measurement equipment can be installed. To this aim, this 2nd protype was analyzed in the Public University of Navarre, where an in-depth study of the TeHP was carried out with the help of a climatic chamber. Both, the methodology proposed for its empirical study, as well as the results obtained, were published in the paper: **Prototype of an air-to-air thermoelectric heat pump integrated with a double flux mechanical ventilation system for passive houses**. (Applied Thermal Engineering 190 (2021) 116801. DOI: 10.1016/j.applthermaleng.2021.116801) and constitute the chapter 3 of this document.

Prototype of an air to air Thermoelectric Heat Pump integrated with a double flux mechanical ventilation system for Passive Houses

S. DiazDeGarayo[1], A. Martínez[2,3], P. Aranguren[2,3], D. Astrain[2,3]

[1] *National Renewable Energy Centre, 31621 Sarriguren, Spain*
[2] *Engineering Department Public University of Navarre, 31006 Pamplona, Spain*
[3] *Smart Cities Institute, Pamplona, Spain*
[*] *e-mail: sdiaz@cener.com*

Keywords: thermoelectricity, heat pump, passive house, HVAC, heat recovery

Abstract

This paper describes the design of an air-to-air thermoelectric heat pump for its integration with a double flux mechanical ventilation system for domestic use in Passive House standard. The prototype has been built and thermally characterized in a test bench reproducing winter and summer conditions, with different gaps between indoor and outdoor temperatures. In addition, two different integration possibilities have been analyzed and tested: a stand-alone installation and the combination with a heat recovery unit.

This prototype is composed of 10 thermoelectric modules and finned heat pipes to transfer the heat between the modules and the incoming and outgoing ventilation flows. The maximum heating capacity with 12V supply was proven to be 1,250 W for heating and 375 W for cooling, with COPs ranging 1.5-4 and 0.5-2.5 respectively. Results show the variations in the performance of the thermoelectric heat pump depending on the voltage supply (3-12V), the air flows (55-130 m3/h) and the temperature gaps between them.

This paper demonstrates the convenience of combining passive and active heat recovery technologies (thermoelectric pump coupled to a heat recovery unit), bringing improvements on the thermal power higher than 25 % for heating and 10 % for cooling, with respect to the thermoelectric heat pump working directly between the incoming and outgoing air flows. The COP is also increased, especially for low energy demands, when the voltage is 3-6 V. In these cases, the COP might be improved by 50 % for heating and 30 % for cooling.

Acronym list

TEM	thermoelectric module	
TeHP	thermoelectric heat pump	
HRU	heat recovery unit for double flux ventilation systems in buildings	
HP	heat pipe	

Nomenclature

α	Seebeck coefficient of a TEM	V/K
ρ_{air}	Density of the air	kg/m^3
b_R	Systematic standard uncertainty	
C_p	Specific heat of the air	J/kgK
COP_h	Coefficient of operation of the TeHP for heating	
COP_c	Coefficient of operation of the TeHP for cooling	
I	Current supply to the TEMs	A
K	Thermal conductance of a TEM	W/K
$\dot{m}_{air}$	Volumetric air flow	m^3/s
$\dot{Q}_c$	Heat flux absorbed by the THP	W
$\dot{Q}_h$	Heat flux emitted by the THP	W
$\dot{Q}_c^{i,TEM}$	Heat flux absorbed by the TEM	W
$\dot{Q}_h^{i,TEM}$	Heat flux emitted by the TEM	W
r	Electric resistivity of a TEM	Ω
R_c^{HP}	Thermal resistance of the cold side heat pipe	K/W
R_h^{HP}	Thermal resistance of the hot side heat pipe	K/W
$s_{\bar{R}}$	Random standard uncertainty of the mean	
$T_c^{i,TEM}$	Temperature of the cold side of the TEM in the intermediate module	K
T_c^i	Temperature of the cooling air in the intermediate module	K
$T_c^{i,IN}$	Inlet temperature of the cooling air in the intermediate module	K
$T_c^{i,OUT}$	Outlet temperature of the cooling air in the intermediate module	K
T_c^{IN}	Inlet temperature of the cooling air stream in the TeHP	K
T_c^{OUT}	Outlet temperature of the cooling air stream in the TeHP	K
$T_h^{i,TEM}$	Temperature of the hot side of the TEM in the intermediate module	K
T_h^i	Temperature of the heating air in the intermediate module	K
$T_h^{i,IN}$	Inlet temperature of the heating air in the intermediate module	K
$T_h^{i,OUT}$	Outlet temperature of the heating air in the intermediate	K
T_h^{IN}	Inlet temperature of the heating air stream	K
T_h^{OUT}	Outlet temperature of the heating air stream	K
U_R	Expanded uncertainty	
V	Voltage supply to the TEMs	V
$\dot{W}^{TEM}$	Power supply to the TEMs	W
$\dot{W}$	Power supply to the THP	W
$\dot{W}_{fan}$	Power supply to the fans	W

1. Introduction

Buildings are responsible for approximately 40% of EU energy consumption and 36% of the CO2 emission [1].This sector is actually the single largest energy consumer in Europe and, hence, a significant player in the achievement of the targets of the 2030 climate and energy framework, aiming at cutting 40% of green gas emissions (from 1990 levels) [2]. In order to boost energy performance of buildings, the EU has established a legislative framework that includes the Energy Performance of Buildings Directive 2010/31/EU (EPBD [1]) and the Energy Efficiency Directive 2012/27/EU [3][4]). These regulations promote a new energy standard called nZEB (nearly ZERO ENERGY BUILDING), obligatory since 2020. This new standard reduces the energy demand of buildings by improving thermal envelop and increasing the in-situ production of renewable energy sources (RES).

In addition to this reduction of heating power demand given by the new regulation, the European Environmental Agency (EEA) reports significant changes in the heating and cooling loads in buildings due to climate change. Heating degree days (HDD) decreased by 6 %, whereas cooling degree days (CDD) increased by 33 % between the periods 1950–1980 and 1981–2017. According to EEA, the trend of reduction of HDD and the increase of CDDs will continue [5].

New better insulated buildings will, hence, require less heating but more cooling. In this context, heat pumps are expected to experience a strong deployment in the coming years [6].

Thermoelectricity is a very promising heat pump technology that presents many advantages: no moving parts, no refrigerants, reliability, scalability, minimum maintenance, easy transition from heating to cooling mode, easy and accurate temperature control and PV integrability among others[7]. Its main disadvantage is the low coefficient of performance (COP), compared with vapor compression technology. In this new scenario of low energy demand required by nZEBs, the cited advantages may outweight the low values of COP.

Many review articles ([8], [9], [10]) have examined the published research studies aiming at integrating thermoelectric heat pumps (TeHP) in buildings trying to maximize the energy performance by identifying favorable heat sinks to provide comfort inside. Most of these studies propose the integration with the thermal envelope (windows, walls, roofs and ceilings), and only some of them combine TeHPs with the air flows in the building.

Most of the reviewed studies are theoretical and only some of them present experimental tests with prototypes, that will be the focus of present analysis.

The review starts in 2006, when S.B. Riffat presented a small TeHP (290 W heating and 70W cooling) with a thermal diode to climatize the indoor air but no specific coupling with the air ventilation [11].

In 2009 Tao Li et al. [12] proposed a TeHP prototype with plate aluminum heat exchangers and cross air flow (60-70m^3/h). Aware of the influence of thermal resistance of heat exchangers in the energy performance of the assembly, this research group presented an evolved prototype [13] including heat pipes. The air flow is still 60 m^3/h and during tests the TeHP was regulated to match outside air temperature with indoor temperature, and thus, with no aim of extra-

heating/cooling the inside. Further studies were carried out to apply TeHP in order to design warm air heaters for bathrooms [14], and more recently this active group integrated the TeHP (53 m^3/h) model with a PVT, working as preheater [15]. The prototype works only for heating and was tested two days: one sunny day and one rainy day, assessing the influence of the radiation in the final performance.

In 2013, Kim et al. [16] suggested the integration of a TeHP with an exhaust/supply HX and an air-to-air heat exchanger in a theoretical study. The internal heat exchangers between the thermoelectric modules (TEMs) and the air are supposed to be finned aluminum with a fix thermal resistance value. In these conditions the researchers find that there is an optimal number of TEMs and electric current to meet a certain heating demand. This theoretical study was further refined with a deeper analysis [17] and the proposal of analytical methods for the design of TeHPs including heat exchangers ([18], [19]).

In 2015 Irshad et al. [20] designed a thermoelectric airduct system to cool a 2.8 m x 2.7 m x 2.5 m test room in a tropical climate. The air duct dissipates heat with outside air and the cooled air flow is drawn into the room. TEMs are directly in contact with cooled air, and the hot side is coupled with some finned aluminum dissipators. This experience was completed with a MATLAB-TRNSYS computational model [21] and further integrated with a PV in-site facility [22].

A similar system was developed by Zeki [23] in 2016 with two antisymmetric ducts and the aim of working as both heater and cooler. Both sides of the TEMs are coupled with aluminum finned heat sinks and the research is strongly focused on the air movement inside the duct, including ANSYS Fluent simulation and thermography.

In 2017 Wang et al. [24] developed a small prototype of 3 TEMs to heat an insulated 1 m^3 box. Again, aluminum fin sinks are used as heat exchangers, but there is no ventilation in the experimental test (the box is closed and airtight). The temperature inside is monitored until it reaches the set point. The conclusions of this study are very optimistic about the possibility to apply TeHP technology in British climate.

More recently, in 2018, Cai et al. [25] carried out a parametric theoretical investigation of thermoelectric heat recovery units applied to buildings, and one year later proposed an active thermoelectric ventilation system for built space cooling [26], including a one TEM experiment to validate the computational simulation. This research combines a thermodynamic model for the thermoelectric cooling effect and the methodology of Effectiveness-Number of Transfer Units methodology.

As a conclusion of present review, all the literature underlines the potential of thermoelectricity for the air conditioning of buildings. Most of the reviewed studies ([8], [9], [10]) are theoretical and only some of them present experimental tests (see Table 9), that mostly focus on validating the proposed mathematical models.

There is, consequently, the need for deeper experimental studies at a higher scale to meet the heating/cooling demand of a nZEB, taking into account the uncertainty of experimental tests

[27]. Moreover, as previously stated, the future will demand the ability to switch between building heating and cooling mode, which only applies to a few of the reviewed references.

Table 9. Review of TeHP prototypes applied to building heating/cooling

REFERENCE	POWER	AIR FLOW	COP_{HEAT}/ COP_{COOL}	REMARKS
S. B. Riffat 2006 [11]	8 TEMs 290W heat 70 W cool	N/A (no air exchange)	1.2-1.4 0.2-0.8	• One thermal diode separates inside and ouside heat sinks • Winter test: 18°C inside and 1-9°C outside • Summer test: 21°C inside and 23-31°C outside
Tao Li et al. 2009 [12]	10 TEMs 490W heat 530W cool (as shown in fig. 2 and 6 of the report)	60-70 m^3/h	2.5 2.5	• Crossed air flows • Combines flat-fin sensible heat exchanger within the same device • Winter test: variable 15-23°C inside and 6-8°C outside • Summer test: variable 22-24°C inside and 35-40°C outside
Tianhe Han et al. 2014 [13]	12 TEMs Not specified	60 m^3/h	2.2-4.16 1.1-4.78	• Heat pipes for TEM-air heat exchange • Winter test: outside temperature ranges 6-14°C, and THP is regulated to reach 20°C of fresh air. • Summer test: outside temp. is 30-35°C and the output fresh air temp is 26°C.
ZhongBing Liu et al. 2018 [15]	12 TEMs 117.3-248.3 W for TEV 75-400W for PVT	53 m^3/h	Comb. PVT-TEV 1.73 (rainy) 6.4 (sunny)	• Only HEATING • PVT preheating of air flow • Heat pipes for TEM-air heat exchange • Winter: outside temperature 4.0-5.3°C and 15.5°C inside.
Irshad et al. 2015 [20]	24 TEMs 350-650W	Not specified	0.6-0.9	• Only COOLING • Direct contact PEM-air for cooling duct and finned Al. dissipattors for heating duct • 12h test with ambient temp. ranging 24-34°C and set point inside the room 24-28°C.
M. Zeki Yilmazoglu 2016 [23]	1 TEM 53.2W heat 9.35W cool	5.6-11.7 m^3/h (hot) 5.9-14.2 m^3/h (cold)	2.5-5 0.4-1	• Finned Al. dissipators • Air flows are drawn into the THP from same room. Inlet temp for heating ~25°C and ~26°C for cooling.

Chend Wang et al. 2016 [24]	3 TEM Not specified	Not applicable	Above 1.8	• Only HEATING • No ventilation coupling • Al. finned heat sinks • 1m^3 enclosed test box • Transient values reported at different voltages • 1-5°C ambient temperature

Finally, most of these tests do not consider the effect of the integration of a heat recovery unit (HRU) that reverses the temperature of exhaust and fresh air flows.

HRUs work as passiv heat recovery systems to mitigate the energy consumption by transferring heat between outgoing and incoming ventilation air flows [28] (but never reaching the set point inside the building). TeHPs and HRUs can be combined integrating both technologies, passive and active heat transfer to enhance the cooling and heating capacity of the ventilation system.

Hence, the objetive of this paper is to design, build and assess the energy performance of a TeHP for the domestic sector in a nZEB. The TeHP is assumed to be integrated with the exhaust/supply mechanical ventilation system of the nZEB, considering two possible configurations: stand-alone installation or combination with an HRU.

Next section 2 focuses on the design of this prototype, that must meet operational design conditions, such as a low weight and reduced dimensions to be successfully integrated with the ventilation systems in false ceilings, coupled or not with an air-to-air heat recovery unit (HRU).

Section 3 describes the methodology employed to thermally characterize the TeHP under test conditions. Both winter and summer conditions have been analyzed, with different gaps between indoor and outdoor temperatures.

Section 4 presents and discusses the obtained results, and final conclusions are reported in section 5.

2. THP Prototype Description

The design of the TeHP is based on the Passive House idea of providing indoor thermal comfort (ISO 7730) by only post-heating or post-cooling the fresh air mass, which is required to achieve sufficient indoor air quality conditions.

In a Passive House certified building the envelope assures a high insulation level, free of thermal bridges, and good quality windows. In addition, an airtight layer and an HRU reduce the thermal losses due to the indoor air change. Under these circumstances, the heating and cooling loads of the building are limited to 10 W/m², irrespective of the climate [29].

In such conditions, raising or lowering the temperature of the incoming fresh air after the HRU might be a solution to meet the heating/cooling need of the building. Besides, the ventilation serves as heating/cooling distribution system.

This prototype is planned to HVAC a dwelling for 1-4 bedrooms, which corresponds to a range of air volumetric flow of 55 - 130 m^3/h [30].

In line with the Passiv House principle, the TeHP will be integrated with an exhaust/supply double flux mechanical ventilation system. As previously mentioned, the ventilation system commonly incorporates an HRU in order to recover the waste heat from the exhaust air ([31], [28]) with and efficiency ranging 80-95% [32].

Instead of this, this paper proposes two alternative strategies: the sole installation of a TeHP for an active heat recovery from exhaust air (replacing the HRU), or the installation of both: the HRU and the TeHP, so that the TeHP continues at absorbing heat from exhaust air once both air streams have gone through the HRU. In summertime the heat flows are reversed.

The heat transfer between air streams is induced by the thermoelectric modules (TEMs), One TEM is an energy converter able to absorb heat from a cold reservoir ($\dot{Q}_c$) and emit heat to a hot one ($\dot{Q}_h$) by consuming DC electric power ($\dot{W}$). Internally, TEMs are composed by thermocouples electrically connected in series and thermally in parallel. This prototype includes TEMs provided by TE Technology (HP-127-1.4-1.15-71), with 127 BiTe thermocouples (1.4x1.4x1.15mm) each [33].

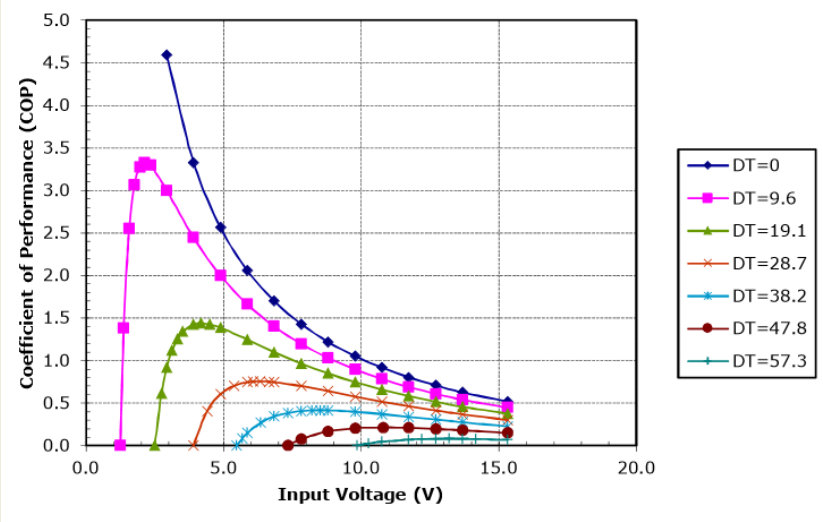

Figure 42. HP-127-1.4-1.15-71 TEM performance (COP) for different voltages (1-15V) and temperature gaps between the TEM sides (0-57.3°C). Source: [33]

The thermal resistance of heat exchangers between TEMs and the air streams is crucial to obtain a good energy performance of a TeHP. A higher thermal resistance increases the temperature gap between the hot and cold sides of the TEM, what drastically decreases the COP [34].

In previous attempts to build an air-to-air TeHP, finned aluminum heat exchangers were employed, leading to a poor COP, ranging 0.2 - 0.4 for cooling ([35], [36]) and a heavy and thick prototype, difficult to be replicated in real applications.

In order to overcome these inconveniences, heat pipes were proposed as heat exchangers, as they help improving the energy performance of the TeHP and are lighter than finned aluminum [13].

The present TeHP design is based on a previous experimental study [37], where the heat pipes that have finally been selected for this application were analyzed and thermally characterized.

The air channel was then reduced to 12 cm high, as the diameter of air ducts in such installations [32]. The TeHP layout is composed of two counter-flow 12 cm square air ducts to maximize the heat flow between both air streams. The direction of the flow of the heating air is, then, opposite to the direction to the flow of the cooling air. The air ducts are divided into 10 modules, with one TEM and two heat exchangers each (see Figure 43).

The TEMs need to be placed between the two air ducts and facilitate the heat exchange between the air streams and both, the hot and cold sides of the TEMs.

The heat exchangers have 5 copper 6 mm heat pipes combined with 40 aluminum fins 5.5 cm deep. The previous analysis of these heat pipes [37] proved that the location in the hot or cold side of the TEM strongly affects their operation, while the horizontal or vertical disposal is not significant. The thermal resistances ranged 0.1 – 0.2 K/W on the hot side and 0.25-0.45 K/W on the cold side, which is still a good result compared with finned aluminum in the previous design ([35], [36]).

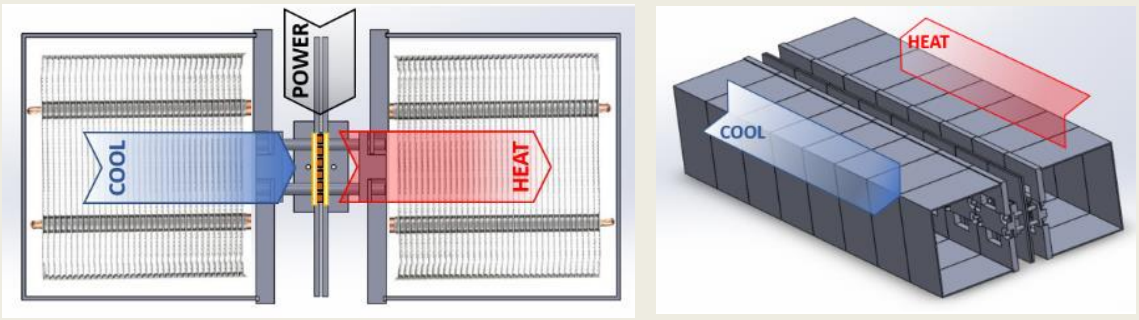

Figure 43. Left image: Crossed section of the TeHP, showing one intermediate module with one TEM in the middle and two HPs connected to both air ducts. Right image:TeHP shell. The module is replicated 10 times, creating two square counter-flow air ducts.

The 10 modules have been carefully assembled with 3D printed parts of polylactic acid (PLA, a vegetable-based plastic material) and insulated with 4 cm of expanded polystyrene (λ = 0.032 W/mK) around the air ducts, and 6 cm of cellulose fiber (λ = 0.039 W/mK) between them. The airtightness in the airducts is guaranteed by a sealing tape used for building constructions.

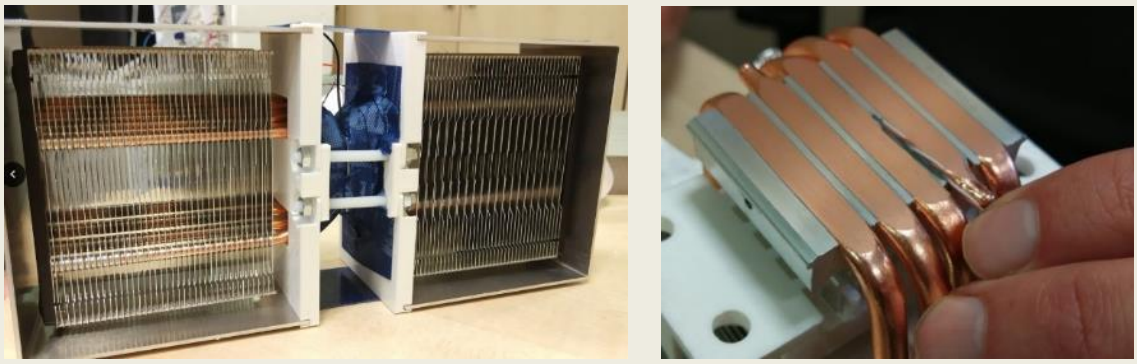

Figure 44. Details of the TeHP fabrication process (left). Installation of a thermocouple in a 1mm slot in the heat exchanger in order to measure the temperature on the cold side of the TEM (right).

The final prototype is 90 cm long and 40cm wide, with a height of 23 cm; and a weight of 15 kg, what makes it a very suitable design for the installation in false ceilings.

Finally, for the experimental characterization of the TeHP one test bench has been planned and deployed.

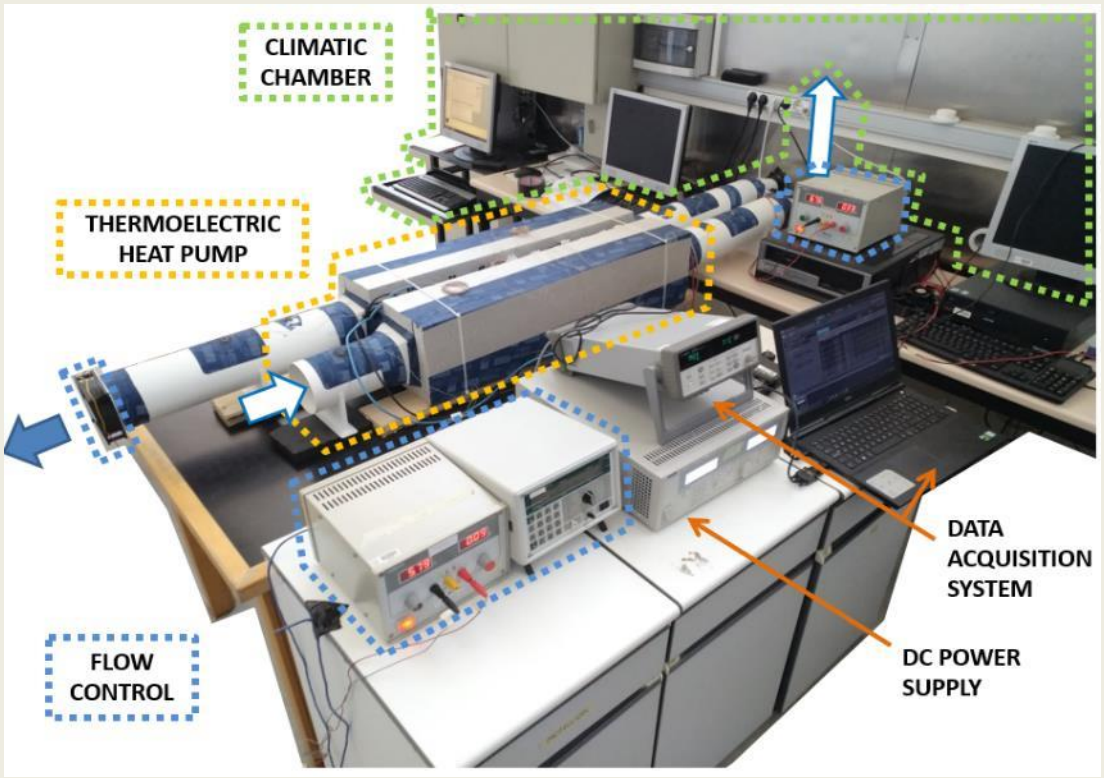

Figure 45. Test bench for the thermal characterization of the TeHP integrated with a climatic chamber.

One fan draws air out from a climatic chamber, where the air temperature is stabilized to a certain set point two hour before the tests; and drives it through the TeHP. Another fan sucks air from the laboratory ambient and sends it through the other air duct of the TeHP with opposite direction.

A complete set of K-Type thermocouples register the temperature at different points of the prototype (see Figure 46), connected to a data acquisition system (AGILENT 34970A). The test bench records the temperature of incoming and outcoming air flows, as well as inner temperatures of one intermediate module. In this module, not only the temperature of air flows is analyzed, but also the temperature on the hot and cold sides of the TEM, as shown in Figure 44.

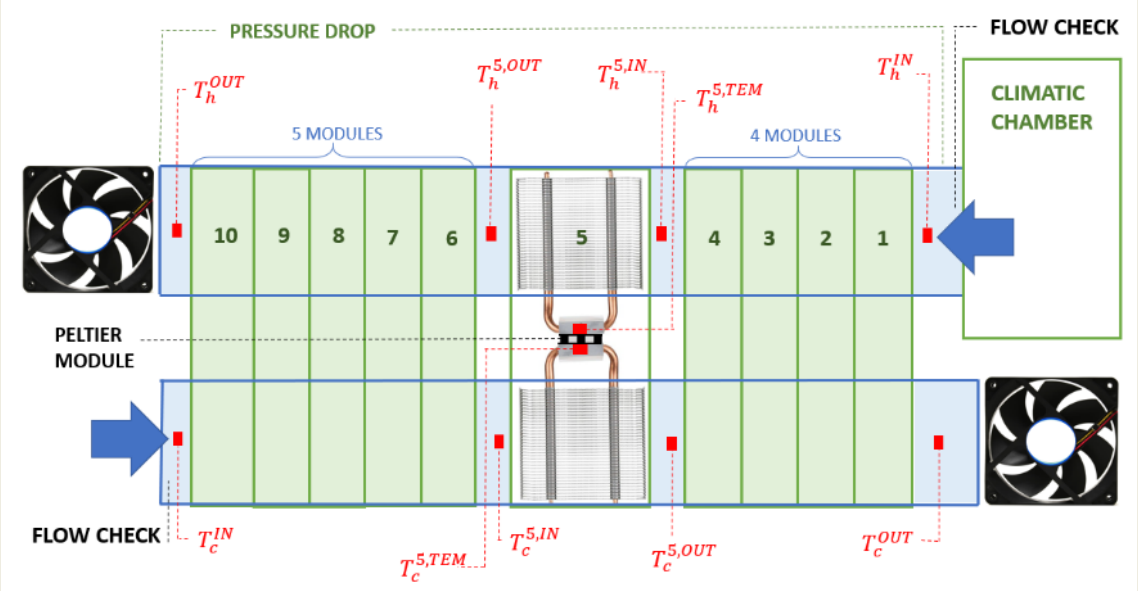

Figure 46. Layout of the test bench to thermally characterize the TeHP in summer and winter conditions.

The TEMs are electrically connected in parallel, activated by a DC Power supply unit (QPX600D), that can switch the voltage polarity to change the TeHP operation from heating to cooling mode.

The air flow is determined by measuring the velocity of the air in the duct at seven vertical equidistant positions to assess the speed profile (see Figure 47), separated 60 cm from the inlet to make sure the speed profile is fully developed, using an anemometer which precision and accuracy are listed in

Table 10, and multiplied by the cross area. Both DC fans are regulated to blow air at the desired flow rate. The tests were repeated three times and next figure shows the average values of the air velocity registered, including the uncertainty of the measurement.

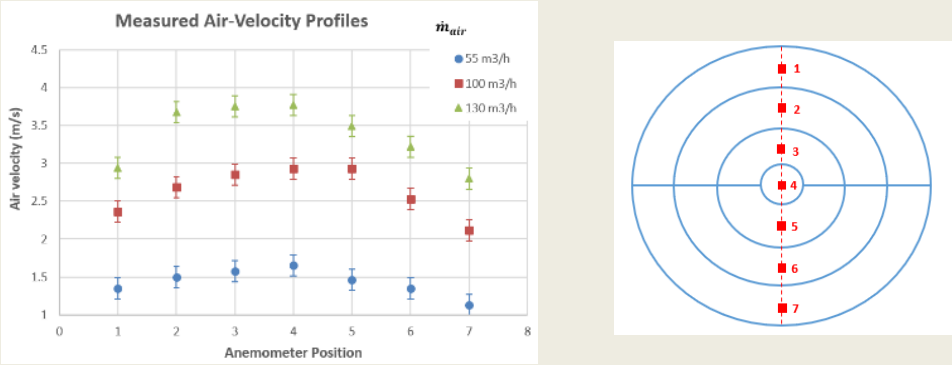

Figure 47. Left image: crossed section of the air duct with the 7 equidistant positions where the air velocity was measured. Right image: air velocity profile measured for the three air flows analyzed (55, 100 and 130 m^3/h).

Table 10. Resolution and accuracy of the measurement probes used

Sensor	Resolution	Accuracy
Temperature (ºC)	0.1	±0.3
Voltmeter (V)	0.1	±0.2
Ammeter (A)	0.01	±0.02
Anemometer (m/s)	0.01	±0.01 + 3% of measured value

3. Methodology

In order to thermally characterize the TeHP we can divide it into ten modules. In each of these modules some heat is absorbed from the cooling duct and drawn into the heating duct with the addition of the electric power consumed by the TEM, as presented in Figure 48.

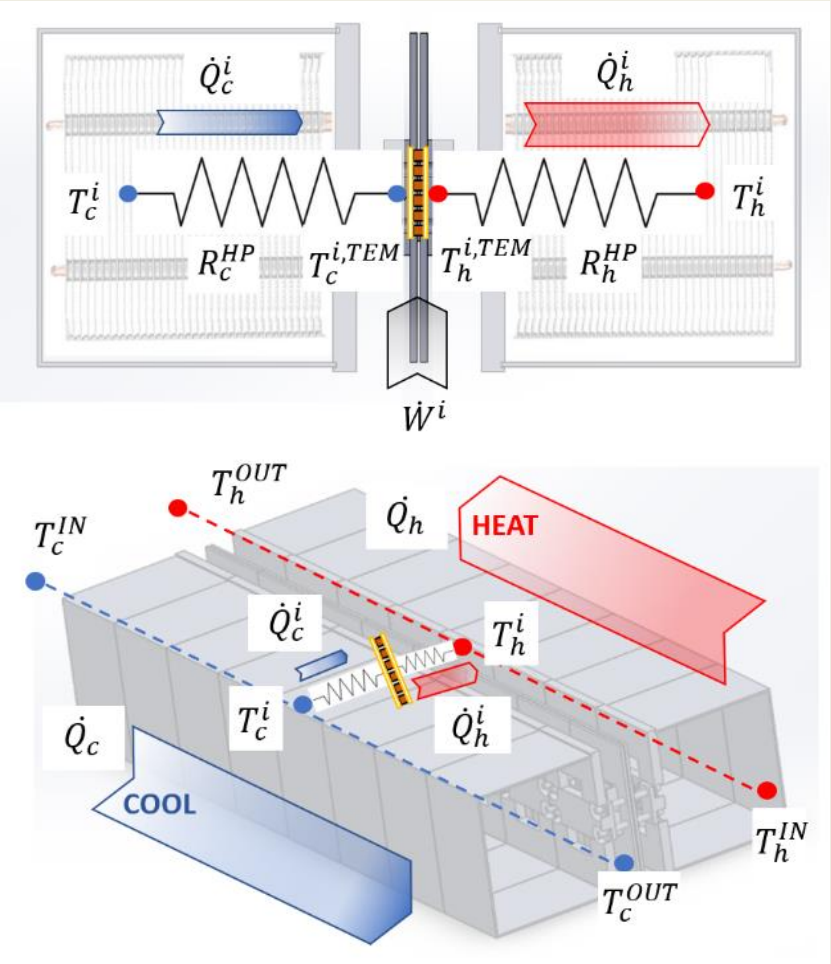

Figure 48. Top figure: crossed section of the TeHP, heat exchange diagram in an intermidate module. Bottom image: overall view of the TeHP with hot and cold counter-flow air streams.

The heat extracted from the cold reservoir can be described by the Eq. (1) in a simple standard method [38] that implies the Peltier and Joule effects, and the thermal conduction, while Eq. (2) presents the heat emitted to the hot reservoir.

$$\dot{Q}_c^i = \alpha I T_c^{i,TEM} - \frac{1}{2} I^2 r - K(T_h^{i,TEM} - T_c^{i,TEM}) \quad (1)$$

$$\dot{Q}_h^i = \alpha I T_h^{i,TEM} + \frac{1}{2} I^2 r - K(T_h^{i,TEM} - T_c^{i,TEM}) \quad (2)$$

Eqs. (3) and (4) show the energy exchanged through the heat pipes between the cold and hot sides of the TEM and the air streams. R^{HP} is variable and depends on the heat flux and the convective coefficient between the air flows and the heat exchanger fins and heat pipes [37].

$$R_c^{HP} = \frac{T_c^i - T_c^{i,TEM}}{\dot{Q}_c^{i,TEM}} \quad (3)$$

$$R_h^{HP} = \frac{T_h^{i,TEM} - T_h^i}{\dot{Q}_h^{i,TEM}} \quad (4)$$

Where T_c^i and T_h^i are emperically calculated as the average temperature between inlet and outlet temperature of the air streams within the intermediate module (see Figure 5):

$$T_c^i = \frac{T_c^{i,IN} + T_c^{i,OUT}}{2} \tag{5}$$

$$T_h^i = \frac{T_h^{i,IN} + T_h^{i,OUT}}{2} \tag{6}$$

The energy balance of the whole TeHP is presented in Figure 48 and described by Eqs. (7), (8) and (9).

$$\dot{Q}_c = \dot{m}_{air}\rho_{air}C_p(T_c^{IN} - T_c^{OUT}) = \sum_{i=1}^{i=10} \dot{Q}_c^i \tag{7}$$

$$\dot{Q}_h = \dot{m}_{air}\rho_{air}C_p(T_h^{OUT} - T_h^{IN}) = \sum_{i=1}^{i=10} \dot{Q}_h^i \tag{8}$$

$$\dot{W} = VI = \dot{Q}_h - \dot{Q}_c = \sum_{i=1}^{i=10} \dot{W}^i \tag{9}$$

The coefficient of performance (COP) is calculated at TeHP level including the electric consumption of the fans, as Eqs. 10 and 11 show:

$$COP_c = \frac{\dot{Q}_c}{\dot{W} + \dot{W}_{fan}} \tag{10}$$

$$COP_h = \frac{\dot{Q}_h}{\dot{W} + \dot{W}_{fan}} \tag{11}$$

The pressure drop in the TeHP has been measured (P3317 Differential Pressure Sensor) obtaining values ranging from 20 to 72 Pa with a ±1% accuracy. These values are very similar to an air to air HRU for domestic use [32] in the same air flow range.

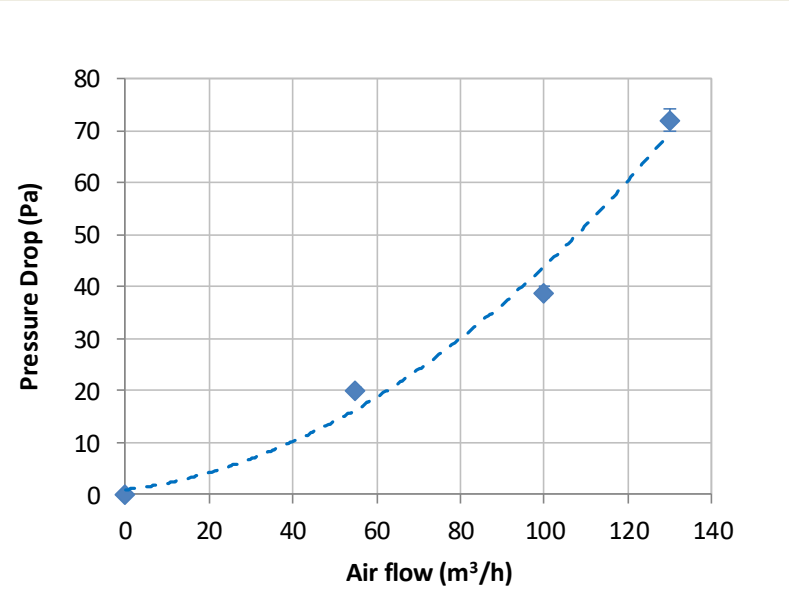

Figure 49. Measured pressure drop (Pa) of the THP with three air flows (55, 100 and 130 m^3/h).

3.1. Experimental tests

Four experimental scenarios have been analyzed: two for wintertime conditions and two for summertime. In winter, air from inside the building is supposed to be blown outside, and same flow of fresh air is drawn inside.

In 1ST SCENARIO the TeHP replaces the installation of HRU (seeTable 11), so that incoming air flow not only aims at matching the temperature of the outside temperature, but it is increased to provide additional heating of inner ambient.

In 2ND SCENARIO the temperature of incoming and outcoming air flows have been reversed after coming through the HRU. In this occasion the TeHP heats up the hotter air stream and cools down the colder one.

In both cases three air flows have been tested: 55, 100 and 130 m^3/h. For each air flow, four voltages were tested (3, 6, 9, 12V) for the TEMs power supply. The temperature in the lab was 20 °C, while the setpoint for the climatic chamber was 0 °C and 10 °C.

Next two scenarios have been tested in summertime, with 25 °C in the lab and 30 °C in the climatic chamber. 3RD SCENARIO reproduces the 1ST SCENARIO scheme for summertime, and 4TH SCENARIO replicates the 2ND SCENARIO in cooling mode. Same number of air flows and voltage supply levels were experienced for summer conditions. In total, 72 tests were carried out.

Table 11. Experimental scenarios analyzed.

WINTER CONDITIONS	1st SCENARIO	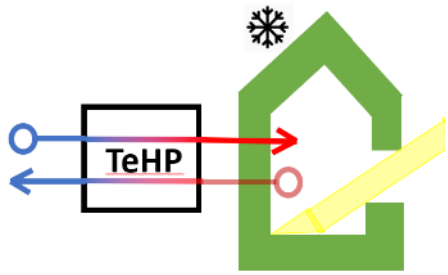	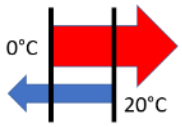 $T_c^{IN} = 20$ °C $T_h^{IN} = 0$ °C	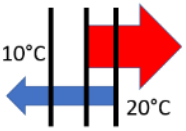 $T_c^{IN} = 20$ °C $T_h^{IN} = 10$ °C
	2nd SCENARIO	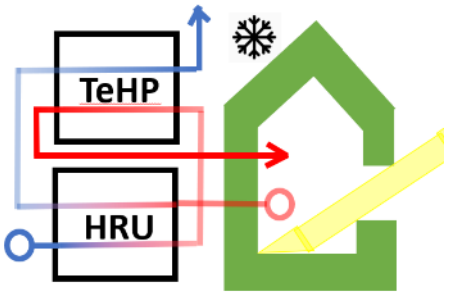	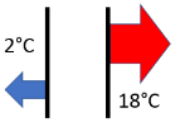 $T_c^{IN} = 2$ °C $T_h^{IN} = 18$ °C	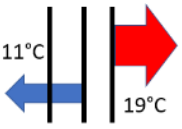 $T_c^{IN} = 11$ °C $T_h^{IN} = 19$ °C
SUMMER CONDITIONS	3rd SCENARIO	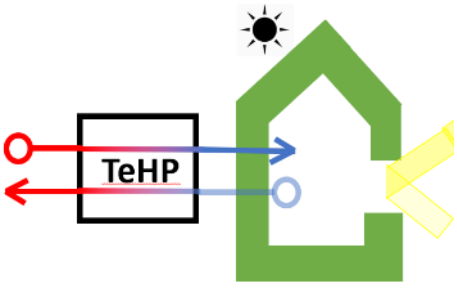	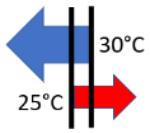 $T_c^{IN} = 30$ °C $T_h^{IN} = 25$ °C	
	4th SCENARIO	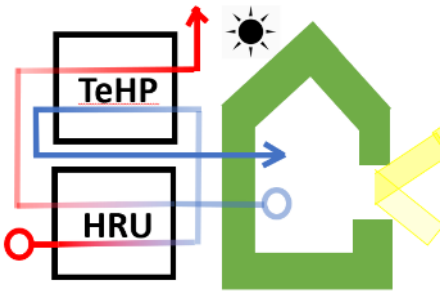	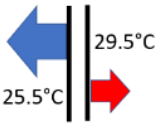 $T_c^{IN} = 25.5$ °C $T_h^{IN} = 29.5$ °C	

3.2. Uncertainty

For every test, 15 min were dedicated to reach stationary conditions. Temperatures were recorded every 10 seconds and only last 30 values were selected to evaluate the average value and the standard deviation of the measure.

For the uncertainty study the Eq. (5) was used, where b_R stands for the systematic standard uncertainty, $s_{\bar{R}}$ is the random standard uncertainty and the coefficient 2 represents a confidence interval of the 95 % for the measure [39].

Even for such a low number of records, $s_{\bar{R}}$ results are virtually insignificant compared to b_R in all the sensors.

$$U_R = 2\left(b_R^2 + s_{\bar{R}}^2\right)^{\frac{1}{2}} \quad (10)$$

The calculation of $\dot{Q}_c$ and $\dot{Q}_h$ as in Eq. (8) and Eq. (7) are subject to the uncertainitiy of the flow rate measurement (estimated as ±7%).Next Figure 50 shows the correlation of $\dot{Q}_h$ calculated for all tests as in Eq. (8) and Eq.(9), as a result of the energy balance considering $\dot{Q}_c$ and $\dot{W}$. The error on these two empirical approaches is below ±15%, which confirms the reliability of the tests carried out.

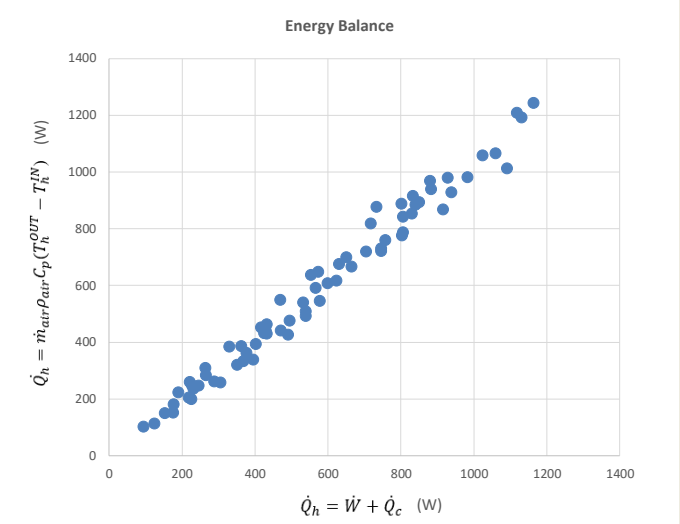

Figure 50. Energy balance: correlation of $\dot{Q}_h$ calculated as in Eq. (8) and Eq. (9) for all tests carried out.

4. Results and discussion

This section reports the experimental results obtained for the 4 scenarios previously described.

4.1. Winter scenarios.

4.1.1. 1ST SCENARIO: Stand-alone installation.

The first series of tests have been dedicated to thermally characterize the TeHP when replacing an HRU in a double flux mechanical ventilation system, as shown in **¡Error! No se encuentra el origen de la referencia.**.

The heating duct draws the air from outside at 0 °C (T_h^{IN}) inside the building (20 °C). The air flow is heated by the TeHP, increasing the air temperature up to T_h^{OUT}. This temperature increase ($T_h^{OUT} - T_h^{IN}$) is represented in Figure 51 (left graph) and shows higher values when the air flow is reduced and the voltage increased. The heating capacity of the TeHP ($\dot{Q}_h$) is the sum of the heat provided by each of the ten modules ($\dot{Q}_h^{i,TEM}$), and it mostly depends on three terms, as described in Eq (2): Peltier effect, Joule effect and the thermal conduction between

both sides of the TEM. When the voltage is increased, the current is almost proportionally increased, and the term $\alpha I T_h^{TEM}$ grows up. The temperature gap between incoming and outgoing air will then be increased as well.

On the other hand, for a given voltage, if the air flow is reduced, the temperature gap will grow (see Eq (8)), but this air flow will also affect to the thermal resistance of the heat exchangers as it will be further explained.

It is important to highlight that while this temperature gap does not exceeds 20°C (left graph, area shaded in blue) the incoming air will be colder than the inside air, which means that the system would be cooling the building. This happens for voltages below 3V for 55 m^3/h, and below 6V for 100 and 130 m^3/h air flows.

When the temperature outside is 10 °C (right graph), the fresh air only needs to gain another additional 10 °C to reach the temperature inside. The shaded area is then reduced, and only applies to voltages under 3V for 100 and 130m^3/h air flows. °

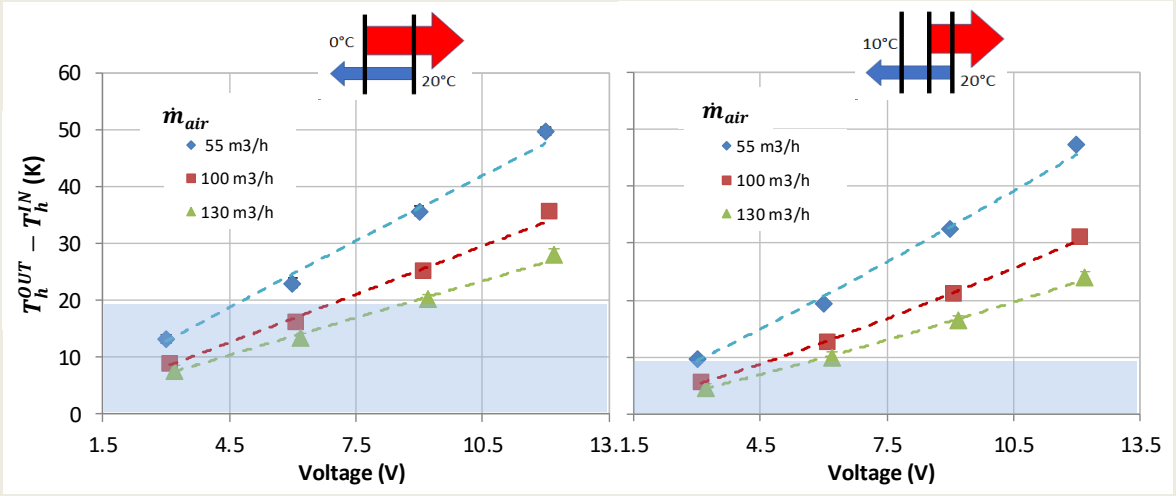

Figure 51. Winter: 1ST SCENARIO. Temperature increase of air in the heating duct ($T_h^{OUT} - T_h^{IN}$) at different operating conditions (3, 6, 9 and 12V TEM voltage; 55,100, 130 m^3/h air flow) and different temperature gap between inside and outside air (LEFT: 20°C; RIGHT:10°C). The uncertainty is ±0.8°C for all values. Shaded area: the temperature increase of the incoming air flow is not enough to provide heating inside.

As shown in Figure 44, the temperature of the cold and heat sides of one TEM in an intermediate module (see Figure 46) have been registered, as well as the incoming and outgoing temperatures of both air streams. The average air temperature is calculated following Eq.(6) and the thermal resistance of the heat exchangers (heat pipes between the air in the heating duct and the hot side of the TEM) can be estimated using Eq.(4). The results are shown in Figure 52. The values of thermal resistance of the heat pipes in the heating air duct range 0.07-0.13 K/W for the different operational conditions, which is coherent with previous studies [37].

The thermal resistance of the heat pipes depends on the phase change of the liquid inside and the condenser section, which is subject to the forced convective cooling due to the air flow inside the heating duct. Higher air flows increase the air velocity, leading to a higher Reynolds

number, and hence an increase of the heat transfer. On the other hand, higher voltages increase the temperature gap between the pipe and the liquid inside, generating a higher heat flux and higher phase change rate, reducing, then, the thermal resistance [40].

In the right graph, we see that when outside temperature is 10 °C, the temperature gap between the heat pipe and the air is reduced, reducing the heat flux, and thus, we appreciate a slight increase (5-10 %) of the thermal resistance.

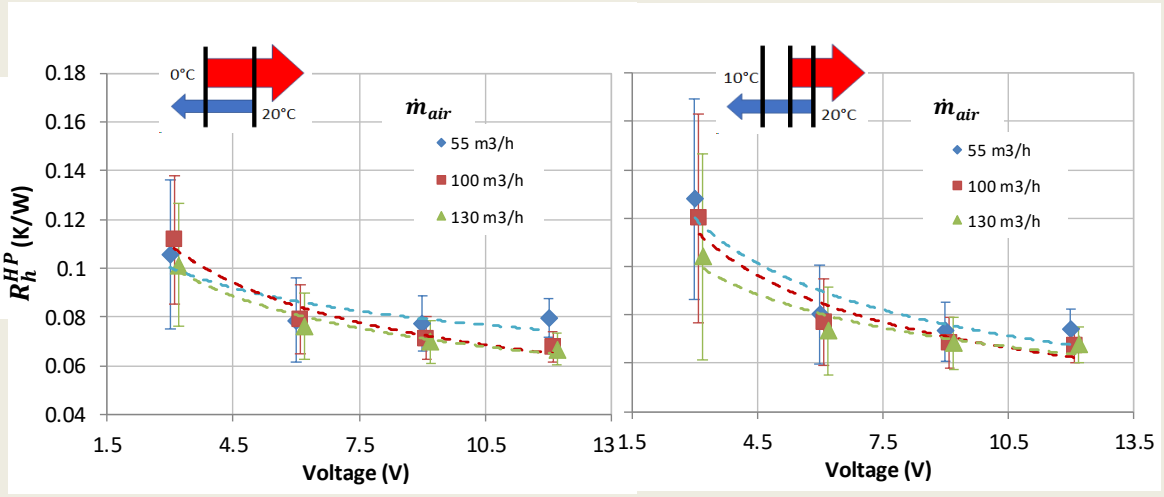

Figure 52. Winter: 1ST SCENARIO. Thermal resistance of TEM-air heat exchangers (R_h^{HP}) at different operating conditions (3, 6, 9 and 12V TEM voltage; 55,100, 130 m³/h air flow) and different temperature gap between inside and outside air (LEFT: 20°C; RIGHT:10 °C).

Figure 53 shows the heating power of the TeHP, calculated with Eq. (8) based on the temperature increase: $T_h^{OUT} - T_h^{IN}$ in the heating duct. This heating capacity is very similar in the case of 100 and 130 m³/h air flows, but it is reduced (about 20 % less) when the air is 55 m³/h, due to the higher thermal resistance of heat pipes, because of a lower convective coefficient between the air and the fins attached to the heat pipes.

The maximum heating capacity reached was 1,243 W (0 °C outdoor temperature, 130 m³/h and 12 V), 16.6 % more than when outside temperature is 10 °C.

In this 1ST SCENARIO the TeHP works as a combination of HRU and heat pump, since it heats a fluid that is colder than the cold sink. For this reason, a higher temperature gap between inside and outside air in the building, favorizes the heat transfer between both air flows, by reducing the temperature gap between both sides of the TEMs.

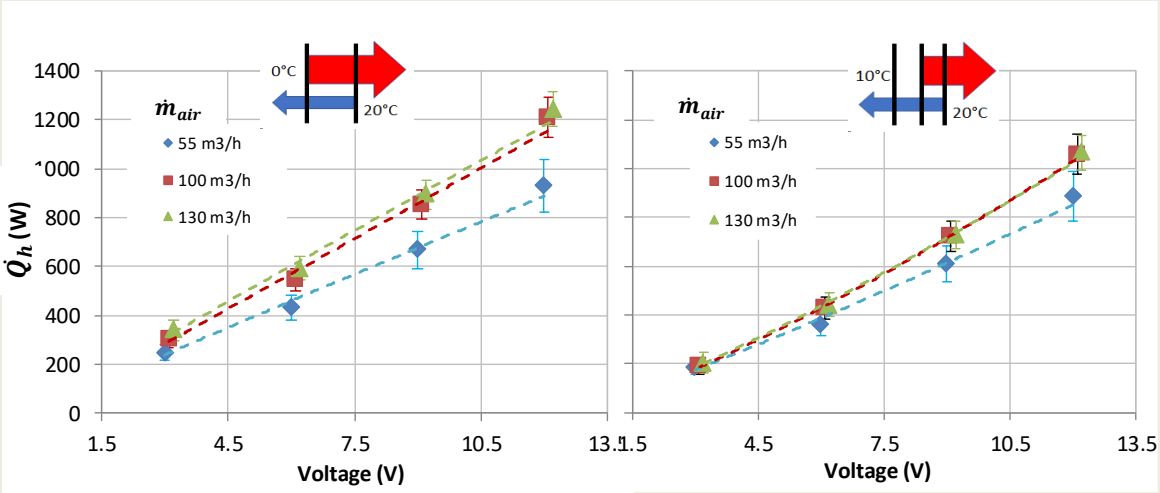

Figure 53. Winter: 1ST SCENARIO. Heating power at different operating conditions (3, 6, 9 and 12V TEM voltage; 55,100, 130 m³/h air flow) and different temperature gap between inside and outside air (LEFT: 20 °C; RIGHT:10 °C).

Figure 54 shows the COP_h (left axis) calculated as in Eq (11) and the temperature gap between the TEM sides ($T_h^{i,TEM} - T_c^{i,TEM}$) (right axis). We can appreciate that this temperature gap in the TEM is about 5 °C lower in the left graph, when the outdoor temperature is 0 °C, since this higher difference between inlet temperatures favorizes this heat transfer, which leads to obtain a higher COP_h that ranges 1.5-4. In the right graph (10 °C outside) the COP_h ranges 1.5-2.5.

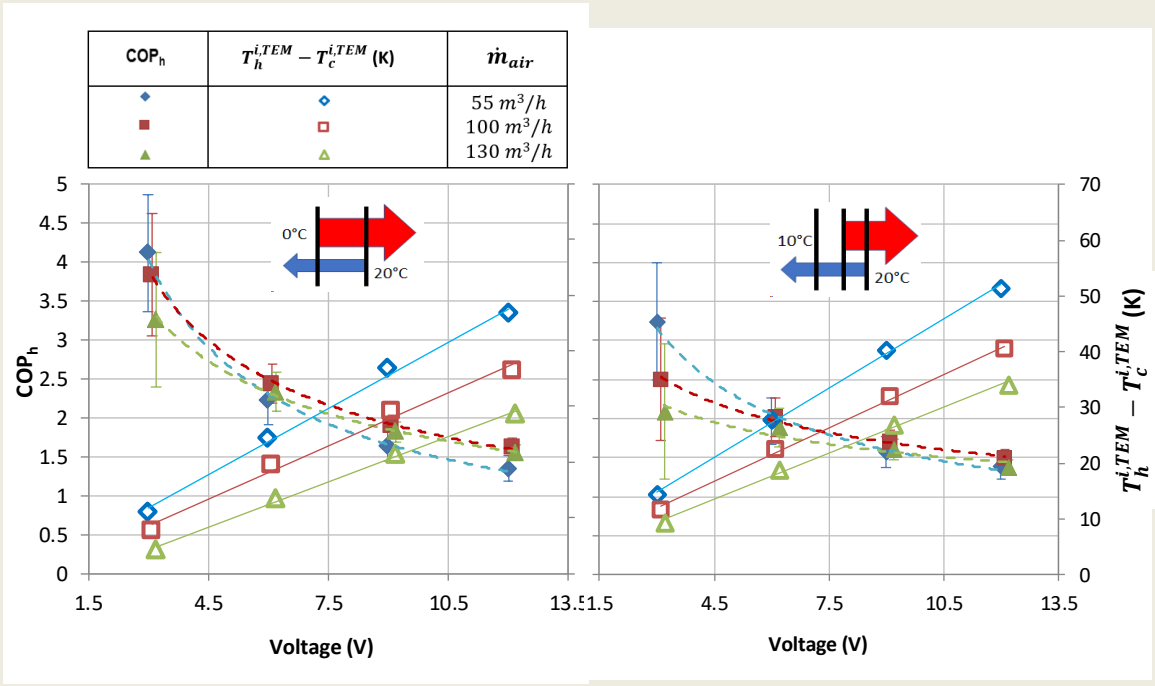

Figure 54. Winter: 1ST SCENARIO. Heating COP and temperature gap between both sides of the TEM ($T_h^{i,TEM} - T_c^{i,TEM}$) at different operating conditions (3, 6, 9 and 12V TEM voltage; 55,100, 130 m³/h air flow) and different temperature gap between inside and outside air (LEFT: 20°C; RIGHT:10°C). The uncertainty for $T_h^{i,TEM} - T_c^{i,TEM}$ values is ±0.8°C.

4.1.2 2ND SCENARIO: Integration of TeHP with an HRU.

The second scenario involves the integration of the TeHP with the HRU, so that the air ventilation air flow is post-heated after going through the HRU. Table 11 shows the integration scheme.

Given an outside temperature of 0 °C and an HRU efficiency of 90 %, the air temperature at the outlet would be 18 °C, just 2 °C below the temperature of the building. In these circumstances the TeHP must raise this temperature as much as possible, pumping heat from the exhausted air duct. This air was originally at 20 °C, but after getting through the HRU, it drops to 2 °C. In this case, the TeHP must work transferring heat between two heat sinks with 16 °C difference between them, heating the hottest one and cooling the coldest one.

Under these conditions, the temperature increase in the heating tube reaches 35°C (Figure 55), below the 50 °C reached in the 1ST SCENARIO. However, as previously explained, the fresh air is at 18 °C before getting through the TeHP, and thus, 3 V supply can guarantee that the outlet air exceeds 20 °C and, therefore, the ventilation system is in all cases heating the interior of the building. The shaded area is in this case below the operating conditions that have been established for the tests.

If the outside temperature is 10 °C, the fresh air temperature after passing through the HRU rises to 19 °C, while the exhausted air temperature drops to 11 °C. Under these conditions, TeHP pumps heat between two heat sinks with 8 °C difference between them (right graphs), which improves TeHP's thermal performance, compared with the 16 °C in the previous case (left graphs).

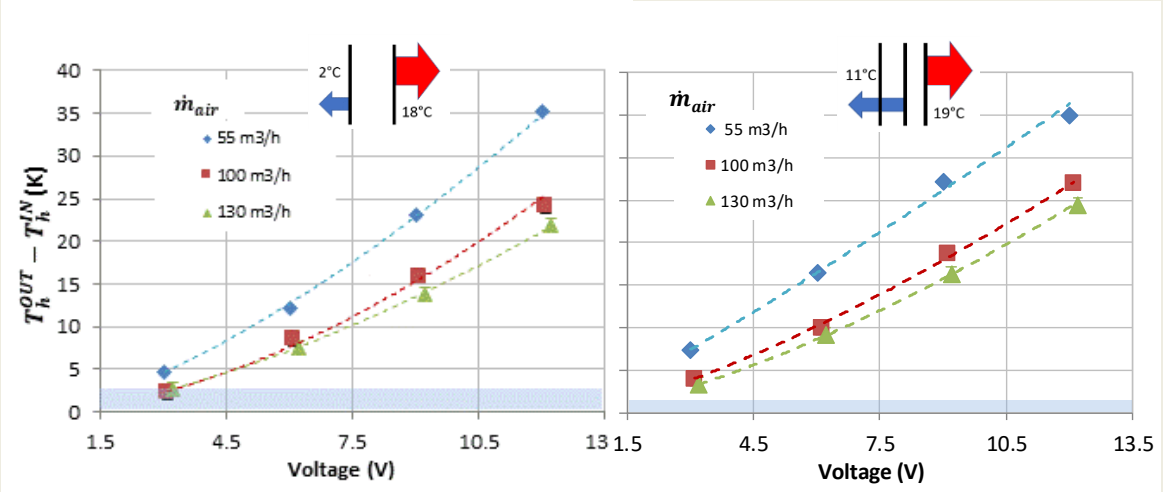

Figure 55. Winter: 2ND SCENARIO. Temperature increase of air in the heating duct ($T_h^{OUT} - T_h^{IN}$) at different operating conditions (3, 6, 9 and 12V TEM voltage; 55,100, 130 m³/h air flow) and different temperature gap between inside and outside air (LEFT: 16°C; RIGHT:8°C). The uncertainty is ±0.8°C for all values.

This situation is different with respect to the 1ST SCENARIO, where the hot sink was colder than the cold sink, and thus, a greater temperature gap between heat sinks (going from an outside

temperature of 10 °C to 0 °C) was in favour of the heat transfer between them. This reduces the temperature difference between the TEM sides ($T_h^{i,TEM} - T_c^{i,TEM}$) and the heat lossses due to thermal conduction ($K(T_h^{i,TEM} - T_c^{i,TEM})$) in Eq (2).

As a result, the $\dot{Q}_h^i$ is lower, which increases the thermal resistance (lower phase change rate) of the heat pipes with respect to 1ST SCENARIO. The estimated values range 0.09-0.25 K/W and are presented in Figure 56.

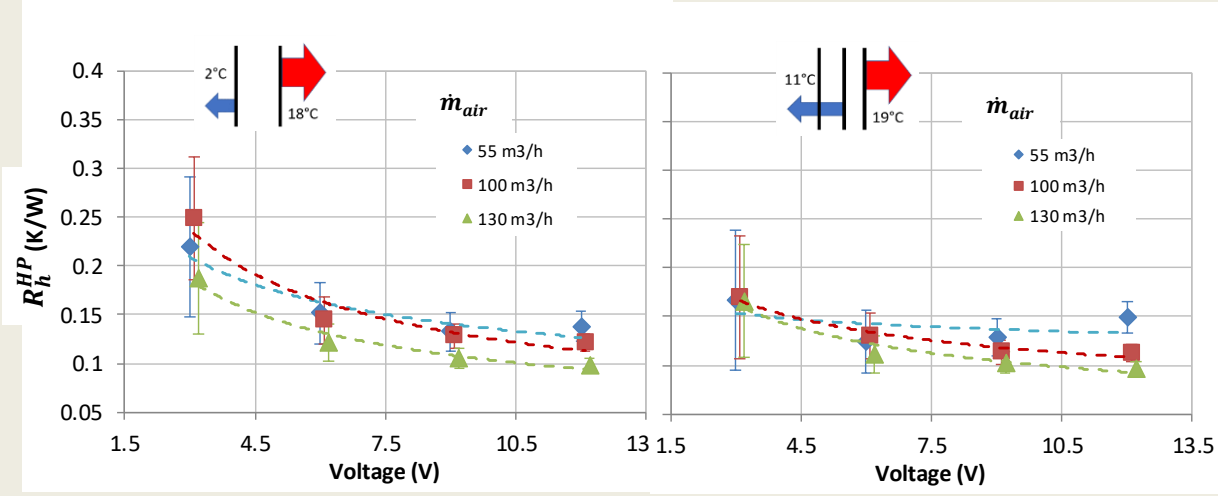

Figure 56. Winter: 2ND SCENARIO. Thermal resistance of TEM-air heat exchangers (R_h^{HP}) at different operating conditions (3, 6, 9 and 12V TEM voltage; 55,100, 130 m³/h air flow) and different temperature gap between inside and outside air (LEFT: 18°C; RIGHT:8°C).

Higher thermal resistances reduce the overall heating capacity of the TeHP ($\dot{Q}_h$), which presents a maximum value of 1,083 W (10 °C outdoor temperature, 130 m³/h and 12 V), 11.5 % more than when outside temperature is 0 °C and 13 % less than the maximum performance in the 1ST SCENARIO.

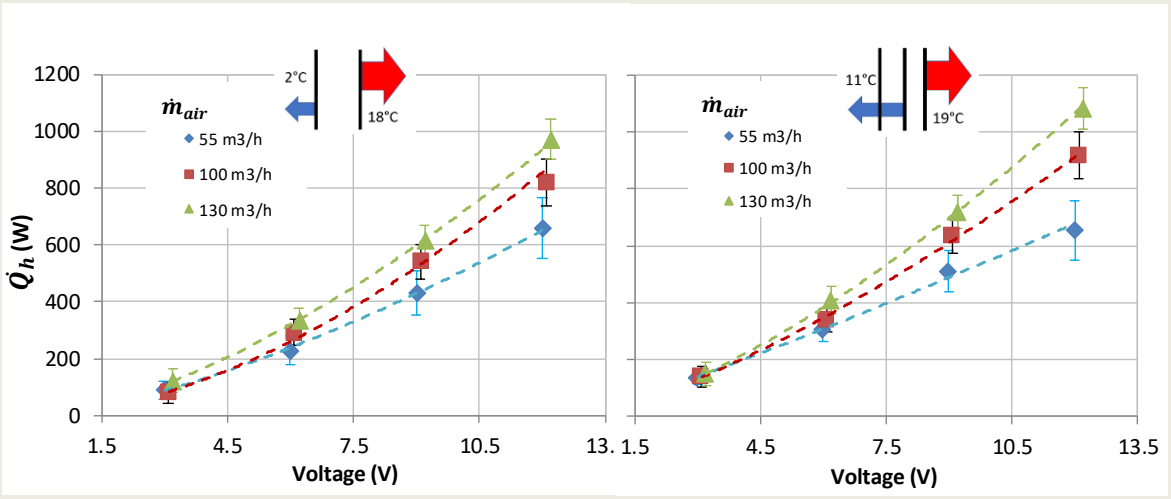

Figure 57. Winter: 2ND SCENARIO. Heating power at different operating conditions (3, 6, 9 and 12V TEM voltage; 55,100, 130 m3/h air flow) and different temperature gap between inside and outside air (LEFT: 16°C; RIGHT:8°C).

Figure 58 shows how a higher termperature gap between the heat sinks forces the TeHP to work with a higher temperature gap between the TEM sides ($T_h^{i,TEM} - T_c^{i,TEM}$), and consequently the COP_h of the TeHP gets reduced. In this case, unlike the 1ST SCENARIO, the COP_h is lower when outdoor temperature is 0 °C, ranging 1-1.5. For 10 °C outside temperature COP_h ranges 1-2.

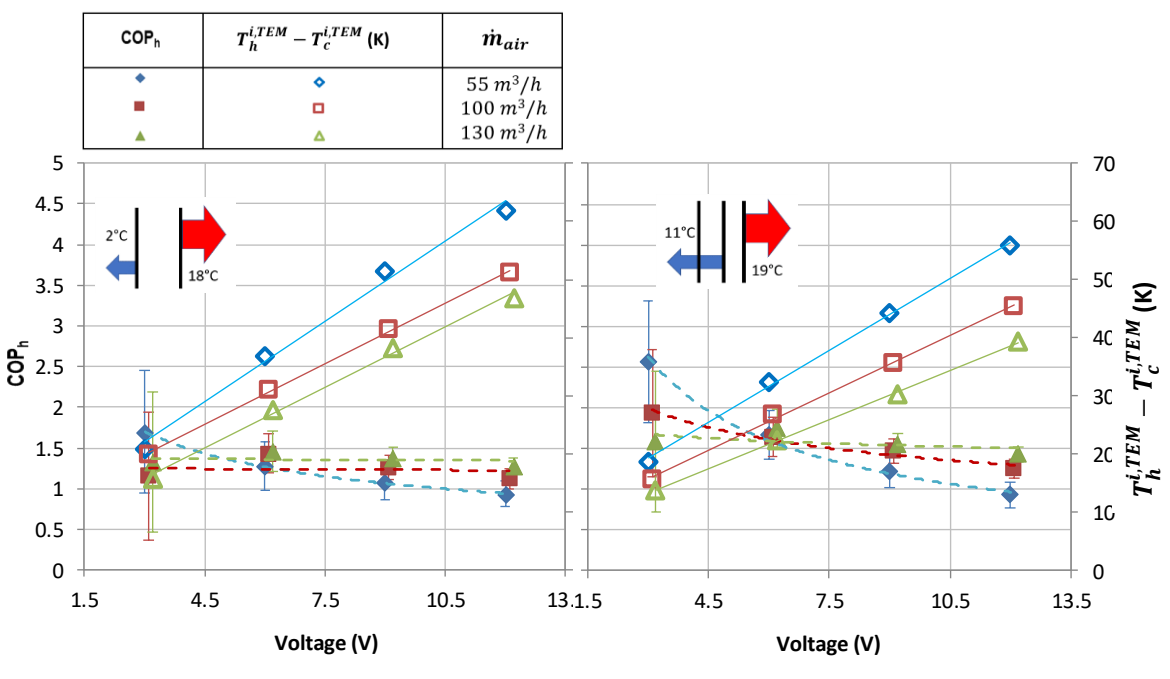

Figure 58. Winter: 2ND SCENARIO. Heating COP and temperature gap between both sides of the TEM ($T_h^{i,TEM} - T_c^{i,TEM}$) at different operating conditions (3, 6, 9 and 12V TEM voltage; 55,100, 130 m^3/h air flow) and different temperature gap between inside and outside air (LEFT: 16°C; RIGHT:8°C). The uncertainty for $T_h^{i,TEM} - T_c^{i,TEM}$ values is ±0.8°C.

Finally, in order to compare 1ST and 2ND SCENARIOS, it is necessary to include the effect of the HRU. With this aim, we take the results for the intermediate air flow of 100 m^3/h, and compare the heating power ($\dot{Q}_c$) of 1ST SCENARIO (in orange) with the addition of the sensible heat provided by the HRU (in blue) and the 2ND SCENARIO (in green). Figure 59 shows this comparisons, left graph for 0 °C outdoor temperature and right graph for 10°C. Although the performance of the TeHP gets reduced, the combination of both, the HRU and the TeHP, provides at least 200 W more heating than the TeHP stand-alone installation.

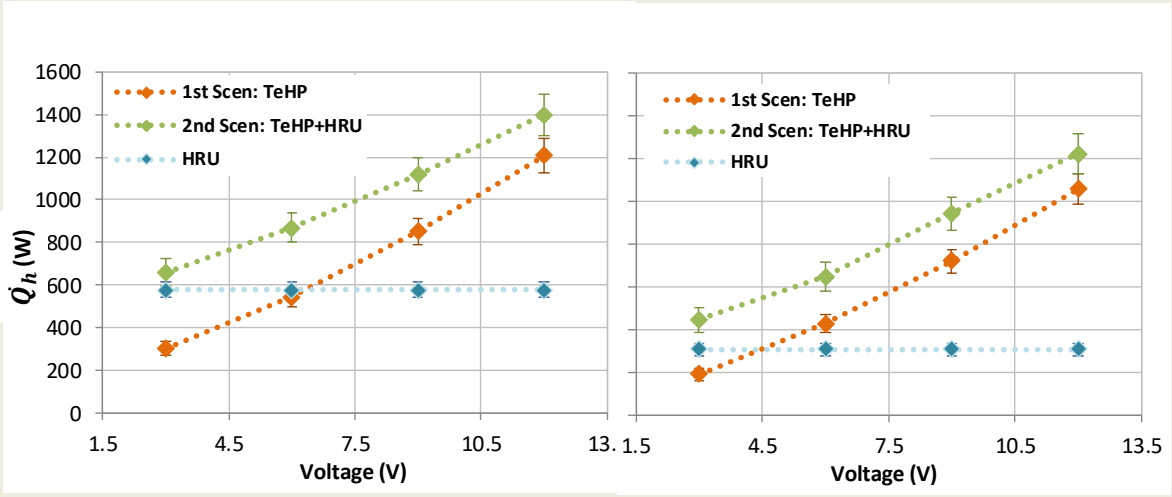

Figure 59. Winter: comparison of the heating power of THP in 1ST SCENARIO and the combination of THP and HX in 2ND SCENARIO for 100 m³/h with different temperature gap between inside and outside air (LEFT: 20°C; RIGHT:10°C).

Figure 60 shows the COP_h comparing 1ST and 2ND SCENARIOS. In both cases (left and right graph corresponding to 0 °C and 10 °C outdoor temperature respectively) the combination of the HRU with the TeHP present a big advantage in terms of COP_h for low voltages, , but this advantage gets reduced as the voltage increases.

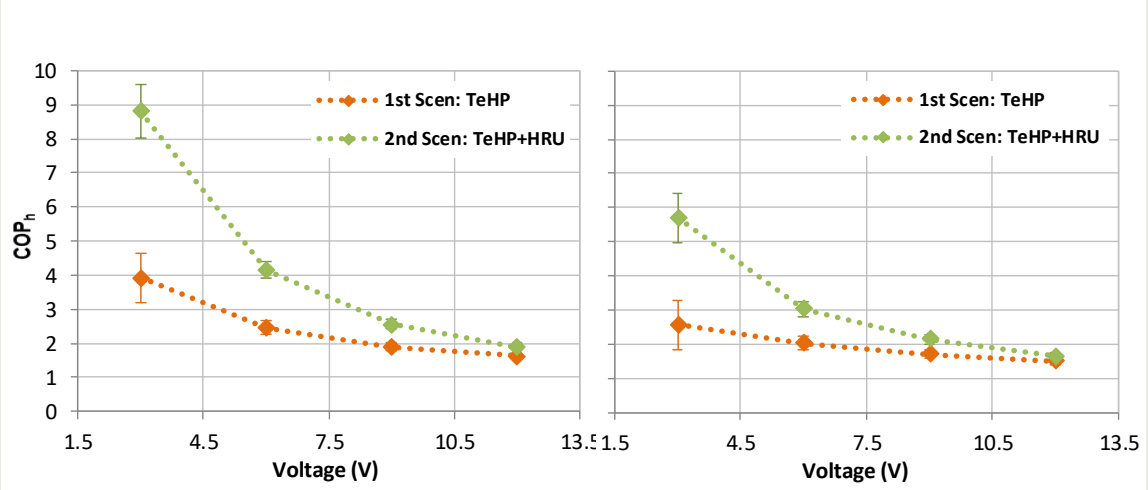

Figure 60. Winter: comparison of the COP_h of THP in 1ST SCENARIO and the combination of THP and HX in 2ND SCENARIO for 100 m³/h with different temperature gap between inside and outside air (LEFT: 20°C; RIGHT:10°C).

4.2. Summer scenarios: 3RD & 4TH SCENARIOS.

In summertime, a simple change of polarity in the TeHP allows the building to be cooled via the ventilation air flow with no additional modifications. In this case, the two configurations proposed in wintertime (stand-alone and integration with HRU) will be studied (Table 11), but with a single thermal gap between the interior and exterior of the building. We assume an indoor air temperature of 25 °C and 30 °C outdoor.

Under these conditions, when the TeHP is installed alone in the double flow ventilation system, the hottest air flow is cooled (30°C) and the exhausted air (25°C) is heated and then expelled outside. When the TeHP is combined with the HRU, the outside air lowers its temperature by 4.5°C, entering the TeHP at 25.5°C; while the exhaust air is preheated up to 29.5°C before reaching the TeHP.

The resulting temperature drop in the ventilation air flow is at least 2°C higher in the 3RD SCENARIO with regard to the 4TH (Figure 61), but, as the air enters 4.5°C colder after getting through the HRU, the overall cooling effect is greater in this second case.

On the other hand, the temperature after the TeHP should be under 25°C to assure the ventilation does not have a heating effect inside the building. This only happens in 3RD SCENARIO for an air flow of 130 m^3/h and 3V supply (see shaded area in left graph of Figure 61).

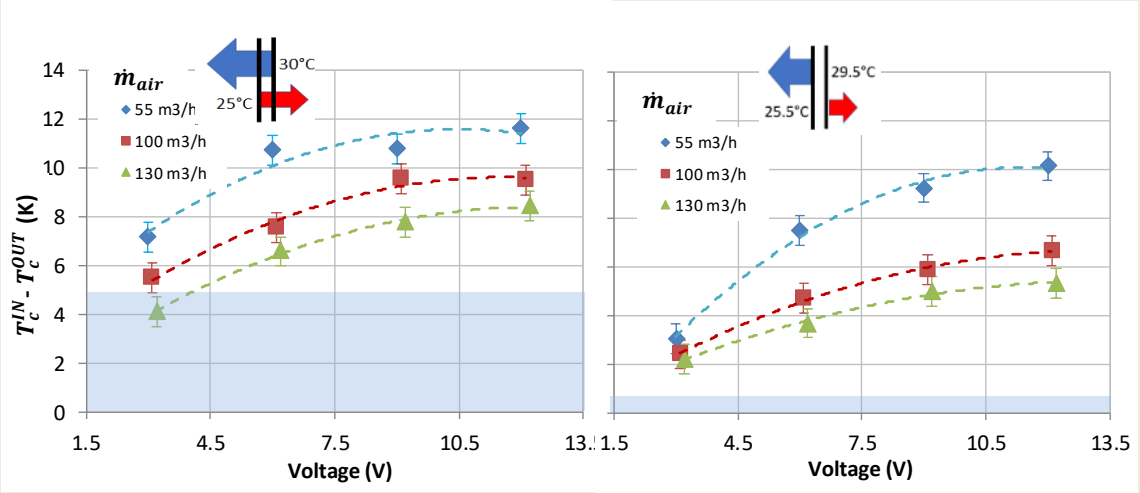

Figure 61. Summer: Temperature drop of air in the cooling duct ($T_c^{IN} - T_c^{OUT}$) at different operating conditions (3, 6, 9 and 12V TEM voltage; 55,100, 130 m^3/h air flow) in two SCENARIOS (LEFT: 3 RD; RIGHT:4TH). The uncertainty is ±0.8°C for all values.

The thermal resistance of the heat exchangers between the TEM's cold side and cooling air stream has been estimated, following same methodology than in previous chapter (Eq. (3)). In this case, the thermal resistance values double the results obtained for the heat pipes in the heating air stream.

The heat pipe works contrary to its design: the finned end of the tubes works as evaporator and the plate as condenser, reducing the condensation area and, hence, increasing its thermal resistance, as Figure 62 shows, compared with results in Figure 52 and Figure 56. As in previous cases, a reduction in the air mass flow increases the thermal resistance due to a lower convective coefficient between the air and the finned end (specially for 55 m^3/h), while higher heat fluxes for higher voltage supplies, reduce it.

The results for 3RD SCENARIO are lower values as in the 4TH SCENARIO, where the air enters at 25.5°C instead of 30°C. When the air is colder, the temperature gap with the air and the finned pipe is lower, which slows down the evaporative process inside the heat pipe.

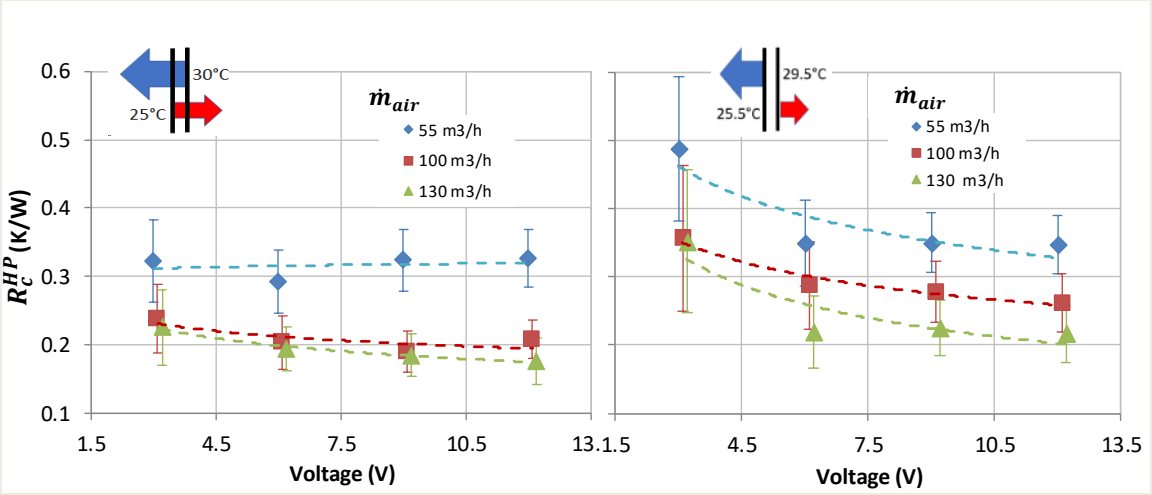

Figure 62. Summer: Thermal resistance of TEM-air heat exchangers (R_c^{HP}) at different operating conditions (3, 6, 9 and 12V TEM voltage; 55,100, 130 m^3/h air flow) in two SCENARIOS (LEFT: 3RD; RIGHT:4TH).

A higher thermal resistance of the heat exchangers and the need to work with higher thermal gaps in the TEMs (Figure 64) make the TeHP have a lower cooling capacity when the ventilation flows go previously through the HRU, as it happened in the comparison between 1ST and 2ND SCENARIOS (winter conditions). The maximum measured cooling capacity is 375W, which corresponds, as in previous cases, with the point of highest voltage and air flow, and being 35% lower in 4TH SCENARIO.

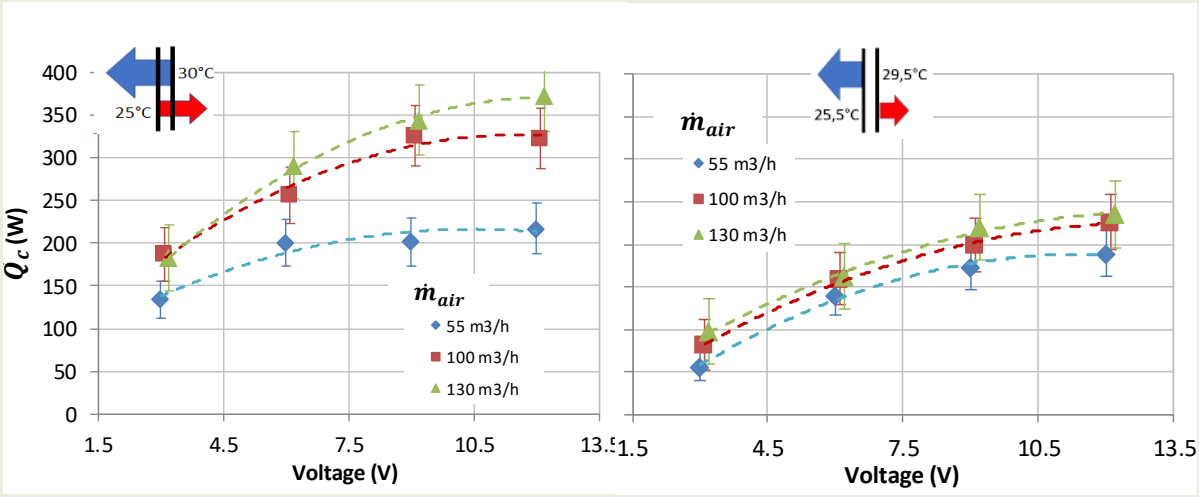

Figure 63. Summer: Cooling power at different operating conditions (3, 6, 9 and 12V TEM voltage; 55,100, 130 m^3/h air flow) in two SCENARIOS (LEFT: 3 RD; RIGHT:4TH).

The Figure 64 represents the comparison of the measured temperature gaps in the TEM (right axis) and COP (left axis) in 3RD and 4TH SCENARIOS.

For the 3RD SCENARIO, the COP varies between 0.5 and 2,5, being higher for higher air flow rates and lower voltages, as in heating mode. In 4TH SCENARIO the temperature gap between

both sides of the TEM is on average 5°C higher than in 3RD SCENARIO, and the COP ranges 0.4-1.

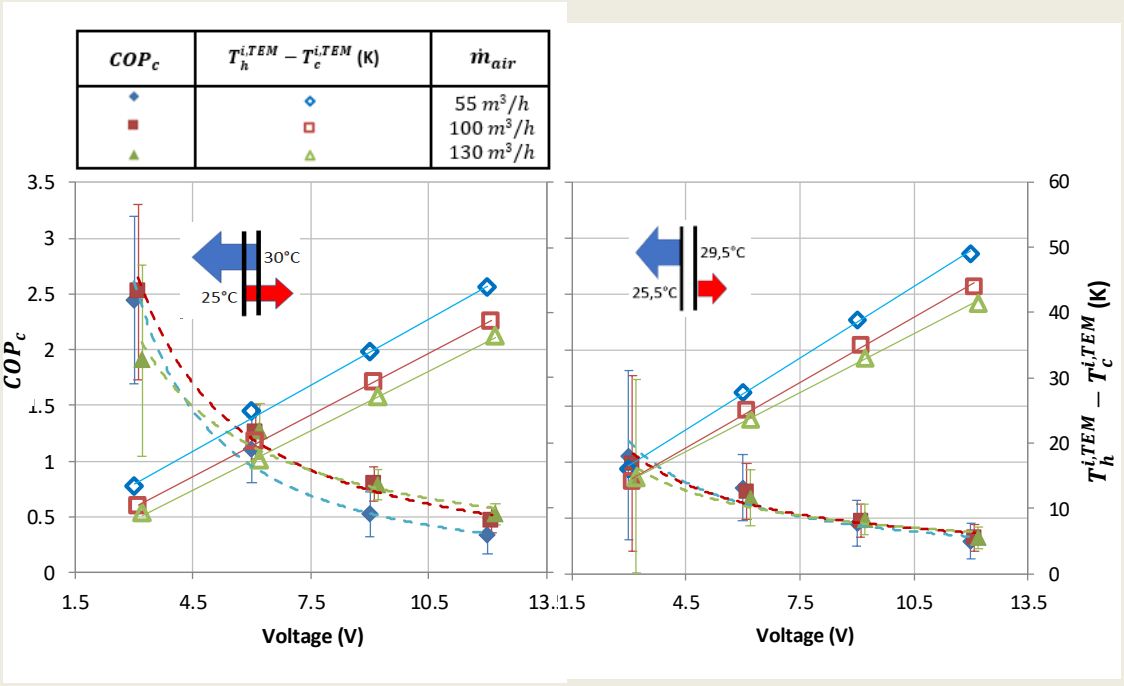

Figure 64. Summer: Cooling COP and temperature gap between both sides of the TEM ($T_h^{i,TEM} - T_c^{i,TEM}$)at different operating conditions (3, 6, 9 and 12V TEM voltage; 55,100, 130 m^3/h air flow) in two SCENARIOS (LEFT: 3^{RD}; RIGHT:4^{TH}). The uncertainty for $T_h^{i,TEM} - T_c^{i,TEM}$ values is ±0.8°C.

Finally, in order to have a better perspective of the performance of these two active ventilation alternatives, both the cooling capacity and COP of 3RD and 4TH SCENARIOS are compared including the effect of the HRU for 100 m^3/h air flow.

Figure 65 shows that the cooling capacity is 50W better in case of 4TH SCENARIO and the COP_c ranges 0.5-3.25 while it varies between 0.5 and 2.5 in 3RD SCENARIO.

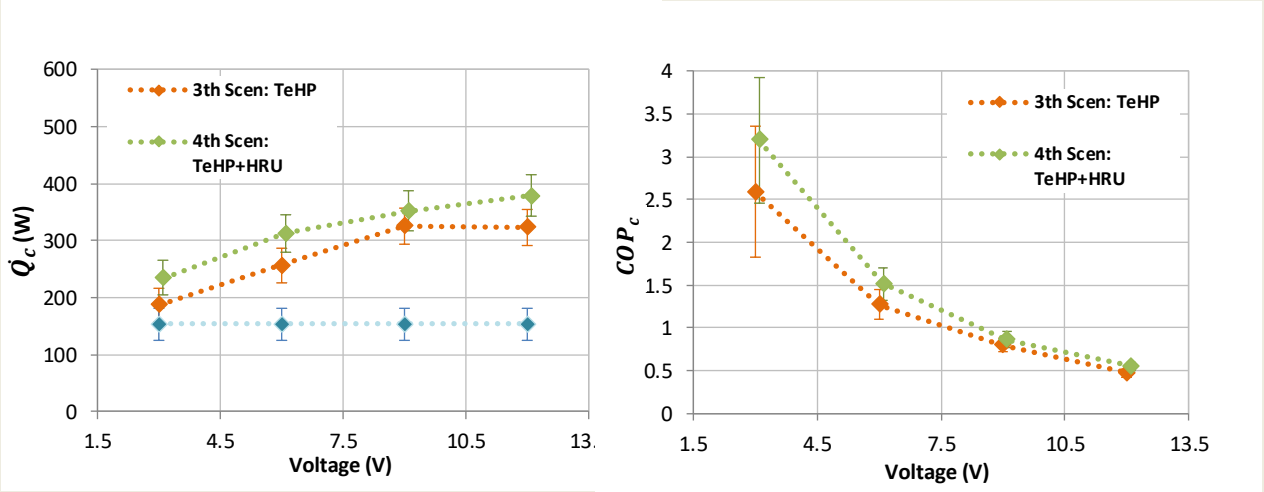

Figure 65. Summer: comparison of the cooling power (left) and COP_c (right) of TeHP in 3^{RD} SCENARIO and the combination of TeHP and HX in 4^{TH} SCENARIO for 100 m^3/h air flow.

Conclusions

In this new paradigm of energy efficient constructions and climate change, it is necessary to find new reliable ventilating and heating alternatives in the domestic sector, with the ability of cooling in order to ensure good comfort conditions inside.

This paper presents the design and construction of an thermoelectric heat pipe prototype to be coupled with a double flux mechanical ventilation system, and empirically analyzes two integration possibilities: stand-alone installation or combined with a heat recovery unit.

In wintertime, the stand-alone installation showed better performance results for the heat pump, with a heating capacity of 1,000-1,250W and COP_h ranging 1.5-4. In this case it is necessary to set a minimum voltage to assure that the incoming air is above the set point inside the building. For a higher temperature outside this performance gets reduced, which is in tune with the lower heating load in the building.

When the thermoelectric heat pump is integrated with a heat recovery unit, both technologies, passive and active heat recovery, have a combined better performance that reaches 1,400-1,650 W with COP_h ranging 1.8-9. In this case, 800-1,000 W of heating capacity are provided by the heat pump, above the maximum heating load required by the Passiv House standard (10 W/m^2) for a 80 m^2 dwelling.

In summertime, the thermoelectric heat pump performance is again better when working as stand-alone installation, reaching 375 W of cooling capacity with COP_c ranging 0.5-2.5. When the power supply exceeds 9 V the cooling capacity is barely increased while the COP_c drops 40%.

The combined effect of heat recovery unit and heat pump obtains better results, the cooling capacity is increased 50 W on average and the COP_c is improved. For more extreme exterior temperatures, this combination would certainly show a better performance compared with the sole use of the heat pump, due to the passive effect of the heat recovery unit.

As an overall conclusion, present work extends the scope of previous experimental works to assess the energy performance of an air-to-air thermoelectric heat pump for Passiv Houses, and demonstrates the convenience to integrate it with an heat recover unit. Future research works need to focus on improving the cooling capacity of this combination.

Acknowledgments

The authors are indebted to the Government of Navarre for the economic support to this work, included in the project PT009 of the R+D Support Program for Technology Centers 2017.

References

[1] EU, Directive 2010/31/EU of the European Parliament and of the Council of 19 May 2010 on the energy performance of buildings (recast), Off. J. Eur. Union. (2010) 13–35. https://doi.org/10.3000/17252555.L_2010.153.eng.

[2] General Secretariat of the Council, Conclusions adopted by the European Council meeting. EUCO 169/14 On The 2030 Climate and Energy Policy Framework, (2014) 1–16. http://data.consilium.europa.eu/doc/document/ST-169-2014-INIT/en/pdf. Access: 3-12-2020.

[3] EED, Directive 2012/27/EU of the European Parliament and of the Council of 25 October 2012 on energy efficiency, (2012) 1–56.

[4] EU, Directive (EU) 2018/844 of the European Parliament and of the Council of 30 May 2018 amending Directive 2010/31/EU on the energy performance of buildings and Directive 2012/27/EU on energy efficiency, Off. J. Eur. Union. 156 (2018) 75–91. https://eur-lex.europa.eu/eli/dir/2018/844/oj. Access: 3-12-2020.

[5] European Environment Agency (EEA), How is climate change affecting total and peak energy demand for space heating and cooling across Europe?, (2019). https://www.eea.europa.eu/data-and-maps/indicators/heating-degree-days-2/assessment. Access: 3-12-2020.

[6] T. Nowak, Heat Pumps: Integrating technologies to decarbonise heating and cooling, (2018) 1–86. https://www.ehpa.org/fileadmin/user_upload/White_Paper_Heat_pumps.pdf. Access: 3-12-2020.

[7] D. Zhao, G. Tan, A review of thermoelectric cooling: Materials, modeling and applications, Appl. Therm. Eng. 66 (2014) 15–24. https://doi.org/10.1016/j.applthermaleng.2014.01.074.

[8] L. Shen, X. Pu, Y. Sun, J. Chen, A study on thermoelectric technology application in net zero energy buildings, Energy. 113 (2016) 9–24. https://doi.org/10.1016/j.energy.2016.07.038.

[9] A. Zuazua-Ros, C. Martín-Gómez, E. Ibáñez-Puy, M. Vidaurre-Arbizu, Y. Gelbstein, Investigation of the thermoelectric potential for heating, cooling and ventilation in buildings: Characterization options and applications, Renew. Energy. 131 (2019) 229–239. https://doi.org/10.1016/j.renene.2018.07.027.

[10] Z. Liu, L. Zhang, G. Gong, H. Li, G. Tang, Review of solar thermoelectric cooling technologies for use in zero energy buildings, Energy Build. 102 (2015) 207–216. https://doi.org/10.1016/j.enbuild.2015.05.029.

[11] S. Riffat, X. Ma, R. Wilson, Performance simulation and experimental testing of a novel thermoelectric heat pump system, Appl. Therm. Eng. 26 (2006) 494–501. https://doi.org/10.1016/j.applthermaleng.2005.07.016.

[12] T. Li, G. Tang, G. Gong, G. Zhang, N. Li, L. Zhang, Investigation of prototype thermoelectric domestic-ventilator, Appl. Therm. Eng. 29 (2009) 2016–2021. https://doi.org/10.1016/j.applthermaleng.2008.10.007.

[13] T. Han, G. Gong, Z. Liu, L. Zhang, Optimum design and experimental study of a thermoelectric ventilator, Appl. Therm. Eng. 67 (2014) 529–539. https://doi.org/10.1016/j.applthermaleng.2014.03.073.

[14] F. Meng, L. Zhang, J. Li, C. Li, L. Xie, Y. Luo, Z. Liu, Investigation of Thermoelectric Warm Air Heater, Energy Procedia. 75 (2015) 621–626. https://doi.org/10.1016/j.egypro.2015.07.470.

[15] Z. Liu, L. Zhang, Y. Luo, Y. Zhang, Z. Wu, Performance evaluation of a photovoltaic thermal-compound thermoelectric ventilator system, Energy Build. 167 (2018) 23–29. https://doi.org/10.1016/j.enbuild.2018.01.058.

[16] Y.W. Kim, J. Ramousse, G. Fraisse, P. Dalicieux, P. Baranek, Optimal performance of air air thermoelectric heat pump (thp) coupled to energy-efficient buildings coupling indifferent climate conditions, Proc. BS 2013 13th Conf. Int. Build. Perform. Simul. Assoc. (2013) 1110–1117.

[17] Y. Kim, J. Ramousse, G. Fraisse, P. Dalicieux, P. Baranek, Optimal sizing of a thermoelectric heat pump (THP) for heating energy-efficient buildings, Energy Build. 70 (2014) 106–116. https://doi.org/10.1016/j.enbuild.2013.11.021.

[18] B. David, J. Ramousse, L. Luo, Optimization of thermoelectric heat pumps by operating condition management and heat exchanger design, Energy Convers. Manag. 60 (2012) 125–133. https://doi.org/10.1016/j.enconman.2012.02.007.

[19] J. Ramousse, D. Sgorlon, G. Fraisse, M. Perier-Muzet, Analytical optimal design of thermoelectric heat pumps, Appl. Therm. Eng. 82 (2015) 48–56. https://doi.org/10.1016/j.applthermaleng.2015.02.042.

[20] K. Irshad, K. Habib, F. Basrawi, N. Thirumalaiswamy, R. Saidur, B. Saha, Thermal comfort study of a building equipped with thermoelectric air duct system for tropical climate, Appl. Therm. Eng. 91 (2015) 1141–1155. https://doi.org/10.1016/j.applthermaleng.2015.08.077.

[21] K. Irshad, K. Habib, N. Thirumalaiswamy, B. Saha, Performance analysis of a thermoelectric air duct system for energy-efficient buildings, Energy. 91 (2015) 1009–1017. https://doi.org/10.1016/j.energy.2015.08.102.

[22] K. Irshad, K. Habib, F. Basrawi, B.B. Saha, Study of a thermoelectric air duct system assisted by photovoltaic wall for space cooling in tropical climate, Energy. 119 (2017) 504–522. https://doi.org/10.1016/j.energy.2016.10.110.

[23] M. Yilmazoglu, Experimental and numerical investigation of a prototype thermoelectric heating and cooling unit, Energy Build. 113 (2016) 51–60. https://doi.org/10.1016/j.enbuild.2015.12.046.

[24] C. Wang, C. Calderón, Y. Wang, An experimental study of a thermoelectric heat exchange module for domestic space heating, Energy Build. 145 (2017) 1–21. https://doi.org/10.1016/j.enbuild.2017.03.050.

[25] Y. Cai, S.J. Mei, D. Liu, F.Y. Zhao, H.Q. Wang, Thermoelectric heat recovery units applied in the energy harvest built ventilation: Parametric investigation and performance optimization, Energy Convers. Manag. 171 (2018) 1163–1176. https://doi.org/10.1016/j.enconman.2018.06.058.

[26] Y. Cai, S. Mei, D. Liu, F. Zhao, H. Wang, Thermoelectric heat recovery units applied in the energy harvest built ventilation: Parametric investigation and performance optimization, Energy Convers. Manag. 171 (2018) 1163–1176. https://doi.org/10.1016/j.enconman.2018.06.058.

[27] A. Martinez, S. Díaz de Garayo, P. Aranguren, D. Astrain, Assessing the reliability of current simulation of thermoelectric heat pumps for nearly zero energy buildings: Expected deviations and general guidelines, Energy Convers. Manag. 198 (2019) 111834. https://doi.org/10.1016/j.enconman.2019.111834.

[28] P. Cuce, S. Riffat, A comprehensive review of heat recovery systems for building applications, Renew. Sustain. Energy Rev. 47 (2015) 665–682. https://doi.org/10.1016/j.rser.2015.03.087.

[29] PASSIPEDIA, The Passive House - definition, (n.d.). https://passipedia.org/basics/the_passive_house_-_definition. Access: 3-12-2020.

[30] S. Guillén-Lambea, B. Rodríguez-Soria, J.M. Marín, Review of European ventilation strategies to meet the cooling and heating demands of nearly zero energy buildings (nZEB)/Passivhaus. Comparison with the USA, Renew. Sustain. Energy Rev. 62 (2016) 561–574. https://doi.org/10.1016/j.rser.2016.05.021.

[31] M.H.C. Javier Crespo, Jesús Soto, Alfredo Bengoa, Sergio Díaz de Garayo, Micheel Wassouf, Amarante Barambio, Rafael Royo, Nuria Díaz, Anne Vogt, Jordina Vidal, GUIA PASSIVHAUS, n.d. M.37.033-2011 https://www.fenercom.com/publicacion/guia-del-estandar-passivhaus-edificios-de-consumo-energetico-casi-nulo-2011/. Access: 3-12-2020.

[32] COMFORT AIR 160 - HX SYSTEM, (n.d.). https://www.zehnder.co.uk/ventilation-units/heat-recovery-centralised/units-smaller-800-m3h/zehnder-comfoair-160. Access: 3-12-2020.

[33] TETechnology, Hp-127-1.4-1.15-71, (2018) 1–7. https://tetech.com/wp-content/uploads/2013/11/HP-127-1.4-1.15-71.pdf. Access: 3-12-2020.

[34] D. Astrain, P. Aranguren, A. Martínez, A. Rodríguez, M.G. Pérez, A comparative study of different heat exchange systems in a thermoelectric refrigerator and their influence on the efficiency, Appl. Therm. Eng. 103 (2016). https://doi.org/10.1016/j.applthermaleng.2016.04.132.

[35] D.A. S. Diaz de Garayo, Alvaro Martinez, Energy performance of an air-to-air thermoelectric heat pump integrated with the mechanical ventilation of a passiv house considering the moisture and CO2 balance, in: 15th Eur. Conf. Thermoelectr. 2017ECT, Padova, 2017.

[36] D.A. Alvaro Martinez, S. Díaz de Garayo, Air-to-air thermoelectric heat pump for heating, ventilation and air conditioning in Passiv Houses, in: 36th Int. Conf. Thermoelectr. - 2017ICT, Pasadena, 2017.

[37] P. Aranguren, S. Díaz de Garayo, A. Martínez, M. Araiz, D. Astrain, Heat pipes thermal performance for a reversible thermoelectric cooler-heat pump for a nZEB, Energy Build. 187 (2019) 163–172. https://doi.org/10.1016/j.enbuild.2019.01.039.

[38] R. DM., CRC Handbook of Thermoelectrics, CRD Press; 1995. DOI: 10.1201/9781420049718.ch3.

[39] H.W. Coleman, W.G. Steele, Experimentation, validation, and uncertainty analysis for engineers, John Wiley & Sons: Fourth edition, 2018. https://doi.org/10.1002/9781119417989.

[40] L. XUE, G. MA, F. ZHOU, L. WANG, Operation characteristics of air–air heat pipe inserted plate heat exchanger for heat recovery, Energy Build. 185 (2019) 66–75. https://doi.org/10.1016/j.enbuild.2018.12.036.

Chapter 4. TeHP performance investigation

Further to the experimental investigation carried out by PT050/2016 and PT009/2017, and the two built prototypes explained in previous chapters, the research must proceed based on computational models in order to optimize the design of the proposed TeHP, and simulate its performance in a real building.

The computational model must not only reproduce the thermal behavior of the TeHP, but also the thermoelectric phenomena, validating its estimations with real data, extracted from the experimental research exposed in previous chapter. To this aim, it is necessary to address the following two questions:

- **Stationary vs dynamic simulation.**

  The steady-state simulation of a process assumes that the variables are not time-dependent, which is not the case of buildings, where outdoor boundary conditions, as the temperature or the solar radiation, are constantly changing, as well as the internal gains and the ventilation. However, many stationary building simulation programs perform an energy balance in a yearly or monthly basis to estimate the heating or even the cooling demand of a building. In this case, the efficiency of the HVAC systems needs to assume a seasonal coefficient of performance, based on a weighted average of the efficiency at different steady-state cases, as the EUROVENT CERTIFICATION system [https://www.eurovent-certification.com/en/third-party-certification/certification-programmes/ac].

  In order to better address the thermal inertia of the building, other simulating tools (as shown in next Chapter) perform a dynamic simulation of the different components of the buildings, but, even in this case, the time-step is commonly between one hour and 10 minutes, since boundary conditions do not change that fast. The duration of transient processes of HVAC systems, as heat pumps, is always lower than this time-step and do not affect significantly to the overall efficiency in one-year-time. Vapor-compression heat pumps performance is normally represented with load curves, where the COP and the heating capacity depend on the temperatures in the condenser and the evaporator.

In the case of the TeHP, the thermal inertia of the prototype is very low. The temperature of the TEM sides change immediately after modifying the supply voltage, and the heat flux in the heat pipes was stabilized in 1-2 minutes during the laboratory tests, whose results have been shown in previous Chapters. Each test (for different air flows, voltage supplies and temperature gaps between indoor and outdoor) lasted 15 min to make sure that the variability of the different measured temperatures was below 2°C, but stationary condition were reached in less than 2 minutes. For all these reasons, the computational model of the TeHP developed within this Chapter will respond to steady conditions and the dynamic character will be implemented in next Chapter, where a quasi-steady-state model will be integrated with the dynamic simulation of a building in an hourly basis.

- Level of complexity: As indicated in section 1.5.2, there are three common models used to simulate the thermal and electrical behavior of thermoelectric applications: the simple model, the improved model and the electrical analogy. All these models reproduce the thermoelectric effects (Seebeck, Peltier, Joule and Thomson) estimating the heat generation and heat absorption carried out in the TEMs. However, this estimation is made based on a number of assumptions and simplifications in order to solve these equations. Actually, the simple model directly discards the Thomson effect. Surprisingly, all the reviewed authors in the scientific literature selected the simple model for their investigations, which seems to reduce the accuracy of the computational model.

  In order to analyze these questions and select the most suitable model, one specific investigation was carried out and published in **Simulation of thermoelectric heat pumps in nearly zero energy buildings: Why do all models seem to be right?**. Energy Conversion and Management 235 (2021) 113992. DOI: 10.1016/j.enconman.2021.113992. This research evaluates up to nine modelling techniques for the simulation of thermoelectric heat pumps within the framework of nearly-zero-energy buildings. These techniques come from the combination of the above-mentioned three simulation models (simple, improved, and electrical-analogy-based) and five methods for implementing the Seebeck coefficient, the electrical resistivity and the thermal conductivity in these simulation models (Lineykin's method, Chen's method, and temperature-dependent expressions from manufacturers Laird, Melcor and Ferrotec).

  As main outcome, the paper proves that there is no statistical difference in the results of coefficient of performance and cooling power provided by these modelling techniques, at 95% level of confidence. The low and non-significant differences in the results between modelling techniques come from the method used to introduce the thermoelectric properties and not from the simulation model deployed for the thermoelectric modules. Therefore, the use of the simple model is recommended for simplicity in the case of TeHPs applied to nZEBs.

However, differences exist in the precision of the results, in terms of the uncertainty of the confidence intervals. The thermal resistance of the heat exchangers per installed thermoelectric module is the key parameter. The minimum values of uncertainty in the results are obtained when this thermal resistance is $0.1KW^{-1}$. Under this condition, uncertainty of ±8% is obtained when using expressions for the thermoelectric properties, independently on the manufacturer. The uncertainty of the Seebeck coefficient (especially in the calculation of the coefficient of performance) and the uncertainty of the electrical resistivity (especially for the cooling power) are the main contributors to the uncertainty in the results. The uncertainty in the results increases dramatically for scenarios with high thermal resistance of the heat exchangers. Under these circumstances, the large end-temperature difference that appear in the thermoelectric modules makes the thermal conductivity gain in influence, which is exacerbated for high voltages and high uncertainties in the thermal resistance. Significant improvements are obtained if the uncertainty of the thermal resistance is reduced by deploying experimental tests for heat exchanger characterization.

- As a result, the proposed computing model is based on a stationary simple model and the expressions for the thermoelectric properties are provided by the manufacturer: TE TECHNOLOGY. Additionally, the thermal resistance of the heat pipes have been characterized experimentally (Chapter 1 and 2), and the double dependency on air flow and the heat flux are introduced in the computing module with an interpolation module. The reliability of the proposed model has been validated with the experimental data obtained in previous Chapter 3, and the result has been published in the paper: **Optimal combination of an air-to-air thermoelectric heat pump with a heat recovery system to HVAC a passive house dwelling** published in **Applied Energy** (Volume 309 (2022) 118443. DOI: 10.1016/j.apenergy.2021.118443), which constitutes the Chapter 4 of the current Ph. D. dissertation.

Besides the validation, the publication explores the performance of the TeHP under different outdoor conditions, heating/cooling load, two different configurations (combined or not with an HRU) and a number of modules for the TeHP that varies from 1 to 100. The analysis demonstrates that 15 TEMs optimize the heating performance of the system regardless of the climate, what constitutes a promising principle to standardize a future thermoelectric heat pump for passive house dwellings that could reach the market.

Optimal combination of an air-to-air thermoelectric heat pump with a heat recovery system to HVAC a passive house dwelling

S. Diaz de Garayo[1], A. Martínez[2,3], D. Astrain[2,3]
[1] *National Renewable Energy Centre, 31621 Sarriguren, Spain*
[2] *Engineering Department Public University of Navarre, 31006 Pamplona, Spain*
[3] *Smart Cities Institute, Pamplona, Spain*
[*] *e-mail: sdiaz@cener.com*

Keywords: thermoelectricity, heat pump, heat recovery unit, passive house, HVAC

Abstract

The main objective of this research is to propose a HVAC system for an 80-100 m^2 passive house dwelling based on a thermoelectric air-to-air heat pump combined with a heat recovery unit. The computational parametric investigation demonstrates that the integration of the heat recovery unit significantly improves the coefficient of performance of the heat pump: 2-3 times for partial load operation and 12.5 % for maximum load. Moreover, the number of required modules to reach the maximum performance is at least 5 times lower.

A second analysis assesses its seasonal heating performance in three climates as stated by the energy labeling Directive 2010/30/EU. The optimum number of thermoelectric modules in all cases is close to 15, regardless of the climate. This 15-modules thermoelectric heat pump provides a maximum heating capacity of 2500 W and 405 W for cooling, which compensates the typical internal heat gains and the transmission heat flux through the building envelope and the ventilation in the passive house dwelling. Finally, the analysis reveals that, in order to increase this cooling capacity, it is more convenient the improvement of the heat exchangers between the thermoelectric modules and the cooling air stream, rather than increasing the number of modules.

Glossary

Acronyms		
ACH	air changes	1/h
DC	direct current	
HP	heat pipe	
HRU	heat recovery unit for double flux ventilation systems in buildings	
TeHP	thermoelectric heat pump	
TEM	thermoelectric module	
Greek letters		
α	seebeck coefficient of a TEM leg	V/K
$\mathcal{E}$	efficiency	
λ	thermal conductivity of a TEM leg	W/mK
γ	aspect ratio of a TEM leg	m
ρ_{air}	air density	kg/m^3
Φ	air relative humidity	%
ω	air humidity ratio	Kg_{H2O}/Kg_{air}
Variables		
A^{TEM}	area of one thermocouple	m^2
b_R	systematic standard uncertainty	
C_p	specific heat of the air	J/kgK
COP	coefficient of Performance	
ΔH_{vap}	vaporization latent heat	
I	current supply to the TEMs	A
K	thermal conductance of a TEM	W/K
l	thermocouple length	m
$\dot{m}_{air}$	air mass flow	Kg/s
$\dot{m}_{cond}$	condensed water	Kg/s
n	number of thermocouples in the TEM	
ΔP	pressure drop	Pa
$\dot{Q}$	heat flux	W
Q	heat	J
r	electric resistivity of a TEM leg	Ωm
R^{HP}	heat pipe thermal resistance	K/W
$SCOP$	seasonal Coefficient of Performance	
R	TEM overall electric resistance	Ω
S	TEM overall Seebeck coefficient	V/°C
$s_{\bar{R}}$	random standard uncertainty of the mean	
T	temperature	K
U_R	expanded uncertainty	
$\dot{V}$	volumetric air flow	m^3/h
V	voltage supply to the TEMs	V
$\dot{W}$	power supply	W

Subscripts / Superscripts		
c	cooling	
cond	condensed water	
exh	exhaust air, air stream coming from building indoor	
fan	fan	
fresh	fresh, air stream coming from building outdoor	
h	heating	
HRU	referring to variables at the outlet of the heat recovery unit	
IN	variables at the inlet of the TeHP	
OUT	variables at the outlet of the TeHP	
sup	supply, referred to the parameters that define the supply ventilation air flow, after going to either the TeHP or HRU+TeHP	

1. Introduction

Buildings are responsible for approximately 40% of EU energy consumption and 36% of the CO_2 emission [1]. This sector is actually the single largest energy consumer in Europe and, hence, a significant player in the achievement of the target of the EU Commission to become climate neutral in 2050 [2]. The Energy Performance of Buildings Directive 2010/31/EU (EPBD [1]) and the Energy Efficiency Directive 2012/27/EU [3][4]) promote the nearly ZERO ENERGY BUILDINGS (nZEBs), obligatory since 2020 for new edifications, which are expected to trigger new construction solutions that must be both energy and cost efficient. Passive houses paved the way for nZEBs, as it is a clearly defined building performance standard based on scientific evidence [5], and characterized by 1) super insulated envelope, 2) airtight construction, 3) high-performance glazing, 4) thermal-bridge-free detailing, and 5) heat recovery ventilation. Under these circumstances, the heating and cooling loads of the building are limited to 10 W/m^2, irrespective of the climate [6]. In such conditions, raising or lowering the temperature of the incoming fresh air with a volumetric flow between 0.35-0.5 air changes (ACH) [7] might provide an indoor comfortable ambient, saving the costs of the heat/cold distribution systems. This is actually the principle upon which the Passive House concept is built [6].

Besides the expected improvement of the buildings' envelope [8], the heating and cooling systems need to be decarbonized [2] as well. In this context, the heat pumps are expected to experiment a strong deployment in the coming years, powered by the increasingly decarbonized electric grid [9], replacing fossil fuel fired boilers. Most of the heat pumps present in the market are based on the electric compression cycle [9]. However, despite the investigations to reduce the global warming potential of the refrigerants, replaced by climate-friendly alternatives [10], and the efforts to integrate the renewable energy production in buildings, there has not been any breakthrough technology on the design of new active HVAC systems [11].

Thermoelectricity is a very promising heat pump technology that presents many advantages: no moving parts, gas free, no chemical reaction, reliability, scalability, minimum maintenance, easy transition from heating to cooling mode, easy and accurate temperature control and PV easy integration, among others [12]. Compared with vapor compression technology, the coefficient of performance (COP) is relatively low, but in the case of building with low energy demand, the cited advantages may well outweigh this aspect. This fact explains the increase in the number of works evaluating the use of thermoelectric heat pumps (TeHP) in the building sector, as it can be seen in several reviews ([13], [11], [14], [15]). A TeHP is a solid-state energy converter that can create a temperature difference when an electric potential is applied to the TEM (thermoelectric module), thanks to the Peltier effect [16]. The TEMs are then able to absorb heat from a cold reservoir and emit heat to a hot one by consuming DC electric power.

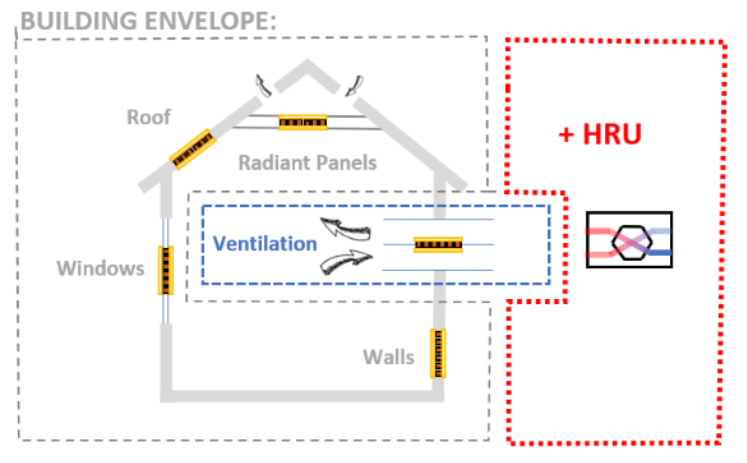

Figure 66. Integration possibilities of a TeHP in a buildings according to the reviewed research works ([13], [11], [14], [15]).

The above-mentioned reviews classify the research works attending to different criteria, but mainly based on the way that the TeHP is integrated in the building. There are basically two main categories:

- Envelope: where the TEMs are inserted in the walls, roofs, radiant panels or windows, compensating the incoming or outgoing heat flows. Most of the built prototypes use finned heat sinks that, in most of the cases, are complemented with PV panels, creating a ventilated façade. However, the thermal bridge created by the TEMs is the main weakness of this strategy, which goes against the passive house philosophy of reducing the thermal losses through the building envelope as much as possible.

- Ventilation: the basic idea in this case is to use exhaust air as either heat or cold reservoir to cool or heat, respectively, the incoming ventilation air stream. This concept fits very well with the passive house principle [6], thus being the approach used in this paper.

One HVAC system in a passive house incorporates a heat recovery unit (HRU). A HRU is a device, able to recover the residual sensible heat of the exhaust air. A typical heat recovery system consists of a core unit, channels for fresh air and exhaust air, and blower fans. The

thermal energy (enthalpy) is transferred from one air stream to another, with no moisture transfer and no air mixture between the air streams [17]. Sensible heat recovery units typically recover about 70–95% of the heat in exhaust air and significantly improve the energy efficiency of buildings [17].

However, noteworthy is the fact that, among all the research works cited by the reviews, only [18], [19] and [20] investigate the combination of a HRU with the TeHP, despite the potential improvement in the global efficiency compared to that of a standalone TeHP. Also, despite being of notable relevance, these papers present some limitations, as subsequently explained, that led to the research presented in this paper. Tao Li et al. [18] built a prototype of domestic thermoelectric ventilator with heat recovery from exhaust air. The prototype combines a thermoelectric module heat exchanger and a cross flat-fin sensible heat exchanger into a device limited to 60 m^3/h volumetric air flow. The fresh air goes through the thermoelectric modules first and then, through the aluminum crossflow HRU, so the temperature of the incoming air is not intended to be higher than the indoor temperature in winter, neither lower in summer. More recently, Seon-Yong Cheon et al. [19] built another crossflow TeHP with aluminum heat sinks. Based on the empirical results, this research proposes its combination with an enthalpy wheel. In this case the fresh air stream recovers the heat from exhaust air first, and then it is conditioned by the TeHP and a desiccant wheel. The modeling results show that the energy consumption for one year is 22 % higher than a reference system composed of an HRU and a vapor compression cycle heat pump. However, in both cases, [18] and [19], the performance of the TeHP is limited due to the high thermal resistance of the finned heat sinks. It is well known that a low thermal resistance of the heat exchangers between the TEMs and the air streams is crucial in order to obtain a good energy performance of the TeHP, since a higher thermal resistance increases the temperature gap between the hot and cold side of the TEM, what drastically reduces the COP [21]. The use of heat pipes as heat exchangers even double the energy performance of a TeHP compared with aluminum flat finned heat sinks. This fact is indeed remarked by [22], presenting a thermoelectric ventilator with heat pipes, as an evolution of a previous design made with aluminum fins [18]. The TeHP demonstrated to perform better, but the prototype is still limited to 60 m^3/h volumetric air flow, and the tests intend to equal the indoor temperature, with no aim of extra-heating/cooling the inside. However, in the mathematical modeling analysis, the thermal resistance of the heat pipes is set up as 0.4 K/W. In real conditions, this thermal resistance is never constant but variable depending on the heat flux and the air flow. Also, its value in the cold side doubles the one in the hot side, since the heat pipe on the cold side works contrary to its design conditions [23]. The natural inaccuracy due to the simplifications and estimated input values for the computational models may drive to deviations higher than 30% between simulated and experimental results [24], especially if a significant aspect as the complexity related to the heat and mass transfer mechanisms in the heat pipes is not well addressed.

Finally, not only the heat exchanger design must be optimized, but also the number of TEMs and the consequent power supply in order to maximize the COP of the system depending on the incoming air temperature. In line with this, the third study that combines a TeHP with a HRU is the interesting simulation analysis carried out by Y.W. Kim et al. [20] to heat one nZEB with a TeHP. This study proposed three different integration possibilities of the TeHP with the ventilation system, and one of them includes a HRU. The simulation results demonstrate the

existence of an optimized number of modules (35-60) driven by the dissipated heat flux and the temperature difference between both sides of the flux. This paper presents some limitations. Firstly, the TeHP has no specific physical representation. Secondly, the thermal resistance of the heat exchangers between the air streams and the TEMs is set to an unrealistic value of 0.001 K/W per installed TEM, based on [25]. Thermal resistances of a heat exchanger below 0.1 K/W per installed TEM [21] are difficult to achieve experimentally when air is present, whereas the reference [25] applies an impinging jet system for liquid-TEM heat exchange. Thirdly, the ventilation scheme includes indoor air recirculation (3 times the ventilation air flow) to reach the estimated energy needs of the building (30 W/m^2), what makes the TeHP work against outdoor air when the HRU is integrated. As previously mentioned the architectural conceptualization and the thermal envelope of a passive house limit the heating/cooling load to 10 W/m^2, what makes it possible the direct integration of the TeHP right after the HRU and, thus, reduce the temperature gap between air streams. This is expected to reduce also the optimum number of modules required in the TeHP.

The present work comes to fill this research void and goes a step forward on the search for the integration of TeHPs+HRU in extremely-high efficient buildings, as passive houses. Additionally, the paper delves into the application of these systems for different climates. The TeHP is used for both, heating and cooling, using outgoing air stream as heat reservoir. It includes finned heat pipes as heat exchangers between the TEMs and the air streams, what considerably improves the experimental performance results of [18] and [19], and reduces the number of optimized modules of [20]. The variable thermal resistance of these heat exchangers was previously measured [23] under different operating conditions, and the empirical results have been introduced in the analytical model used in the present study. Moreover, the TeHP design is based on a previous experimental work [26], where one real 10-TEM-prototype was built and tested. Additionally, some of the findings of the present study are in contradiction with the conclusions of [20], wherein it is stated that, for higher indoor temperature or higher heating demand, the number of modules to reach the maximum COP needs to be higher as well.

The research work is presented in three sections. Section 2 deals with the methodology of the study describing the proposed HVAC system and the TeHP model: section 2.1 explains the computational model, while section 2.2 reports the validation, comparing the experimental results with the calculated outputs. Section 3 presents the results of the parametric investigation with two primary objectives: the first one is to compare the maximum energy performance of the HVAC system when the TeHP works alone or integrated with the HRU under different operating conditions. To this aim, section 3.1 presents the optimization of the number of modules for different temperature and humidity conditions outdoor and indoor, in both heating and cooling modes for both configurations. The second objective is to consider the relationship between the passive house thermal envelope, the heating and cooling loads and the outdoor conditions in different climates, what permits the optimization of the seasonal performance of the TeHP in winter conditions, and the maximum cooling capacity in summer conditions. This study is reported in section 3.2. Finally, section 4 provides the main conclusions of the paper.

2. Methodology

This paper proposes an HVAC system for a passive house dwelling, where one air-to-air thermoelectric heat pump (TeHP) provides heating or cooling, by raising or lowering the temperature of the ventilation air flow before entering the building, using the outgoing exhaust air stream as either cold or hot reservoirs. Two possible configurations are present in the literature, and will be analyzed here (Figure 67):

- **1st Config:** the TeHP works alone, so it is directly installed between both incoming and outgoing air streams (where, $T_c^{IN} = T_{exh}$ and $T_h^{IN} = T_{fresh}$ in heating mode). The TeHP works as both passive and active heat recovery system, that can raise/lower the T_{fresh} up/down to T_{sup}, that will be above/bellow T_{exh} in order to air condition the indoor ambient. This configuration is the simplest, thus facilitating the installation .

- **2nd Config:** the TeHP is installed in combination with an HRU. The heat pumped to/from the fresh air stream from/to the exhaust air stream, after going through the HRU (where, $T_c^{IN} = T_{exh}^{HRU}$ and $T_h^{IN} = T_{fresh}^{HRU}$ in heating mode, T_{fresh}^{HRU} will be then lower than T_{exh}, since the passive heat recovery can never perform at 100% efficiency).

In both scenarios a polarity reversion in the electric supply of the TEMs easily switches the HVAC system from heating to cooling mode. The scope of the present study is to ventilate, heat or cool a passive house dwelling of 80-100 m^2, so the volumetric air flow rate will be set at 100 m^3/h, corresponding to the ventilation needs of 0.4-0.5 ACH for a room height of 2.5 m (200-250 m^3 of air conditioned space) [7]. The technical characteristics of the HRU (efficiency, pressure drop and blower electric consumption) are based on a commercial model limited to 200 m^3/h of maximum volumetric air flow [27], that normally operates at 80-120 m^3/h.

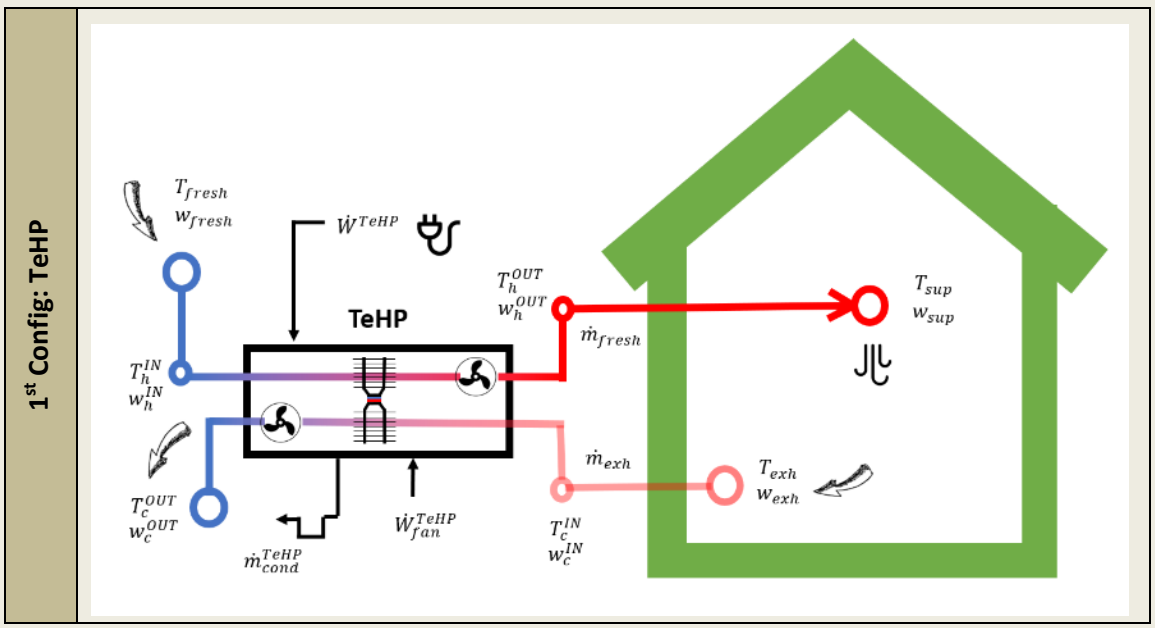

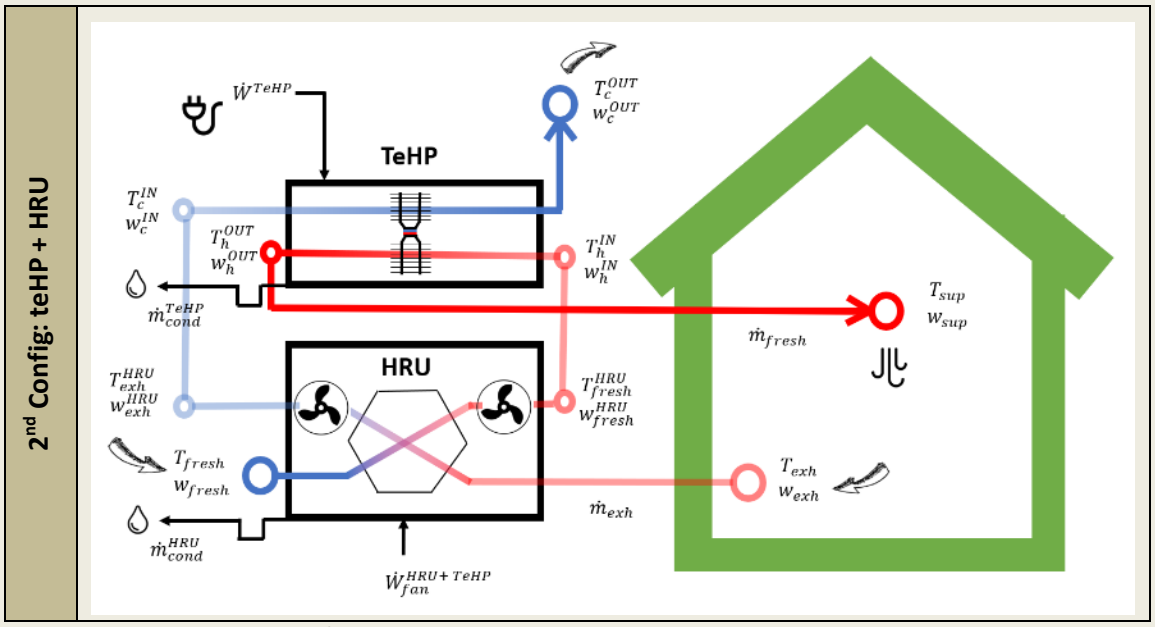

Figure 67. Detailed scheme of the two proposed HVAC systems to provide ventilation, heating and cooling in a Passive House building (heating mode in the picture). The 1st Config proposes the sole installation of a TeHP to work as both passive and active heat recovery system. The 2nd Config integrates the TeHP with a HRU.

The air-to-air TeHP design is based on a previous empirical research work [26] (see Figure 68), that includes the construction and test of the energy performance of a thermoelectric heat pump prototype. This prototype is composed of two counter-flow 12 cm square air ducts. The heat transfer between the air streams is induced by the thermoelectric modules (TEMs). The TeHP has a modular design. Each module is composed of a TEM and two heat exchangers to transfer the heat between the TEM's cold and hot faces and the air streams. Each heat exchanger is composed of 5 copper 6 mm heat pipes (HP) combined with 40 aluminum fins 5.5 cm deep. These HP have been analyzed and thermally characterized in a previous experimental study [23]. In both, the TeHP or the HRU, the vapor contained in the cooling air stream may condense when the temperature goes below the dew point, so a condensate drain port is also necessary in order to evacuate the condensed water.

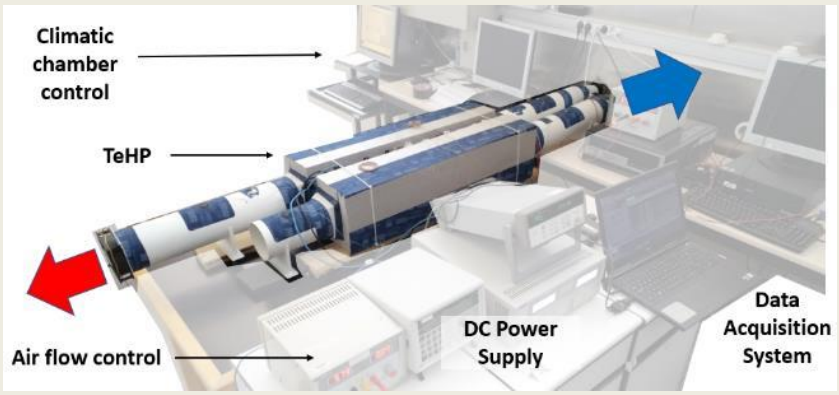

Figure 68. TeHP prototype investigated. The thermal resistance of the heat sinks is based on empirical data and the mathematical model has been validated with the results a previous empirical invesgitagion [26].

2.1. Computational model

This section describes the analytical model that has been programed in Engineering Equation Solver (EES) developed by F-Chart Software [28], and further validated with experimental data. The mathematical model must not only reproduce the thermal behaviour of the different components, but also the thermoelectric phenomena, as well as the pressure drop in the air ducts and the water condensation in the cooling air streams.

2.1.1. Heat Recovery Unit (HRU)

In order to model the HRU, the effectiveness – minimum capacitance approach is used [29]. The HVAC system is regulated to ensure that $\dot{m}_{fresh}$ is equal to $\dot{m}_{exh}$, so that the air pressure inside is equal to the one outside. In this situation, the minimum capacitance belongs to the hotter air stream (as having lower specific heat): the exhaust air flow in winter and the fresh air in summer. The efficiency is considered constant, with a value of 0.9 [27], that is, the transferred sensible heat is then 90 % of the maximum possible energy transfer between the two air streams, as in Eq. (1) [30], where exhaust air is considered the minimum capacity fluid, as it is commonly the hotter air stream during winter season and, therefore, with lower Cp.

$$\dot{Q}^{HRU} = \mathcal{E}^{HRU}\, \dot{m}_{exh} Cp_{exh} (T_{exh} - T_{fresh}) \tag{1}$$

The enthalpy of the fresh air stream outlet can be determined using Eq. (2).

$$h_{fresh}^{HRU} = h_{fresh} + \frac{\dot{Q}^{HRU}}{\dot{m}_{fresh}} \tag{2}$$

While the enthalpy of the exhaust air stream is calculated following Eq. (3):

$$h_{exh}^{HRU} = h_{exh} - \frac{\dot{Q}^{HRU}}{\dot{m}_{fresh}} \tag{3}$$

The outlet humidity ratios are expected to remain constant, as the HRU only transfers sensible heat. However, in the case that the enthalpy at the outlet is lower than the enthalpy at the dew point, condensation is expected to happen. Then, Eq. (4) is used to calculate the condensed water:

$$\dot{m}_{cond}^{HRU} = \dot{m}_{exh}\, (\omega_{exh} - \omega_{exh}^{HRU}) \tag{4}$$

This condensation occurs in the cooling air duct (exhaust air duct in winter). In order to solve these equations, the EES psychrometrics routines are employed. The pressure drop caused by the HRU is commonly provided by the manufacturer, and depends on the air flow. For this research work, one commercial model has been considered specific for small dwellings (less than 100 m^2) [27]:

$$\Delta P^{HRU} = 0.0012\, \dot{V}_{air}{}^{2} + 0.3478\, \dot{V}_{air} \tag{5}$$

The electricity consumed by HRU is due to the blower fans that adjust the fan speed to meet a certain air flow depending on the pressure drop in the air ducts, caused by both the HRU and the TeHP. For $\dot{V}_{air}$ = 100 m^3/h the ΔP^{HRU} = 46.78 Pa and the fans electric consumption associated is 20 W.

2.1.2. Termoelectric Heat Pump (TeHP)

As well as in the HRU, in the TeHP, two counter-flow air streams exchange heat with no moisture transfer between them. Thanks to the Peltier effect in the TEMs, heat can be pumped from the colder to the hotter air stream. The operation of a TEM with n pairs of thermoelectric legs can be described with a standard simple method that implies Peltier and Joule Effects, as well as the thermal conduction, disregarding the Thomson effect [31]. According to [32], the simulation of a TeHP does not require the deployment of a more complex model. The heat extracted from the cold reservoir in one TEM can be described then by the Eq. (6), while Eq. (7) presents the heat emitted to the hot reservoir.

$$\dot{Q}_c^i = SIT_c^{TEM,i} - \frac{1}{2}I^2R - K(T_h^{TEM,i} - T_c^{TEM,i}) \quad (6)$$

$$\dot{Q}_h^i = SIT_h^{TEM,i} + \frac{1}{2}I^2R - K(T_h^{TEM,i} - T_c^{TEM,i}) \quad (7)$$

The parameters S, R and K are, respectively, the Seebeck coefficient, the electrical resistance and thermal conductance of the TEM, and they depend on the number of thermocouples, the thermoelectric material and the TEM geometry. The simple model assumes opposite Seebeck coefficient but equal electric resistivity, thermal conductivity and aspect ratio in n-doped and p-doped legs. In this case:

$$S = 2\,n\,\alpha \quad (8)$$

$$R = 2\,n\,r\,/\gamma \quad (9)$$

$$K = 2\,n\,\lambda\,\gamma \quad (10)$$

Where γ is the aspect ratio of the thermocouple, calculated as the area of one leg divided by its lenght:

$$\gamma = \frac{A^{TEM}}{l} \quad (11)$$

The α, r and λ thermoelectric properties are temperature dependent variables [20], but for building HVAC applications, can be considered constant (at a temperature of 398K), as their variation in the range of heat sinks operation conditions can be disregarded [33].

For this specific research work, the TEM selected has been the HP-127-1.4-1.15-71 made by TE Technology with 127 thermocouples of Bi_2Te_3 [34]. Its properties are shown in Table 12:

Table 12. Properties of HP-127-1.4-1.15-71 thermoelectric module [34].

Parameters	Values
TEM lenght (mm)	40
TEM width (mm)	40
TEM thickness (mm)	3.4
Number of thermocouples (n)	127
$\dot{Q}_{max}$ (W)	80
ΔT_{max} (°C)	71
I_{max} (A)	8
V_{max} (V)	16.1
S (V/K) at 298 K	0.053
K (W/K) at 298 K	0.72
R (Ω) at 298 K	1.45

The TeHP consists of a series of N modules. Each of these modules (i) has one TEM pumping heat from the cooling duct to the heating duct through two HP heat exchangers.

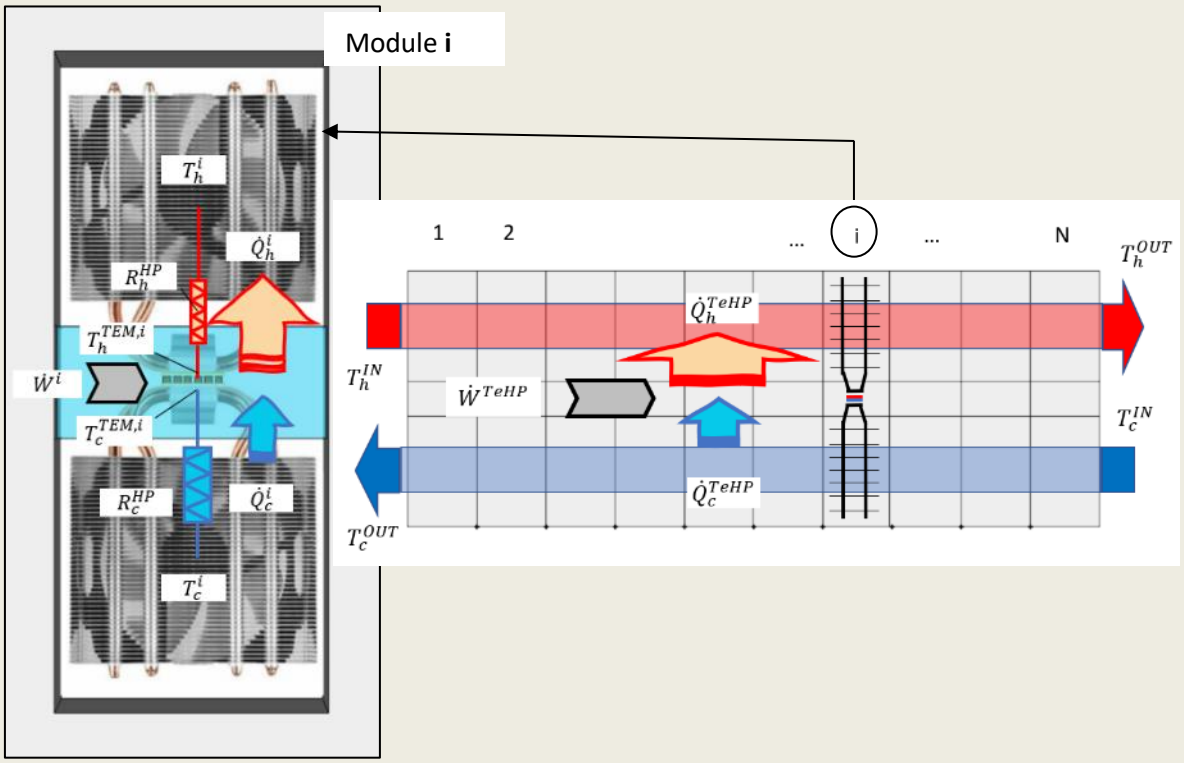

Figure 69. Left: cross-section of one module of the TeHP showing the TEM and the heat pipe heat exchangers with both the cooling and the heating air streams. Right: top view showing the overall energy balance of the TeHP.

Eqs. (12) and (13) show the heat flux exchanged through the HP, between the cold and hot sides of the TEM and the air streams.

$$\dot{Q}_c^{TEM,i} = \frac{T_c^i - T_c^{TEM,i}}{R_c^{HP}} \quad (12)$$

$$\dot{Q}_h^{TEM,i} = \frac{T_h^{TEM,i} - T_h^i}{R_h^{HP}} \quad (13)$$

Where the temperature of the air streams is calculated as the average temperature between the inlet and the outlet, according to Eq (14) and Eq (15).

$$T_c^i = \frac{T_c^{IN} + T_c^{OUT}}{2} \quad (14)$$

$$T_h^i = \frac{T_h^{IN} + T_h^{OUT}}{2} \quad (15)$$

The HP present a variable value of R^{HP}, that clearly influence the calculation of $\dot{Q}_{c/h}^{TEM,i}$. In the case of the hot air stream, the HP works evaporating the internal fluid in the plate attached to the hot side of the TEM, while the condensation happens in the area attached to the aluminum fins in contact with the air flow. R^{HP} value depends on the heat flux (mainly related with the voltage of the TEM electric supply) and the air flow (which affects to the convective heat transfer coefficient between the air and the aluminum fins). In these conditions, R^{HP} ranges from 0.08 to 0.18 K/W [23], as shown in Figure 70.

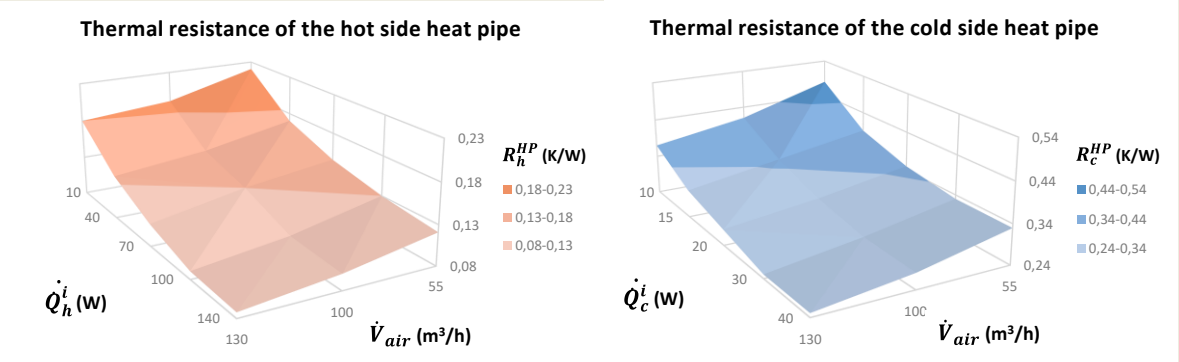

Figure 70. Thermal resistance empirical values of the heat pipes used as heat exchangers between the TEM and air streams depending on the volumetric air flow and the heat flux going through the heat exchangers [26].

However, in the case of the cold air stream, the condensation of the internal fluid of the heat pipe occurs in the plate attached to the cold side of the TEM, which is opposite to the original design. In this case, the R^{HP} is significantly higher: 0.24 - 0.44 K/W. These values, based on the previous experimental research, have been included in the computational model with an interpolation module. Finally, the energy balance of the whole TeHP is presented in Figure 48 and described by Eqs. (16), (17) and (18).

$$\dot{Q}_c^{TeHP} = \dot{m}_{exh}\rho_{air}C_p(T_c^{IN} - T_c^{OUT}) = N\,\dot{Q}_c^i \quad (16)$$

$$\dot{Q}_h^{TeHP} = \dot{m}_{fresh}\rho_{air}C_p\left(T_h^{OUT} - T_h^{IN}\right) = N\,\dot{Q}_h^i \quad (17)$$

$$\dot{W}^{TeHP} = N\,V\,I = \dot{Q}_h^{TeHP} - \dot{Q}_c^{TeHP} \quad (18)$$

As in the HRU, the TeHP simulation also considers possible condensation. In case that the cooling air stream is saturated, then the energy balance of eq. (16) turns into eq. (19) to take into account the condensed water, which can be calculated with eq. (20).

$$\dot{Q}_c^{TeHP} = \dot{m}_{exh}\rho_{air}C_p(T_c^{IN} - T_c^{OUT}) - \dot{m}_{cond}^{TeHP}\,\Delta H_{\,vap} \quad (19)$$

$$\dot{m}_{cond}^{TeHP} = \dot{m}_{exh}\,\rho_{air}\,(w_c^{IN} - w_c^{OUT}) \quad (20)$$

The electric consumption of the TeHP is due to the TEMs ($\dot{W}^{TeHP}$) and the blower fans ($\dot{W}_{fan}^{TeHP}$). $\dot{W}^{TeHP}$ is calculated with Eq. (18), while $\dot{W}_{fan}^{TeHP}$ depends on the pressure drop caused by the heat exchangers in the air ducts. This pressure drop was experimentally measured in the prototype, and the following Eq. (21) represents the pressure drop per module depending on the volumetric air flow:

$$\Delta P^i = 0.00033\,\dot{V}_{air}{}^2 + 0.00997\,\dot{V}_{air} \quad (21)$$

According to the number of modules (N) and the volumetric air flow ($\dot{V}$), the pressure drop is estimated and added to the pressure drop caused by the HRU, and the final fan electric consumption is recalculated for the whole system ($\dot{W}_{fan}^{HRU+TeHP}$) [27]. For 10 modules (as in the case of the experimental prototype) ΔP = 43 Pa when $\dot{V}_{air}$ = 100 m^3/h and the associated fans consumption is 18.5 W (only TeHP).

2.2. Validation

The proposed computational model has been validated by comparing the simulated results with empirical evidence obtained in a deep experimental study of the 10 modules TeHP prototype [26]. Three experimental scenarios were analyzed with the help of an environmental chamber Figure 68: two for winter conditions (T_{fresh}= 0°C and T_{fresh} = 10 °C) and one for summer conditions (T_{fresh}= 30°C). The volumetric air flows ($\dot{V}_{air}$) tested were: 55, 100 and 130 m3/h and the voltage supply: 3, 6, 9 and 12 V. In total, 72 tests were carried out, reaching stationary conditions: 36 for heating and 24 for cooling. All these air inlet conditions were introduced in the computational model, and the outputs compared with the experimental results.

Figure 71 shows the test and estimated values of $\dot{Q}_h$ (left graph) and $\dot{Q}_c$ (right graph) when increasing the voltage of the DC supply of the TEMs for three volumetric air flows. The results show a clear similar trend of both experimental and simulated results, inside the confidence band of the lab tests. The uncertainty of the experimental results was assessed with Eq. (22), where b_R stands for the systematic standard uncertainty, $s_{\bar{R}}$ is the random standard uncertainty and the coefficient 2 represents a confidence interval of the 95 % for the measure. An in-depth explanation about the test can be found elsewhere [26].

$$U_R = 2\sqrt{b_R^2 + s_{\bar{R}}^2} \tag{22}$$

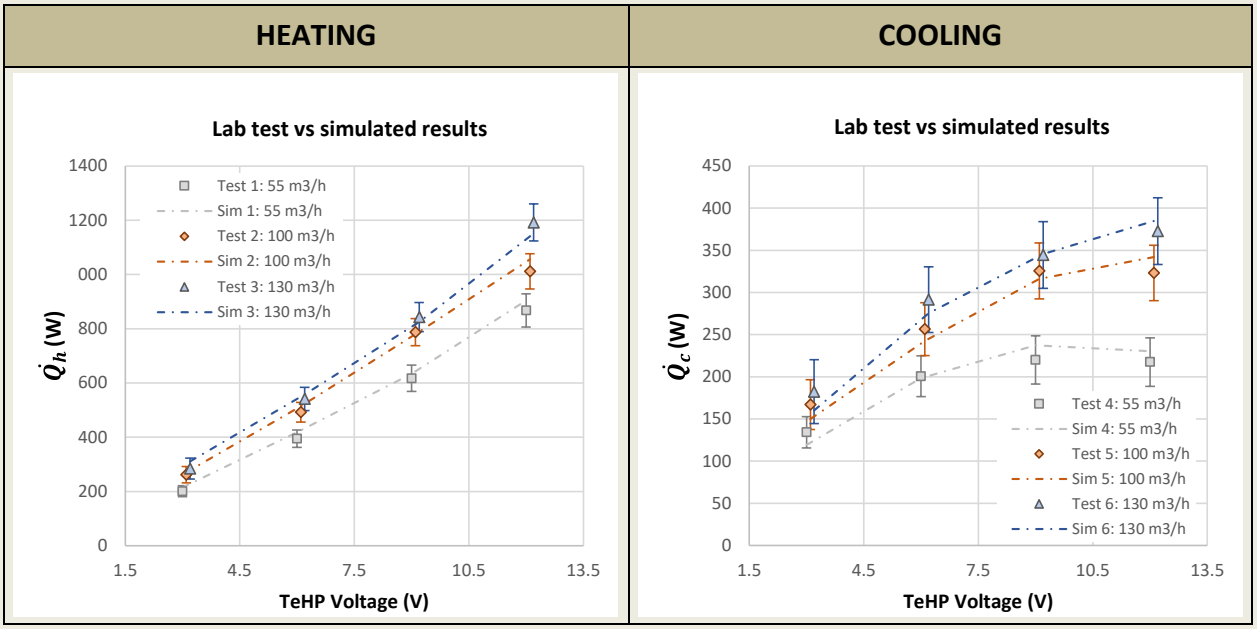

Figure 71. Comparison of experimental and simulated results trends when increasing the TeHP DC supply in heating and cooling tests at different air volumetric flows (m3/h).

Figure 72 shows $\dot{Q}_{c/h}$ and $COP_{\boldsymbol{c/h}}$ correlating experimental and simulated results for the 72 lab tests. The horizontal error bars reproduce the uncertainity, as calculated in Eq (22), which is percentually higher for the lower TEM voltage supply.

The results show a maximum deviation of ±13% for the prediction of the $\dot{Q}_h^{TeHP}$ and the COP_h^{TeHP}. In the case of the cooling tests, the lower temperature gaps in the tests lead to higher uncertainity in the experimental results, specially for 3 V TEM supply. The confidence interval is ±14% for $\dot{Q}_c^{TeHP}$ and ±15% for COP_c^{TeHP}. We can then conclude that the maximum deviation of the experimental and simulated resuls is ±15%, which is a good result and coherent with the uncertainty analysis associated to the thermoelectric properties of the TEMs [35].

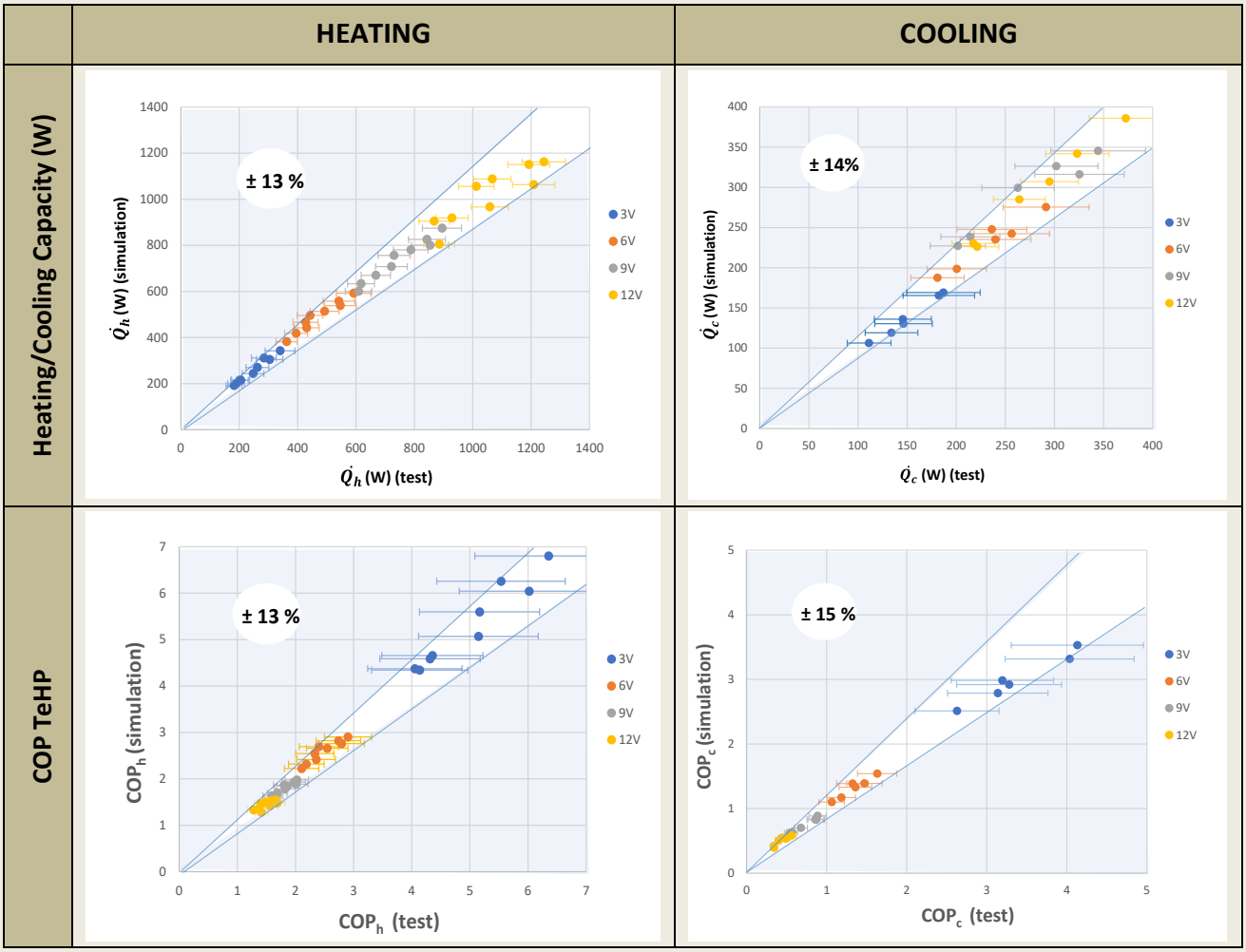

Figure 72. Validation of the computational model comparing the simulated results with 72 empirical tests.

3. Parametric investigation of the proposed HVAC systems and further discussion

The parametric investigation is divided into two studies. The first one is presented in section 3.1 and its main objective is to reveal the maximum performance that the two configurations can reach by varying the number of modules, connected in series, that constitute the TeHP. Heating mode is addressed in the first place, followed by the cooling mode. The second study is presented in section 3.2 and analyzes the seasonal performance of the TeHP for three different climates, evaluating the heating model in the first place, and the cooling mode after that.

3.1. Maximization of the energy performance for different operating conditions

Usually, the parametric investigation of thermoelectric devices are carried out by setting the temperature of the heat sinks and the thermal resistance of the heat exchangers between the

heat sink and the TEMs, varying the number of TEMs and the power supply voltage, in order to analyze the energy flows of the device. By doing so, it is generally concluded that, for a greater amount of heat exchanged, the optimum performance is obtained for a greater number of TEMs [20]. However, in this specific application, the TeHP regulation responds to specific needs for heating or cooling the interior of the building. As already indicated, in the case of a passive house, this specific heat demand is limited by the Standard itself and never exceeds 10 W/m^2 [36], what will lead to results non-expected beforehand.

3.1.1. Heating

For this study, we have considered a fixed volumetric air ventilation flow of 100 m^3/h (corresponding to the ventilation need of a 80-100 m^2 dwelling). The heating demand will therefore never exceed 1000 W, so we have considered a heating demand ($\dot{Q}_h^{TeHP}$) varying from 100 to 1000 W. Building indoor conditions are set to T_{exh} = 20 °C and Φ_{exh} = 40 %, while for outdoor, two weather conditions will be studied: an extreme one (T_{fresh} = 0 °C, Φ_{fresh} = 60 %) and a mild one (T_{fresh} = 10 °C, Φ_{fresh} = 70 %). Note that in a standarized passive house (where a HRU is always installed), the heating demand is always calculated considering the effect of the HRU [36]; that is, the heating demand is the heat needed to increase the temperature of the ventilation airflow from the outlet of the HRU (T_{fresh}^{HRU}) to the supply air temperature (T_{sup}). Given that the ventilation air flow is set according to health criteria and fixed (100 m^3/h in this case), the air supply temperature is defined by the heating demand, according to Eq. (17). Therefore there is a setpoint temperature at the outlet of the TeHP heating channel (T_h^{OUT} or T_{sup}) associated with each heating demand, according to Table 2. As an example, if T_{fresh} = 0 °C and T_{exh} = 20 °C, for a $\mathcal{E}^{HRU}$= 0.9, $\dot{Q}^{HRU}$ can be calculated with Eq. (1), being 609 W. Then, T_{HRU} can be then estimated with Eq. (23), yielding 17.9°C.

$$T_{HRU} = T_{fresh} + \frac{\dot{Q}^{HRU}}{\dot{m}_{fresh} Cp_{fresh}} \quad (23)$$

Finally, T_{sup} is calculated also with Eq. (23), substituting $\dot{Q}^{HRU}$ by $\dot{Q}_h^{TeHP}$, and T_{fresh} by T_{HRU}.

Table 13. T_{sup} of ventilation air flow (100 m^3/h) to provide different levels of heating capacity inside the building at two different outdoor conditions: T_{fresh}= 0°C and 10°C, being indoor air temperatura: T_{exh}= 20°C .

T_{fresh}	$\dot{Q}^{HRU}$	T_{HRU}	$\dot{Q}_h^{TeHP}$	T_{sup}
0°C	609 W	17.9 °C	100 W	20.8 °C
			200 W	23. 8 °C
			400 W	29.7 °C
			600 W	35.6 °C
			800 W	41.5 °C
			1000 W	47.5 °C

10°C	306 W	19 °C	100 W	21.8 °C
			200 W	24. 8 °C
			400 W	30.7 °C
			600 W	36.6 °C
			800 W	42.5 °C
			1000 W	48.5 °C

Table 2 describes the temperatures for the 2nd Config. In this configuration the heating demand coincides with the heat transferred from the hot side of the TEMs to the ventilation airflow. However, in the case of the 1st Config, there is no HRU, so the TeHP has the dual role of recovering the residual heat from the exhaust air and also providing additional heat to warm the ventilation airflow. Therefore, to compare the two configurations under equal conditions, the same temperature is set at the outlet of the HVAC (T_{sup}) in both cases. This means that in the 1st Config, the heat emitted by the TEMs must be greater than the heating demand. For example, if the heating demand of the building is 100W, the TeHP in the 2nd configuration must provide 100W to the ventilation air to increase its temperature from 17.9 to 20.8 °C, whereas 609W are recovered in the HRU to increase its temperature from 0 to 17.9 °C. However, for the same heating demand of 100 W, the TeHP in the 1st configuration must provide 709 W, to increase the temperature of the ventilation air from 0 to 20.8 °C.

Twelve cases for simulation arise from Table 2. For each, the number of modules (arranged in series) is varied up to 100. The mathematical model iteratively calculates the necessary feeding voltage of the TEMs to make the ventilation air reach the necessary temperature T_{sup}. The model provides as output the electric consumption, so the COP_h is calculated with Eq. (24). Remember that the heat delivered to the ventilation air is provided just by the TeHP in the 1st Config, but by both the HRU and TeHP in the 2nd Config. This $\dot{Q}_h$ is calculated with Eq. (25).

$$COP_h = \frac{\dot{Q}_h}{\dot{W}^{TeHP} + \dot{W}_{fan}^{TeHP+HRU}} \tag{24}$$

$$\dot{Q}_h = \dot{m}_{fresh}\rho_{air}\left(h_h^{OUT} - h_{fresh}\right) = \dot{m}_{fresh}\rho_{air}C_p\left(T_{sup} - T_{fresh}\right) \tag{25}$$

Figure 73 shows the evolution of COP_h as a function of the number of modules N for the two configurations under study (arranged in columns) and the two external conditions (arranged in rows).

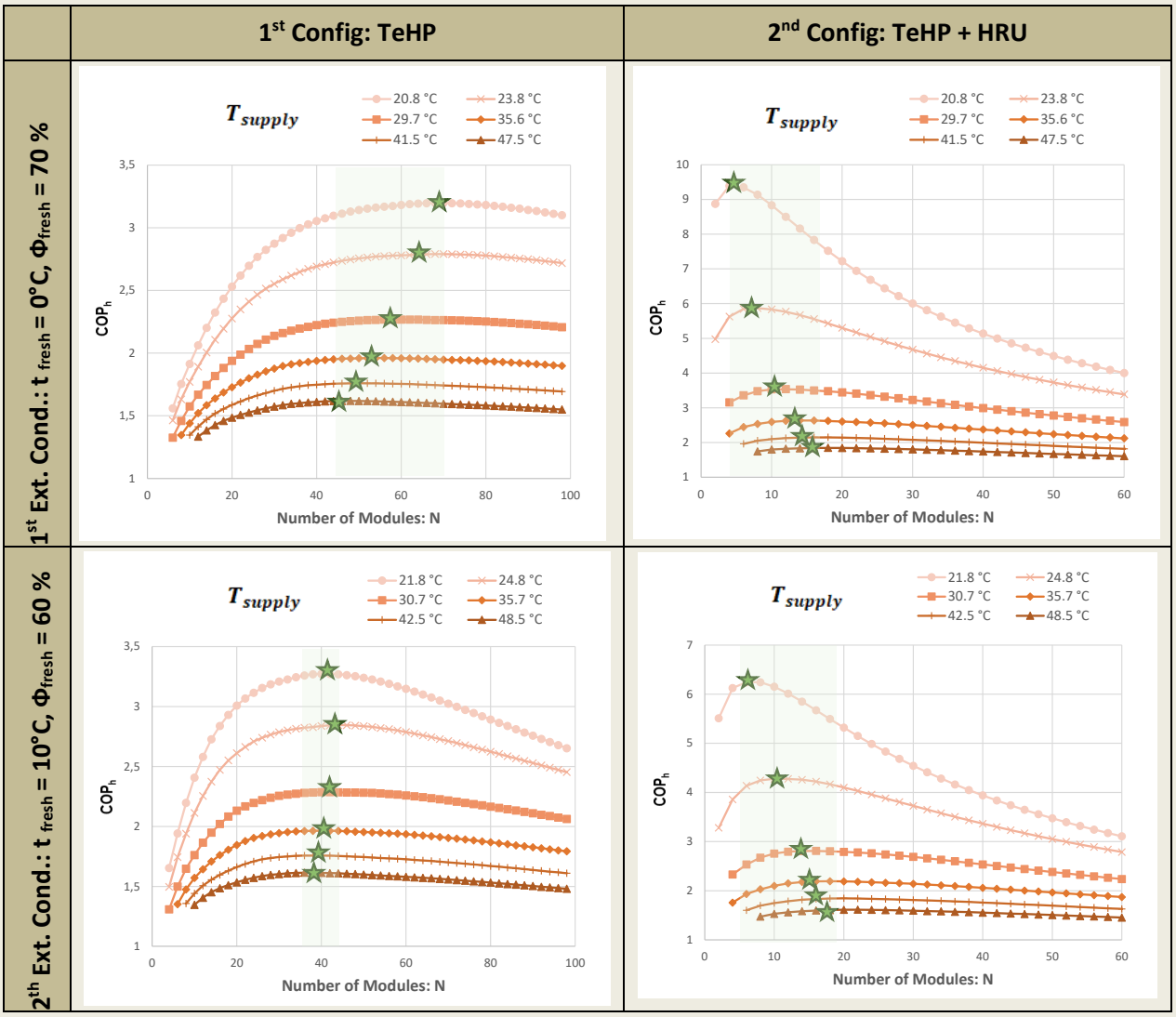

Figure 73. COP_h for two system configurations and two weather conditions, for N ranging 1-100 and T_{sup}= 20.8°C, 23.8°C, 29.7°C, 35.6°C, 41.5°C and 47.5°C. Green stars point the optimum values of COP_h for each T_{sup}.

Figure 73 indicates that COP_h follows a similar trend in both external conditions, increasing up to a maximum and decreasing with the growing number of modules. As expected, the maximum COP_h is lower when T_{sup} rises. The comparison of the two configurations for the 1st Ext. Cond. (1st row) reveals that the maximum COP_h values are notably higher in the case of the 2nd Config (1.8-9.4) with respect to the 1st Config (1.6-3.2), requiring also a smaller number of modules (2-16 and 48-70 respectively). This outcome also occurs for the 2nd Ext.Cond (2nd row). This comparison clearly confirms the convenience of integrating the TeHP with the HRU, anticipated in previous works ([18], [19], [20]).

Two controversial issues arise from the results, that require further explanation. In the first place, a more detailed analisys shows that in the 1st Config (1st column), the increase of T_{sup}

means an unexpected progressively lower number of modules for maximum COP_h, which seems at odds with previous research [20], while in the 2nd Config (2nd column) the opposite happens. To analyze this unexpected fact, we need to focus on the denominator of Eq. (24), since the numerator remains constant for a fixed T_{sup}. On the one hand, the fan consumption grows proportionally with the number of modules, given the increase in pressure drop with a constant flow rate. This pressure loss calculation also takes into account the HRU in the 2nd Config, as indicated in Section 2. On the other hand, there is the consumption of TeHP, which, according to Eq. (26) (obtained from Eqs. (18), (6) and (7)), presents two terms: one due to the Joule effect (NRI^2) and another one due to the Peltier effect ($NSI\left(T_h^{TEM,i} - T_c^{TEM,i}\right)$).

$$\dot{W}^{TeHP} = N\,V\,I = N\,(SI\left(T_h^{TEM,i} - T_c^{TEM,i}\right) + RI^2) \tag{26}$$

As N increases, the required supply voltage of the TEMs decreases. This decrease is notable when the number of modules is low, but becomes insignificant when more modules are added.

Figure 74 proves so, showing the evolution of $\dot{W}^{TeHP}$ and $\dot{W}_{fan}^{TeHP+HRU}$ for T_{sup}= 23.8 °C and T_{sup}= 35.6°C in both configurations. It can be seen that $\dot{W}^{TeHP}$ always decreases with the number of modules in the 1st Config, while in the 2nd Config it reaches a minumum for a number of modules lower than 20. Therefore, the minimum power consumption (and the maximum COP_h) in the 1st Config is determined by the fan consumption, whereas $\dot{W}^{TeHP}$ determines so for the 2nd Config.

The second controversial result is the unexpected behavior of $\dot{W}^{TeHP}$ for increasing number of modules in the 2nd Config. The general consensus recommends that, for a given heating power, one should increase the number of modules to reduce the required voltage and, in turn, the electric power, so that the COP is expected to rise. A first explanation can be found in the fact that the thermal resistance of the HP is increased when the heat flux per TEM is reduced (see Figure 70) and, therefore, the $\dot{W}^{TeHP}$ is increased. This effect is further studied in the second row of

Figure 74, where the $\dot{W}^{TeHP}$ is calculated with the variable thermal resistance of the HP, and compared with a fixed thermal resistance employing maximum empirical values ($R_c^{HP} = 0.48\,K/W$ and $R_h^{HP} = 0.22\,K/W$) and minimum values ($R_c^{HP} = 0.25\,K/W$ and $R_h^{HP} = 0.087\,K/W$). The analysis demonstrates that, although this effect prioritizes a lower N, $\dot{W}^{TeHP}$ still shows a decreasing tendency in the 1st Config (first column) whereas there is clear minim value of $\dot{W}^{TeHP}$ even when R^{HP} is fixed in the 2nd Config (second column).

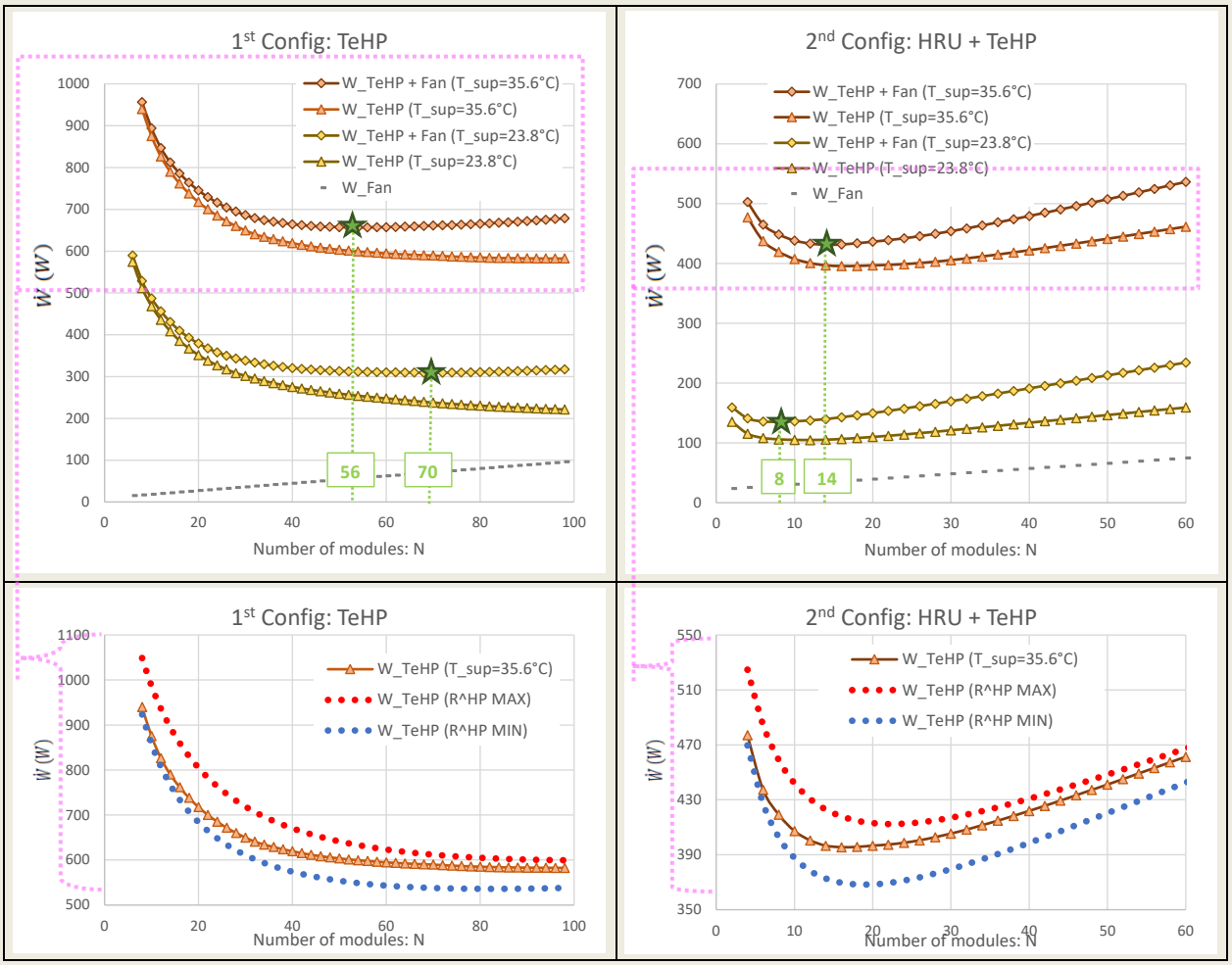

Figure 74. First row: electric consumption of the TeHP ($\dot{W}^{TeHP}$) and the fans ($\dot{W}_{fan}^{TeHP+HRU}$) depending on N for $T_{sup} = 23.8\ °C$ and 35.6 °C in both configurations with 100 m^3/h air flow. Second row: comparison of $\dot{W}^{TeHP}$ for $T_{sup} = 35.6\ °C$ and variable thermal resitance of the HP with fixed maximum R^{HP} ($R_c^{HP} = 0.48\ K/W$; $R_h^{HP} = 0.22\ K/W$) and minimum R^{HP} ($R_c^{HP} = 0.25\ K/W$ and $R_h^{HP} = 0.087\ K/W$).

The reason behind is related to the working conditions of the TEM, as explained subsequently. The energy balance of the TeHP heating duct is shown in Figure 75, following Eq. (27) and the scheme of Figure 76 for $T_{sup} = 35.6\ °C$.

$$\dot{Q}_h^{TeHP} = \dot{m}_{fresh}\rho_{air}\left(h_h^{OUT} - h_h^{IN}\right) = \dot{Q}_{Peltier} + \dot{Q}_{Joule} - \dot{Q}_{Conduction} \qquad (27)$$

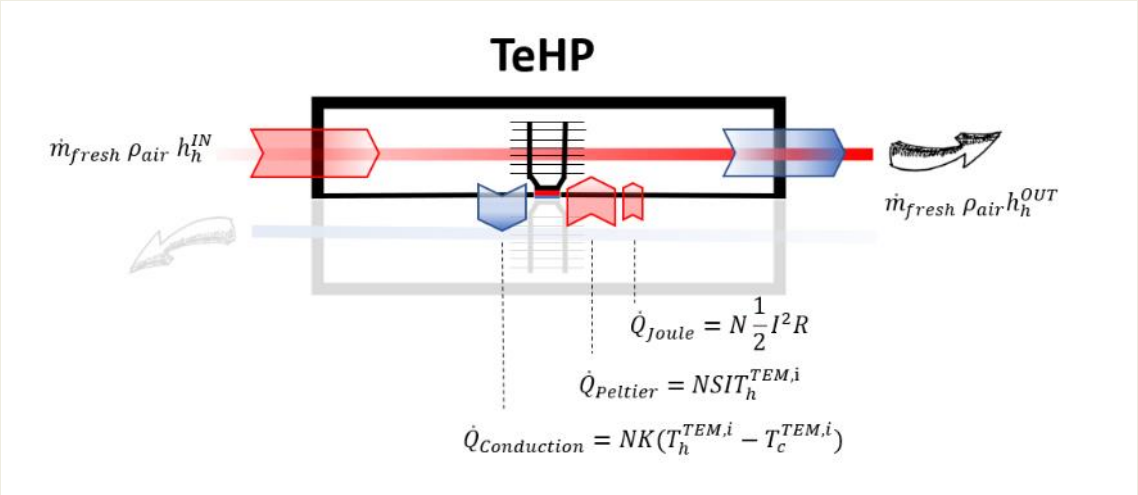

Figure 75. Energy balance in the heating air duct.

In the 1st Config the air enters the TeHP at 0 °C and reaches 35.6 °C. Three different heat fluxes can be analyzed on each module and each TEM, according to Eq. (26): on the one hand, the heat delivered by the Peltier effect ($\dot{Q}_{Peltier}$), another due to the Joule effect ($\dot{Q}_{Joule}$) and, finally, heat conduction through the TEMs due to the temperature difference between their faces ($\dot{Q}_{Conduction}$). The heat necessary for the ventilation air to reach 35.6 °C is 1209 W ($\dot{Q}_h^{TeHP}$), which remains constant for all N analyzed, while $\dot{Q}_{Peltier}$, $\dot{Q}_{Joule}$ and $\dot{Q}_{Conduction}$ vary. For N = 56 modules (when the maximum COP_h = 1.69 is obtained) $\dot{Q}_{Peltier}$= 2033.4 W, $\dot{Q}_{Joule}$= 195.7 W and $\dot{Q}_{Conduction}$= 1019.9 W, being I = 2.3 A per TEM. The average temperature of the hot side of the TEM is 27.1°C and that of the air 17.8 °C, while on the other side (cooling duct) the air is at 11.3 °C and the temperature of the cold side of the TEM is 2.8 °C. In the 2nd Config the ventilation air goes through the HRU first, receiving 609 W from the exhaust air passively, reaching 17.9 °C, while the exhaust air flow temperature drops from 20 °C to 3.9 °C, condensing 98 g/h of water in the HRU. From here, the TeHP provides the remaining 600 W and the ventilation air reaches 35.6 °C, but in more unfavorable conditions than in the 1st Config, since the ventilation air is hotter and the air in the cooling duct is colder. For N = 14 modules we obtain a maximum COP_h of 2.8, with an I = 3.7 A per TEM. The average temperature of the hot side of the TEM is 35 °C and that of the air is 26.8 °C, while in the cooling duct the cold side of the TEM is at -4.8 °C and the air is at 2.4 °C.

In general, for a given N, the $\dot{Q}_{Conduction}$ are 20 % lower in the 1st Config with respect to the 2nd Config due to the lower temperature gap between TEM faces, but the TeHP needs to double the heat flux from the TEMs to the ventilation air flow. Consequently, in the 1st Config more modules are required, working in more favorable conditions, so that the number could be increased to reduce $\dot{W}^{TeHP}$ and increase the COP. The unfavorable conditions of 2nd Config limits the reduction in $\dot{W}^{TeHP}$.

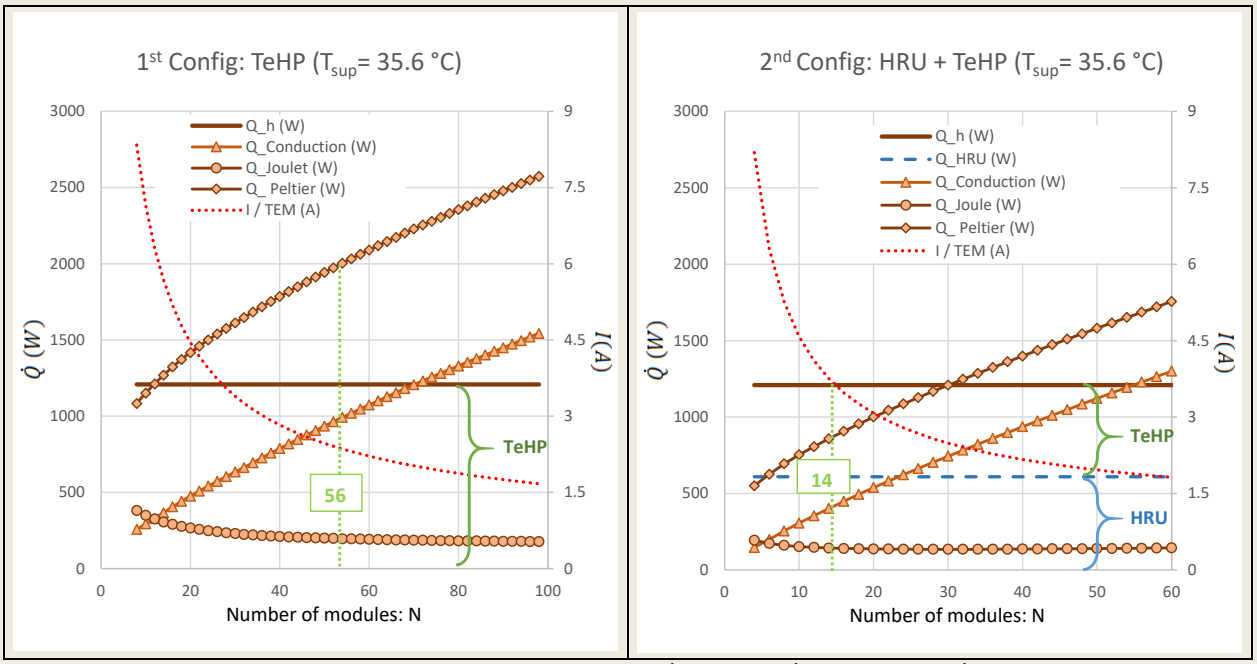

Figure 76. Energy balance in the heating air duct representing $\dot{Q}_{Peltier}$ and $\dot{Q}_{Joule}$ gains and $\dot{Q}_{Conduction}$ losses for both configurations when $T_{sup} = 35.6$ °C.

Finally, Figure 73 also allows the study of the variation of the TeHP operating parameters when outdoor environmental conditions improve in winter, increasing the temperature from 0°C to 10°C. In this case, the maximum COP_h values of the 1st Config remain almost the same, while the range of N, for which these values are obtained, decreases considerably, going from 48-70 to 36-44. The $\dot{W}^{TeHP}$ is then reduced, proportionally to $\dot{Q}_h$. By contrast, in the 2nd Config, the COP_h maximum values decrease from 1.8-9.4 to 1.6-6.2, due mainly to the lower heat recovery potential in the HRU. However, as one of the main conclusions, the range of optimal N remains practically constant, with a slight increase of 2 modules.

3.1.2. Cooling

In cooling mode, the same analysis is carried out, setting T_{sup} below the temperature at the outlet of the ventilation air in the HRU. In this case, the building indoor temperature is considered 25 °C and the relative humidity 60%, while the external environmental conditions under study will be T_{fresh}= 40 °C and Φ_{fresh} = 20 % as extreme conditions (4th Ext. Cond.) and T_{fresh}= 30°C and Φ_{fresh} = 30 % (3rd Ext. Cond.) as mild conditions.

Table 14. T_{sup} of ventilation air flow (100 m^3/h) to provide different levels of cooling capacity inside the building at two different outdoor conditions: T_{fresh} = 30°C and 40°C , being indoor air temperature: T_{exh} = 25°C.

T_{fresh}	$\dot{Q}^{HRU}$	T_{HRU}	$\dot{Q}_c^{TeHP}$	T_{sup}
30°C	150.8 W	25.5 °C	50 W	24.0 °C
			150 W	21. 0 °C
			250 W	18.1 °C
			300 W	16.5 °C
			350 W	15.1 °C
			400 W	13.7 °C
40°C	452.5 W	26.5 °C	50 W	24.9 °C
			100 W	23.5 °C
			150 W	22.0 °C
			200 W	20.5 °C
			250 W	19.0 °C
			300 W	17.6 °C

In this case, when decreasing the T_{sup} there is not only a minimum number of modules to achieve the envisaged cooling effect, but there is also a maximum N. For higher number of modules T_{sup} is not achievable at the outlet of the cooling air duct. The reason behind is that, following Eq. (26) but applied to $\dot{Q}_c^{TeHP}$, $\dot{Q}_{Peltier}$ needs now to compensate both $\dot{Q}_{Conduction}$ and also $\dot{Q}_{Joule}$, and that is not possible above a certain N. This happens, for example, in the 1st Config, when T_{sup} = 15.1 °C and N exceeds 80 modules.

	1st Config: TeHP	2nd Config: TeHP + HRU
3rd Ext. Cond.: t_{fresh} = 30°C, Φ_{fresh} = 30 %	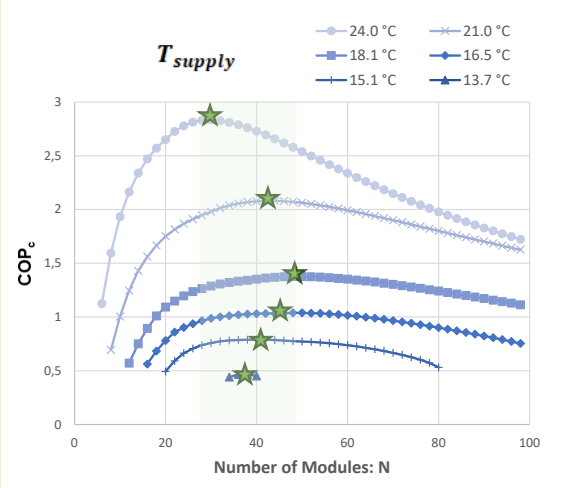	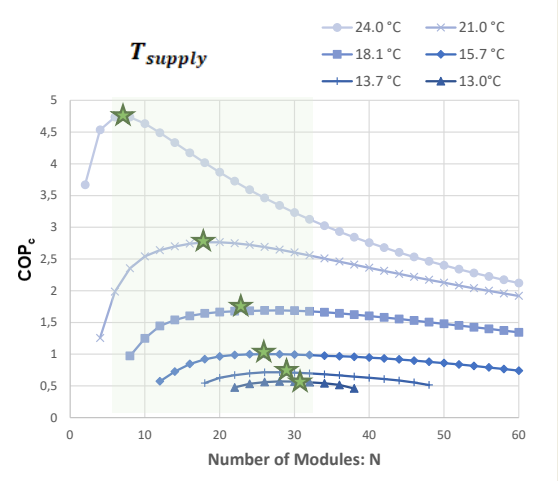

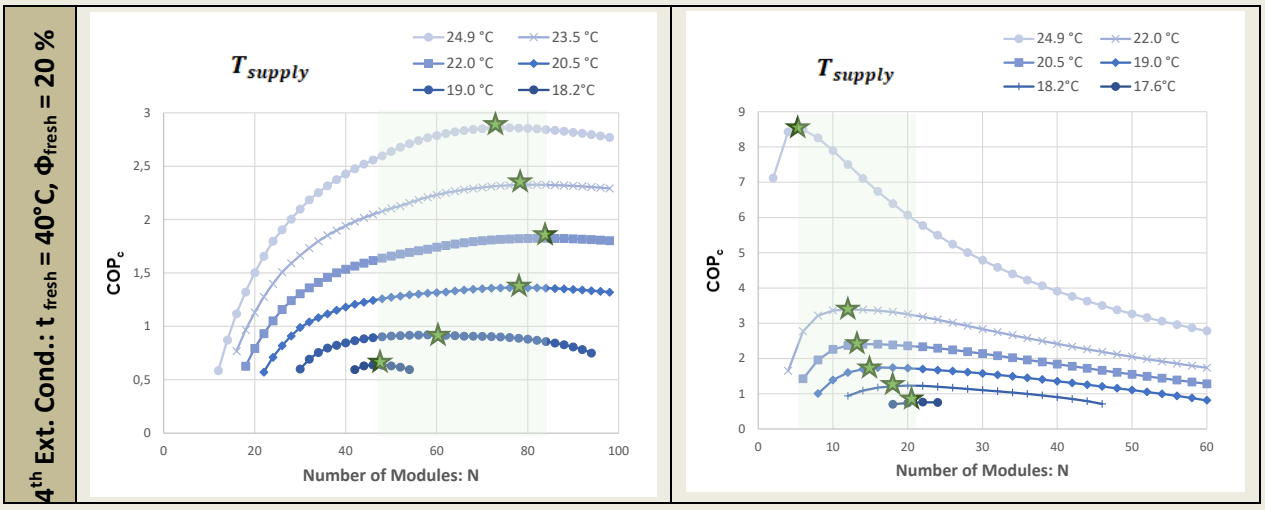

Figure 77. COP_c for two system configurations and two weather conditions, for N ranging 1-100 and T_{sup} = 24°C, 21°C, 18.1°C. 16.5°C, 15.1°C and 13.7°C. Green stars point the optimum values of COP_c for each T_{sup}.

Figure 77 shows that the 2nd Config manages to decrease 0.7 °C more the T_{sup}, presenting a higher COP_c and requiring a lower number of modules. The air flow temperature does not fall below 13 °C, which implies a cooling capacity limitation of 420 W, in addition to the 150 W previously absorbed by the HRU. When the outside temperature is more extreme ($T_{fresh} = 40°C$), the HRU recovers 450 W and the TeHP absorbs another additional 300 W.

As a result of the previous study, Figure 78 shows the maximum values of COP_h and COP_c obtained for the different T_{sup}, the two analyzed configurations and the two external weather conditions in both heating and cooling modes. The efficiency of the 2nd Config is always superior to that of the 1st Config, demonstrating, again, the convenience of incorporating an HRU with the TeHP. Although the TeHP in the 1st Config works in more favorable conditions than the 2nd Config, due to a favorable temperature gap between heating and cooling ducts, the combination of the HRU and the TeHP is much more efficient, especially at partial loads with values that reach triple the COP of the 1st Config. For higher air conditioning demands these values converge, but, even at maximum heating or cooling demand, the COP still remains 12.5% superior.

The original idea of having, in the case of the 1st Config, a more simple configuration of the HVAC system with a double function of passive and active heat recovery unit to provide ventilation, heating and cooling, has been discarded, since the optimized number of modules required is excessively high, with values that exceed N = 40. Taking into account that each module has a width of 8 cm, the constructive result is not operative. Finally, the study also reveals that 2nd Config shows higher COPs and a lower number of modules to reach the heating or cooling set points when the outdoor conditions are more adverse. The higher COP, in this case, is due to the higher heat recovery potential of the HRU. Instead, the lower N required is due the higher temperature gap between cooling and heating incoming air flows, what, as it has been shown in

Figure 74, Figure 75 and Figure 76, means a higher minimum feeding voltage of the TEMs, what induces a higher $\dot{Q}_h^{TeHP}$ or $\dot{Q}_c^{TeHP}$ per module and, consequently, a lower N for a given T_{sup}. This means that not always a higher N is required to optimize the peformance of the TeHP when the heating demand is increased, as satated in [20]. N must be optimized considering both the heating demand and the temperature gap between indoor and outdoor, in addition to other operating factors, as the thermal resistance of the heat exchangers between the TEMs and air streams.

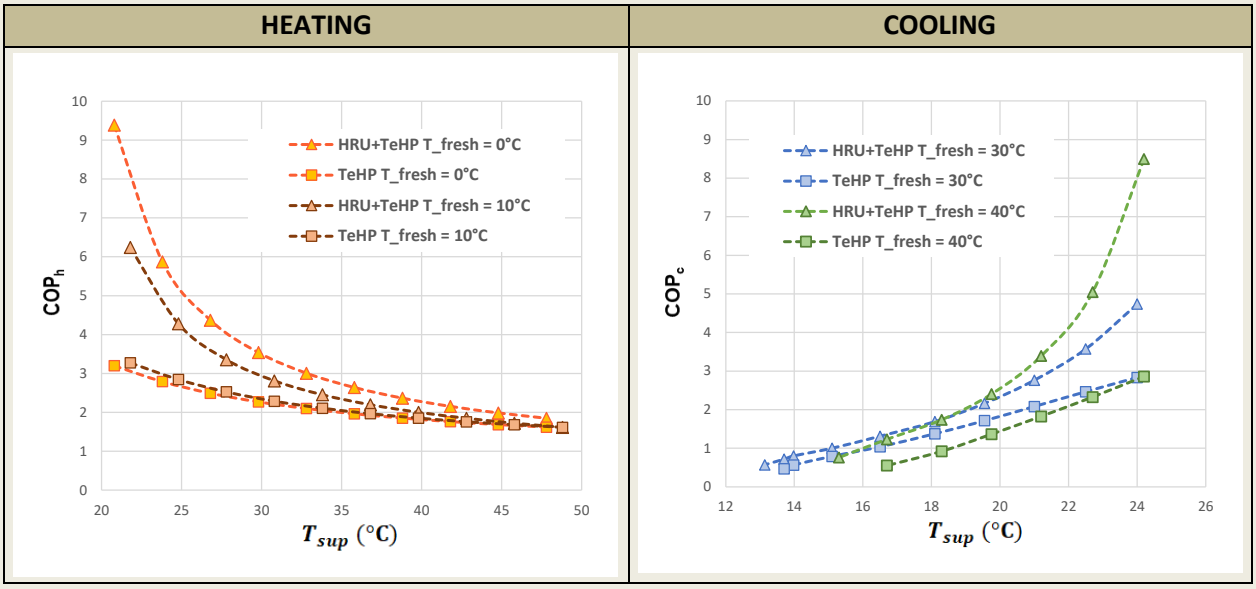

Figure 78. Maximum values of COP_h and COP_c for different T_{sup} in the four scenarios previosly analyzed (1st and 2nd configurations and two different outdoor conditions).

3.2. Optimization of the seasonal performance for heating and maximum capacity for cooling

Once 1st Config has been dismissed, the definitive optimized number of modules of the TeHP must be calculated. In the previous section, an optimum COP value has been found at a certain N for each T_{sup}, corresponding to a certain heating or cooling need of the building, in four different external conditions. However, the set point for T_{sup} is not independent of the external environmental conditions. The heating and cooling needs depend, basically, on the outside temperature and the quality of the building envelope.

3.2.1. Heating

According to UNE 13790, the heating needs of a building can be calculated through a global loss coefficient that depends on the level of insulation of the envelope and the efficiency of the heat recovery unit (if any) integrated with the ventilation. The heat losses are proportional

to the difference between the interior and exterior temperatures [37], establishing a limit for the specific power demanded by the building of 10 W/m^2 (according to passive house standard), which ensures the possibility of heating or cooling the interior through the ventilation air flow. This precept makes the definition of a passive house building independent of the climate where it is located, having to adapt the design and the thermal insulation level to comply with this functional principle. The objective of this study is to assess and optimize the seasonal performance of the TeHP (set as in 2nd Config), considering the dependency of the heating needs, and therefore, the T_{sup} of the incoming ventilation air flow, with respect to the external conditions.

To this purpose, the reference methodology for the energy certification of heat pumps in Europe will be followed, according to Directive 2010/30/EU [38] and the delegated regulation No 626/2011 [39], where three reference climates are established to characterize the heating needs in the continent (see Figure 79): Helsinki for the colder climates, Strasbourg for intermediate climates, and Athens for warmer climates.

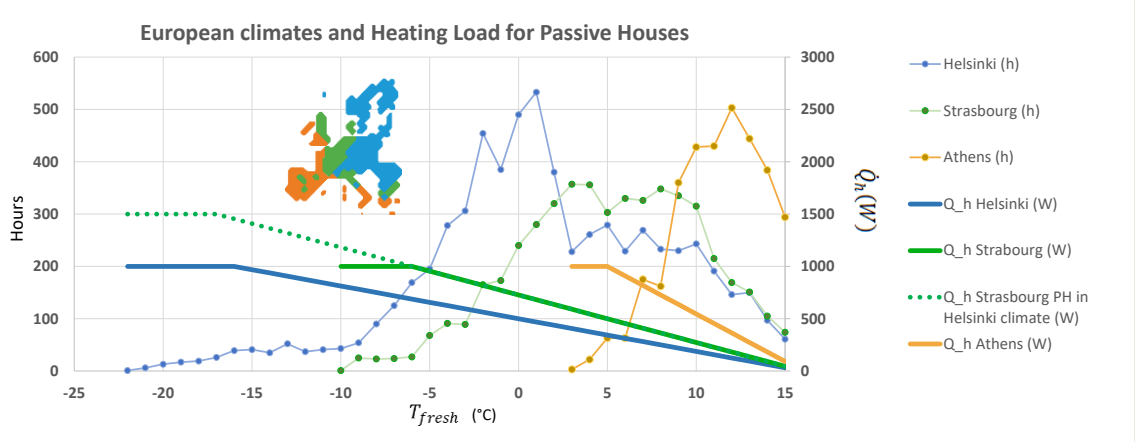

Figure 79. Number of hours at different outdoor temperatures during heating season in the three reference climates [39]: Helsinki, Strasbourg and Athens. In right axis specific heating load of a Passive House building adapted to each of the three climates.

In this analysis, to assess the performance of the TeHP we need to exclude the effect of the HRU, redefining the COP as the ratio of the heat delivered by the TeHP and the electrical consumption of the TeHP and the fans, according to Eq. (30):

$$COP_h^{TeHP} = \frac{\dot{Q}_h^{TeHP}}{\dot{W}^{TeHP} + \dot{W}_{fan}^{TeHP+HRU}} \tag{30}$$

And, therefore, assessing the seasonal performance of the TeHP as the ponderated average of the COP_h^{TeHP} for different external temperatures depending on the frecuency of these temperatures during the winter season in the three reference climates:

$$SCOP_h^{TeHP} = \frac{\sum_j COP_h^{TeHP}\left(T_j\right) Hours\left(T_j\right)}{\sum_j Hours\left(T_j\right)} \tag{31}$$

In this way, we have a specific number of hours for each climate and for each temperature of the outdoor environment, associated with a specific heat demand, which corresponds to the specific passive house envelope design for that climate. According to PHPP, we are going to assume a heating demand limited to 10 W/m^2, corresponding to a temperature below which we only expect 1% of the hours of the heating season. In the case of Helsinky this temperature is -16°C °C, in the case of Strausbourg -6°C and in Athens this is 5°C. The number of hours of each outside temperature and the corresponding $\dot{Q}_h^{TeHP}$ for the three climates are stated in Figure 79. According to this methodology, $SCOP_h^{TeHP}$ is calculated varying N from 8 to 22 modules, obtaining the results shown in Figure 80.

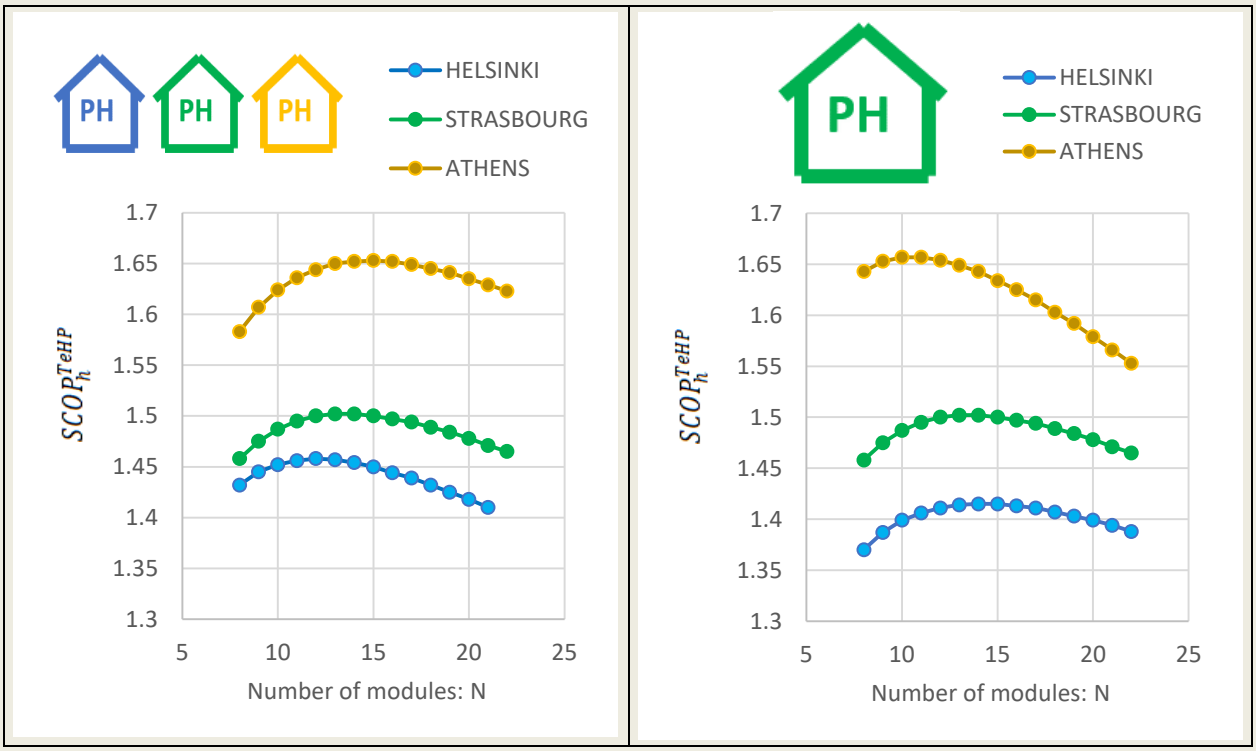

Figure 80. Optimization of $SCOP_h^{TeHP}$ for the three european winter climates (Helsinki, Strasbourg and Athens) varying N. Left graph: the building envelope is adapted to the Passive House requirements in the three climates. Right graph: same building envelope complying with the Passive House standard in Strasbourg is assessed in Athens and Helsinki.

For each climate we find an optimal $SCOP_h^{TeHP}$ for a specific N, although the performance variations are not significant and the optimal N range obtained is very narrow: 12-16. This is due to two reasons: on the one hand, the heating demand curve is different in all three cases, with an envelope that guarantees an equivalent maximum level of heating in the three climates (Figure 79). On the other hand, the HRU acts by reversing the inlet temperatures in the TeHP, so that the effect of the different outside temperature levels is dampened. However, it may seem paradoxical that the maximum $SCOP_h^{TeHP}$ is obtained for a slighly lower number of modules in the case of colder climates. Here again applies the same explanation found in previous section, where, for higher temperature gaps between incoming air flows, the optimum N is reduced, due to the need to maintain higher TEM feeding voltages to reach the

envisaged T_{sup}. Finally, this analysis is repeated but, in this case, keeping the same thermal insulation level needed for a Strasbourg Passive House envelope (10 W/m^2 at -6 °C outside temperature, see Figure 79 with the dashed green line) for the three climates, up to a maximum of 15 W/ m^2 in the case of the Helsinki climate. In this case, the $SCOP_h^{TeHP}$ is slightly higher for Athens, with a lower number of N to reach this new maximum, given the very low heating demand with this overinsulated envelope. On the other hand, the $SCOP_h^{TeHP}$ is lower in the case of Helsinki, since we are demanding more heating capacity and a greater number of modules is necessary to reach these new heating set points. The results show that a 15-modules TeHP is very close to the optimized $SCOP_h^{TeHP}$ in all cases, reaching a maximum heating capacity of 2500 W at highest voltage supply (16 V) when the temperature outside is 0°C and the TeHP is combined with the HRU.

3.2.2. Cooling

Finally, in the case of refrigeration and given the cooling capacity limitations analyzed in the previous section 3.1.2, the objective is to assure that the maximum cooling capacity of the TeHP meets the energy demand of the passive house dwelling. The focus is not, then, the optimization of the energy peformance, that can be easly compensated with PV production when the solar radiation is at its maximum, but the analysis of the maximum cooling capacity of the TeHP at different circumstances, looking for alternatives to improve this capacity and, therefore, guarantee indoor comfort conditions in summertime. To this end, the analysis considers an indoor temperature of 25 °C and Φ = 60 %, while outdoor temperatures goes from 25°C to 40°C with fixed humidity ratio ω = 8 g/Kg, increasing the $\dot{Q}_c^{TeHP}$ up to a point from which the heat absorbed by the Peltier effect ($\dot{Q}_{Peltier}$) cannot compensate the heat gains due the conduction losses ($\dot{Q}_{Conduction}$) and the Joule effect ($\dot{Q}_{Peltier}$) (see Figure 76 for the heating energy balance). This is the point of maximum $\dot{Q}_c^{TeHP}$ for a given outside temperature and a given N.

The scope of the TeHP must be to at least compensate the internal gains due to the use of the building (inhabitants, electrical appliances, lighting ...) and the gains due to the heat transmission through the building envelope and the ventilation, that can be estimated as $\sim 4\ \mathrm{W/m^2}$ [35].

The base line is described by N = 15, as this configuration was proved to optimize the heating capacity of the TeHP. In such a case, the TeHP provides 405 W of cooling capacity when outside temperature is 25 °C, which is reduced to 330 W when the temperature rises to 40 °C. The analsys compares this results with N = 25, given the results obtained in Section 3.1.2, with the aim of exploring the potential expansion of the number of modules to provide more cooling capacity.

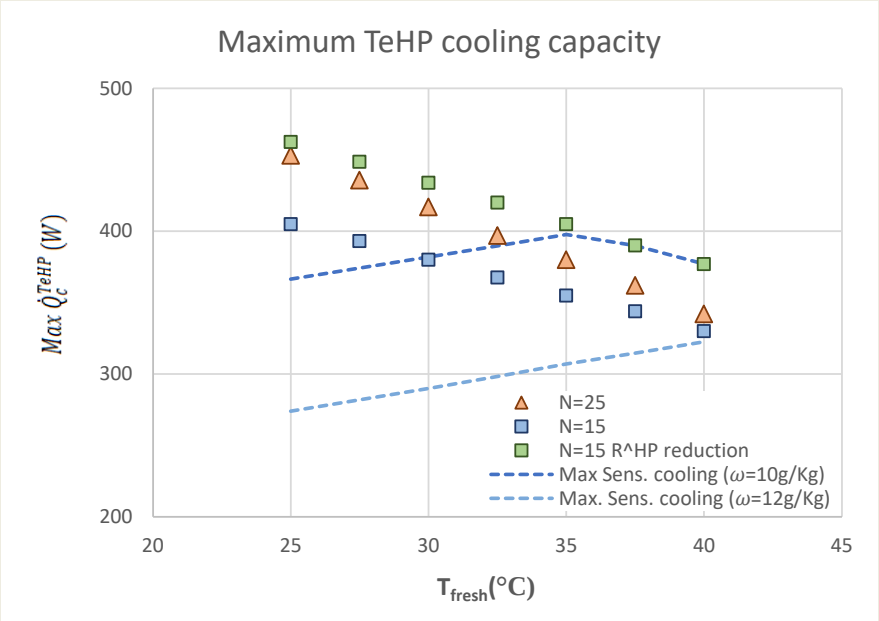

Figure 81. Maximum cooling capacity ($\dot{Q}_c^{TeHP}$) of the TeHP for different outdoor conditions with different configurations: N=25, N=15 and N=15 reducing the thermal resistance of the HP heat exchangers (R_c^{HP}) by 0.2 K/W thanks to a potential optimized design. Dotted lines show the maximum sensible cooling achievable when outdoor humidify is ω = 10 g/Kg and ω = 12 g/Kg.

Figure 81 shows that the addition of these 10 modules barely increases the cooling capacity of the TeHP by 50 W with an outside temperature of 25 °C and it turns to almost cero when the outside temperature rises up to 40 °C. However, given the scarce increase in cooling capacity compared with the significant increase of modules, it seems interesting to explore other alternatives for improvement, such as reducing the thermal resistance of HP heat exchangers in the cooling duct. As seen in Section 2, the HP heat exchangers work in this application evaporating the internal liquid in the place that, according to the design, should condense. A potential dedicated optimized design of these heat exchangers could easily bring improvements that would reduce the thermal resistance by 0.2 K/W. This improvement would increase the cooling capacity by 60 W for all the range of outside temperatures under study with the same TeHP size. Another alternative is the indirect adiabatic cooling, which consists of humidifying the exhaust air flow of the building before entering the HRU. The humidification reduces the air temperature that is afterwards transferred to the incoming air flow through the HRU. Under this study conditions and assuming that the air is humidified up to the 80 % of its maximum capacity, an extra 120 W of cooling could be provided, reducing the T_{sup} by 3 °C.

In either case, the cooling through the ventilation air flow is limited by the humidity of the outside air. If the assumption of the outdoor humidity rises from ω = 8 g/Kg to ω = 12 g/Kg, as in the case of a coastal city, then the sensible cooling capacity would be limited to 390 W for 30 °C outside temperature. The additional cooling capacity would be then dedicated to dry the aire condensing air water, limiting T_{sup} to 15.9 °C.

As a consequence of the analysis, it is concluded that it is not worth expanding the number of modules, but it is worth exploring other ways of experimentation that improve the assembly and thermal resistance of the heat sinks, the performance of the TEMs themselves (or their

connection in cascaded form) and the combination with other cooling strategies (adiabatic cooling, freecooling ...). The study has been limited to a constant ventilation flow, but it is possible to increase the cooling and heating capacity, incresing the ventilation air (at the cost of increasing the demand) or recirculating indoor air.

4. Conclusions

This research work proposes the use of a thermoelectric air-to-air heat pump integrated in a double flux ventilation system with a heat recovery unit for an 80-100 m^2 passive house to provide both heating and cooling in different climates. The use of a thermoelectric air-to-air heat pump with a heat recovery unit is scarce in current literature, which is surprising given the increase in efficiency compared to a standalone thermoelectric heat pump. The first study in this paper confirms so, demonstrating a better performance with a more reduced number of modules. The analysis was assessed for a range of 100-1000 W of heating demand and 50-420 W of cooling demand, and four weather conditions. The inclusion of a heat recovery unit along with the thermoelectric heat pump doubles or even triples the COP for low heating/cooling demand, and it stays at least 12.5 % higher when maximum demand is required. The number of modules needed to reach this maximum COP is also considerably lower, being 2-16 modules vs 48-70 for heating, while 6-20 vs 46-84 for cooling. More important is that this analysis raised two controversial results. Firstly, for a standalone TeHP, an increasing heating demand led to an unexpected progressively lower number of modules needed to reach the maximum COP. Secondly, for the TeHP+HRU, the electric consumption of the modules increases for an increased number of modules, but just up to a certain point. From that value, this expected statement is no longer true.

An in-depth analysis reveals that, given that the heating and cooling demands are correlated in these applications with the outgoing air temperature, there is a minimum temperature gap that needs to be set in thermoelectric modules and, therefore, a minimum feeding voltage. This means that a minimum heat flux per module is required, below which the system is useless. This explains the first controversial result, and also explains the limited reduction of the electric current intensity when the number of modules grows, thus justifying the second controversial finding. Consequently, no general rule can be given beforehand about the number of modules for maximum COP, which contradicts previous research, so it must be evaluated in each application. As a consequence of previous findings, the standalone TeHP installation has been discarded. The second and most relevant outcome concerning a passive house is that the number of modules for maximum COP is virtually constant and independent on the climate, when combined with a heat recovery unit. The optimization of the number of modules is carried out calculating a seasonal coefficient of performance for three European climates: Athens, Strasbourg and Helsinki, with very different winter seasons. The analysis reveals that the optimized number of modules is almost constant (and very close to 15 in all cases), although the energy consumption is different. This number of modules is very low, compared with previous research studies, and makes the potential construction and further installation of this TeHP very viable in terms of dimensions and costs.

In the case of cooling, due to the cooling capacity limitations arise during the first analysis, it is crucial to find how much this system can help to keep comfort conditions inside, depending on outside temperature. The thermoelectric heat pump with 15 modules provides 405 W of cooling capacity when outside temperature is 25 °C, which is reduced to 330 W when the temperature rises to 40 °C. Even though this cooling capacity may compensate the internal heat gains and the transmission heat flux through the building envelope and the ventilation to a high extent, higher cooling capacity would be desirable. Several measures are proposed, which should be evaluated in future research. Among them, the reduction in the thermal resistance of the heat sinks should be the first option, once the study has indicated that the inclusion of more thermoelectric modules would provide insignificant improvements in the system.

References

[1] EU. Directive 2010/31/EU of the European Parliament and of the Council of 19 May 2010 on the energy performance of buildings (recast). Off J Eur Union 2010:13–35. https://doi.org/10.3000/17252555.L_2010.153.eng.

[2] European Commission. The European Green Deal. Eur Comm 2019;53:24. https://doi.org/10.1017/CBO9781107415324.004.

[3] EU. Directive 2012/27/EU of the European Parliament and of the Council of 25 October 2012 on energy efficiency (EED) 2012:1–56.

[4] EU. Directive (EU) 2018/844 of the European Parliament and of the Council of 30 May 2018 amending Directive 2010/31/EU on the energy performance of buildings and Directive 2012/27/EU on energy efficiency. Off J Eur Union 2018;156:75–91.

[5] Müller L, Berker T. Passive House at the crossroads: The past and the present of a voluntary standard that managed to bridge the energy efficiency gap. Energy Policy 2013;60:586–93. https://doi.org/10.1016/j.enpol.2013.05.057.

[6] Moreno-Rangel Alejandro. 2021. "Passivhaus" Encyclopedia, no. 1: 20–29. https://doi.org/10.3390/encyclopedia1010005.

[7] Guillén-Lambea S, Rodríguez-Soria B, Marín JM. Review of European ventilation strategies to meet the cooling and heating demands of nearly zero energy buildings (nZEB)/Passivhaus. Comparison with the USA. Renew Sustain Energy Rev 2016;62:561–74. https://doi.org/10.1016/j.rser.2016.05.021.

[8] Renovation Wave n.d. https://ec.europa.eu/energy/topics/energy-efficiency/energy-efficient-buildings/renovation-wave_en (accessed September 14, 2021).

[9] Nowak T. White paper: Heat Pumps - Integrating technologies to decarbonise heating and cooling. EPHA -European Heat Pump Assoc 2018:1–86. https://www.ehpa.org/fileadmin/user_upload/White_Paper_Heat_pumps.pdf (accessed October 5, 2021).

[10] Parliament THEE, Council THE, The OF, Union E. F-Gas Regulation. Eur Comm 2014;2014:195–230. https://eur-lex.europa.eu/legal-content/EN/TXT/PDF/?uri=CELEX:32014R0517&from=EN.

[11] Zuazua-Ros A, Martín-Gómez C, Ibáñez-Puy E, Vidaurre-Arbizu M, Gelbstein Y. Investigation of the thermoelectric potential for heating, cooling and ventilation in buildings: Characterization options and applications. Renew Energy 2019;131:229–39. https://doi.org/10.1016/j.renene.2018.07.027.

[12] Zhao D, Tan G. A review of thermoelectric cooling: Materials, modeling and applications. Appl Therm Eng 2014;66:15–24. https://doi.org/10.1016/j.applthermaleng.2014.01.074.

[13] Shen L, Pu X, Sun Y, Chen J. A study on thermoelectric technology application in net zero energy buildings. Energy 2016;113:9–24. https://doi.org/10.1016/j.energy.2016.07.038.

[14] Liu Z, Zhang L, Gong G, Li H, Tang G. Review of solar thermoelectric cooling technologies for use in zero energy buildings. Energy Build 2015;102:207–16. https://doi.org/10.1016/j.enbuild.2015.05.029.

[15] Sarbu I, Dorca A. A comprehensive review of solar thermoelectric cooling systems. Int J Energy Res 2018;42:395–415. https://doi.org/10.1002/er.3795.

[16] Irshad K, Habib K, Basrawi F, Thirumalaiswamy N, Saidur R, Saha B. Thermal comfort study of a building equipped with thermoelectric air duct system for tropical climate. Appl Therm Eng 2015;91:1141–55. https://doi.org/10.1016/j.applthermaleng.2015.08.077.

[17] Shah RK. Fundamentals of heat technology. vol. 4. 1960. https://doi.org/10.1007/bf00740254.

[18] Li T, Tang G, Gong G, Zhang G, Li N, Zhang L. Investigation of prototype thermoelectric domestic-ventilator. Appl Therm Eng 2009;29:2016–21. https://doi.org/10.1016/j.applthermaleng.2008.10.007.

[19] Cheon S, Lim H, Jeong J. Applicability of thermoelectric heat pump in a dedicated outdoor air system. Energy 2019;173:244–62. https://doi.org/10.1016/j.energy.2019.02.012.

[20] Kim Y, Ramousse J, Fraisse G, Dalicieux P, Baranek P. Optimal sizing of a thermoelectric heat pump (THP) for heating energy-efficient buildings. Energy Build 2014;70:106–16. https://doi.org/10.1016/j.enbuild.2013.11.021.

[21] Astrain D, Aranguren P, Martínez A, Rodríguez A, Pérez MG. A comparative study of different heat exchange systems in a thermoelectric refrigerator and their influence on the efficiency. Appl Therm Eng 2016;103. https://doi.org/10.1016/j.applthermaleng.2016.04.132.

[22] Han T, Gong G, Liu Z, Zhang L. Optimum design and experimental study of a thermoelectric ventilator. Appl Therm Eng 2014;67:529–39. https://doi.org/10.1016/j.applthermaleng.2014.03.073.

[23] Aranguren P, Díaz de Garayo S, Martínez A, Araiz M, Astrain D. Heat pipes thermal performance for a reversible thermoelectric cooler-heat pump for a nZEB. Energy Build 2019;187:163–72. https://doi.org/10.1016/j.enbuild.2019.01.039.

[24] Shen L, Tu Z, Hu Q, Tao C, Chen H. The optimization design and parametric study of thermoelectric radiant cooling and heating panel. Appl Therm Eng 2017;112:688–97. https://doi.org/10.1016/j.applthermaleng.2016.10.094.

[25] Karwa N, Stanley C, Intwala H, Rosengarten G. Development of a low thermal resistance water jet cooled heat sink for thermoelectric refrigerators. Appl Therm Eng 2017;111:1596–602. https://doi.org/10.1016/j.applthermaleng.2016.06.118.

[26] Diaz de Garayo, S.; Martínez, A.; Aranguren, P.; Astrain D. Prototype of an air to air thermoelectric heat pump integrated with a double flux mechanical ventilation system for passive houses. Appl Therm Eng 2021. https://doi.org/https://doi.org/10.1016/j.applthermaleng.2021.116801.

[27] HRU commercial model: Siber EVO2 n.d. https://www.siberzone.es/descarga/siber-df-evo-2-15328/ (accessed September 14, 2021).

[28] EES Sofware: Engineering Equation Solver n.d. http://fchartsoftware.com/ees/ (accessed September 14, 2021).

[29] Picallo-Perez A, Sala JM, Odriozola-Maritorena M, Hidalgo JM, Gomez-Arriaran I. Ventilation of buildings with heat recovery systems: Thorough energy and exergy analysis for indoor thermal wellness. J Build Eng 2021;39:102255. https://doi.org/10.1016/j.jobe.2021.102255.

[30] J.E. Hesselgreaves, Richard Law DR. Compact Heat Exchangers. Elsevier; 2017. ISBN: 9780081003060.

[31] Cai Y, Mei SJ, Liu D, Zhao FY, Wang HQ. Thermoelectric heat recovery units applied in the energy harvest built ventilation: Parametric investigation and performance optimization. Energy Convers Manag 2018;171:1163–76. https://doi.org/10.1016/j.enconman.2018.06.058.

[32] Martinez A, Díaz S, Garayo D, Aranguren P, Araiz M, Catal L. Simulation of thermoelectric heat pumps in nearly zero energy buildings : Why do all models seem to be right ? 2021;235. https://doi.org/10.1016/j.enconman.2021.113992.

[33] Han T, Gong G, Liu Z, Zhang L. Optimum design and experimental study of a thermoelectric ventilator. Appl Therm Eng 2014;67:529–39. https://doi.org/10.1016/j.applthermaleng.2014.03.073.

[34] TE Technology. TEM Module: Hp-127-1.4-1.15-71 2018:1–7. https://tetech.com/product/hp-127-1-4-1-15-71/ (accessed January 20, 2007).

[35] Martínez A, Díaz de Garayo S, Aranguren P, Astrain D. Assessing the reliability of current simulation of thermoelectric heat pumps for nearly zero energy buildings: Expected

deviations and general guidelines. Energy Convers Manag 2019;198:111834. https://doi.org/10.1016/j.enconman.2019.111834.

[36] Schnieders J, Feist W, Rongen L. Passive Houses for different climate zones. Energy Build 2015;105:71–87. https://doi.org/10.1016/j.enbuild.2015.07.032.

[37] PHI. Sofware: Passive House Planning Package (PHPP) n.d. https://passivehouse.com/04_phpp/04_phpp.htm (accessed September 14, 2021).

[38] EU. Directive 2010/30/EU on the indication by labelling and standard product information of the consumption of energy and other resources by energy-related products (recast). 2010.

[39] EU. EU Regulation No. 626/2011 - Energy labelling of air conditioners 2011:1–72.

Chapter 5. The TeHP integrated in a pilot case

As demonstrated in the previous chapter, one 15-TEMs-air-to-air heat pump, based on heat pipes as heat exchangers, optimizes the performance of the system, when being combined with a HRU, in a passive house, where the heat load is lower than 10 W/m^2. However, this optimization is based on stationary conditions, and further analysis of the thermal behavior of such a system needs to be done in a dwelling, where the occupancy, the solar radiation and the temperature are changing constantly.

To this purpose, one pilot case has been selected in Pamplona (Spain), as part of the Navarra Social Housing (NSH), a public rental plan trying to respond to the growing social demand for rental housing, promoting high quality and energy efficient dwellings at affordable price, in this case, under the PH standard. NSH will promote a total of 524 dwellings by 2022, from which 322 have been already built. The case study is focused on one particular dwelling of the 42 apartments block, in Mutilva (Valle de Aranguren-Navarra).The selected dwelling is in a second floor and south oriented, what means that the specific heating needs are lower than the certification of the entire building, but presents some cooling needs if strict solar shading control is not guaranteed.

The PH certification is based on Passive House Planning Package (PHPP), the building energy modelling software. It is an essential part of the building design process and its certification. The PHPP enables the building designer to introduce all the individual components such as wall insulation, windows, etc. assessing their influence on the energy balance of the building in winter and in summer. PHPP calculates the heating and cooling load of the building concluding whether the building meets the required criteria for a PH certification. The PHPP has been thoroughly validated against measured performance data of real buildings in various climates, so it is a reliable tool in terms of heating and cooling demand prediction for building close to the PH requirements. However, the PHPP is a stationary building simulation program that assesses a double monthly and yearly energy balance, which does not consider the dynamic thermal behavior of the HVAC systems. Moreover, the energy balance is made at building level, since the dwellings of an apartment block cannot be individually certified.

For this reason, the input parameters of the energy simulation of the building are being extracted from the PHPP results for the PH certification and further introduced in TRNSYS dynamic simulation program, calibrating the results of both models. TRNSYS is a transient

systems simulation program with a modular structure. Many of the components that commonly make part of a thermal or electrical system can be found in the library and can be connected between them, as well as different routines to handle input of weather data or other time-dependent forcing functions and output of simulation results. TRNSYS is well suited to detailed analyses of any system whose behaviour is dependent on the passage of time, as buildings. To this purpose TYPE 56 provides a multizone building calculation method that allows a very detailed description of the building, including the solar radiation, the blinds, internal gains per zone and the air flow exchange between indoor and outdoor, as well as between the different zones of the building. The building can actually be drawn in SketchUp and then exported to either PHPP via designPH plug-in or TRNSYS-TYPE56 via Trnsys 3D plug-in.

In addition, TRNSYS can be connected with the software EES (Engineering Equation Solver). EES is a non-linear equations solver, that includes heat transfer subroutines and the thermodynamic properties of different substances, as psychometrics in the case of the air. This software is the tool employed for the computing analysis performed in previous chapter, and the TeHP model that has been already validated with empirical data can be directly integrated with the PH dynamic simulation model through TYPE 66.

TRNSYS has been the basis for the next investigation, where the thermal behaviour of a 15-TEM TeHP has been analyzed with this quasi-steady simulation model in an hourly basis. In each time-step, the weather conditions, as well as the building thermal behaviour, are simulated, providing the input for the TeHP-EES model. EES provides the output parameter back to TRNSYS, and so, the quasi-study model represents the interaction of both systems: the TeHP and the building including all the additional HVAC components.

The focus of this research is to analyze the annual performance of the air-to-air TeHP in the context of the case study, comparing the results with a similar heat pump with vapor-compression technology. The purpose is to find out how much consumes the thermoelectric device more than the VCHP, and see up to which point this energy can be easily supplied with an on-site RES production, as PV panels. In case this happens, the benefits of thermoelectricity, namely: refrigerant free, no moving parts, noise free, reliability, scalability, good control and minimum maintenance can well outweigh its lower efficiency, becoming a realistic alternative to vapor-compression heat pumps to air condition nZEBs and, more specifically, passive houses.

All the results of this in-depth analysis have been published in the paper: **Annual energy performance of a thermoelectric heat pump combined with a heat recover unit to HVAC one passive house dwelling,** published in **Applied Thermal Engineering** (Volume 204 (2022) 117832. DOI: 10.1016/j.applthermaleng.2021.117832), which constitutes the Chapter 5 of the current Ph. D. dissertation.

Annual energy performance of a thermoelectric heat pump combined with a heat recover unit to HVAC one passive house dwelling

S. Diaz de Garayo[1], A. Martínez[2,3], D. Astrain[2,3]

[1] *National Renewable Energy Centre, 31621 Sarriguren, Spain*
[2] *Engineering Department Public University of Navarre, 31006 Pamplona, Spain*
[3] *Smart Cities Institute, Pamplona, Spain*
[*] *e-mail: sdiaz@cener.com*

Keywords: thermoelectricity, heat pump, passive house, HVAC, heat recovery

Abstract

This paper proposes a HVAC system that integrates a thermoelectric heat pump with a double flux ventilation system and a sensible heat recovery unit able to provide heating, cooling and ventilation to a 74.3 m^2 Passive House certified dwelling in Pamplona (Spain). This study computationally investigates the energy performance of the system and the comfort conditions of the dwelling for one year long.

The thermoelectric HVAC system maintains adequate comfort conditions with an indoor temperature between 20 – 23 °C in wintertime and 23 – 25 °C during summer, thanks to the precise control of the voltage supplied to the thermoelectric heat pump that can regulate the heating/cooling capacity from 5 to 100 %. The system consumes 1143.3 kWh/y (15.3 kWh/m^2y) of electric energy, that can be provided by 4 photovoltaic panels of 250 Wp each. This system is then compared with a vapor compression heat pump with a COP of 4.5. The vapor compression system reduces the electric energy consumption by 36.1 % with respect to the thermoelectric system, which allows saving only 270 Wp (1 - 2 PV panels). This demonstrates the promising application of thermoelectricity for HVAC in passive houses.

Glossary

Acronyms		
ACH	air volume changes	1/h
COP	coefficient of performance	
DC	direct current	
HPipe	heat pipe	
HRU	heat recovery unit for double flux ventilation systems in buildings	
nZEB	nearly zero energy building	
PV	Photovoltaic	
TE	Thermoelectric	
TeHP	thermoelectric heat pump	
TEM	thermoelectric module	
VCHP	vapor compression heat pump	
Greek letters		
ρ_{air}	air density	kg/m^3
Φ	air relative humidity	%
ω	air humidity ratio	Kg_{H2O}/Kg_{air}
Variables		
C_p	specific heat of the air	J/kgK
COP	coefficient of Performance	
I	current supply to the TEMs	A
K	thermal conductance of a TEM	W/K
L_{water}	water latent heat of condensation	J/kg
$\dot{m}_{air}$	air mass flow	Kg/s
$\dot{m}_{cond}$	condensed water	Kg/s
N	number of modules in the TeHP	
$\dot{Q}$	heat flux	W
R^{HPipe}	heat pipe thermal resistance	K/W
R	TEM overall electric resistance	Ω
S	TEM overall Seebeck coefficient	V/K
T	temperature	K
V	voltage supply to the TEMs	V
$\dot{V}$	volumetric air flow	m^3/h
$\dot{W}$	power supply	W
Subscripts / Superscripts		
c	Cooling	
cond	condensed water	
exh	exhaust air, air stream coming from building indoor	
fan	Fan	
fresh	fresh, air stream coming from building outdoor	
h	Heating	
HRU	referring to variables at the outlet of the HRU	

i	relative to one of the modules that constitute the TeHP	
IN	variables at the inlet of the TeHP	
OUT	variables at the outlet of the TeHP	
Supply	variables for the ventilation air supply, that can as ambient conditions (Freecooling), the HRU or the TeHP/VCHP outlets	
TeHP	referring to variables at the outlet of the TeHP	
VCHP	referring to variables at the outlet of the VCHP	

1. Introduction

The European Union Commission has the ambitious target of becoming carbon neutral in 2050 [1]. In Europe 52 % of final energy demand comes from heating and cooling; 25% are used for electricity generation and 23 % in transport. The final energy demand for heating and cooling is then 6352 TWh, with fossil gas being the dominant energy carrier (42 %), followed by oil, biomass and electricity (all 12 %). Buildings are responsible for 80 % of this heating and cooling energy demand (approximately 40 % of EU energy consumption) and represent the 36 % of the European CO_2 emissions [2], what means that the decarbonization plans need to tackle the construction sector from many perspectives. One the one hand, buildings need to reduce their energy demand. To this purpose the Energy Performance of Buildings Directive 2010/31/EU (EPBD [2], recast in 2018 [3]) and the Energy Efficiency Directive 2012/27/EU [4]) promote the nearly ZERO ENERGY BUILDING (nZEB) standard, obligatory since 2020 for new buildings. Additionally, the Commission aims to accelerate the energy refurbishment of the existing stock of buildings doubling the current rate of 1 % of renovation every year (Renovation Wave [5]). On the other hand, buildings need to be fossil fuels free, what leads to the electrification of heat [6], with a strong promotion of heat pumps, in combination with other RES (biomass, solar, geothermal…)[7] and waste heat recovery [8]. Passive houses paved the way for nZEBs, as it is a clearly defined building performance standard based on scientific evidence [9], and characterized by 1) super insulated envelope, 2) airtight construction, 3) high-performance glazing, 4) thermal-bridge-free detailing, and 5) heat recovery ventilation. Under these circumstances, the heating and cooling loads of the building are limited to 10 W/m^2, irrespective of the climate [10]. In such conditions, raising or lowering the temperature of the incoming fresh air with a volumetric flow between 0.35-0.5 air changes (ACH) [11] might provide an indoor comfortable ambient, saving the costs of the heat/cold distribution systems. This is actually the principle upon which the passive house concept is built [10], and this passive house concept permits the integration of a heat pump between both incoming and outgoing air streams as heat sinks [8]. This paper explores this possibility introducing thermoelectric modules (TEMs) replacing the conventional vapor compression heat pumps (VCHP). A thermoelectric heat pump (TeHP) is a solid-state energy converter that can create a temperature difference when an electric potential is applied to the TEM, thanks to the Peltier effect [12]. Thermoelectricity is a very promising technology that presents many advantages: no moving parts, noise free, gas free, no chemical reaction, reliability, scalability and minimum maintenance [13]. Thus, TEMs present zero Global Warming Potential, zero Ozone Depletion Potential and easy transition from heating to cooling mode [14]. TEMs require direct current

(DC) power supply and permit an accurate temperature control by regulating the voltage, as well as an easy integration with PV panels. Compared with vapor compression technology, the coefficient of performance (COP) of a TeHP is relatively low, but in the case of applications with so extremely low energy demand, as is the case of passive houses, the cited advantages and the small size of these devices may well outweigh this aspect. Moreover, new material research is increasingly improving the efficiency of TEMs [15]. These advantages explain the increase in the number of works evaluating the use of TeHPs in the building sector, as it can be seen in several reviews ([16], [17], [18], [19]). The different reported investigations propose different TeHP prototypes integrated in the building envelope or the ventilation system, showing a variety of TeHP designs, mathematical validated models and parametric investigations. On the one hand, as first alternative, many researchers explore the insertion of the TEMs in the walls, roofs, radiant panels or windows; however, the main disadvantage in this case is the thermal bridge created by the TEMs, which goes against the passive house philosophy of reducing the thermal losses through the building envelope as much as possible. On the other hand, many other investigations analyze the integration of the TEMs with the ventilation system, using the exhaust air as either heat or cold reservoir to cool or heat, respectively, the incoming air stream, what better fits with the passive house principle [10]. As being the best alternative, this is the approach used in this paper.

The main objective of this research is to evaluate the operating energy performance and comfort conditions provided by a thermoelectric HVAC system, compared with a reference system. To this aim, it is necessary to evaluate the annual energy balance of the building, analyzing the interaction of the proposed HVAC system with heat losses through the envelope and ventilation, as well as the heat and solar gains. This topic is scarcely addressed in the literature, since among all the research works included in the cited reviews, only [20], [21], [22], [23] and [24] perform an annual energy balance of a TeHP and the building, and only [23] do so for a nZEB.

The first reference [20] presents a solution for domestic indoor space heating. The TeHP is made with aluminum heat sinks and integrated in the wall. The prototype is tested in a 1 m^3 insulated box, and the resulting validated model is afterward extrapolated to assess the energy peformance in a pre-1900s mid-terrace UK dwelling. The TeHP can partly meet the domestic heating demand, which is covered by an on-site renvewable energy hybrid system. Instead, [21] and [22] references present TeHP protoypes only for cooling. While [21] describes a building integrated photovoltaic (PV) thermoelectric wall system, combining the concept of a PV façade and solar cooling, [22] focuses on improving the cooling COP by linking the TeHP with a cold water tank, refrigerated with radiative sky cooling panels. Reference [23] provides solutions for both, heating and cooling, in a nZEB. The investigation proposed the combination of various technologies. On the one hand, the production of electricity using the Seebeck effect, by integrating the TEMs in both a PV panel and a solar thermal collector. On the other hand, the substitution of air conditioners by employing a thermoelectric radiant ceiling and a thermoelectric primary air handing unit.

Despite well documented, defined and developed, none of these four references include the evaluation of a heat recovery unit (HRU) in combination with the TeHP, which was proven to

provide a better performance than a standalone TeHP [25], requiring also a lower number of TEMs. Therefore, better results could be obtained.

Only ref [24] evaluates this possibility. The proposed protype is an air-to-air crossflow TeHP that uses aluminum heat sinks to exchange heat between the TEMs and air streams. Based on the empirical results, this research proposes its combination with an enthalpy wheel, so that the fresh air stream recovers the heat from exhaust air first, and then it is conditioned by the TeHP and a desiccant wheel. The modeling results show that the energy consumption for one year is 22 % higher than a reference system composed of an HRU and a vapor compression cycle heat pump. However, the performance of the TeHP is limited due to the crossflow configuration and, more importantly, due to the type of heat exchangers deployed (finned heat sinks). A low thermal resistance of the heat exchangers between the TEMs and the air streams is crucial in order to obtain a good energy performance of the TeHP. A high thermal resistance increases the temperature gap between the hot and cold sides of the TEM, what drastically reduces the COP [26]. The use of heat pipes as heat exchangers even doubles the energy performance of a TeHP compared with aluminum finned heat sinks. This fact is remarked by [27], who presents a thermoelectric ventilator with heat pipes, as an evolution of a previous design made with aluminum finned sinks [28]. Therefore, there is room for improvement with respect to ref. [23].

The present work comes to fill this research void and goes a step forward on the search of application of thermoelectricity to nZEBs. This paper presents the first study on integrating a passive house with an air-to-air TeHP and a HRU, presenting the annual energy balance in a case study. A “passive house” certified building is a particular case of nZEB where the heating and cooling loads of the building are specifically limited, what allows the proposed TeHP to meet the energy demand in combination with the HRU. The TeHP design presents a counter-flow disposal and uses heat pipes to exchange heat between the TEMs and air streams.

The study involves the use of TrnSYS software for the simulation of the building, the HRU and other involved systems, but it requires a specific model for the TeHP. In this regard, the modeling of heat pipes thermal behavior is complex. In real conditions, the thermal resistance is never constant but variable depending on the heat flux and the air flow. Also, its value in the cold side doubles the one in the hot side, since the heat pipe on the cold side works contrary to its design conditions [29]. The natural inaccuracy due to the simplifications and estimated input values for the computational models may drive to deviations higher than 30% between simulated and experimental results [30], especially if a significant aspect as the complexity related to the heat and mass transfer mechanisms in the heat pipes is not well addressed.

The design of the TeHP is based on previous experimental work, that tested and modeled the thermal behavior of the heat pipes [29] and a subsequent research that constructed and tested one 10-TEM TeHP prototype [31]. The computational model employed for the TeHP is validated by comparing the simulated results with empirical results of these works.

This paper analyzes a real passive house case study, aiming at studying the feasibility of this innovative system to HVAC one 74.3 m^2 dwelling in the city of Pamplona (Spain). The analysis includes the comparison of the proposed system with a VCHP, assessing the number of PV panels needed to compensate the better performance of VCHP technology in two grid-

integration scenarios: net balance and self-consumption. Next section 2 describes the selected case study for the analysis: the building, the proposed HVAC system and the TeHP design, followed by section 3, that reports the investigation methodology. Section 4 presents the validation by comparing the calculated outputs with the experimental results. The next section 5 shows the results related to the energy performance and the comfort temperatures in the dwelling, including the comparison of the TeHP with the VCHP, and the production of PV panels on the roof. Finally, main conclusions are introduced in section 6.

2. Case study description

The case study house selected to explore the viability and replicability of the proposed HVAC system is one residential block built as part of the Navarra Social Housing Plan (NSH), an ambitious public plan to provide high quality rental houses to vulnerable population. The NSH aims at building 524 dwellings Passive House certified by 2022, providing high comfort conditions with minimum energy consumption, aiming at having best value for money.

2.1. Building

Figure 82. Picture of the south-east, south-wes façades of the case study building with 21 dwellings.

This 21-dwellings-block has been already built and previously simulated with the Passive House Planning Package (PHPP) [32] for the Passive House certification, estimating a heating demand of 15 kWh/m^{2}y and a maximum heat load of 10 W/m^2. Further details on the building envelope and the energy balance are provided in Figure 83.

For the purpose of this study, one dwelling of 74.3 m^2 in second floor and south oriented was selected. The dwelling has two bedrooms, two toilets, one kitchen and one living room with a small entrance (see Figure 82). The ventilation air flow, calculated to comply with the building code [33] is 0.54 ACH. The double flux ventilation system drives the fresh air to the living rooms and both, the master and the secundary bedrooms, while the exhaust air is collected from the kitchen, the bathroom and the toilet. The HRU harvests the sensible heat of the exhaust air with an efficiency of 82% [34]. The infiltrations are supposed to be 0.033 ACH,

based on the experimental blower door test with a result of n_{50}=0.5 ACH and the Ref. [35]. PHPP is used to estimate the energy balance of a building as a whole, since it is a simplified unizone model with monthly basis calculation. As one of the main goals of this study is the analysis of the performance of the novel HVAC system in different operating conditions, we use a dynamic simulation model (TYPE 56 - Multizone Building modeling) [36], introducing same inputs for the thermal envolope, ventilation and climate conditions [37], as in PHPP. For this detailed simulation study three people are estimated to live in the dwelling with the occupancy schedule shown in Figure 84. Total internal gains summarized account for 16 kWh/m^2 during the heating season, same as in the case of PHPP and [38]. Finally, the internal humidity production (due to people's breath, cooking, plants or personal hygiene) considered is 4.5 l/day (distributed according to the occupancy schedule), coherent with other prior specific studies [38]. PHPP does not foresees the use of dehumidification in the building, estimating a maximum indoor absolute humidity of 10.9 g/Kg (while dehumidification is applied when it exceeds 12 g/Kg more than 10% of summertime).

Parameters	Surf. (m^2)	U (W/m^{2}K)
External wall	1,040.5	0.196
Roof	416.8	0.141
Floor	396.9	0.159
Seperation with parking	46.4	0.366
Separation with not heated-space	517.7	0.766
Windows	215.4	0.984
Door	24.6	0.749
Thermal bridges	1,364.0	0.086

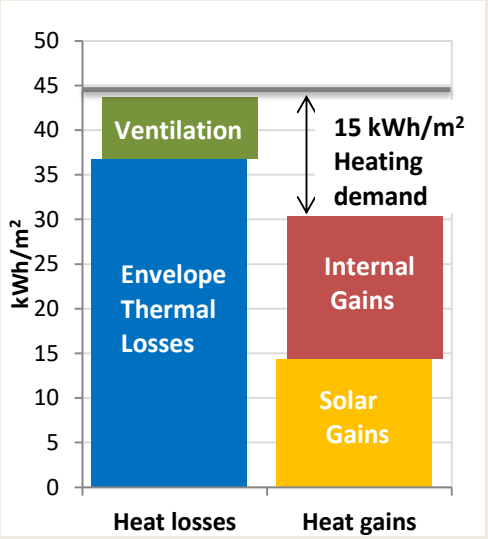

Figure 83. Left: Thermal properties of the case study building envelope. Right: Energy balance of building according to PHPP and the Passive House certification.

The dwelling is south oriented, with 3 openings in SE and 2 in SW. The external solar protection system is supposed to favor the entrance of solar radiation in wintertime and block it during summer. Under these circumstances and operational conditions, the heating demand calculated with the dynamic model (considering and ideal heating/cooling system with no power limitation and 20 °C - 25 °C as respective set points) for this dwelling is 11.6 kWh/m^{2}y with a peak demand of 12.4 W/m^2. The cooling demand, however, depends very much on the effectiveness of the blinds control system that, in this case, is manual, and, hence, depends on the tenants. PHPP assumes that, for this climate, the overheating situation is limited to the 2% of the time in summer season. For this study we estimate that the blinds will only be lowered when the incident radion exceeds 300 W/m^2, blocking only 80 % of the radiation. In this case, there is a cooling demand of 4.7 kWh/m^{2}y and a peak demand of 9.5 W/m^2, that will be the baseline to simulate the operation of the HVAC system proposed by this paper. Finally, the

simulations show that this refrigeration demand may be lowered to 1.8 kWh/m^{2}y if night ventilation is applied during summer with 1 ACH. The heating and cooling power demand hourly values are depycted in Figure 84 with a cumulative histogram.

	Oc.	Timetable
Bedrooms	2+1	24:00-8:00
Living room	1.5	14:00-20:00 & 21:00-24:00
Kitchen	2	7:00-9:00 & 21:00-22:00
Bathrooms	1.5	7:00-8:00 & 20:00-21:00

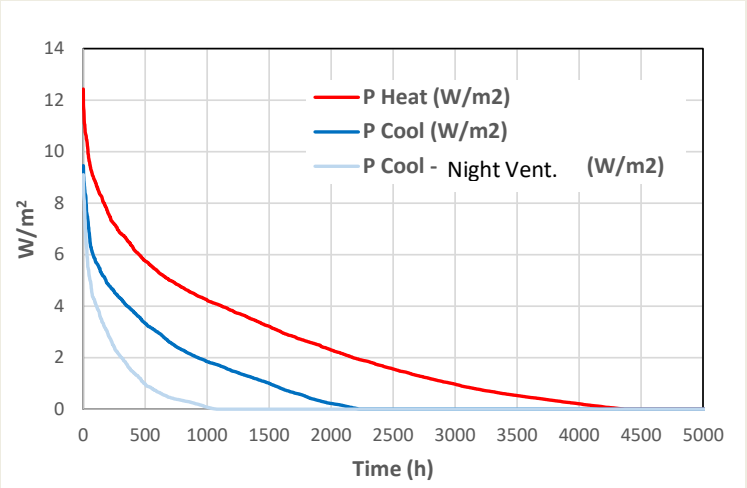

Figure 84. Left: occupancy schedule; right: cumulative histogram of heating and cooling capacity hourly demands of the dwelling (W/m^2) one year long. Results of the energy simulation of the dwelling considering an ideal heating / cooling system with no power limit, and 20°C set point for heating and 25°C for cooling. The clear blue line shows the cooling demand when night ventilation is applied in summer time.

2.2. HVAC

This paper proposes an HVAC system to renovate the indoor air and work as either heating or cooling device by solely raising or lowering the temperature of the incoming air. The ventilation system blows the fresh air to the dry zones (bedrooms and living rooms) and extracts the exhaust air from the humid zones (bathrooms and kitchens). The exhaust air goes through the HRU exchanging sensible heat with the incoming air. The heat flows naturally in wintertime since the exhaust air is hotter than the air outside, and the only energy consumption is due to the fans. For this case study the commercial model Zehnder-ComfoAir-200-D250-WHR920 has been selected (same as in the real facility), with a proven efficiency of 82 % [34]. After the HRU the incoming air is hotter than the exhaust air, and both air streams enter the TeHP, where heat is again pumped from the exhaust air to the fresh air, but, in this case, forced by thermoelectric modules (TEMs). In summertime, the HVAC system may work in cooling mode by only reversing the polarity of the electric supply of the TEMs, as shown in Figure 85.

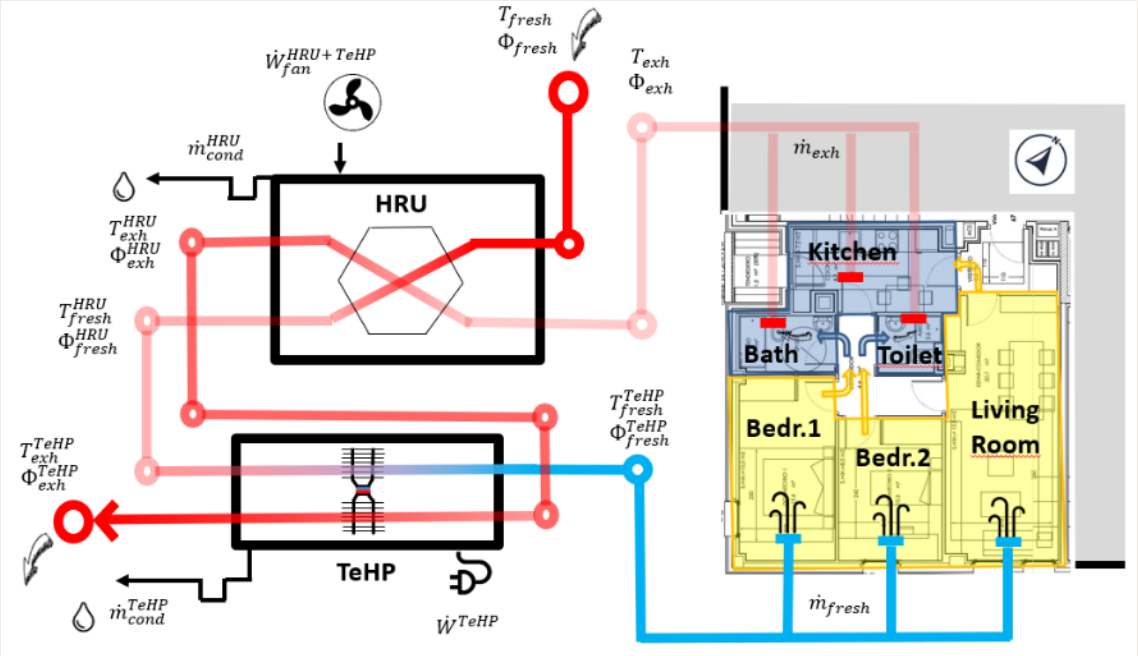

Figure 85. Cooling mode of the HVAC proposed system to meet the heating needs of the Passive House dwelling.

The air-to-air TeHP investigated is composed of two counter-flow 12 cm square air ducts. The heat transfer between the air streams is induced by the thermoelectric modules (TEMs). Each TEM is an energy converter able to absorb heat from a cold reservoir ($\dot{Q}_c$) and emit heat to a hot one ($\dot{Q}_h$) by consuming DC electric power ($\dot{W}$). The TeHP has a modular design, based on previous experimental study [39], composed of several TEMs and heat sinks to transfer the heat between the TEM's cold and hot faces, and the air streams. Each heat sink includes 5 copper 6 mm heat pipes combined with 40 aluminum fins 5.5 cm deep. Figure 86 shows the hot and cold counter-flow air ducts.

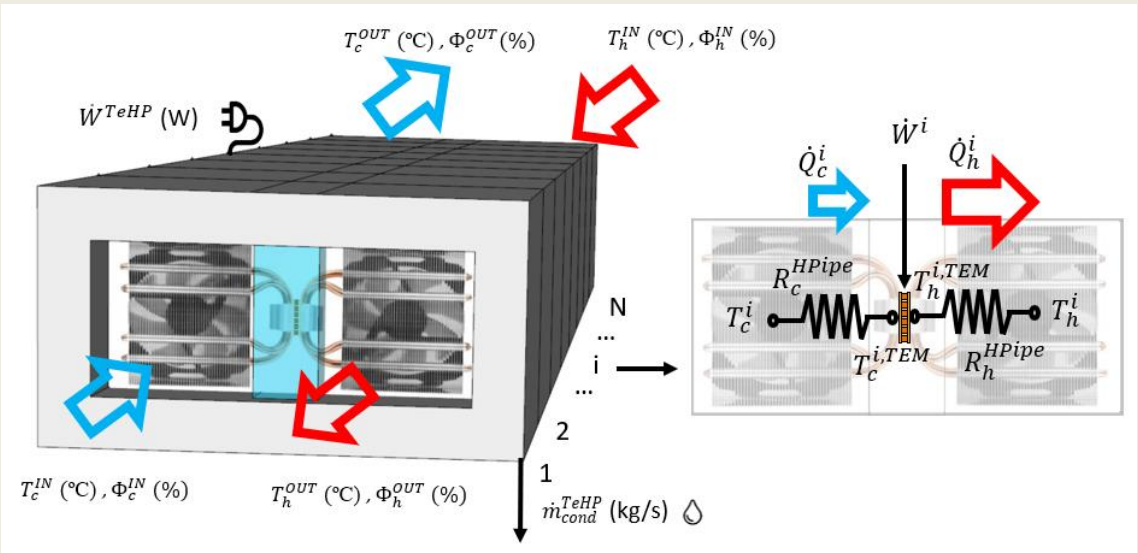

Figure 86. TeHP design with hot and cold counter-flow air streams. Right figure shows a crossed section with the energy balance of one module, including the thermal resistance of the heat sinks.

As one of the aims of the present work is the comparison between the performance of thermoelectric heat pump and the vapor compression cycle, the TeHP will be replaced by a VCHP, with the same scheme as shown in Figure 85. As the efficiency of the VCHP may differ depending on the refrigerants and the compressor technology, this study includes two scenarios: regular technology with a nominal COP of 2.5 for heating and 2.2 for cooling [40], and a highly efficient heat pump for this particular application with a COP of 4.5 for heating and 4 for cooling.

Finally, the analysis includes the contribution of PV pannels on the roof in order to compensate the energy consumption of the HVAC system. To this purpose we employ the thechnical specifications of one commercial model with 250 W peak production and 16 % efficiency: Kyocera - KD250GH-4FB2 - 250Wp - Poly – Secondsol [41], considering 10% of conducting and switching losses due to the inverter and the facility inefficiencies.

3. Methodology: computational model

The goal of this study is to analyze the performance and viability of the previously defined HVAC system in the proposed passive house certified pilot case. The simulation method must then consider the dynamic thermal behaviour of the building, estimating the thermal gains and losses, as well as the ventilation system sweeping the air from the dry to the humid zones. To this aim TRNSYS17 software is selected [42]. TRNSYS is a modular based simulation environment for the transient simulation of systems, including multi-zone buildings.

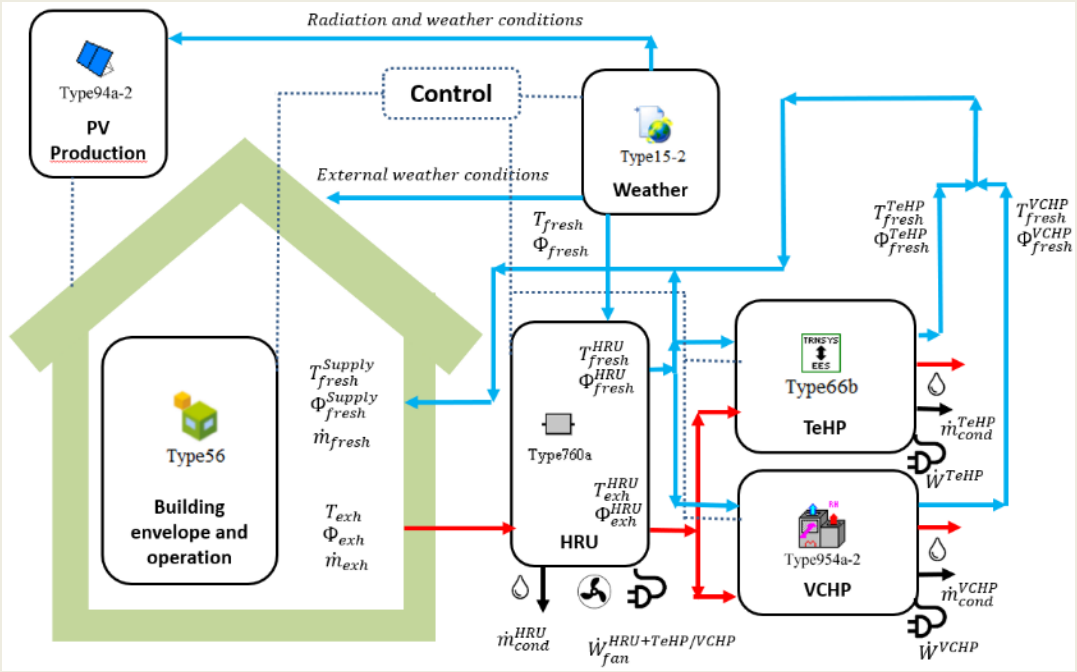

Figure 87. TRNSYS model structure for the dynamic simulation of the dwelling and the HVAC system with either the TeHP or the VCHP.

The building has been modeled with TYPE56 [36], which is able to reproduce the geometric details of the multizone building, as well as the thermal properties of the envelope, the internal gains, solar radiation, infiltrations, ventilation and the water vapor mass balance of the different dwelling zones. The weather conditions are provided by TYPE15 based on METEONORM data from Pamplona [37] and the HRU is reproduced by TYPE760a (TESS library [43]), based on the effectiveness-minimum capacitance method.

3.1. TeHP

The simulation of the TeHP must not only consider the thermal, but also the thermoelectric phenomena. For this specific research work, the TEM selected is HP-127-1.4-1.15-71 made by TE Technology with 127 thermocouples of Bi_2Te_3 [44]. Its properties are shown in Table 15:

Table 15. Properties of HP-127-1.4-1.15-71 thermoelectric module [44].

Parameters	Values
Lenght (mm)	40
Width (mm)	40
Thickness (mm)	3.4
Number of thermocouples (n)	127
$\dot{Q}_{max}$ (W)	80
ΔT_{max} (°C)	71
I_{max} (A)	8
V_{max} (V)	16.1
S (V/K) at 298 K	0.053
K (W/K) at 298 K	0.72
R (Ω) at 298 K	1.45

After comparing nine different modelling techniques for the simulation of TeHPs applied to air condition nZEBs, one previous research work carried out by the authors [45] concluded that there is no statistical difference in the predicted results of the coefficient of performance and the cooling capacity at 95 % level of condidence. In order to reduce the computational cost of the analysis, this investigation describes the TEM operation with a standard widely used simple method that implies Peltier and Joule Effects and thermal conduction (disregarding the Thomson effect) [46]. For each of the modules of the TeHP (represented with the superscript i), the heat absorbed by the cold side of the TEM can be described as in Eq. (1), while Eq. (2) presents the heat emitted by the hot side, where superscript TEM stands for the surface temperature on both, the cold and hot sides of the thermoelectric module, as shown in Figure 86.

$$\dot{Q}_c^i = SIT_c^{i,TEM} - \frac{1}{2}I^2R - K(T_h^{i,TEM} - T_c^{i,TEM}) \quad (1)$$

$$\dot{Q}_h^i = SIT_h^{i,TEM} + \frac{1}{2}I^2R - K(T_h^{i,TEM} - T_c^{i,TEM}) \quad (2)$$

This heat is absorbed or emitted to the air through the heat pipes (as TEM-air heat exchangers) described in section 2.3. These heat pipes were analyzed and thermally characterized in a previous experimental research [29].

$$\dot{Q}_c^{i,TEM} = \frac{T_c^i - T_c^{i,TEM}}{R_c^{HPipe}} \quad (3)$$

$$\dot{Q}_h^{i,TEM} = \frac{T_h^{i,TEM} - T_h^i}{R_h^{HPipe}} \quad (4)$$

Eqs. (3) and (4) show the heat exchange depending on the thermal resistance of the heat pipes R^{HPipe}, which is variable and depends on the heat flux (mainly related with the voltage of the TEM electric supply) and the air flow (which affects to the convective heat transfer coefficient between the air and the aluminum fins). The obtained thermal resistance values are shown in Figure 88, and were included in the computational model with an interpolation function.

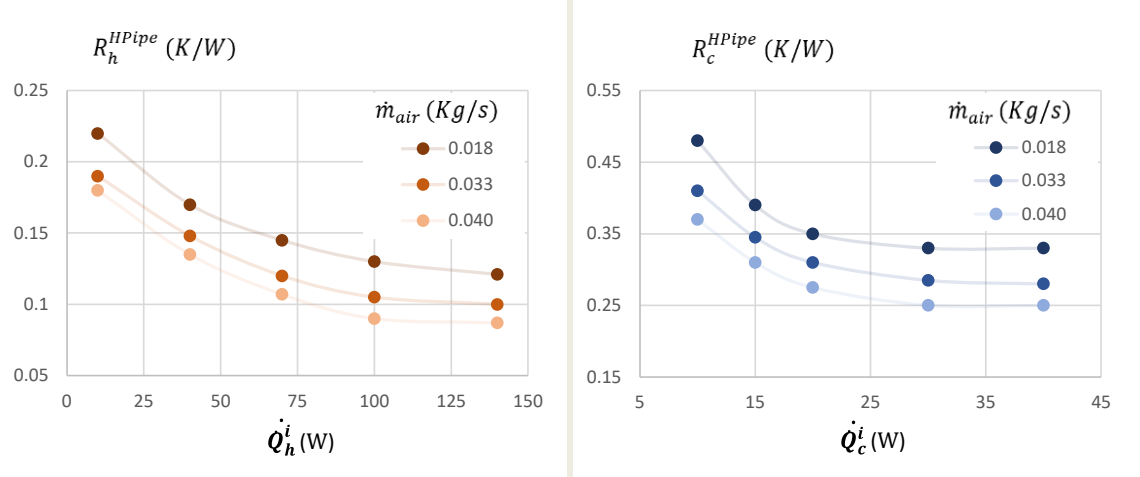

Figure 88. Thermal resistance values of the heat pipes used as heat sinks between the TEM and the heating (left) and the cooling (right) air streams [29]

Finally, the energy balance of the whole TeHP (see Figure 86) is described by Eqs. (5), (6) and (7):

$$\dot{Q}_c^{TeHP} = \dot{m}_{air}\rho_{air}C_p(T_c^{IN} - T_c^{OUT}) - \dot{m}_{cond}^{TeHP}\,L_{water} = N\,\dot{Q}_c^{i,TEM} \quad (5)$$

$$\dot{Q}_h^{TeHP} = \dot{m}_{air}\ \rho_{air}C_p\left(T_h^{OUT} - T_h^{IN}\right) = N\,\dot{Q}_h^{i,TEM} \quad (6)$$

$$\dot{W}^{TeHP} = N\,V\,I = \dot{Q}_h^{TeHP} - \dot{Q}_c^{TeHP} \quad (7)$$

$$\dot{m}_{cond}^{TeHP} = \dot{m}_{air}\,\rho_{air}\,(w_c^{IN} - w_c^{OUT}) \quad (8)$$

The air mass flow ($\dot{m}_{air}$) in both, the cooling and heating ducts, is the same, since the air extrated ($\dot{m}_{exh}$) and blown into the dwelling ($\dot{m}_{fresh}$) must be balanced in order to prevent

overpressure or under-pressure indoor conditions. If the air temperature in the cooling duct undergoes the saturation point, then a certain amount of water is condensed and calculated through the latent heat in Eq. (5) and the water mass balance in Eq. (8). This model has been programed in Engineering Equation Solver (EES) [47] and the results were validated, as shown in next Section 4.

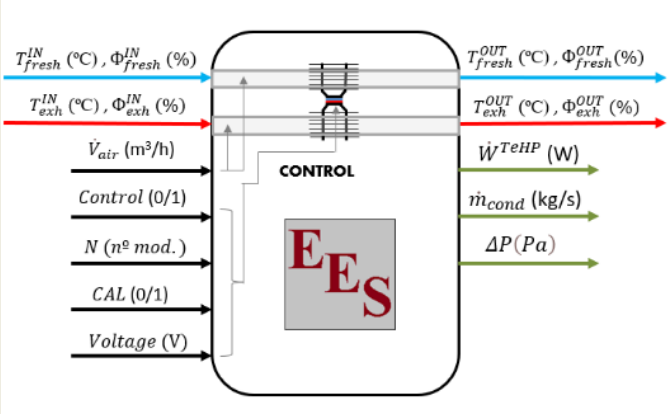

Figure 89. Type 66 scheme used for the simulation of the TeHP. The figure shows the input and output parameters used between Trnsys17 and the EES model to reproduce the thermal behaviour of the TeHP.

For the purpose of the present research work, this computational model has been integrated with TRNSYS17 by using TYPE 66 (see Figure 89). This type has been configured to introduce the temperature and humidity of the fresh and the exhaust air ducts, the air flow, the number of modules, the voltage and two control signals (one signal to activate the TYPE in each timestep, and the signal CAL which is set to 1 when operating in heating mode and 0 for cooling). The number of modules that constitute the TeHP affects its performance. A higher number of modules permits to reach a certain heating capacity with less TEM voltage and, thus, have a better energy performance [48]. However, depending on the temperature of incoming air streams, a minimum voltage is required, since the temperature gap between the hot and cold sides of the TEM needs to be higher than the temperature gap between the air streams to assure that the heat is transferred from one air duct to the other. Moreover, a higher number of modules also means a higher pressure drop in the air ducts and, thus, a higher electric consumption due to the fans. This means that, depending on the temperature gap of the incoming air streams and the heating/cooling needs, there is an optimum value of modules that maximize the efficiency of the TeHP. For this investigation the number of modules was set at 15, as a result of a previous optimization assessment considering the estimated operating conditions. In the TRNSYS simulation model, TYPE 66 calls EES program with the TeHP computational model described in this section returning the air temperature and humidity of the outgoing air ducts, the electric DC consumption of the TEMs, the pressure drop (based on empirical research [39]) and the condensated water (if so) in the cooling duct. For this study we consider an additional 10 % of electric consumption to contemplate the AC-DC conversion to feed the TEMs (this electric conversion inefficiencies could be lowered if the PV facility is directly connected to the TeHP by using a DC-DC converter).

3.2. VCHP

In order to reproduce the thermal behaviour of the VCHP we employ the TYPE 954, which uses a manufacturer's catalog data approach to model an air source heat pump. The model utilizes normalized off-performance data, based on 340/360 Standard of ARI (Air-conditioning & Refrigeration Institute) [49]. The coefficient operation depends on the temperature of both heat sinks for heating and it also includes the humidity of fresh air when cooling. The heating capacity is 700 - 1500 W and the cooling capacity 550-1000 W). For the envisaged ventilation volumetric air flow (100 m^3/h) the heating capacity is limited to 800-1200 W and the cooling capacity 600-800 W.

3.3. Regulation

The TeHP is able to regulate the heating/cooling capacity from 5 % to 100 % by modifying the voltage of the DC supply to the TEMs (see Figure 90). For heating the control thermostat is set to 21 °C with an hysteresis cycle of 1 °C. The DC supply is also regulated depending on the dwelling air temperature (living room), going from 0.5 V when the inside temperature is 22 °C up to 15 V when this temperature undergoes 18 °C. For cooling, the set point is 24 °C with also 1 °C hysteresis and the voltage ranging from 0.5 V for 23 °C up to 12 V for indoor temperatures higher than 27 °C. Ref. [39] demonstrated that higher voltages are inefficient for cooling due to the Joule effect. In the case of the VCHP, the regulation is more limited. One limitation factor is the maximum temperature of the supply air, that should never go above 50 °C to avoid the dust burning (bad smell) and the discomfort due to high temperature gradients [38]. On the other hand, VCHP can never go under a specific heating capacity. For the simulations carried out, the heating/cooling capacity depends on the temperature of heat sinks (as previously explained) and the volumetric air flow [49] (which is fixed to 100 m^3/h). The VCHP is regulated following an hysteresis cycle, as described in Figure 90. The minimum temperature set point is 20 °C, and it continues working until indoor temperature reaches 23 °C (3°C hystereris), in order to reduce the switching cycles, that lower the overall efficiency of the heat pump [50]. Likewise, the cooling set point is 25 °C and the hysteresis cycle is 2 °C.

In both case studies (TeHP and VCHP) the freecooling option is included, and it is activated when the HVAC is in cooling mode (according to the above mentioned conditions) and the temperature outside is 3°C lower than the inside temperature. The heat exchange system inside the HRU is then shorcut, and the fans increase the air flow reaching 1 ACH.

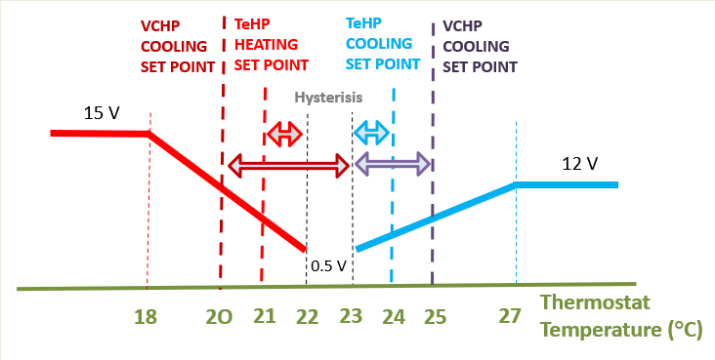

Figure 90. Set points and hysteresis cycles to regulate the TeHP and the VCHP. The TeHP heating set point is 21°C and regulates de voltage from 0.5 to 15V with 1°C hysteresis. For cooling the set point is 24°C and the voltage goes 0.5-12V with 1°C hysteresis. The VCHP set points are 20°C for heating and 25°C for cooling with 3°C and 2°C hysteresis respectively.

3.4 Fans electric consumption

The fans of the HRU are regulated to assure a minimum 0.54 ACH of ventilation, that is increased to 1 ACH when freecooling. The pressure drop is calculated as the addition of the pressure drop in the air ducts, the ventilation grills, the HRU and the TeHP/VCHP. This presure drop is based on empirical evidence in the case of the TeHP [39], the technical characteristics in the case of the HRU [34] and the estimation for the installed air ducts and grills in the dwelling (100 Pa for 0.54 ACH [51] and a parabolic increase of the pressure drop air flow dependent, being 354 Pa for 1 ACH). As a result, the electric consumption of the fans is calculated according to the fan technical specifications [34], being 58.4 W when ventilating with the HRU, 75.3 W when the TeHP/VCHP is activated and, finally, 98.5 W when dragging outdoor air for freecooling (allthough the HRU is shortcut, the air flow is increased and, therefore, the pressure drop is increased as well, resulting in an increase of the fan electric consumption).

3.5 RES production: PV panels

The photovoltaic array used to compensate the energy consumption of the HVAC system is simulated employing TYPE 94 [52]. It uses the equations of an empirical equivalent circuit model to predict the current-voltage characteristics of a single module, based on the cataloghe specifications of the PV panel [41]. The strength of the current source is dependent on solar radiation and the efficiency of the cells is temperature-dependent. This model estimates, as metioned in the previous chapter, 10 % energy looses due mainly to DC/AC conversion. The panels are assumed to be installed south oriented with a 30 ° slope.

4. **Validation**

The mathematical models that describe the thermal behavior of the building (TYPE 56 [36]), the HRU (TYPE 760a (TESS library [43])) and the electric production of the PV panels (TYPE 94

[52]) have been widely validated, with specific references in the corresponding mathematical descriptions. In the case of the energy demand of the building, the 21-dwelling-block has been firstly simulated with PHPP [32], that employs the monthly calculation method of EN-ISO 13790, adapted to the passive house characteristics. The simulation results were certified by the Passivhaus Institute. Moreover, the results of the monitoring carried out by NASUVINSA, public building company and owner of the building, have shown that the energy consumption during the first winter season are 27550 kWh of primary energy (biomass), one 5 % less than expected. The purpose of using this particular dwelling for this research is to simulate a realistic case study in a certified passive house building. The dwelling has been drawn in SketchUp and exported to the TYPE 56 using Trnsys3d software, considering 8 zones, as explained in Section 2.1. The main input parameters have been described in this section and are coherent with the PHPP assumptions. The resulting dynamic model is also coherent with the obtained annual results.

Finally, and more importantly, the TeHP requires a specific validation, given that it needs to reproduce, not only the thermal, but also thermoelectric phenomena, and it is at the core of the investigation. To this aim, the proposed computational model has been validated by comparing the simulated results with empirical evidence obtained in a deep experimental study of the 10-modules-TeHP prototype [26]. Three experimental scenarios were analyzed with the help of an environmental chamber (Figure 68): two for winter conditions (T_{fresh}= 0°C and T_{fresh} = 10 °C) and one for summer conditions (T_{fresh}= 30°C). The volumetric air flows ($\dot{V}_{air}$) tested were: 55, 100 and 130 m^3/h and the voltage supply: 3, 6, 9 and 12 V. In total, 72 tests were carried out, reaching stationary conditions: 36 for heating and 24 for cooling.

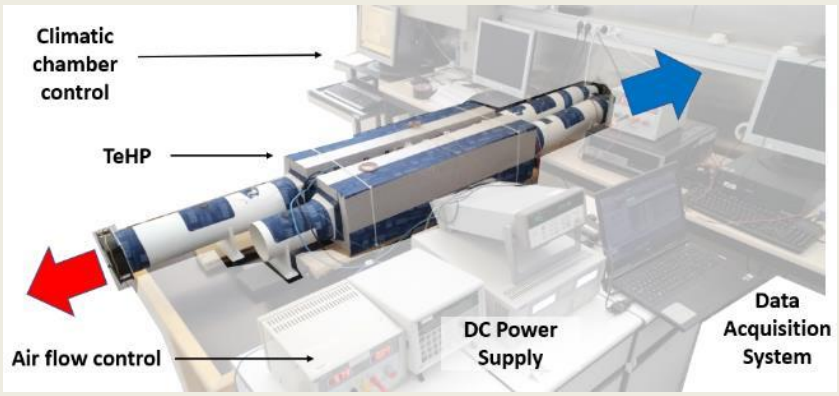

Figure 91. TeHP prototype investigated. The thermal resistance of the heat sinks is based on empirical data and the mathematical model has been validated with the results a previous empirical invesgitagion [26].

All these air inlet conditions were introduced in the computational model, and the outputs compared with the experimental results. The results show a maximum deviation of ±13% for the prediction of the $\dot{Q}_h^{TeHP}$ and the COP_h^{TeHP}. In the case of the cooling tests, the lower temperature gaps in the tests lead to higher uncertainity in the experimental results, specially for 3 V TEM supply. The confidence interval is ±14% for $\dot{Q}_c^{TeHP}$ and ±15% for COP_c^{TeHP}. We can then conclude that the maximum deviation of the experimental and simulated resuls is ±15%,

which is a good result and coherent with the uncertainity analysis associated to the thermoelectric properties of the TEMs [34].

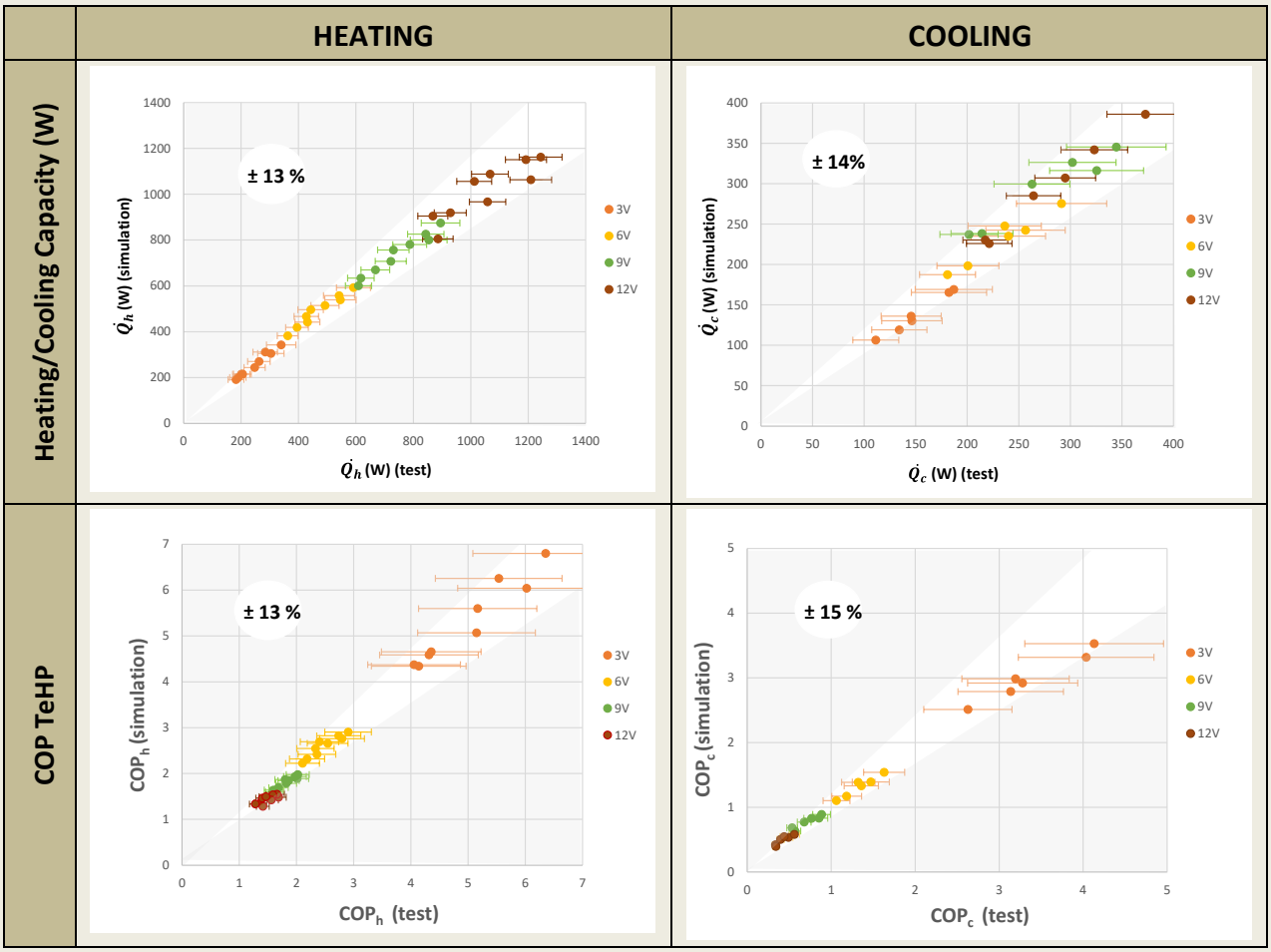

Figure 92. Validation of the computational model comparing the simulated results with 72 empirical tests. The horizontal error bars reproduce the uncertainity of the measured data.

5. Simulated results and discussion

This section presents the results of the simulations, focusing first on the dynamic evolution of the air temperature in the different HVAC components integrated with the building. This analysis is carried out for the TeHP (section 5.1) first and, then, for the VCHP (section 5.2), what therefore helps to better understand the operating characteristics of both systems and the results in terms of comfort and energy performance. Next section 5.3 compares the overall one-year performance and the final section 5.4 assesses the energy balance of the building considering the electric production of PV panels integrated on the roof.

5.1. TeHP Results

Figure 93 shows the evolution of the HVAC temperatures in a cold week [37]. The first two days present night cold temperatures close to 0°C, but the temperatures rise to a maximum of 15 °C and 7 °C respectively during the day. The weather is sunny, as reflected by the building temperature (T_{exh}, red line, calculated as the average temperature of the 8 zones in TYPE56) increase during midday due to the solar gains (see more detailed information in the additional documentation, including the evolution of indoor temperature when no heating or cooling are supplied to the ventilation system). The fresh air goes first through the HRU. The temperature of the ventilation air flow is initially similar to the outdoor temperature (T_{fresh}, blue line) and it rises up to T_{fresh}^{HRU} (yellow line) after crossing the HRU. As long as the building temperature is above 21 °C (during 12 hours the first days and 6 hours the second day), this air is directly provided to the building, keeping the TeHP switched off. The temperature of the ventilation fresh air is reproduced with T_{fresh}^{Supply} and indicated with a gross dark green line. When the indoor temperature udergoes the set-point of 21 °C, the TeHP is switched on increasing the temperature of the incoming air up to T_{fresh}^{TeHP}, reproduced by a light green line. This temperature depends on the DC voltage supplied to the TeHP, and this voltage is regulated following Figure 90, being proportionally higher when the building temperature (T_{exh}, red line) decreases. The night of the second day (23rd of December) the TeHP works 10 hours, and the incoming air temperature is slightly raised from 18 °C to 24 °C, with voltages between 3-4 V.

During the next 5 days the outdoor temperature (T_{fresh}, blue line) goes below 0 °C four times, with maximum daily temperatures below 5 °C. There are no solar gains, what indicates a foggy weather. The TeHP is constantly on, and the incoming air reaches 33 °C with a DC supply of 6-8 V. The continuous regulation of T_{fresh}^{HRU} maintains the building indoor temperature stable and always above 20 °C.

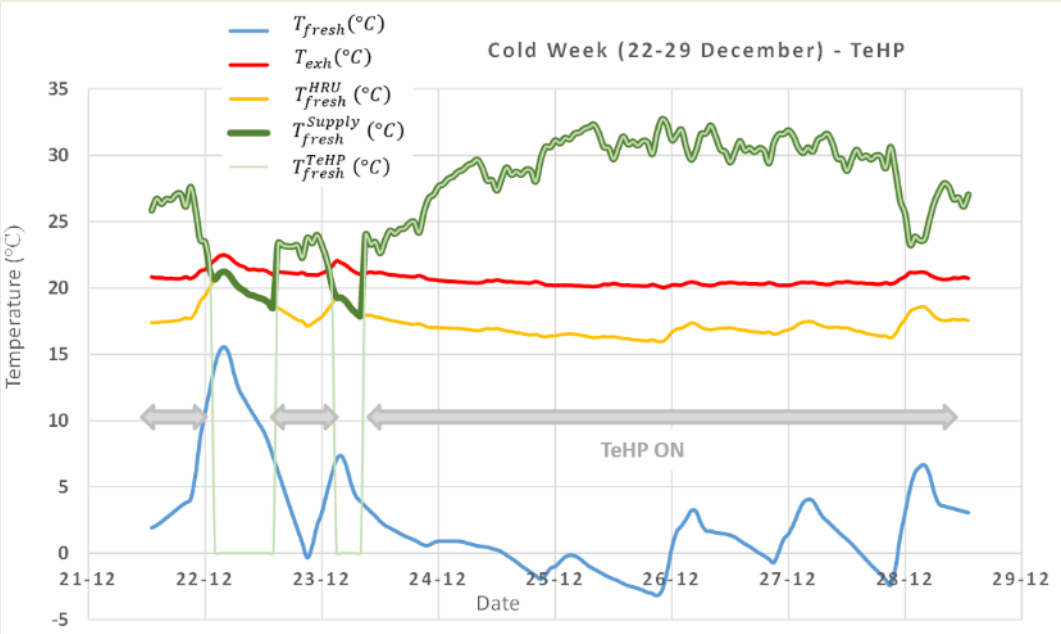

Figure 93. Evolution of the temperature of the dwelling and the TeHP HVAC components one cold week (22-29 December) with four days having ambient temperatures under 0°C.

Passive houses are well known for the weak coupling with the environment, what certainly helps to keep living comfort in wintertime, with the contribution of the internal and solar gains to reduce the heating demand. However, in summertime, the solar gains must be prevented to reduce the risk of overheating.

Figure 94 shows how the indoor temperature evolves in a hot summer week. The windows are programmed to block 80 % of the incident radiation when it exceeds 300 W/m^2, but the internal gains continue to increase the temperature inside and cooling is required 90 % of the time during this week. The morning of the first day (18th of July) the indoor air temperature is 23 °C and, therefore, the TeHP is off and the ventilation supply air temperature (T_{fresh}^{Supply}) is T_{fresh}^{HRU}. The outside temperature reaches a maximum of 28 °C and T_{fresh}^{Supply} rises up to 25 °C, what constitutes another heat gain for the indoor ambient. At a certain point the indoor temperature (T_{exh}) is above 24 °C and the TeHP is then switched on. The DC voltage supply depends again on the building temperature, being higher when the temperature is increased, following Figure 90. The voltage ranges 2.5-3 V and the T_{fresh}^{Supply} is then lowered to 18-20 °C, remainin the indoor air below 24.5 °C. When outside temperature (T_{fresh}) decreases and goes 3 °C below the indoor air, the freecooling mode is activated (if cooling is still required). The direct introduction of outside air refrigerates the indoor ambient. To this aim, the TeHP is turned off and the HRU is shortcut, while the ventilation air flow is increased to 1 ACH. The outside air (16-21 °C) is then directly blown inside the building. The second day (19th of July) the HVAC system operates in a very similar way. The outdoor temperature reaches a maximum of 31 °C and goes below 12 °C at nightime. This low temperature outside makes indoor temperature go under 23 °C and, according to Figure 90, deactive the freecooling mode. The 4th and 5th days (21st and 22nd of July) the weather is very hot with maximum temperatures of 35 °C and night temperatures above 19 °C. The building in this case precise permanent cooling. During the day the TeHP is activated with 5.5-6.5 V and during the night the freecooling is turned on. Under these conditions the HVAC system is demonstrated to guarantee the indoor temperature below 25 °C the whole week.

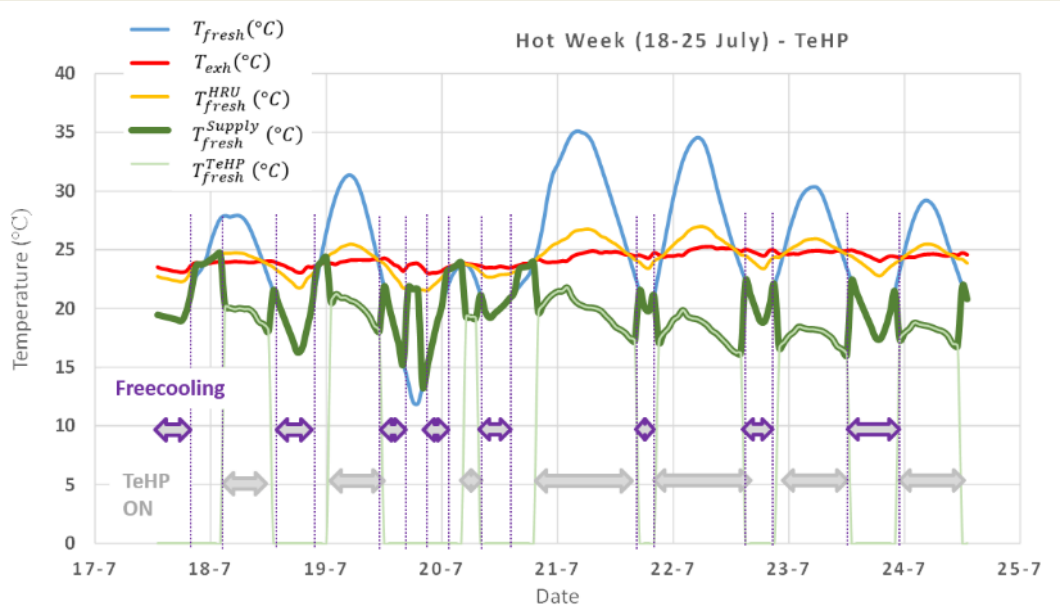

Figure 94. Evolution of the temperature of the dwelling and the HVAC components one hot week (18-25 July) with two days of ambient temperatures close to 35 °C. The figure shows when the TeHP or the freecooling are activated.

5.2. VCHP Results

This section analyzes the same building and weather conditions as in the previous section replacing the TeHP by a VCHP. Figure 95 shows the evolution of the air temperatures in the HVAC system the same cold week as in Figure 93, but, in this case, the ventilation air flow goes through the VCHP when additional heating is required, regulated as shown in Figure 90. The first two days heating is not even needed, with a set point of 20 °C. The following five cold days the VCHP is activated. Given the higher heating capacity, the reaction of the increase of indoor air temperature is quicker. The ventilation incoming air temperature rises to almost 50 °C (as explained in Section 3.3) and the VCHP works 8-12 hours per day. By contrast, the TeHP was constantly on, but with the ability of reducing the heating capacity to a minimum of 100 W. In the case of the VCHP the heating capacity and energy consumption depend on the temperature difference between the heat reservoirs (fresh and exhaust air flows after going through the HRU) following the heat curve [49]. Additionally, this analysis considers two scenarios for the energy performance of the VCHP with two different nominal COPs (section 2.2). The result is that the VCHP operates less time than the TeHP in heating mode and consumes less energy, but presents less regulation capacity and the time in HRU mode is then increased.

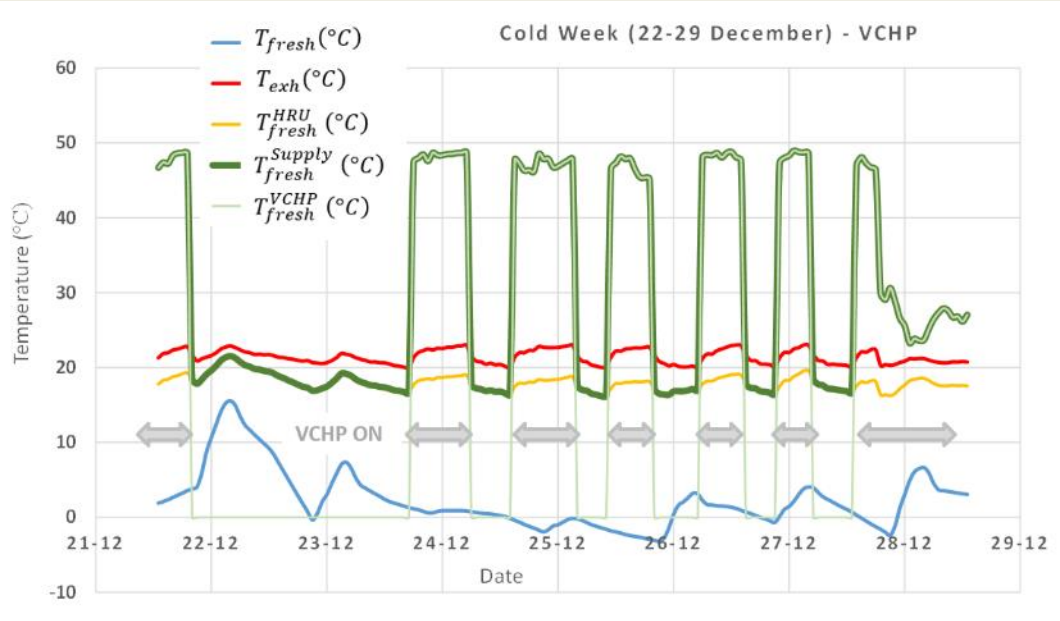

Figure 95. Evolution of the temperatures with the VCHP replacing the TeHP during the cold week. An hysteresis cycle of 20-23°C is set to avoid the intermitent functioning of the VCHP.

Figure 96 shows the same analysis as in Figure 94, replacing the TeHP by the VCHP. The situation is similar as in the previous case, being the fresh air stream cooled by the VCHP. The higher cooling capacity lowers T_{fresh}^{Supply} to a minimum of 10 °C the second day (compared to 17.5 °C same day in Figure 94). This makes the VCHP reach the set point faster, reducing the cooling operating time. As in Figure 94, when outside temperature is 3 °C lower than the temperature inside the building and cooling is required, the freecooling mode is activated.

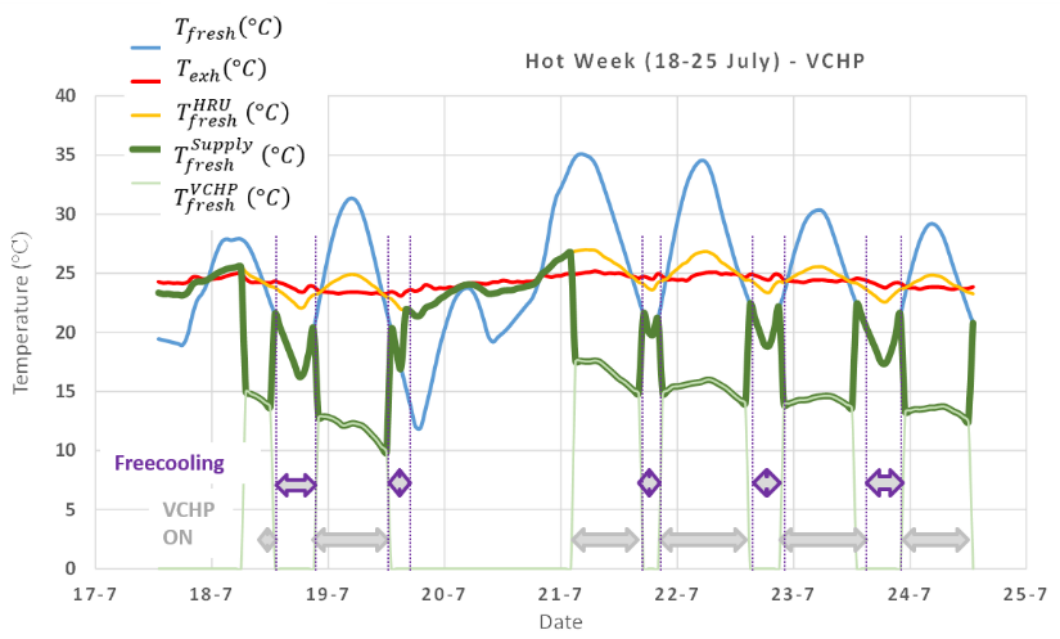

Figure 96. Evolution of the temperatures with the VCHP replacing the TeHP during the hot week. An hysteresis cycle of 25-23°C is set to avoid the intermitent functioning of the VCHP. The figure shows when the VCHP or the freecooling are activated.

5.3. Comparison TeHP vs VCHP

The conclusions of the evolution of the air temperature in the HVAC systems shown in previous sections (5.1 and 5.2) need to be extended to one year, as well as the comparison of the energy balance and the comfort conditions inside the building. As a first deduction of the previous study for extreme weather conditions, both systems guarantee indoor comfort inside the building. Figure 97 reproduces the annual analysis, where a box plot reproduces the range of indoor temperature in both: winter and summer seasons. The average indoor temperature in wintertime is very similar in both cases: 21.3 °C with the VCHP and 21.4 °C with the TeHP. However, the regulation is demonstrated to be more precise in this last case, thanks to the wide range of heating capacity regulation. The interquartile range is below 0.6 °C, while in the case of the VCHP it is 1.4 °C, which is mainly due to the higher hysteresis cycle that these systems normally employ. The temperature never goes below 20 °C in none of the two cases, and maximum temperatures reached inside the dwelling go up to 24.4 - 24.8 °C due to solar gains in sunny days.

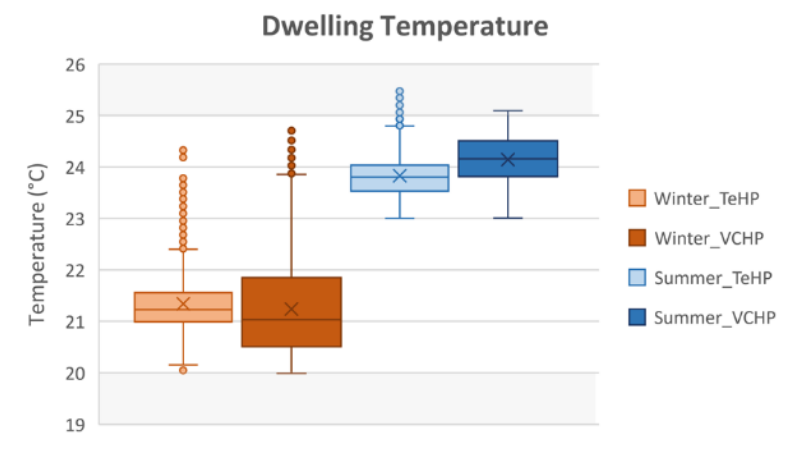

Figure 97. Comparison of the indoor temperature during winter and summer seasons with the TeHP and the VCHP HVAC systems.

In summertime the minimum indoor temperature is 23 °C in both cases. The temperature interquartile range is still lower in the case of the TeHP, but closer to the VCHP (TeHP: 0.5 °C, VCHP: 0.8 °C). The regulation has shown to be more precise with the TeHP, maintaining the third quartile below 24.1 °C, compared with 24.6 °C in the case of the VCHP. However, the analysis reveals that during 2 % of the studied period the temperature goes above 25 °C in the TeHP case study, what indicates a lack of cooling capacity at some certain points.

The efficiency of the heat pumps is calculated with Eq. (9):

$$COP_{c/h} = \frac{\dot{Q}_{c/h}^{TeHP/VCHP}}{\dot{W}^{TeHP/VCHP} + \dot{W}_{fan}^{TeHP/VCHP+HRU+Air\ ducts}} \quad (9)$$

The Coefficient of Performance relates the cooling or heating capacity with the energy consumption. In this case the electric consumption not only considers the energy consumed by the heat pumps (TeHP or VCHP) but also includes the electric consumption of the fans, that blow the incoming and outgoing air flow through the air ducts/filters/grills, the HRU and the heat exchangers TEM-air of the TeHP (and the condenser/evaporator in the case of the VCHP), calculated as explained in section 3. This COP varies depending on the air temperature in the air ducts, being higher when the temperature gap between incoming and outgoing air streams is lower. In the case of the TeHP it also depends on the voltage, presenting higher COP with lower voltages, which is required (according to the proposed regulation) when temperature gaps between air streams is lower as well. For heating the COP_h^{TeHP} ranges 1 - 2 with an average value of 1.4. With vapor compression technology, the COP_h^{VCHP} is at least 1 unit higher: 2.2 - 2-8, when considering a low performance system, and could go up to a range of 4 - 5 for a high performance system (see Figure 98).

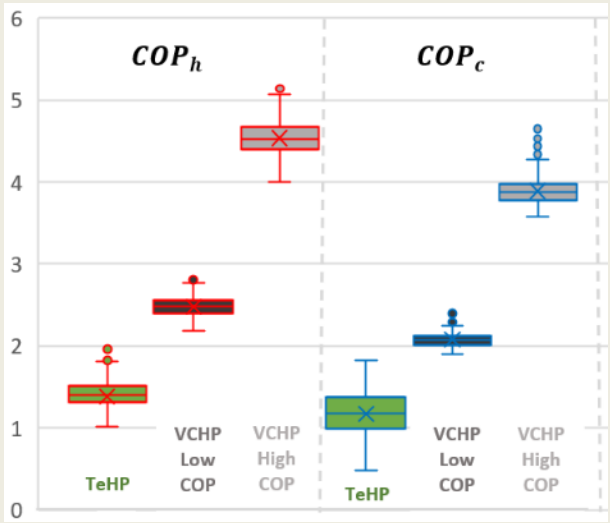

Figure 98. Comparison of the COP of the TeHP and VCHP in heating and cooling mode.

When cooling, the less efficient VCHP has an average COP_c^{VCHP} value of 2.1, and 3.9 in the case of the efficient system; while the COP_c^{TeHP} of the TeHP presents a value range that goes from 0.5 to 1.7. This performance is higher than expected, with an average value of 1.2. The reason behind is that most of the operating time it works with low voltage values ranging 2-6 V (with occasional 8 V peaks). This part-load but constant operating mode meets the dwelling cooling demand, as previously shown, with an acceptable energy efficiency. Moreover, this modulated cooling capacity reduces the condensed water (just 2.7 l during the summer period), being more effective in terms of air sensible cooling, compared with the VCHP, that condenses up to 107.4 l of water during the summer season. This fact is reflected in the results shown in Table 16: the VCHP works 30 % less time in cooling mode (247 h) with respect to the TeHP, but the energy saving is only 15 % in the case of the low COP VCHP with respect to the TeHP, and 46% for the high COP VCHP. However, this conclusion only stands when

dehumidification is not specifically required. In such a case the TeHP can contribute to dehumidifying but the regulation must be modified accordingly and the energy balance would be different. In heating mode, the VCHP works 82 % less time (2858 h) than the TeHP and the energy savings are between 57 % (low COP) and 74 % (high COP).

Table 16. Comparison of annual energy consumption and operating time for the TeHP and VCHP HVAC systems in different working modes: heating, cooling, freecooling and HRU.

		TeHP	VCHP_LowCOP	VCHP_HighCOP
Heating	*Operating Time (h)*	3,480	622	622
	Consumption (kWh)	662.0	284.7	170.4
Cooling	*Operating Time (h)*	811	564	564
	Consumption (kWh)	190.0	162.5	103.4
Freecooling	*Operating Time (h)*	733	351	351
	Consumption (kWh)	72.2	34.6	34.6
HRU	*Operating Time (h)*	3,736	7,223	7,223
	Consumption (kWh)	218.3	422.0	422.0
TOTAL	*Consumption (kWh)*	1,143.2	903.4	730.4

Additionally, these high relative saving values for heating and cooling modes are not so significant in the overall one-year energy balance, since the HVAC system continues working providing ventilation with 0.54 ACH so, less time of heating or cooling modes implies more time operation in HRU mode. The total energy consumption of the TeHP HVAC system is 1143.2 kWh, which is reduced by 20.9 % in the case of VCHP with low COP and 36.1 % in the case of VCHP with a high COP.

5.4. Integration of RES: PV production

Passive houses have a limited energy demand and are intended to produce their own energy, as much as possible, from renewable energy sources on site or nearby. In this context, minor inefficiencies of the HVAC system may be easily compensated by a slight increase of local renewable energies production. This research work includes the analysis of the PV production on the roof of the building. The calculations (Section 3.5) indicate that in Pamplona, the electric production of a Kyocera PV panel [41] can reach 1350 equivalent hours, what means that three panels (0.75 kWp) may produce more energy than the electric consumption of the HVAC system with a VCHP (see Figure 99) one year long. The single addition of one PV panel (1 kWp) compensates the lower efficiency of the TeHP compared with the VCHP. More

information of the monthly energy balance, comparing the PV production and electric consumption of both, the TeHP and the VCHP can be found in the additional documentation.

However, this PV facility do not produce the energy when the HVAC system requires, so most of the time we will find that either the energy consumption exceeds the power generation, or the PV production is greater than the consumption. The price of the energy delivered to grid is usually lower than the kWh taken from the grid. Considering the simulated hourly HVAC consumption profile and the PV production profile one year long, assuming that the price of the kWh consumed from the grid is 0.14 €/kWh and 0.04 €/kWh the energy produced and delivered to the grid, the annual economic balance remains as shown in Figure 99 (right figure) and it is further explained in the additional material. 4 PV panels (1 kWp) contribute to have a 0 € balance by the end of the year for the cost of the energy in the case of the VCHP with the high COP. One more panel (1.25 kWp) is required to compensate the energy cost when the VCHP has a low COP, and one single additional panel (1.5 kWp) meets the cero energy cost when replacing the VCHP by a TeHP. This, in terms of life cycle cost, means that the cost of the TeHP is competitive from an economic perspective with a price that results of subtracting the cost of 1-2 panels (150-300 €) to the cost of the VCHP. Moreover, the robustness of the TeHP could entail additional maintenance cost reductions that are beyond the scope of the present research.

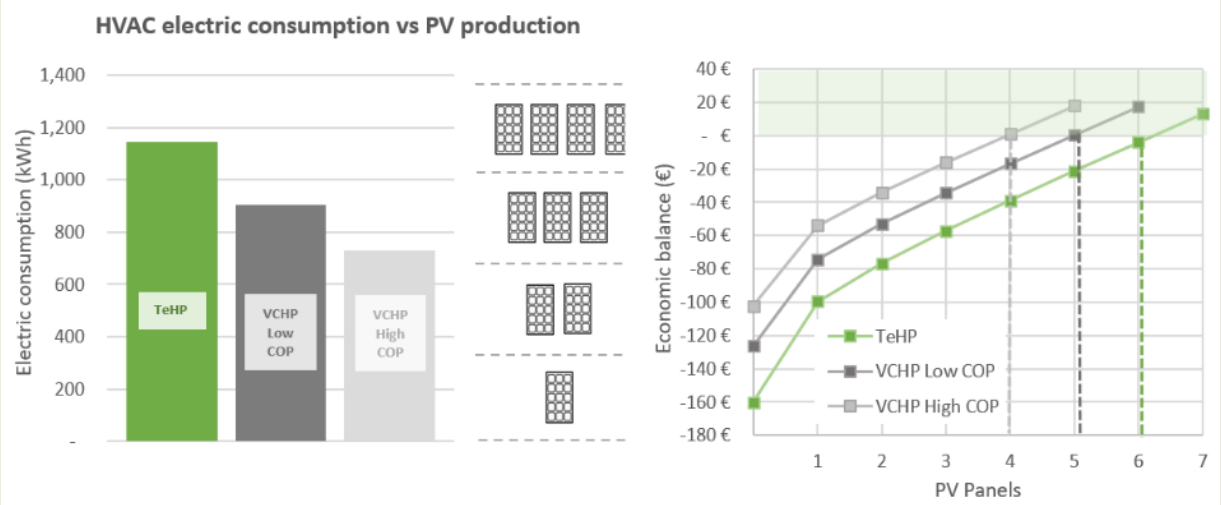

Figure 99. Comparison of the energy consumption of the TeHP and the VCHP based HVAC systems and the energy production of PV panels on the roof. Left figure: energy consumption and production in kWh, the figure shows that 1 kWp (four panels) may produce the energy consumed by the HVAC with the TeHP, while 0.75kWp (three panels) compensate the energy consumed by the HVAC with the VCHP. Right figure: one year energy cost balance considering the PV production and the hourly consumption profile.

This research represents a step forward for thermoelectrics, as they can find a potential niche application in the heating and cooling of individual single-family apartments (50-100 m^2) of passive house certified buildings, where the peak heating demand is calculated to be below 10 W/m^2; and no specific dehumidification is required (maximum indoor absolute humidity below 12 g/Kg more than 90% of summertime). The objective of the present study is the evaluation

of thermoelectric heat pumps as a potential market alternative to HVAC these indoor spaces, restricted to the application of individual systems.

6. Conclusions

This research work demonstrates the reliability of a thermoelectric air-to-air heat pump that, integrated with a double flux ventilation system and a heat recovery unit, provides ventilation (0.54 - 1 ACH), heating and cooling for a 74.3 m^2 Passive House certified dwelling in Pamplona (Spain) consuming 1143.2 kWh/y (15.3 kWh/m^2y) of electricity. The results show that:

1) Given the low specific energy demand of passive houses, thanks to the highly isolated envelope, the indoor ambient may be conditioned by only raising or lowering the temperature of the incoming air flow.

2) The thermoelectric heat pump permits a wide operation range (5 - 100 % regulation) by controlling the voltage of the DC supply, which keeps indoor air within the comfort range very accurately (20 - 23 °C in winter and 23 - 25 °C in summer).

3) The COP ranged between 1 - 2 for heating and 0.5 - 1.7 for cooling.

This thermoelectric heat pump has been compared with a small vapor compression heat pump unit with a low and a high COP (2.5 - 4.5 for heating and 2.2 - 4 for cooling). The study shows that:

4) Vapor compression heat pumps reduce the operation time (82 % in heating mode and 30 % in cooling mode) and improves the overall efficiency (20.9 % with the low COP vapor compression heat pump and 36.1 % with the high COP).

5) The energy saving may be easily compensated with the production of 1 PV panel (250 Wp) and, in economic terms, with 1 or 2 PV panels per dwelling (250 - 500 Wp): 1 in case the price for the kWh imported from the grid is similar to the kWh exported, and 2 when the imported kWh is 0.14 € and 0.04 € the kWh exported.

The results presented in this paper demonstrate the great potential of the use of TEMs as a breakthrough and cost-effective technology to air condition low energy demand buildings, with a peak heating demand below 10 W/m^2. The refrigerant-free technology, the compactness, and the silent operation, together with the potentially lower costs and the integrability with PV facilities (that would reduce the extra 10 % electric consumption of the TeHPs considered in this paper for the AC-DC conversion and the 10 % electric losses for the DC-AC conversion in the PV facility) outweigh the additional energy consumption, when comparing its performance with vapor compression technology.

Acknowledgements

The authors would like to thank the public construction company NASUVINSA for the detailed information of the 21 dwellings Passive house certified residential building case study and the great interest in the outcomes of this investigation.

References

[1] European Commission, The European Green Deal, Eur. Comm. 53 (2019) 24. https://doi.org/10.1017/CBO9781107415324.004.

[2] EU, Directive 2010/31/EU of the European Parliament and of the Council of 19 May 2010 on the energy performance of buildings (recast), Off. J. Eur. Union. (2010) 13–35. https://doi.org/10.3000/17252555.L_2010.153.eng.

[3] EU, Directive (EU) 2018/844 of the European Parliament and of the Council of 30 May 2018 amending Directive 2010/31/EU on the energy performance of buildings and Directive 2012/27/EU on energy efficiency, Off. J. Eur. Union. 156 (2018) 75–91. https://eur-lex.europa.eu/eli/dir/2018/844/oj.

[4] EU, Directive 2012/27/EU of the European Parliament and of the Council of 25 October 2012 on energy efficiency (EED), (2012) 1–56. https://ec.europa.eu/energy/topics/energy-efficiency/targets-directive-and-rules/energy-efficiency-directive_en.

[5] Renovation Wave, (n.d.). https://ec.europa.eu/energy/topics/energy-efficiency/energy-efficient-buildings/renovation-wave_en (accesed July 2, 2021).

[6] K. Dennis, Environmentally Beneficial Electrification: Electricity as the End-Use Option, Electr. J. 28 (2015) 100–112. https://doi.org/10.1016/j.tej.2015.09.019.

[7] T. Nowak, Heat Pumps: Integrating technologies to decarbonise heating and cooling, (2018) 1–86. https://www.ehpa.org/fileadmin/user_upload/White_Paper_Heat_pumps.pdf (accesed July 5, 2021).

[8] P. Cuce, S. Riffat, A comprehensive review of heat recovery systems for building applications, Renew. Sustain. Energy Rev. 47 (2015) 665–682. https://doi.org/10.1016/j.rser.2015.03.087.

[9] L. Müller, T. Berker, Passive House at the crossroads: The past and the present of a voluntary standard that managed to bridge the energy efficiency gap, Energy Policy. 60 (2013) 586–593. https://doi.org/10.1016/j.enpol.2013.05.057.

[10] PHI, Passipedia: Passive House concepts, (n.d.). https://passipedia.org/ (accesed July 5, 2021).

[11] S. Guillén-Lambea, B. Rodríguez-Soria, J.M. Marín, Review of European ventilation strategies to meet the cooling and heating demands of nearly zero energy buildings

(nZEB)/Passivhaus. Comparison with the USA, Renew. Sustain. Energy Rev. 62 (2016) 561–574. https://doi.org/10.1016/j.rser.2016.05.021.

[12] K. Irshad, K. Habib, F. Basrawi, N. Thirumalaiswamy, R. Saidur, B. Saha, Thermal comfort study of a building equipped with thermoelectric air duct system for tropical climate, Appl. Therm. Eng. 91 (2015) 1141–1155. https://doi.org/10.1016/j.applthermaleng.2015.08.077.

[13] D. Zhao, G. Tan, A review of thermoelectric cooling: Materials, modeling and applications, Appl. Therm. Eng. 66 (2014) 15–24. https://doi.org/10.1016/j.applthermaleng.2014.01.074.

[14] J. Sarkar, S. Bhattacharyya, Application of graphene and graphene-based materials in clean energy-related devices Minghui, Arch. Thermodyn. 33 (2012) 23–40. https://doi.org/10.1002/er.

[15] S.M. Pourkiaei, M.H. Ahmadi, M. Sadeghzadeh, S. Moosavi, F. Pourfayaz, L. Chen, M.A. Pour Yazdi, R. Kumar, Thermoelectric cooler and thermoelectric generator devices: A review of present and potential applications, modeling and materials, Energy. 186 (2019) 115849. https://doi.org/10.1016/j.energy.2019.07.179.

[16] L. Shen, X. Pu, Y. Sun, J. Chen, A study on thermoelectric technology application in net zero energy buildings, Energy. 113 (2016) 9–24. https://doi.org/10.1016/j.energy.2016.07.038.

[17] A. Zuazua-Ros, C. Martín-Gómez, E. Ibáñez-Puy, M. Vidaurre-Arbizu, Y. Gelbstein, Investigation of the thermoelectric potential for heating, cooling and ventilation in buildings: Characterization options and applications, Renew. Energy. 131 (2019) 229–239. https://doi.org/10.1016/j.renene.2018.07.027.

[18] Z. Liu, L. Zhang, G. Gong, H. Li, G. Tang, Review of solar thermoelectric cooling technologies for use in zero energy buildings, Energy Build. 102 (2015) 207–216. https://doi.org/10.1016/j.enbuild.2015.05.029.

[19] I. Sarbu, A. Dorca, A comprehensive review of solar thermoelectric cooling systems, Int. J. Energy Res. 42 (2018) 395–415. https://doi.org/10.1002/er.3795.

[20] C. Wang, C. Calderón, Y. Wang, An experimental study of a thermoelectric heat exchange module for domestic space heating, Energy Build. 145 (2017) 1–21. https://doi.org/10.1016/j.enbuild.2017.03.050.

[21] Y. Luo, L. Zhang, Z. Liu, J. Wu, Y. Zhang, Z. Wu, Numerical evaluation on energy saving potential of a solar photovoltaic thermoelectric radiant wall system in cooling dominant climates, Energy. 142 (2018) 384–399. https://doi.org/10.1016/j.energy.2017.10.050.

[22] D. Zhao, X. Yin, J. Xu, G. Tan, R. Yang, Radiative sky cooling-assisted thermoelectric cooling system for building applications, Energy. 190 (2020) 116322. https://doi.org/10.1016/j.energy.2019.116322.

[23] L. Shen, X. Pu, Y. Sun, J. Chen, A study on thermoelectric technology application in net zero energy buildings, Energy. 113 (2016) 9–24. https://doi.org/10.1016/j.energy.2016.07.038.

[24] S. Cheon, H. Lim, J. Jeong, Applicability of thermoelectric heat pump in a dedicated outdoor air system, Energy. 173 (2019) 244–262. https://doi.org/10.1016/j.energy.2019.02.012.

[25] Y. Kim, J. Ramousse, G. Fraisse, P. Dalicieux, P. Baranek, Optimal sizing of a thermoelectric heat pump (THP) for heating energy-efficient buildings, Energy Build. 70 (2014) 106–116. https://doi.org/10.1016/j.enbuild.2013.11.021.

[26] D. Astrain, P. Aranguren, A. Martínez, A. Rodríguez, M.G. Pérez, A comparative study of different heat exchange systems in a thermoelectric refrigerator and their influence on the efficiency, Appl. Therm. Eng. 103 (2016). https://doi.org/10.1016/j.applthermaleng.2016.04.132.

[27] T. Han, G. Gong, Z. Liu, L. Zhang, Optimum design and experimental study of a thermoelectric ventilator, Appl. Therm. Eng. 67 (2014) 529–539. https://doi.org/10.1016/j.applthermaleng.2014.03.073.

[28] T. Li, G. Tang, G. Gong, G. Zhang, N. Li, L. Zhang, Investigation of prototype thermoelectric domestic-ventilator, Appl. Therm. Eng. 29 (2009) 2016–2021. https://doi.org/10.1016/j.applthermaleng.2008.10.007.

[29] P. Aranguren, S. Díaz de Garayo, A. Martínez, M. Araiz, D. Astrain, Heat pipes thermal performance for a reversible thermoelectric cooler-heat pump for a nZEB, Energy Build. 187 (2019) 163–172. https://doi.org/10.1016/j.enbuild.2019.01.039.

[30] L. Shen, Z. Tu, Q. Hu, C. Tao, H. Chen, The optimization design and parametric study of thermoelectric radiant cooling and heating panel, Appl. Therm. Eng. 112 (2017) 688–697. https://doi.org/10.1016/j.applthermaleng.2016.10.094.

[31] Prototype of an air to air thermoelectric heat pump integrated with a double flux mechanical ventilation system for passive houses, Appl. Therm. Eng. (2021). https://doi.org/https://doi.org/10.1016/j.applthermaleng.2021.116801.

[32] PHI, Sofware: Passive House Planning Package (PHPP), (n.d.). https://passivehouse.com/04_phpp/04_phpp.htm (accesed July 5, 2021).

[33] Ministerio de Fomento, Documento Básico HS Salubridad 2019, Septiembre. 2013 (2007) 1–129. http://www.arquitectura-tecnica.com/hit/Hit2016-2/DBHE.pdf (accesed June 2, 2021).

[34] Z. Comfoair, Z. Comfoair, Z. Comfoair, Zehnder ComfoAir 200 -Technical Specifications, n.d. https://www.international.zehnder-systems.com/products-and-systems/comfosystems/zehnder-comfoair-200 (accesed June 2, 2021).

[35] AENOR, Prestaciones térmicas de los edificios. Cálculo del uso de energía para calefacción de los espacios (UNE-EN_ISO_13790:2004).

[36] M. Kummert, TYPE 56 - TRNSYS, Program. 5 (2007) 1–11. http://web.mit.edu/parmstr/Public/Documentation/06-MultizoneBuilding.pdf (accesed May 12, 2021).

[37] METEONORM, Weather database. https://meteonorm.com/en/product/meteonorm-software (accesed May 12, 2021).

[38] J. Schnieders, W. Feist, L. Rongen, Passive Houses for different climate zones, Energy Build. 105 (2015) 71–87. https://doi.org/10.1016/j.enbuild.2015.07.032.

[39] D. Diaz de Garayo, S.; Martínez, A.; Aranguren, P.; Astrain, Prototype of an air to air thermoelectric heat pump integrated with a double flux mechanical ventilation system for passive houses, Appl. Therm. Eng. (2021). https://doi.org/https://doi.org/10.1016/j.applthermaleng.2021.116801.

[40] S.B. Riffat, G. Qiu, Comparative investigation of thermoelectric air-conditioners versus vapour compression and absorption air-conditioners, 24 (2004) 1979–1993. https://doi.org/10.1016/j.applthermaleng.2004.02.010.

[41] Kyocera Solar, PV Pannel KD250 GH-4FB2. https://global.kyocera.com/prdct/solar/ (accessed May 12, 2021).

[42] TRNSYS, Program. 5 (2007) 1–11. http://web.mit.edu/parmstr/Public/Documentation/06-MultizoneBuilding.pdf. (accessed May 12, 2021).

[43] TRNSYS, TESS COMPONENT LIBRARIES Volume 7 – The Hydronic Component Library, TRNSYS17 Doc. (2014) 1–79. http://www.trnsys.de/download/en/tesslibary_shortinfo_en.pdf (accessed May 12, 2021).

[44] TETechnology, Hp-127-1.4-1.15-71, (2018) 1–7. https://tetech.com/wp-content/uploads/2013/11/HP-127-1.4-1.15-71.pdf (accessed May 12, 2021).

[45] A. Martinez, S. Díaz, D. Garayo, P. Aranguren, M. Araiz, L. Catal, Simulation of thermoelectric heat pumps in nearly zero energy buildings : Why do all models seem to be right ?, 235 (2021). https://doi.org/10.1016/j.enconman.2021.113992.

[46] Y. Cai, S.J. Mei, D. Liu, F.Y. Zhao, H.Q. Wang, Thermoelectric heat recovery units applied in the energy harvest built ventilation: Parametric investigation and performance optimization, Energy Convers. Manag. 171 (2018) 1163–1176. https://doi.org/10.1016/j.enconman.2018.06.058.

[47] Software: EES - Engineering Equation Solver. http://fchartsoftware.com/ees/. (accessed April 2, 2021).

[48] P. Aranguren, S. Díaz de Garayo, A. Martínez, M. Araiz, D. Astrain, Heat pipes thermal performance for a reversible thermoelectric cooler-heat pump for a nZEB, Energy Build. 187 (2019) 163–172. https://doi.org/10.1016/j.enbuild.2019.01.039.

[49] Air-Conditioning and Refrigeration Institute (ARI), Standard for Performance Rating of Commercial and Industrial Unitary Air-Conditioning. Standard 340-360-2019. https://www.ahrinet.org/App_Content/ahri/files/STANDARDS/AHRI/AHRI_Standard_340-360_I-P_2019.pdf (accessed May 7, 2021).

[50] N. Karali, N. Shah, W.Y. Park, N. Khanna, C. Ding, J. Lin, N. Zhou, Improving the energy efficiency of room air conditioners in China : Costs and benefits, Appl. Energy. 258 (2020) 114023. https://doi.org/10.1016/j.apenergy.2019.114023.

[51] A. Picallo-Perez, J.M. Sala, M. Odriozola-Maritorena, J.M. Hidalgo, I. Gomez-Arriaran, Ventilation of buildings with heat recovery systems: Thorough energy and exergy analysis for indoor thermal wellness, J. Build. Eng. 39 (2021) 102255. https://doi.org/10.1016/j.jobe.2021.102255.

[52] Trnsys, Mathematical Reference (Volume 4). http://web.mit.edu/parmstr/Public/TRNSYS/04-MathematicalReference.pdf (accessed April 7, 2021).

Annual energy performance of a thermoelectric heat pump combined with a heat recover unit to HVAC one passive house dwelling

- Supplementary material –

The present document includes some additional figures to complement the content of the original paper. In particular, three aspects have been added:

Sup. 1. Passive and active thermal behavior of the building.

Figure S1 shows the evolution of indoor temperature (in red) under ambient temperature and solar radiation with no heating or cooling, during a cold week of wintertime. On Monday (22nd of December) and Tuesday (23rd of December) the indoor temperature rises up to 17.5 °C due to solar gains, but the following 5 days the ambient temperature (in blue) goes below 0 °C and there is no solar radiation, so indoor temperature continues falling down to 10.5 °C.

When the heat pump integrated with the ventilation system is activated, the indoor temperature keeps above 20 °C. In the case of the TeHP, the supply air temperature is precisely regulated to keep indoor temperature stable working 24 h/day during these five cold days. In the case of the VCHP, it works 10-12 h/day and indoor temperature ranges 20-23 °C, following the hysteresis cycle programed and described in section 3.3.

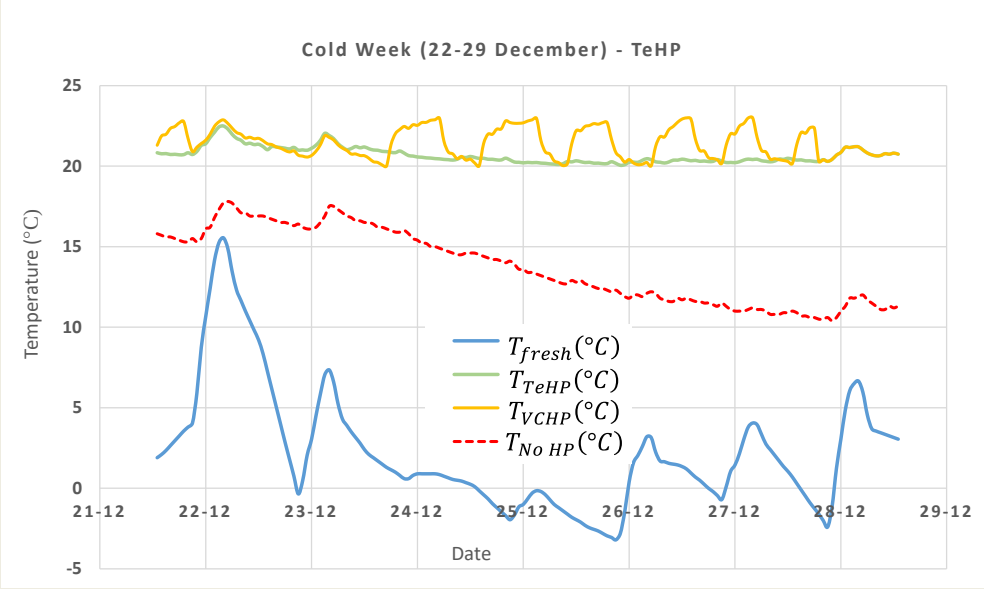

Figure S100. Comparison of the ambient temperature and indoor temperature in three scenarios: TeHP, VCHP and no HP one a cold week (22-29 December). The red line indicates the thermal behaviour of the building with ventilation but no active system to heat indoor ambient.

Next Fig. S2 shows the same comparison in a hot week of summertime. The rise of ambient temperature up to 35 °C two consecutive days (21st and 22nd of July) with minimum temperatures of 20 °C makes indoor temperature go up to 28 °C, while it keeps below 25 °C if the heat pump (any of both, the TeHP or the VCHP) is activated.

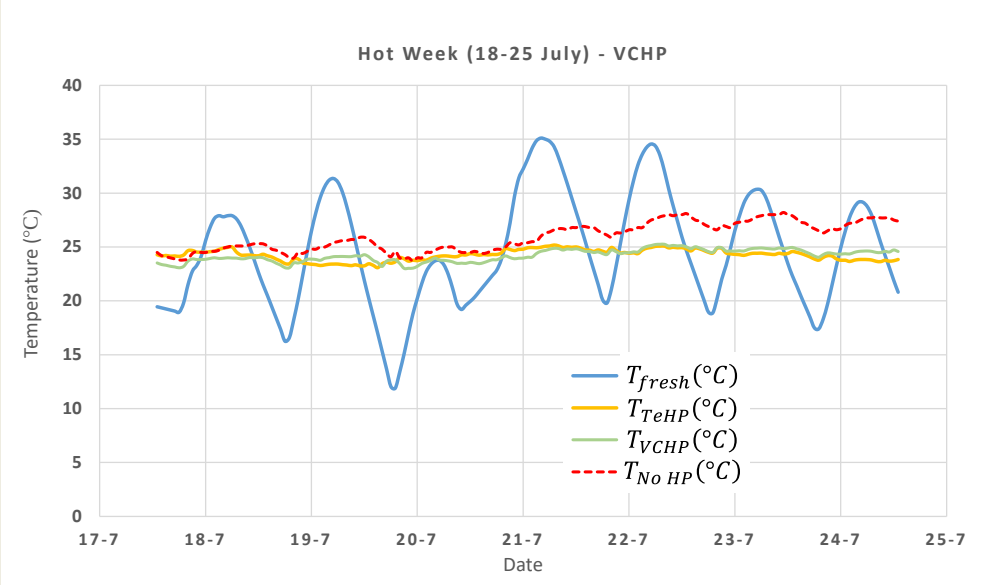

Figure S101. Comparison of the ambient temperature and indoor temperature in three scenarios: TeHP, VCHP and no HP one a hot week (18-25 July). The red line indicates the thermal behaviour of the building with ventilation but no active system to cool indoor ambient.

Sup. 2. Dynamic evolution of the electric consumption of the heat pumps compared with the PV production in a cold and a hot week of the year.

In coherence with Fig. S1, Fig. S3 shows the electric consumption of the TeHP and both, the VCHP with the high and low COP, during same cold week (22nd -29th of December). This figure clearly shows the working time of the heat pumps and the comparison of the electric consumption with the PV production that, in this case, is low due to four foggy days.

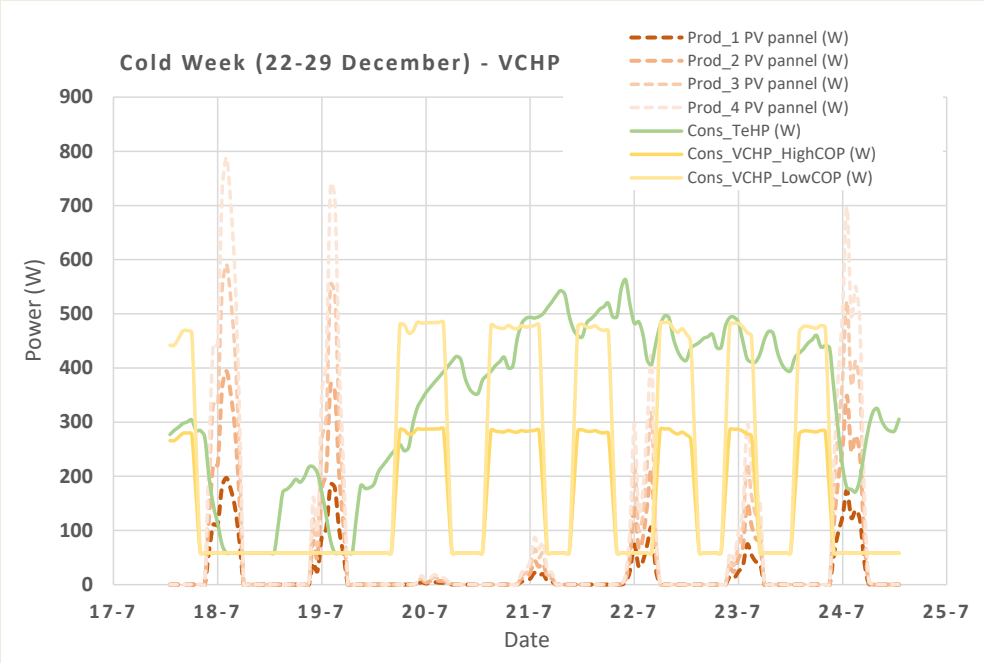

Figure S102. Comparison of the power generated in a PV facility on the roof with 1, 2, 3 or 4 PV pannels, with the energy consumped by the TeHP, the VCHP with the high COP and th VCHP with the low COP one a cold week (22-29 December).

However, during the hot week, the PV production is clearly increased, reaching 900 W in the case of the 4 panels (1 kWp) PV facility. In this week, the heat pumps need to work during daytime and freecooling is activated during nighttime. This 4 panel PV facility outweighs the electric consumption of the TeHP, in the one-year-balance, as it can be seen in next chapter.

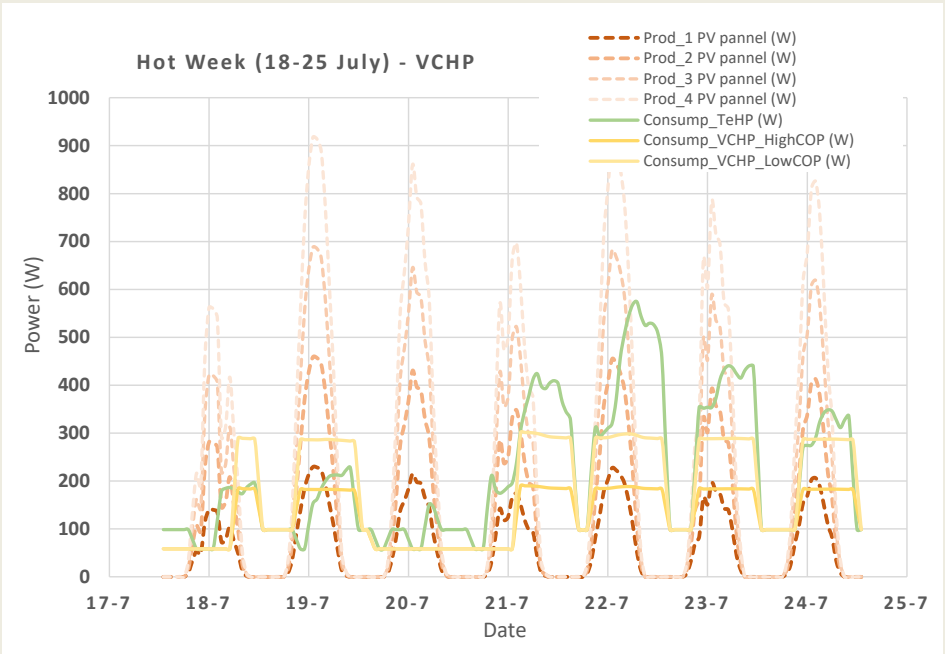

Figure S103. Comparison of the power generated by a PV facility on the roof with 1, 2, 3 or 4 PV pannels, with the energy consumped by the TeHP, the VCHP with the high COP and th VCHP with the low COP one a hot week (18-25 July).

Sup. 3. Monthly energy and economic balance of the HVAC consumption and the PV production:

This section specifies the monthly energy balance of the electric consumption of the TeHP, the VCHP with the high and the low COP, and the PV facility with 1, 2, 3 and 4 panels.

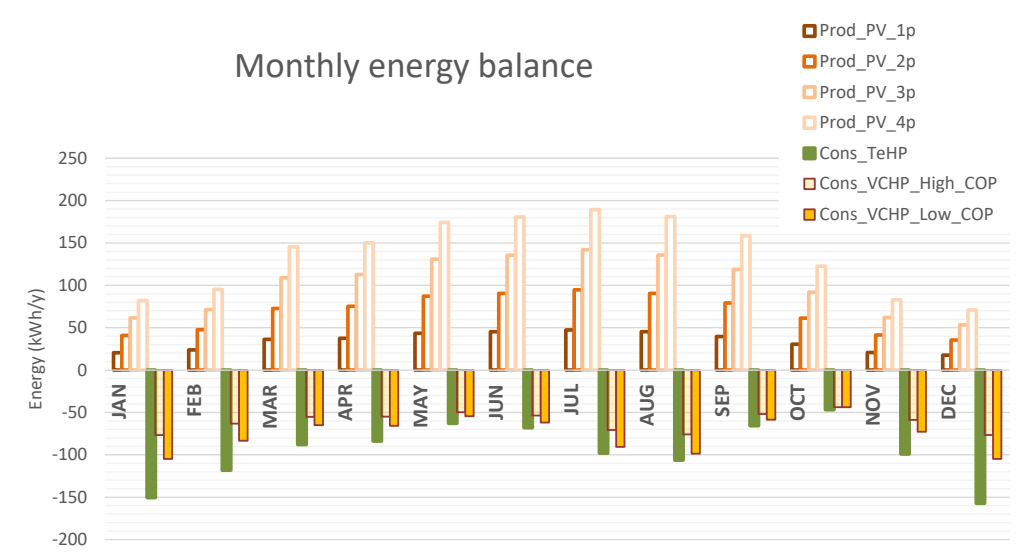

Figure S104. Comparison of the energy generated by a PV facility on the roof with 1, 2, 3 or 4 PV pannels, with the energy consumped by the TeHP, the VCHP with the high COP and the VCHP with the low COP.

Fig. S5 shows the monthly overal energy consumption and production in kWh. Next Fig. S6 analyzes the fact that the energy production of the PV panels does not happen when it is required by the TeHP. This means that, at certain points, it is necessary to consume electricity from the grid, or deliver electricity to the grid, when the PV production exceeds the electric consumption of the heat pump. Fig. S6 shows this balance for the TeHP and a 4 panels PV facility, representing the energy simultaneusly produced by the PV facility and consumed by the TeHP (in green), while red colour represents the electricity consumed from the grid and blue colour the electricity delivered to the grid.

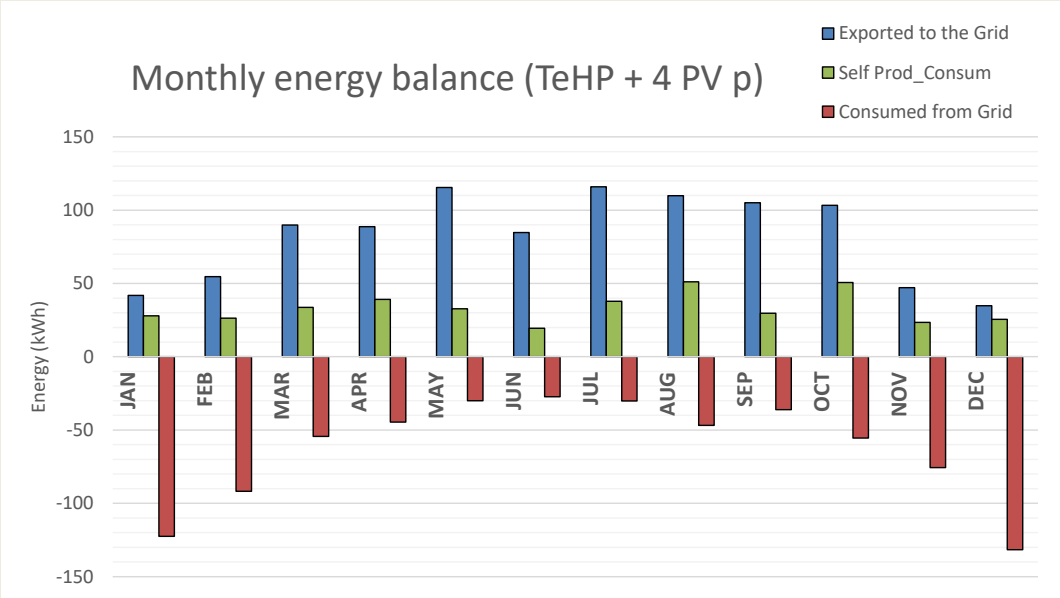

Figure S105. Monthly energy balance of the energy consumed by the TeHP and a PV facility on the roof with 4 PV pannels, considering the energy produced and silmultaneusly consumed by the TeHP (green colour), the energy imported from the grid (red) and energy exported to the grid (blue).

The electricity consumed from the grid and delivered to grid should be compensated by the end of the year. In this case, with 4 PV panels, the electricity delivered to the grid exceeds in 245 kWh the electricity consumed by the TeHP.

Finally, as normally the energy consumed from the grid is more expensive than the energy delivered to the grid, Fig. S7 shows the economic balance of the energy costs assuming 0.14 c€/kWh for the energy taken from the grid and 0.04 c€/kWh for the energy delivered to the grid , increasing, in this case, the number of PV panels from 4 to 6, in order to compensate this difference in the energy price.

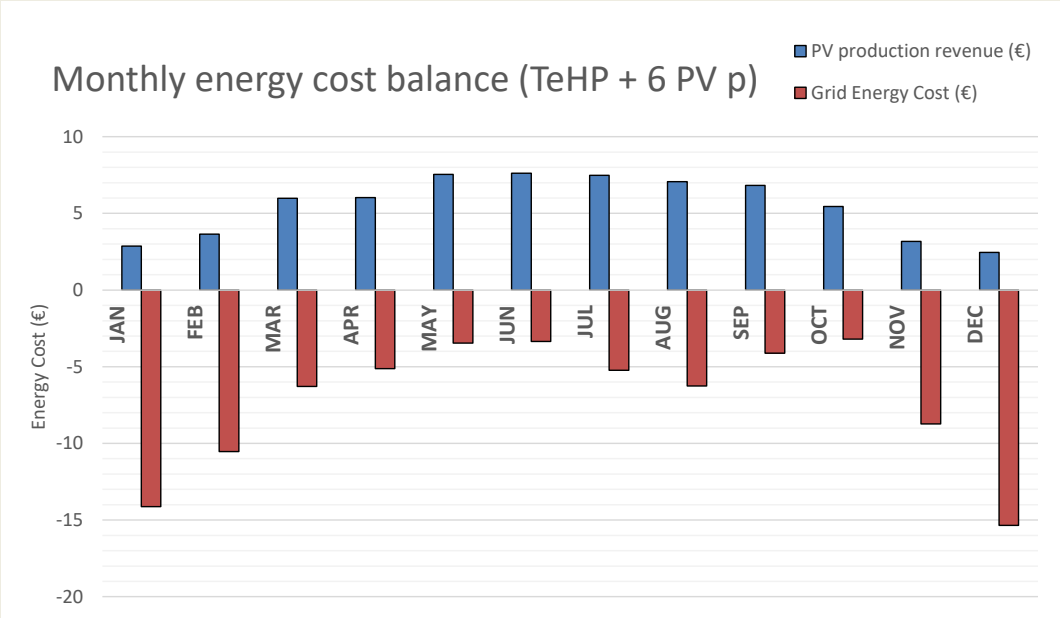

Figure S106. Monthly energy cost balance of the energy consumed by the TeHP and a PV facility on the roof with 6 PV pannels, considering the revenue due the energy exported to the grid (blue colour, 0.04 c€/kWh) and the cost of the energy imported from the grid (red colour – 0.14 c€/kWh).

Chapter 6. Conclusions and future lines

This last chapter summarizes the most relevant conclusions and results obtained in the studies and developments performed during the attainment of the present Ph. D. dissertation, in which one air-to-air thermoelectric heat pump has been developed and optimized for the air-conditioning of a PH dwelling.

Section 6.1 includes the general conclusions of the thesis, which have been divided into four subsections that do not strictly correspond to the published articles, but to the following four research activities: in the case of Subsection 6.1.1 the conclusions derive from the state of the art, in Subsection 6.1.2 the conclusions correspond to the analysis of the thermal characterization of the heat exchangers installed between the TEM and the air stream, while 6.1.3 focuses on the TeHP performance optimization and, finally, conclusions derived from the integration of the TeHP in a PH pilot case are presented in Subsection 6.1.4.

Afterwards, Section 6.2 comprises the recommendations for future works intended to continue with this research line.

Finally, Section 6.3 presents the most relevant scientific contributions made during the time devoted to the fulfillment of the is Ph. D. dissertation, including not only results directly related to the thesis, but also other contributions performed during the same period.

6.1. Conclusions

The main conclusions reached after the completion of this Ph. D. dissertation are described below, starting with those derived from the state of the art, and followed by the outcomes of the investigation of the TEM-air HE, the TeHP optimization and TeHP integration in a pilot case. Moreover, the attainment of the different specific objectives of the thesis is also pointed out.

6.1.1. Conclusions derived from the state of the art

The conclusions relative to the state of the art address the research necessities derived from the bibliographic review, which have led to the development of the present Ph. D. dissertation.

1. Buildings will demand less heating per square meter in the future, with a lower heating load, due to renovated or new better insulated and air-sailed envelopes. Moreover,

they will require more cooling, due to a higher comfort demand and the climate warming. This fact, together with the need to decarbonize the economy and phase-out the fossil fuel boilers, will strongly promote the use of heat pumps in the future.

2. According to the Sustainable Development Scenario 2030 of the IAE, a total of 14.52 TW of thermal output with heat pumps will be deployed. From these figures, 1.5 TW will correspond to non-vapor compression technologies, that will help to phase out high-global warming potential refrigerants. This is a great opportunity to thermoelectricity as an alternative to vapor-compression in certain applications.

3. Thermoelectricity is a solid-state heat pump technology that presents many advantages compared with vapor-compression: no refrigerant, no moving parts, noise free, gas free, no chemical reaction, reliability, scalability, minimum maintenance, easy transition from heating to cooling mode, accurate control and direct integration with PV panels.

4. Thermoelectricity has reached the market in certain niche applications as small refrigerators, automobile cooling, medical equipment, temperature-regulated clothes… but not in the buildings heating and cooling sector, although many investigations can be reported in the scientific literature. Most of these attempts propose the integration of thermoelectric modules in the thermal envelope, but this causes a thermal bridge when the modules are not supplied with DC current.

5. Passive houses are characterized by heating/cooling load lower than 10 W/m^2. In these conditions, the thermal comfort can be achieved by solely post-heating or post-cooling the fresh ventilation air mass. Hence, one heat pump can be integrated with the double flux ventilation system of a passive house, as some commercial models based on vapor-compression do. Thermoelectricity can be an interesting alternative to vapor-compression in small spaces (< 100 m^2) due to the low energy demand and the above-mentioned advantages, in addition to a compact and light-weight design.

6. An air-to-air thermoelectric heat pump requires an optimized design that reduces the thermal resistance of the heat exchangers between the TEMs and the air. This thermal resistance is proved to be determinant in the final coefficient of performance of the heat pump.

7. In the last years, computational models have emerged as an indispensable tool for the design and optimization of thermoelectric heat pumps and can greatly contribute to the development of this particular application. Nonetheless, in order to obtain a reliable instrument, it is necessary that these models take into account all the thermoelectric effects and incorporate the modeling of the heat exchangers and the heat reservoirs.

6.1.2. Conclusions derived from the analysis and thermal characterization of heat exchangers

The first phase of the study of the present Ph. D. dissertation is the empirical work done in the frame of two research projects: SMART CLIMA-1 (PT050/2016) and SMART CLIMA-2 (PT009/2017) funded by the Government of Navarre. In this frame two TeHP prototypes have been designed and tested: the first prototype is based on finned heat sinks and a cross-flow layout, while the second prototype is based on finned heat pipes and a counter-flow layout.

1. The advantage of the first prototype with the use of heat sinks as HE is that the thermal resistance is the same in both, the heat and the cold air ducts. However, the thermal resistance measured ranged 0.74-0.8 KW^{-1}. In a lab test, the maximum temperature decrease in the cooled air channel is limited to 5 °C for 7.5 V, and it drops when the supply voltage is higher. Additionally, the final weight of the prototype is estimated in 40 Kg and the thickness is 26 cm.

2. The heat pipes have proved to be a better alternative. The second prototype of TeHP presents a modular design, with one TEM and two heat pipe HE per module. It weighs 15 Kg, 10 Kg less than a common HRU, and is 16.5 cm thick (before insulation). With only 10 TEMs (corresponding to 10 modules), the temperature decrease in the cooling air duct is 70% higher, compared with first prototype (that employs 40 TEMs) in same test conditions.

3. The thermal characterization of the HPp is difficult due to three main aspects: the thermal resistance of the HPp depend not only on the convective coefficient, but also on the heat flux, being lower for higher supply voltages; moreover, the heat pipe HE in the cold side of the TEM works contrary to its original design; finally, the position of the heat pipe may affect to the reposition of the interior working fluid, being optimal for vertical position and heat generation on the bottom. This characterization cannot be found in catalogues, and it has been carried following a novel empirical methodology: firstly, the heat pipe dissipating heat from the TEM is characterized by placing a calibrated heat plate in the evaporator, and the condenser in an air duct, with different controlled air flows and a well-insulated envelope. The temperature gap between the evaporator and the air is measured at different heat fluxes and air flows. Then the experience can be replicated replacing the heat plate by one TEM and two air ducts: one for the cool air and one for the hot air. As the thermal resistance of the HE in the hot side is well known, the heat flux in the cold side can be deduced and the thermal resistance of the HE in the cold side calculated. This thermal characterization has demonstrated that that the operation of the heat pipes is not significantly affected by the vertical or horizontal position, with deviations lower than 3 %. This fact facilitates a TeHP design where the HPp are placed horizontally, resulting in a TeHP design with a thickness lower than 16 cm (before insulation).

4. However, the HPp thermal characterization shows that the thermal resistance is strongly affected if located on the hot or cold side. The thermal resistance of the HPp in hot side is very low, with a range 0.19-0.25 KW^{-1}, while the obtained thermal resistance in the cold side double the previous values (0.38-0.45 KW^{-1}). However, this is still 40 % better than the thermal resistance of the finned heat sinks, so it is worth to install finned heat pipes in the cold side, even if they work contrary to their original design. This permits to conceive a reversible air-to-air TeHP that switches from heating to cooling mode by solely changing the DC supply polarity.

5. This prototype has been deeply analyzed at different temperature gaps with the help of one climatic chamber. The tests reproduce two integration possibilities in a dwelling: the stand-alone installation between incoming and outgoing ventilation air flows, replacing the HRU; and the combination of both the HRU and the heat pump. In winter mode, the stand-alone installation showed better performance results for the heat pump, with a heating capacity of 1,000-1,250W and COP_h ranging 1.5-4. In this case it is necessary to set a minimum voltage to assure that the incoming air is above the set point inside the building. For a higher temperature outside this performance gets reduced, which is in tune with the lower heating load in the building.

6. When the thermoelectric heat pump is integrated with a heat recovery unit, both technologies, passive and active heat recovery, have a combined better performance that reaches 1,400-1,650 W with COP_h ranging 1.8-9. Maximum COP values are reached when the air flow is higher, since the coefficient of convection is increased.

7. In summertime, the thermoelectric heat pump performance is again better when working as stand-alone installation, reaching 375 W of cooling capacity with COP_c ranging 0.5-2.5. When the power supply exceeds 9 V the cooling capacity is barely increased while the COP_c drops 40%.

8. The combined effect of heat recovery unit and heat pump obtains better results, the cooling capacity is increased 50 W on average and the COP_c is improved. For more extreme exterior temperatures, this combination would certainly show a better performance compared with the sole use of the heat pump, due to the passive effect of the heat recovery unit.

6.1.3. Conclusions derived from the TeHP design and optimization

As a result of the thermal characterization of the heat pipes and the second prototype, the final TeHP design proposed by this Ph. D dissertation is based on the parametric optimization carried out by a computational model developed to reproduce the thermal behavior of the TeHP in all operating conditions.

1. A computational model has been developed and programmed in EES software, including the simple method, as there is no statistical difference in the calculated results of coefficient of performance and cooling power compared with other more complex modelling techniques at 95% level of confidence, according to a previous research work. The thermoelectric properties are provided by the manufacturer, and the thermal resistance of the HE in the hot and cold air ducts are based on the measured experimental data, and integrated with an interpolation module considering the double dependency on air flow and the heat flux. This is a key parameter, as it affects to the uncertainty of the simulation model, according to the previously cited research, comparing various modelling techniques.
   The resulting computing module has been validated with the empirical results obtained in the laboratory tests for the second prototype, showing a maximum deviation of 13 % for the estimation of the heating capacity and 14 % for the cooling capacity.

2. The parametric investigation carried out with this model compares the stand-alone installation of the TeHP and the combination with the HRU, but this time optimizing the COP for a variable number of modules and different outside weather conditions. The integration with the HRU along with the TeHP doubles or even triples the COP for low heating/cooling demand, and it stays at least 12.5 % higher when maximum demand is required.

3. The number of modules needed to reach this maximum COP is also considerably lower in the case of the combination with an HRU, being 2-16 modules vs 48-70 for heating, while it is 6-20 vs 46-84 for cooling. The standalone installation is then discarded for the final proposed design.

4. More important is that this analysis raised two controversial results. Firstly, for a standalone TeHP, an increasing heating demand led to an unexpected progressively lower number of modules needed to reach the maximum COP. Secondly, for the TeHP+HRU, the electric consumption of the modules increases for an increased number of modules, but just up to a certain point. From that value, this expected statement is no longer true.
   An in-depth analysis reveals that, given that the heating and cooling demands are correlated in this applications with the outgoing air temperature, there is a minimum temperature gap that needs to be set in thermoelectric modules and, therefore, a minimum feeding voltage. This means that a minimum heat flux per module is required, below which the system is uselles. This explains the first controversial result, and also explains the limited reduction of the electric current intensity when the

number of modules grows, thus justifying the second controversial finding. Consequently, no general rule can be given beforehand about the number of modules for maximum COP, which contradicts previous research, so it must be evaluated in each application.

5. The second and most relevant outcome concerning a PH is that the number of modules for maximum COP is virtually constant and independent on the climate. The optimization of the number of modules is carried out calculating a seasonal coeffient of performance for three European climates: Athens, Strasbourg and Helsinki, with very different winter seasons. The analisys reveals that the optimized number of modules is almost constant (and very close to 15 in all cases), although the energy consumption is different. This number of modules is very low, compared with previous research studies, and makes the potential construction and further installation of this TeHP very viable in terms of dimensions and costs.

6. The thermoelectric heat pump with 15 modules provides 405 W of cooling capacity when outside temperature is 25 °C, which is reduced to 330 W when the temperature rises up to 40 °C. Eventhough this cooling capacity may compensate the internal heat gains and the transmission heat flux through the building envelope and the ventilation to a high extent, higher cooling capacity is desiderable.

6.1.4. Conclusions derived from the integration of the TeHP in a PH pilot case

With the aim of optimizing the TeHP design and its operation in a PH dwelling, one computational model has been developed by integrating the previously validated TeHP model with the dynamic simulation of the building and the ventilation system in TrNSYS, based on the PH certification data. This computational model allows for the comparison of the TeHP with VCHP and the integration of a PV facility. The most relevant conclusions of this investigation are summarized as follows:

1. The results demonstrate that the thermoelectric air-to-air heat pump integrated with a double flux ventilation system and a heat recovery unit is a reliable system, able to provide ventilation (0.54 - 1 ACH), heating and cooling for a pilot case of 74.3 m^2 PH certified dwelling in Pamplona (Spain) consuming 1143.2 kWh/y (15.3 kWh/m^2y) of electricity per year.

2. The results show that, given the low specific energy demand of PH, thanks to the highly isolated envelope, the indoor ambient may be conditioned by only raising or lowering the temperature of the incoming air flow. The thermoelectric heat pump permits a wide operation range (5 - 100 % regulation) by controlling the voltage of the DC supply, which keeps indoor air within the comfort range very accurately (20 - 23 °C in winter and 23 - 25 °C in summer), with a COP between 1 - 2 for heating and 0.5 - 1.7 for cooling.

3. This thermoelectric heat pump has been compared with a small VCHP unit with a low and a high COP (2.5 - 4.5 for heating and 2.2 - 4 for cooling). The study shows that VCHP reduces the operation time (82 % in heating mode and 30 % in cooling mode) and improves the overall efficiency (20.9 % with the low COP vapor compression heat pump and 36.1 % with the high COP), but the energy saving may be easily compensated with the production of just 1 PV panel (250 Wp) and, in economic terms, with 1 or 2 PV panels per dwelling (250 - 500 Wp): 1 in case the price for the kWh imported from the grid is similar to the kWh exported, and 2 when the imported kWh is 0.14 € and 0.04 € the kWh exported. This means that if the TeHP RRP may be 150-300€ lower than the VCHP, it is then competitive from a life cycle cost perspective.

4. The provision of heating is guaranteed by both the TeHP and the VCHP, since the temperature gap between the indoor temperature (20 - 23 °C) and the supply temperature (< 50 °C) with the ventilation air flow allows to deliver a heating capacity above 10 W/m^2 through the ventilation air mass. However, in the case of cooling, the temperature of the supply air is limited by the dew point of the fresh air. The system has showed to provide enough cooling capacity to compensate the internal gains in the domestic sector, but in case of unexpected heat gains (i.e. deficient blind regulation with totally open windows during midday) transient overheating situations may occur.

5. The results presented in this Ph. D. dissertation demonstrate the great potential of the use of TEMs as a breakthrough and cost-effective technology to air condition low energy demand buildings, with a peak heating demand below 10 W/m^2.
   The refrigerant-free technology, the compactness, and the silent operation, together with the potentially lower costs and the integrability with PV facilities (that would reduce the extra 10 % electric consumption of the TeHPs considered in this Ph. D dissertation for the AC-DC conversion and the 10 % electric losses for the DC-AC conversion in the PV facility) outweigh the additional energy consumption, when comparing its performance with vapor compression technology.

6.2. Future Lines

The promising results shown the present Ph. D dissertation will the basis of a research line in thermoelectricity applied to high efficiency building, that will follow the recommendations presented in this section:

- **Optimized design of the TEM-air heat exchanger in the cold side to reduce the thermal resistance:**

  As demonstrated in the 2nd chapter of the dissertation, the thermal resistance of the cold side doubles the values obtained for the hot side in all operational conditions tested. This is clearly due to the fact that the HPp works contrary to the original design, since the condensation of the inner fluid takes place in the evaporator, whereas the vaporization happens in the condenser. However, the thermal resistance is still 40% better than finned heat sinks and, therefore they have been used for the final prototype, with the additional benefit of the reversible working model.
  Additional research is needed to reduce the thermal resistance of the HPp in the cold air duct by testing alternative inner fluids and HPp designs to enhance the thermal flux in low temperature ranges (0-5 ° C of cooled air).

- **Cascade TEM configuration for new thermoelectric heat pump:**

  For high temperature gaps between indoor and outdoor analyzed in winter conditions the TEM needs to be stressed, working at high voltages to make sure the hot side is hotter than the air in the hot air duct, while the cold side is colder than the cooling air. High voltages naturally derive into bad COPs, which is a common rule in thermoelectric devices. There are commercially available TEMs with a multistep pyramidal design by setting two or three layers of thermocouples thermally connected in series. As a result, the temperature gap reached by the TEM is higher. These TEMs are used for cooling very specific and small areas at low temperatures, as laser diodes. There is an interesting field to experiment with multi-step TEMs, with cascade connection to extend the temperature gaps and work at low voltages, optimizing the heat flow in the heat pump.

- **Exploration of synergies between ventilation and the production of DHW with thermoelectric devices:**

  nZEBs and Passive Houses have reduced the energy demand for heating and cooling tremendously. However, the DHW remains the same, as sanitary needs of the occupants have not changed. The economy decarbonization goal and the resulting electrification of heating and cooling in buildings need to also address the production of DHW. TeHP have also a great potential in this field. One great disadvantage in this case is the need for 60 °C of DHW. However, the thermal resistance of a HE between of the TEM and the water can be significantly lower, and the cascade connection of the TEMs, as explained in previous recommendation, can help on this matter. Additionally,

there are clear synergies between heating and DHW, enabling the use of a common tank to provide both.

- **Additional heat recovery possibilities in the building sector with thermoelectric devices:**

  In line with the previous recommendation, there is the possibility to explore new residual heat sources for the heat generation and the integration of thermoelectric modules as heat pumps to provide DHW and heating. One of this heat reservoirs is the collection of grey water before reaching the sewage network. A TeHP can be integrated to preheat the tap water before reaching the DHW tank.

- **Optimization of the TEM regulation:**

  In Chapter 5 the regulation proposed for the TeHP in the pilot case study is explained. The voltage of the electric supply to the TEMs is proportional to the temperature difference between the indoor temperature and the setpoint. The analysis demonstrates the good results in terms of comfort conditions inside. However, the wide range of regulation capacity of both, the heating and cooling power, and the dependency of the TeHP efficiency on the supply voltage, infer a great potential of energy saving and optimized comfort based on new strategies or the use of artificial intelligence.

- **Additional strategies to improve the cooling capacity:**

  Chapter 4 explores the limitation in terms of cooling capacity, as the air volumetric flow is limited by the ventilation need, and the temperature of the cooled air due the humidity of the outside air, in addition to the limitation of the Seebeck effect in the TEMs. Some of the potential alternatives to improve the cooling capacity of the system are proposed in the paper. Adiabatic cooling, in combination with free cooling and air recirculation are suggested and would need additional research to adapt the system to climates with hot summers and high cooling loads above 5 W/m^2.

- **Direct integration of the TeHP and the PV facilities:**

  Finally, more additional research is required to analyze the direct integrability of a PV installation with the TeHP in order to reduce the energy losses in the DC-AC and AC-DC conversion. This system must enable the voltage regulation of the electricity supply and reduce the PV peak-power, and analyze the potential addition of the energy storage to optimize the energy flow and economic results.

6.3. Scientific Contributions

The research carried out during the fulfillment of this thesis has been presented in different formats: publications in JCR journals, communications in conferences, publication in conference proceedings or Bachelor's Thesis supervised. This section enumerates these scientific contributions distinguishing into those contributions directly related to the present Ph. D. dissertation, and those performed at the same time due to the participation of the Ph. D. candidate in other research activities.

Research projects related to the Ph. D dissertation:

- **Main researcher** in **SMART CLIMA -1** funded by the Government of Navarre (PT050). 1st Prototype of air-to-air thermoelectric heat pump with heat sinks. February 2016 - December 2016.
- **Main researcher** in **SMART CLIMA -2** funded by the Government of Navarre (PT009). 2nd Prototype of air-to-air thermoelectric heat pump with heat pipes. January 2017 - December 2017.

Other significant research project activities as project manager at CENER:

- **Project coordinator** and technical director in **STARDUST** - **Holistic and integrated urban model for smart cities.** GA774094 SCC01-HORIZONTE 2020: 2017. September 2017-September 2022.
- **Main researcher and technical director** in **LIFE ZEROSTORE** – Supermarket retrofit for zero energy consumption. LIFE12 ENV/ES/000787 March 2014 - September 2017.
- **Researcher** in **TROMBE** (**"Muro TROMBE de agua activo para fachadas modular y ligero"**) Código Expediente: 0011-1411-2018-000007 Convocatoria Proyectos estratégicos I+D 2018-2020.
- **Co-leader** of Subtask D of **International Energy Agency (IEA) – EBC ANNEX 83:** Positive Energy Districts (PED).
- **Co-leader** of **Monitoring and Evaluation Task Group** and member of the **Board of Coordinators** in the Smart Cities European Network.

Awards:

- **SCIENCE EKAITZA 2019 - RENEWABLE ENERGIES in the "II Gala científica de Navarra"** organized by ADITECH the 26th of June 2019 with the proposal: ZERO CO2 DATA: decarbonized data centers using freecooling of water reservoirs and the integration with smart RES grids.

The Ph. D. candidate founded a Start Up called Monitoring S.L. (www.inbiot.es) in 2018 that provides indoor air quality technology in order to monitor and analyze the comfort and heath conditions of indoor environments. This initiative received the following awards:

- **"INICIATE" AWARD** organized by CEIN the 23rd of March 3018 with the proposal of an IAQ monitoring system connected to an IoT platform.

- **"EMPRENDEDOR" AWARD** organized by CEIN, Gobierno de Navarra, Caja Rural de Navarra, Cinfa, Corporación Mondragón, Correos, Inycom, MTorres, Mutua Navarra, Uscal, Viscofán and Zabala Innovation the 29th of May 2018 with the proposal of monitoring indoor environments' wellness beyond thermal comfort.

- **"CLH EMPRENDE 2018" AWARD** organized by CAMPUS IBERUS (Universidad Pública de Navarra, Universidad de Zaragoza and Universidad e Lérida) with the proposal of inBiot business model.

- **SMART IRUÑA LAB 2019** program organized by the City of Pamplona to test products and services of emerging technological Start Ups in the urban context as a living lab.

- **NEOTEC 2020 – 2021:** support program of the Centre for the Development of Industrial Technology (CDTI) for technological SMEs in order to develop the business model and consolidate the company.

Publications in JCR Journals:

The publications in JCR Journals directly related to the thesis are the four articles that endorse the present Ph. D. dissertation as a compendium.

- P. Aranguren, S. Díaz de Garayo, A. Martínez, D. Astrain. **Heat pipes thermal performance for a reversible thermoelectric cooler-heat pump for a nZEBs**. Enery & Buildings 187 (2019) 163-172. DOI: 10.1016/j.enbuild.2019.01.039

- S. Díaz de Garayo, A. Martínez, P. Aranguren, D. Astrain. **Prototype of an air to air thermoelectric heat pump integrated with a double flux mechanical ventilation system for passive houses**. Applied Thermal Engineering 190 (2021) 116801. DOI: 10.1016/j.applthermaleng.2021.116801

- S. Díaz de Garayo, A. Martínez, P. Aranguren, D. Astrain. **Optimal combination of an air-to-air thermoelectric heat pump with a heat recovery system to HVAC a passive house dwelling**. Applied Energy 309 (2022) 118443. DOI: 10.1016/j.apenergy.2021.118443

- S. Díaz de Garayo, A. Martínez, P. Aranguren, D. Astrain. **Annual energy performance of a thermoelectric heat pump combined with a heat recover unit to HVAC one passive house dwelling.** Applied Thermal Engineering 204 (2022) 117832. DOI: 10.1016/j.applthermaleng.2021.117832

Besides them, the Ph. D. candidate has also published the following two articles in JCR journals focused on the simulation models of the thermoelectric heat pumps applied to field analyzed in the present dissertation.

- A. Martínez, S. Díaz de Garayo, P. Aranguren, D. Astrain. **Assessing the reliability of current simulation of thermoelectric heat pumps for nearly zero energy buildings: expected deviations and general guidelines**. Energy Conversion and Management 198 (2019) 111834. DOI: 10.1016/j.enconman.2019.111834

- A. Martínez, S. Díaz de Garayo, P. Aranguren, M. Araiz, L. Catalán. **Simulation of thermoelectric heat pumps in nearly zero energy buildings: Why do all models seem to be right?**. Energy Conversion and Management 235 (2021) 113992. DOI: 10.1016/j.enconman.2021.113992

Other publications:

- Paper: S. Díaz de Garayo, J. Llorente "SISTEMA DE GESTIÓN DE LA ENERGÍA Y ANÁLISIS AVANZADO DE DATOS: APLICACIÓN EN EL SECTOR RETAIL", Revista ENERGÉTICA XXI (n° 165, April 2017).

- Paper: S. Díaz de Garayo, J. Llorente, D. Zambrano "PROYECTO ZEROSTORE: MODERNIZANDO SUPERMERCADOS HACIA LA SOSTENIBILIDAD", FUTURENERGIA Magazine (May, 2016).

Publications in conference proceedings:

Related to the Ph. D dissertation:

- S. Díaz de Garayo, **"La tecnología termoeléctrica como alternativa al uso de refrigerantes para climatizar casas pasivas"**. Libro de comunicaciones 13ª Conferencia Passivhaus. Publicaciones Plataforma de Edificación Passivhaus. Octubre 2021.

- S. Díaz de Garayo, A. Martínez, P. Aranguren, D. Astrain. **"Bomba de calor aire-aire termoeléctrica para refrigeración de edificios residenciales"**. X Iberian and VIII Ibero-American Congress in Cooling Science and Techniques Proceedings (CYTEF 2020) 2020. ISBN: 978-2-36215-043-2.

- S. Díaz de Garayo, A. Martínez, D. Astrain. **"Air-to-air thermoelectric heat pump for heating, ventilation and air-conditioning in a nearly zero energy building"**. IX Iberian and VII Ibero-American Congress in Cooling Science and Techniques Proceedings (CYTEF 2018) 2018. ISBN: 978-84-09-01619-8.

Others:

- J. Llorente, S. Díaz de Garayo, A. Miranda. **"Aprovechamiento energético de las redes de agua en la Mancomunidad de la Comarca de Pamplona".** Actas del IX International Greencities Congress9° Foro de Inteligencia y Sostenibilidad Urbana. ISBN: 978-84-09-01166-7.

- S. Díaz de Garayo, J. Llorente, D. Zambrano, **"Biomass trigeneration system for retail stores"**. 9th International Conference Improving Energy Efficiency in Commercial Buildings and Smart Communities (IEECB&SC'16). JRC Conference and Workshop Report. ISBN: 978-92-79-59779-4.

Communication in Conferences:

- Oral: S. Díaz de Garayo, **"La tecnología termoeléctrica como alternativa al uso de refrigerantes para climatizar casas pasivas"**. 13ª Conferencia Passivhaus | PEP (Murcia, Spain, 2021).

- Plenary session: S. Díaz de Garayo, **"Tendencias en la Energética Edificatoria"**. X Congreso Ibérico | VIII Congreso Iberoamericano de las Ciencias y Técnicas del Frío (Pamplona, Spain, 2020).

- Oral: S. Díaz de Garayo, A. Martínez, P. Aranguren, D. Astrain. **"Bomba de calor aire-aire termoeléctrica para refrigeración de edificios residenciales"**. X Congreso Ibérico | VIII Congreso Iberoamericano de las Ciencias y Técnicas del Frío (Pamplona, Spain, 2020).

- Oral: S. Díaz de Garayo, A. Martínez, D. Astrain. **"New prototype of a thermoelectric heat pump with heat pipes for the air condition of a Nearly Zero Energy Building"**. 37th International and 16th European Conference on Thermoelectrics (Caen, France, 2018).

- Oral: S. Díaz de Garayo, A. Martínez, D. Astrain. **"Air-to-air thermoelectric heat pump for heating, ventilation and air-conditioning in a nearly zero energy building"**. IX Congreso Ibérico | VII Congreso Iberoamericano de las Ciencias y Técnicas del Frío (Valencia, Spain, 2018).

- Oral: S. Díaz de Garayo, A. Martínez, D. Astrain, X. Aláez. **"Integration of an air-to-air thermoelectric heat pump and a heat exchanger in the ventilation system of a passive house".** 15th European Conference on Thermoelectrics (Padua, Italy, 2017).

- Oral: A. Martínez, S. Díaz de Garayo, D. Astrain, **"Air-to-air thermoelectric heat pump for heating, ventilation, and air-conditioning in passive houses".** 36th International Conference on Thermoelectrics (Pasadena, EEUU, 2017).

Others:

- Oral: J. Llorente. :"Water source heat pump and PV installation to reduce CO2emissions in drinking water treatment stations", 11th International Conference on Improving Energy Efficiency in Commercial Buildings and Smart Communities (IEECB&SC'20)(ON-LINE, 2020).

- Oral: J. Llorente, S. Díaz de Garayo, A. Miranda. "Aplicación en climatización del aprovechamiento energético de las redes de agua en la mancomunidad de la comarca de Pamplona". XXXV CONGRESO AEAS (Valencia, España, 2019).

- Oral: S. Díaz de Garayo, "STARDUST Project", Portugal Smart Cities Summit (Lisboa, Lisboa 2019)

- Ponencia: S. Díaz de Garayo. "Los sistemas HVAC, los edificios inteligentes y la conectividad", XIII Encuentro Anual de ATECYR –REFUNDICIÓN DE LA DIRECTIVA DE EFICIENCIA ENERGÉTICA EN LOS EDIFICIOS (Pamplona, Spain, 2018).

- CENER representative: Technologic Mission Japan (MITC 20180001): "Thermal heat recovery" ENEX 2018 (Tokyo, Japan, 2018).

- Oral: J. Llorente, S. Díaz de Garayo, A. Miranda "APROVECHAMIENTO ENERGÉTICO DE LAS REDES DE AGUA EN LA MANCOMUNIDAD DE LA COMARCA DE PAMPLONA" Congreso Green Cities – 9° Foro de Inteligencia y Sostenibilidad Urbana (Málaga, Spain, 2018).

- Oral: S. Díaz de Garayo, "STARDUST Project", Jornadas sobre Ciudades Inteligentes RED-RTI, Smart Cities Institute, Universidad Pública de Navarra (Pamplona, Spain, 2018).

- Chair: S. Díaz de Garayo, 8ª Conferencia Española Passivhaus (Pamplona, Spain, 2016) and 9ª Conferencia Española Passivhaus (Sevilla, Spain, 2017) Plataforma de Edificación Passivhaus (PEP).

- Oral: S. Díaz de Garayo, J. Llorente, D. Zambrano, "Biomass trigeneration system for retail stores". 9th International Congress Improving Energy Efficiency in Commercial Buildings, (Frankfurt, Germany, 2016).

- Poster: J. Llorente, S. Díaz de Garayo, D. Zambrano "Biomass Trigeneration System for Retail Stores", 1st International Conference on Bioenergy & Climate Change (Soria, Spain, 2016).

Other remarcable profesional activities:

- Founder member of PEP (Plataforma de Edificación Passivhaus): www.plataforma-pep.org
- Founder member of Cluster IAQ (Indoor Air Quality): www.clusteriaq.com

Supervision of Bachelor's Thesis

During the fulfillment of the thesis, the following Bachellor's thesis have been supervised:

- D. Zambrano, "Evaluación energética de un sistema de trigeneración con energías renovables", June 2016.
- X. Alaez, "Simulación y desarrollo de prototipo para la climatización de nZEB mediante una bomba de calor termoeléctrica integrada en un sistema de ventilación mecánica de doble flujo", June 2017
- I. Retegi, "Análisis de la eficiencia energética y propuestas de mejora para Centro de Procesamiento de Datos de CENER", September 2020.

upna
Universidad Pública de Navarra
Nafarroako Unibertsitate Publikoa